Ruby laser-assisted depilation: the mode of action and potential ways of improving outcome

Adam Topping FRCS

2000

A thesis submitted to the University of London
for the degree of
Doctor of Medicine (M.D.)

The RAFT Institute of Plastic Surgery
Mount Vernon Hospital
Northwood
Middlesex
&
The Northwick Park Institute for Medical Research
Northwick Park Hospital
Harrow
London

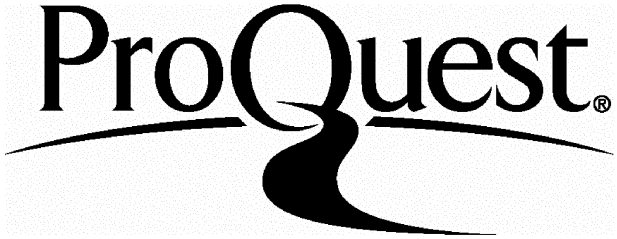

DESCRIPTION OF THESIS

Name of candidate Adam Partington Topping

Title of thesis Ruby laser-assisted depilation: The mode of action and potential ways of improving outcome.

TEXT

The technique of ruby laser-assisted depilation has become commonly used in the fields of reconstructive and cosmetic plastic surgery. Nevertheless it is clear that this technique, as presently practised, produces sub-optimal results in the majority of patients. One of the contributing factors towards the inefficiency of current treatment regimes is the reluctance to produce the side effect of epidermal damage.

This thesis examines the clinical technique of ruby laser-assisted depilation. Attempts are made to define this technique's mode of action and then to devise new methods of protecting the skin from the associated side effect of epidermal damage. The work presented uses cell biology and biochemical techniques, specifically: human cell and tissue explant culture, animal models, histology, immunohistochemistry, protein gel analysis (SDS PAGE and western blotting), thermal imaging.

The work shows that laser depilation treatment causes heat production within the confines of the hair follicle which then dissipates to the surrounding dermal stroma. The maximum temperature induced in each follicle differs between follicles within the same treatment area and also between different individuals. Laser light penetration through the skin's depth was found to be deeper than previously theorised. In addition, an acceptable animal model was established and characterised. Two differing methods of potentially protecting the epidermis from side effect damage were assessed. The first relied on physical blocking of the laser light from reaching the viable cells of the epidermis, whilst the second involved the induction of the cells' own intrinsic stress protection mechanisms (specifically heat shock proteins). Both potential techniques were assessed *in vitro* using cell and/or tissue explant culture and *in vivo* using the mouse model. It is hoped that in future a small clinical trial of these techniques will prove their worth in patients.

Acknowledgements

This thesis is dedicated to my wife, Lucy and my son Sam.

I wish to thank my supervisors Dr C Linge and Professor C Green for their invaluable supervision and constant enthusiasm, Mr D T Gault for his support and supply of material, Mr A O Grobbelaar for his advice and help and Professor R Sanders for making it all possible. I also thank Dr A Cambrey for her help and advice during the progress of my work.

I also would like to thank Mr J Shelton for teaching me tissue culture techniques, Mrs F Daley for immunohistochemical assistance and Mrs S Barnet, Ms C Noel and Mrs E Clayton for the preparation of all the histological sections. I would furthermore like to thank Mr K Ladhani for all his help and assistance during my two years of research.

My thanks go to Dr Paul Sibbons for his help in obtaining the Animal Licence and for being the Project Licence holder during the work performed at Northwick Park. I am also grateful for the assistance of the theatre staff at Northwick Park during the experimental work performed at the Institute, in particular to Mr D Shepherd and Ms C Grey.

I would finally like to thank everyone at RAFT, both trustees and employees, for finding the necessary funds to continue my work and for making my research time there so enjoyable.

ABSTRACT

Aim - To improve efficacy and lessen side effects resulting from normal mode ruby laser (NMRL)-assisted depilation via a greater understanding of its mode of action and the development of novel methods of reducing associated epidermal damage.

Employing a thermal imaging camera and *ex vivo* hair-bearing skin, the targets for the NMRL (pulse duration 900 μsec and spot size 7 mm) were defined, the temperatures reached and the heat dissipation rates determined. Production of heat was confined to the hair follicles, with the peak temperatures reached varying considerably between hairs within the same treatment area and also between individuals. Histological assessment for a known indicator of cellular damage (p53 expression) identified the sites and extent of damage, which correlated with the peak temperatures measured. An energy meter was used to detect the penetration of NMRL light through *ex vivo* skin, which was found to be deeper than previously theorised. The black-haired mouse (C57Bl/10) was assessed both macroscopically and histologically and found to be an acceptable animal model of NMRL depilation and associated epidermal damage. Attempts to reduce the epidermal damage by simply stopping the light reaching the epidermis using a chromophore block were assessed. Chromophore did indeed reduce the amount of epidermal damage detected in laser-irradiated *ex vivo* human skin, whereas in contrast it increased the wounding seen in the much thinner skin of the mouse. Nevertheless the mouse model showed that this technique did not affect the depilation efficacy. An alternative method of reducing epidermal damage using induction of the cells' intrinsic protective mechanisms (heat shock proteins, HSP) was assessed using cultured keratinocytes and the mouse model. Primarily, the sub-lethal temperature optimum for HSP expression in human keratinocytes was determined, then an *in vitro* model of NMRL-associated epidermal damage was established and the heat pre-treatment assessed. The temperature to precondition mouse skin was then determined and its protective capacity and effect on depilatory efficacy examined *in vivo*. In both models heat pretreatment was found to

significantly protect from NMRL-associated damage whilst having no detectable affect on depilatory efficacy.

CONTENTS

CHAPTER 1 – GENERAL INTRODUCTION

CHAPTER 2 – MATERIALS AND METHODS

CHAPTER 3 – THE INTERACTION BETWEEN A LASER PULSE AND HUMAN SKIN

CHAPTER 4 – AN ANIMAL MODEL ASSESSING RUBY LASER-ASSISTED DEPILATION

CHAPTER 5 – THE EFFECT ADDITIONAL CHROMOPHORE HAS UPON RUBY LASER/SKIN INTERACTION

CHAPTER 6 – POTENTIAL PROTECTION FROM EPIDERMAL SIDE EFFECTS BY PRETREATMENT – *IN VITRO* PROOF OF PRINCIPLE

CHAPTER 7 – POTENTIAL PROTECTION FROM EPIDERMAL SIDE EFFECTS BY PRE-HEATING – *IN VIVO* PROOF OF PRINCIPLE

CHAPTER 8 – DISCUSSION

APPENDICES

LIST OF FIGURES

CHAPTER 1

CHAPTER 3

CHAPTER 4

CHAPTER 6

LIST OF TABLES

CHAPTER 1

CHAPTER 2

CHAPTER 3

CHAPTER 5

CHAPTER 1 - GENERAL INTRODUCTION

Recent advances in the field of laser technology have led to the development and production of a variety of lasers with the ability to target and destroy hairs within the skin. The capacity to permanently depilate skin could have important consequences in the fields of both reconstructive and cosmetic surgery but as yet, studies performed have only reported a moderate and mainly temporary success rate. Skin side effects have been noted including superficial burning, hypopigmentation and hyperpigmentation which can limit the strength of treatment. This thesis aims to improve laser-assisted depilation by firstly understanding the interaction between the laser and skin and then determining methods to lessen the side effects whilst either not affecting or even improving depilatory efficacy. To enable this requires an intimate knowledge of both lasers and skin before discussing the present data available on how lasers interact with skin.

1.1 HAIR

The precise role of hair on the human body is not known. In primates and ancestors it would have been primarily that of heat retention for the warm-blooded mammals. Since then the human has experienced loss of total body hair through evolution stated to be a selective advantage on descending from trees and hunting in a warm climate so allowing greater temperature control (Ebling, et al., 1991). Presently its surmised role is predominantly that of sociosexual interaction (eyebrows, axillae and pubis). This occurs through visual signalling and olfactory means by scent dispersal from neighbouring apocrine and sebaceous glands. The greater psychological than physical effect of abnormalities of hair on the individual concerned would serve to reinforce this belief, as does the change of hair type and distribution that occurs upon sexual maturity. Its protective role is minimal except possibly against irradiation and heat loss, particularly upon the scalp region. Hair also supplies a sensory function that compliments the skin.

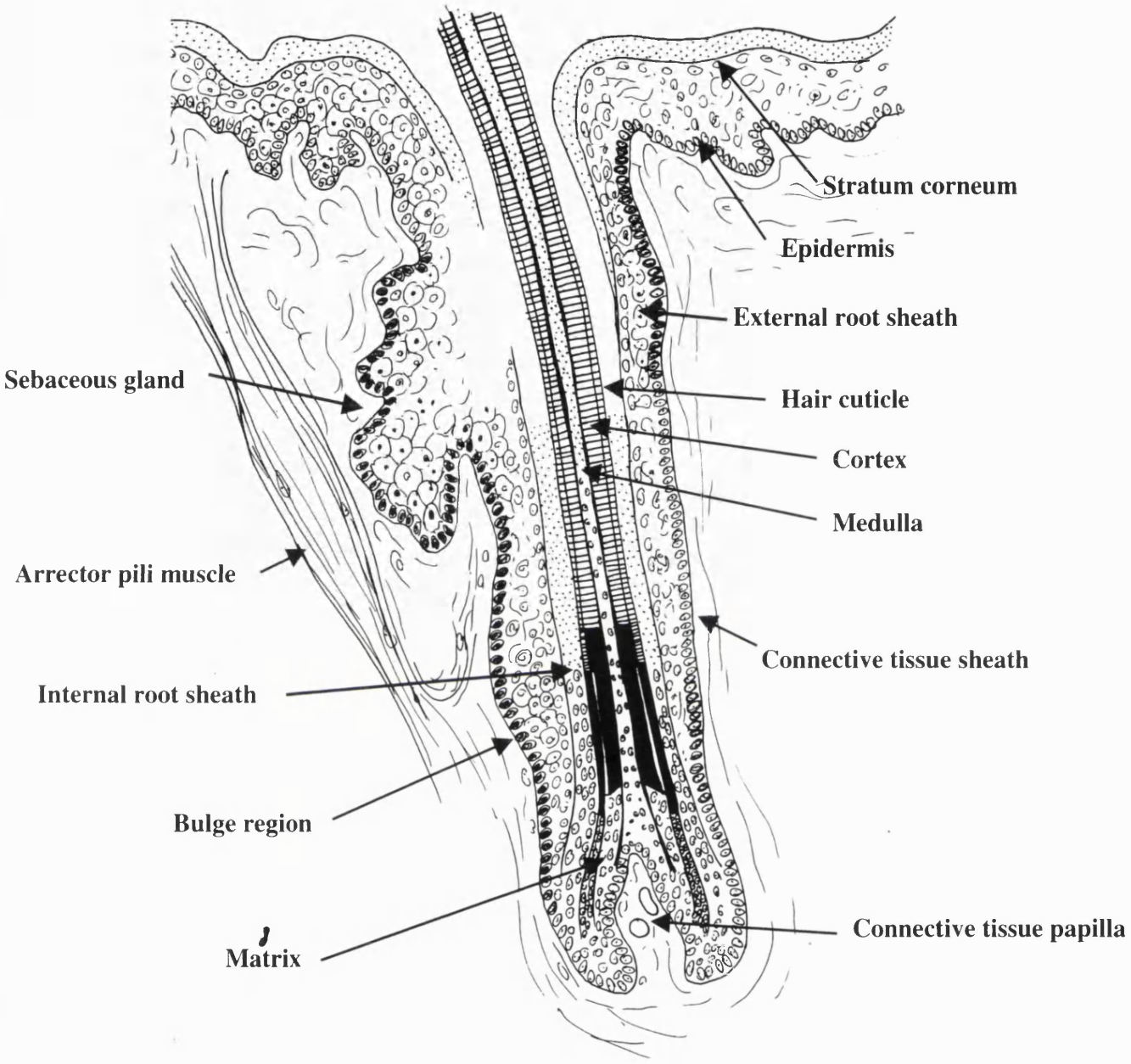

Figure 1.1: Anatomical representation of a human hair follicle. The solid black region represents the keratogeneous zone, the straight-line regions the hard keratin and the speckled regions the soft keratin.

1.2 ANATOMY OF HAIR

Hair is a filamentous, keratinised structure forming part of the Pilosebaceous Unit, which in addition, consists of the follicle, the arrector pilli muscle, sebaceous gland and depending on the site, an apocrine gland (see Figure 1.1). Keratins are a group of insoluble proteins of which there are two types, hard and soft. Hair contains hard keratin whilst desquamating tissues such as skin contain soft keratin. Keratins form long fibres which are bound tightly via di-sulphide bonds and cross-linking with other proteins. Consequently, they show great resistance to changes in pH, temperature and enzymatic digestion (Rushmer, et al., 1966). Hair is essentially dead except at its base where the growing region, or hair bulb, is situated. Hair tracts have been mapped in man showing that a general "flow" of hair exists particularly noticeable on the forearm and fingers in the ulnar direction. There are parts of the body where hair is absent. These are the palms of the hands, soles of the feet, the umbilicus, nipples, glans penis, clitoris and labia minora where it is probable that their presence would be a hindrance to function.

Hair is contained within a follicle whose depth can vary from between 1 and 3 mm below the dermis so the lower end protrudes into subcutaneous fat. The hair emerges from the skin surface at an oblique angle which can be changed by action of the arrector pilli muscle. This muscle originates from the papillary dermis and attaches to the follicle at approximately 1/3rd the way down the hair shaft. Action of the muscle, which is influenced by cold and the sympathetic nervous system, makes the angle between skin and hair more acute and so the hair "stands on end". The diameter of hair can vary between 15 to 120 μm and is dependent on the type and the site the hair originates from (see Figure 1.2).

Microscopically, the mature hair shaft has been described as usually having 3 concentric zones differing in the type of keratin present. From inside out the zones are described as the medulla, the cortex and the cuticle. The medulla may be absent in thinner hairs. It is formed of disintegrating cells producing columns which contain air cavities above the level of the epidermis. The cortex is the largest component of the

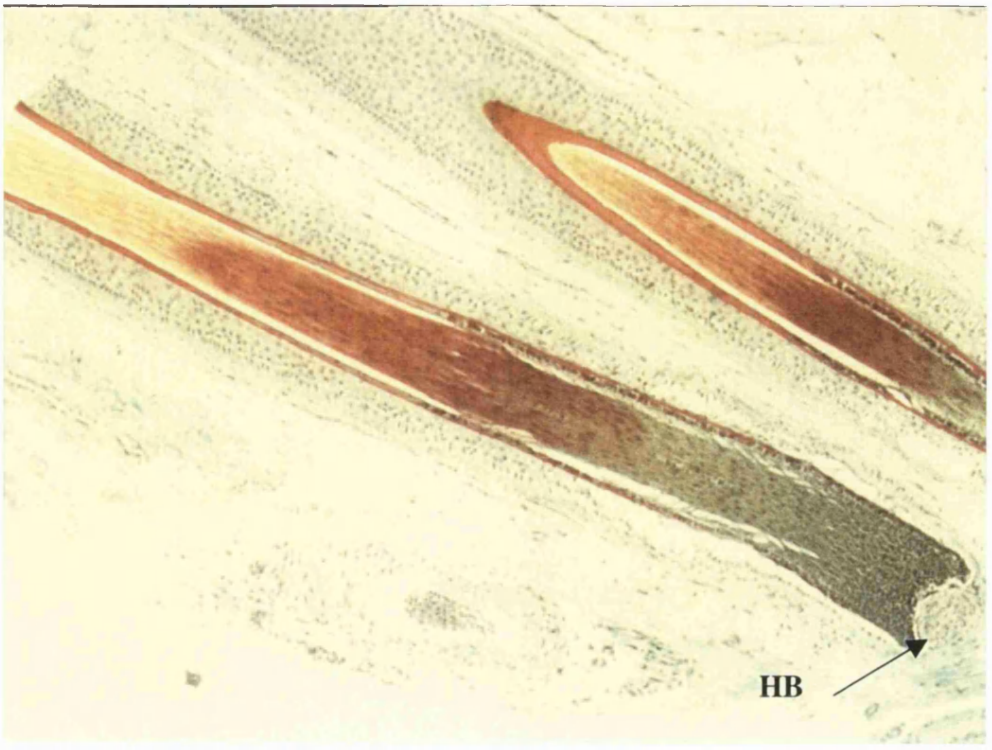

Figure 1.2: Modified SACPIC stain of a transverse section taken from human hair-bearing skin showing the different keratinised regions of a hair shaft. The viable hair keratinocytes are stained green, whilst those in the keratogenous zone are stained red. The fully keratinised, mature cells of the hair shaft are stained yellow. HB is the hair bulb (x100).

hair-shaft and is composed of many tightly packed keratinised cells set in a dense matrix. The cells contain melanosomes and nuclear remnants. The cuticle, which forms the surface of the hair, consists of several layers of keratinised squamous epithelial cells directed in an upward and slightly outward direction similar to the tiles on a roof. They are fused with the cells of the inner root sheath at the level of the isthmus (just below the sebaceous gland) so helping to fix the hair-shaft in its containing piliary canal. The outer surface of the cuticle cells is rich in high sulphur protein which increases their environmental resistance. Nevertheless, as the hair shaft emerges from the skin so wear and tear causes it to become jagged as the cells are removed until ultimately it gains a brush-like appearance.

The inner root sheath is a layer which lies adjacent to the hair shaft almost up to the level of the duct of the sebaceous gland (isthmus) but then degenerates just before reaching it. Its role has been described as that of a temporary filling material for the growing hair shaft. It consists of 3 layers; an inner cuticle, a middle Huxley's layer and an outer Henle's layer. The cuticle layer undergoes keratinisation as the cells ascend the canal. Huxley's layer keratinises after those of the cuticle at the level of the middle of the follicle and Henle's at the level of the upper bulb. All layers then degenerate at the level of the isthmus.

The outer root sheath extends from the level of the upper bulb as a single or double layer of undifferentiated cells becoming multilayered higher up the follicle and then continuous with the superficial epithelium of the skin. Melanocytes and Langerhans cells are contained within it. At the level of the sebaceous duct the outer root sheath forms the wall of the piliary canal after the breakdown of the inner root sheath. Two types of cells containing different keratin and antigen expressions during differentiation have been described recently within the outer root sheath (Ito, et al., 1986). Further to this, a bulge region situated at and below the insertion of the arrector pilli muscle has been described. The cells within this region have features consistent with those of stem cells (Cotsarelis, et al., 1990), (Rochat, et al., 1994) and could play a fundamental part in hair cycling to be discussed later (see physiology section). Melanocytes have been described in the bulge region interspersed with the

keratinocytes which have occasionally been seen to contain melanin under electron microscopy (Narisawa, et al., 1995). Narisawa looked at scalp and eyebrow hair with reference to the bulge and found that melanisation was independent of hair cycling (Narisawa, et al., 1997). The bulge of eyebrow hair follicles always contained melanin in varying amounts whilst the bulge of scalp hair was free of melanin, it only being seen in the bulb and during specific growth phases. Thus the site and distribution of melanocytes and the melanin they produce would appear to vary throughout the body, particularly in the two regions most associated with hair growth, which could have an important influence on ruby laser-assisted depilation described later. Surrounding the outer root sheath is the glassy membrane which is a non-cellular layer equivalent to the basal layer of the skin. The whole follicle is invested in a connective tissue sheath called the outer dermal sheath into which is inserted the arrector pilli muscle.

The base of the pilosebaceous unit is called the hair bulb being the lowermost part of the follicular epithelium. It encloses the dermal papilla, which during hair growth consists predominantly of highly cellular connective tissue continuous with the outer dermal sheath, but during development induces formation of the hair germ. The hair bulb generates the hair and its inner root sheath and can be divided into two sections. The lower section, called the germinal matrix, consists of close-packed, mitotically active pluripotential keratinocytes interspersed with melanocytes and Langerhans cells. The upper section, or the upper bulb, consists of cells derived from the lower germinal matrix which move apically, differentiating along several lines. Those at the centre form the hair medulla whilst successive, radial cells give rise to the cortex and cuticle of the hair and finally the layers of the inner root sheath respectively.

Hair pigmentation derives from melanocytes present in the bulb adjacent to the apex of the dermal papilla. Melanocytes are also present in the outer root sheath and other parts of the follicle as described earlier. Within the bulb the melanocytes donate melanosomes to the medulla and cortex of the hair mainly and are active during hair growth alone producing both eumelanin (dark brown) and pheomelanin (red/yellow) in varying quantities depending on genetic predisposition. Hair that contains less

melanin (eu or phaeo) becomes lighter in colour. The melanin granules present in the hair cortex are at a stronger concentration at the periphery.

Hair colouration appears to have no protective role against environmental irradiation. The colour may change, usually during adolescence, as a result of the change in the dominant melanin. This is primarily under genetic control via the probable production of melanocyte stimulating hormone. However, other factors can affect hair colour such as drugs (Chloroquine), nutritional deficiencies and metabolic disorders (Phenylketonuria). Hair greying results from a reduction in the number and activity of melanocytes. Albinism occurs when the melanocytes are present at the normal quantity but are inactive. Both circumstances appear to be genetically determined.

The blood supply of the hair follicle is via collateral vessels from the reticular arteriolar plexus to the dermal papilla and from ascending branches to networks around the bulb and the inferior segment of the follicle. These latter vessels travel with the sensory nerve endings within the outer dermal sheath.

Embryologically, the hair follicle is composed of epidermal and dermal tissue. The latter, namely the dermal papilla and dermal sheath, are derived from mesenchymal tissue. This is situated just below the epidermis and instructs the epidermis to form a downward projection which progresses and envelopes the mesenchymal grouping so becoming the dermal papilla and sheath. This is accomplished by a series of messages sent between the two embryological cell lines during the 2nd and 5th month of fetal life. Approximately equal numbers of such groupings occur in all regions of the body initially taking the form of focal crowding of basal cell nuclei in the epidermis of the eyebrow, upper-lip and chin (Pinkus, 1958). These are the primary germs and subsequently more primary, and then secondary germs form between existing follicles so forming groups of three. Production of hair follicles is complete by 6 months gestation and is equal in amount in both males and females (Szabo, 1958). The total number has been estimated at 5 million. After birth, new follicles are not thought to appear (Billingham, 1958) except in certain tumours, namely trichofolliculomas, but

uneven regional growth of the skin causes the differing densities noted over the body. After its development, a certain follicle may produce several different types of hair.

Three types of hair are recognised on the human; lanugo (lana = wool), vellus (Fleece) and terminal (Rook, 1965). Lanugo covers the fetus by the fifth or sixth month in-utero and is shed before birth except in the region of the eyelids, eyebrows and scalp where it becomes initially stronger but then replaced several months post-partum. New hair growth then occurs over the body giving a downy appearance. These are the vellus hairs which persist until puberty. They are soft, rarely exceed a length of 2cm, are occasionally pigmented and do not have a medulla. At puberty, in certain regions of the body and under hormonal control, coarse hairs develop. This occurs most notably in the axilla and groin in both sexes and the back and chest to a greater or lesser extent in the male. They are termed, along with the hairs of the scalp and eyebrows, the terminal hairs. These hairs are longer and coarser than vellus hairs and are often medullated and pigmented, although there are gradations between the two. The process from vellus to terminal may reverse with ageing.

Of the estimated 5 million hair follicles on the body, approximately 1 million are present on the scalp. 100 000 of these have been stated to be terminal but this number appears to vary according to the hairs pigmentation; light hairs 140 000, dark 102 000 and red 88 000 (Friedenthal, 1908). Ageing seems to produce a reduction in follicular count on the scalp from 615 per cm^2 between 20 and 30 years to 435 per cm^2 between 80-90 years and baldness reduces this figure still further (305 per cm^2 on average between ages 45 and 85) (Giacommetti, 1965). Distribution of hair follicles in other bodily regions has been classified by Szabo and tabulated below.

Area	Number of Specimens Investigated	Number of Hair Follicles +/- s.e. (mean per cm^2)
Cheek	11	880 +/- 60
Forehead	4	770 +/- 60
Forearm	5	100 +/- 50
Thigh	21	55 +/- 5
Leg	5	50 +/- 20
Upper Arm	10	40 +/- 10
Abdomen	3	40 +/- 30

In men, 90% of the hairs on the chest, trunk, shoulders, arms and legs are stated to be terminal. In women, this figure has been estimated to be approximately 35% (Danforth, 1925).

1.3 PHYSIOLOGY OF HAIR

Follicular growth in the human is cyclical in nature with periods of active growth, regression and rest (see Figure 1.3). In addition it is dysynchronous with neighbouring follicles in different phases of the cycle, unlike most wild mammals. This mosaic pattern is shared only by the Guinea-pig. The three stages of the hair cycle are known as anagen, catagen and telogen although it is in fact a continuum (Dry, 1926), (Chase, 1954). The hair follicle grows in length during anagen until, during the late phase, mitotic activity of the stem cells in the hair bulb ceases along with melanin production from the melanocytes, and the hair root becomes keratinised and amelanotic forming a club. This is the catagen phase and the bulb then continues to keratinise. In addition, the club hair starts to ascend releasing the dermal papilla from its epidermal investment. During telogen, the column continues to rise with the dermal papilla following until it reaches the level of the insertion of the arrector pili muscle adjacent to the bulge region. Follicular reactivation occurs from the base of the resting structure. These germ cells grow deeper surrounding the dermal papilla cells. Adjacent hair matrix cells then divide producing the hair and inner root sheath which

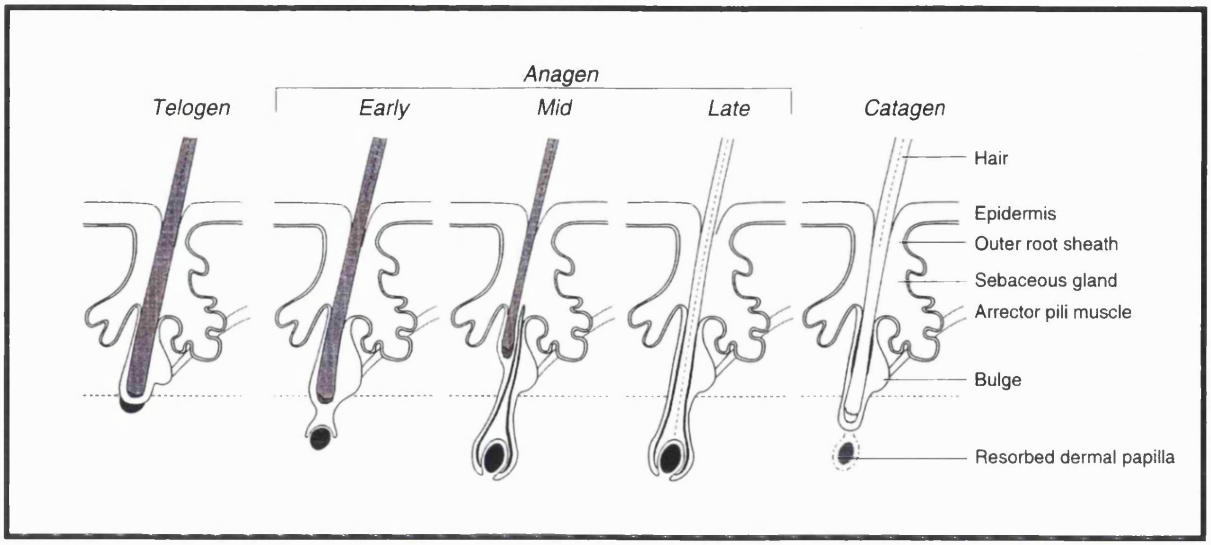

Figure 1.3: The three stages of the hair cycle. Note that during the telogen phase the position of the resorbed dermal papilla of the old hair bulb lies adjacent to the bulge region.

grows into the old canal eventually shedding the original hair. Work by Oliver in 1966 (Oliver, 1966) showed that whisker growth occurred in the hooded rat after removal of the dermal papilla and lengths of the follicle suggesting a different source for the stem cells than the papilla itself. Cotsarelis in 1990 (Cotsarelis, et al., 1990) performed isotope labelling studies on keratinocytes in the bulge region of the outer root sheath located at and below the insertion of the arrector pili muscle. The results lent support to the earlier work by Oliver that hair stem cells could reside in this region. More recent studies have again noticed characteristics of these keratinocytes being similar to stem cells by clonal analysis (Rochat, et al., 1994). Rochat et al also stated that the so-called bulge region was at approximately two thirds the way down the hair follicle. It would thus appear that these probable stem cells migrate to surround the dermal papilla during telogen when the papilla lies adjacent to the bulge region and so initiates a new anagen phase.

The length of the hair cycle varies in humans between anatomical regions. Scalp hair has been studied the most and is known to have the longest cycle lasting from 2 to 6 years (Kligman, 1961) with catagen approximately 2 to 3 weeks and telogen several months. Of those scalp hairs, overall 85 - 95% have been stated to be in anagen, 1% catagen and 4-14% telogen at any one time (Rook, 1965). The total cycle appears to be much shorter in other terminal hair regions with an average of 2 cycles per year (Flesch, 1954); their resting periods equaling their growing periods in duration. Saitoh (Saitoh, et al., 1970) observed hair growth at the vertex, temple, finger, arm and leg of 3 Japanese men over a 2 year period. The leg had the longest cycle at an average of 37 weeks, the temple 26 weeks, arm 24 weeks, moustache 19 weeks and the finger 18 weeks.

Individual hairs grow at different rates according to site. For example, hairs at the vertex grow at 0.44 mm/day, chest 0.44 mm/day, temple 0.39 mm/day and beard 0.27 mm/day (Saitoh, et al., 1970). The daily rate of growth of leg hairs has been found to increase with increasing age whilst those of the hand, axilla and pubis, decrease (Trotter, 1924). Further effects of ageing have been characterised showing a reduction in the duration of hair growth and hair-shaft diameter and an increase in the interval

separating the loss of the hair and the appearance of a replacement as the individual ages (Courtois, et al., 1995). The daily rate of hair growth is greater in males than females and in summer rather than winter (Casey, et al., 1966). The latter statement has been supported by recent work in Sheffield on scalp hair (Randall and Ebling, 1991). The percentage of hairs in anagen was found to rise to a peak of 90% in March falling to a trough of 80% in September when an increase in shed hairs and decreased percentage anagen status was noted.

The hair type and colour of an individual shows genetically-determined variations. This occurs not only between races but within the same race aswell. Mongoloids have coarse, straight hair, which has the largest diameter and is circular on cross-section. They have in general, less pubic, axillary, beard and body hair and the colour is dark and eumelanotic. Negroes have curly hair which is oval on cross-section and the colour also mainly eumelanotic. They are three times less likely to have hair on their feet and more likely to have hair on their thighs than caucasians (Setty, 1966), (Setty, 1968). Caucasians have hair which is the most varied, displaying a range of textures and curls and being moderately eliptical on cross-section. The hair colouration varies between phaeomelanin and eumelanin with frequently a combination of the two being present. Such expression can manifest itself within the shaft of the same follicle and also in different follicles, with adjacent shafts on the same individual displaying different hair colours.

Factors affecting hair growth include the individuals age and sex plus genetic predisposition, hormonal levels and the season. The influences of all but hormonal levels have been discussed previously. Hormones and their effects can be subdivided into local and systemic factors. Local factors were first shown to exist by experiments performed on rats. Hair-bearing skin flaps were raised and reversed through 180 degrees. Subsequent moulting was seen to occur in the same original direction and this continued for a prolonged period (Durward and Randall, 1949). What the local factors are, though, have not been elucidated. Systemic control occurs particularly under the influence of the anterior pituitary, which includes mainly the sex hormones (the important group) plus thyroid, adrenal cortex and growth hormones with

parathyroid hormone also having an effect. Hormonal secretions from the pineal gland (Ebling, et al., 1991), which is light sensitive, is believed to cause the seasonal growing and shedding effect previously mentioned.

Androgens stimulate facial and general body hair formation by changing vellus follicles to terminal. They alter the size of the hair follicle and the diameter of the hair fibre produced and thus are believed to act via the dermal papilla which causes these effects (Choudry, et al., 1992), (Randall, et al., 1992). However, in susceptible men they also cause baldness, usually after the first 30 years. The thick terminal hairs are then converted to small vellus hairs causing hair-line recession. It seems likely, discovered through experimentation, that the uptake and metabolism of testosterone is increased in the scalp hair follicles of such men (Price, 1975) and even moreso in those hair follicles in balding regions than non-balding regions of the same man. Oestrogens appear to maintain vellus hair formation and consequently their decrease post-menopause leads to increased terminal hair formation. An increase in the proportion of follicles in anagen occurs during pregnancy (Lynfield, 1960). This is believed to be related to the increase in oestrogen (Ebling and Johnson, 1964) which slows both the passage of follicles into catagen and the release of club hairs from the piliary canal. A noticeable shedding of hair occurs post-partum when the oestrogen levels return to normal.

Thyroid hormones profoundly affect the hair. Diffuse alopecia is a feature common to thyroid deficiency along with a reduction in hair diameter and an increase in the number of follicles in telogen. This effect can be reversed by replacement using the hormone thyroxine. Cortisol retards hair growth in experimental animals (Ferguson, et al., 1965) whilst parathyroid hormone makes the body hair coarse, dry and sparse.

1.4 PATHOLOGY OF HAIR

1.4.1 Excess Hair

"Hair growth occurring at any site and being coarser, longer or at a greater quantity than normal for the age, sex and race of the individual is viewed as excessive" (Dawber, et al., 1992). Two terms are applied to this occurrence, hirsutism and hypertrichosis. Hirsutism is defined as an excess of terminal body hair in the male distribution affecting women. It is restricted to androgen-dependent mechanisms. Hypertrichosis is the term given to an excess of vellus hair growth either at a particular site or generally over the body, affecting both sexes and being non-androgen dependent.

The prevalence of hirsutism is difficult to establish as it is a subjective notion. Not only that but there are differences in hair distribution between races anyway. Work in the 1960's, however, attempted to establish the prevalence of hirsutism within the female "European" population. 400 female students at the University of Wales were examined and their hair distribution compared with 239 adult, white males. "Non-Europeans" were excluded. 9% of females were described as "particularly hairy" with male pattern hair growth. It was felt that if women had terminal hair on the breast, lumbo-sacral region and shoulders they were more likely to complain and to have an endocrine imbalance as the cause of their problem. In this study 0.005% (2 patients of the 400) were found to have adrenal virilism (McKnight, 1964). A scoring mechanism devised by Ferriman and Galway (Ferriman and Galway, 1961), also in the 1960's, stated that 5% of American women were hirsute. Both these studies were subjective, attempting to define a "norm" on the part of the examiner and the individual concerned. Both would probably be influenced by current vogues and society which define normality, usually via the media and tend to select non-hairy individuals as being beautiful. More modern techniques for detecting hyperandrogenaemia could now raise the original percentage recorded. Several studies have attempted to discover the possible psychological effects of hirsutism with one showing increased anxiety

levels in women deemed as hirsute when compared to an equivalent non-hirsute cohort (Rabinowitz and Cohen, 1983).

Hypertrichosis is rare in comparison to hirsutism and as such has been studied little. Its prevalence within the population is consequently unknown. The causes of excessive hair growth have been tabulated below.

Hypertrichosis	Hirsutism
Congenital Hypertrichosis lanuginosa	**Polycystic Ovary Syndrome**
Acquired Hypertrichosis lanuginosa	**Ovarian Tumours**
Universal Hypertrichosis	**Adrenal**
Naevoid Hypertrichosis	Congenital Adrenal Hyperplasia
Symptomatic Hypertrichosis	Cushing's Disease
Hereditary	**Prolactinoma**
Porphyria	**Gonadal Dysgenesis**
Epidermolysis bullosa	**Androgen Therapy**
Hurler's Syndrome	**Idiopathic Hirsuties**
Congenital Macrogingivae	**? Stress**
Cornelia de Lange Syndrome	**Acquired Hirsuties**
Winchester Syndrome	
Trisomy 18	
Endocrine Disturbances	
Hypothyroidism	
Hyperthyroidism	
Berardinelli's Syndrome	
Teratogenic Syndromes	
Fetal Alcohol Syndrome	
Other Conditions	
Malnutrition	
Anorexia nervosa	
Acrodynia	
Dermatomyositis	
Iatrogenic Hypertrichosis	
Acquired Circumscribed Hypertrichosis	

Hypertrichosis

Congenital hypertrichosis lanuginosae occurs when the fetal pellage is not replaced by vellus or terminal hairs. In the acquired form it is associated usually with malignant disease later in life. The Universal form describes a condition where the hair pattern is normal but the hairs are longer and coarser. Naevoid hypertrichosis occurs either from birth or develops at puberty resulting in coarse hair associated with a melanocytic naevus.

Symptomatic hypertrichosis develops as a manifestation of an underlying pathology. This may be endocrine in origin or related to a connective tissue phenomenon. However, the majority are unknown in both cause and effect. The group can be sub-divided into separate headings as shown in the table. Under hereditary disorders, porphyria commonly results in hair growth on exposed skin, usually the face. Gross hypertrichosis of the face occurs in Epidermolysis bullosa whilst in Hurler's syndrome, this feature extends to the trunk and limbs, though not to as great an extent. A similar pattern is seen with Congenital macrogingivae. Cornelia de Lange syndrome associates mentally retarded, microcephalic children with a low hairline and eyebrow overgrowth. In both Winchester syndrome and Trisomy 18, general hypertrichosis occurs.

Endocrine disturbances have been mentioned in the physiology section as a cause of excess hair growth. Hypothyroidsm can produce hair growth on the back in some children whilst hyperthyroidism can result in coarse hair over the tibia. Berardinelli's syndrome has accelerated growth, lipodystrophy and muscular hypertrophy as its features. The skin is usually coarse with hypertrichosis. Mothers who are chronic alcoholics may have children who are both mentally and physically retarded. The so called fetal alcohol syndrome can result in cutaneous abnormalities with hypertrichosis. Other conditions include malnutrition which can result in profuse, generalised hypertrichosis in children. Anorexia nervosa has been shown to increase the growth of fine hair on the face, trunk and arms in 20% of sufferers. Acrodynia is also associated with general hair growth, particularly on the limbs, as is

dermatomyositis. Iatrogenic hypertrichosis occurs as a complication of drug therapy. Uniform fine hair growth over the trunk, hands and face is noted not at androgen-dependent sites. How the drugs cause this form of excess hair growth is not known but certain drug types such as cortisone and penicillamine work probably via the connective tissue which is their primary mode of action. The effect of sunlight appears to be enhanced by psoralens inducing hypertrichosis in predisposed individuals. Medications known to produce this phenomenon are listed below.

Diphenylhydantoin	Diazoxide
Minoxidil	Cyclosporin
Benoxaprofen	Streptomycin
Cortisone	Penicillamine
Psoralens	Phenytoin

Acquired circumscribed hypertrichosis is the term given to an area of increased hair growth resulting from repeated or longterm inflammatory changes involving the dermis. An example is hypertrichosis occurring at a site following prolonged use of a Plaster of Paris.

Hirsutism

Hirsutism describes excess terminal hair growth in the female as a result of an increase in circulating androgen levels and/or an increase in the sensitivity of the pilosebaceous unit to normal androgen levels. The latter is termed idiopathic hirsutism as normal androgen levels are discovered on testing and would suggest that a family history of excessive terminal hair growth, particularly in the non-sexual areas (legs and arms), is an important factor relating to increased sensitivity of the follicle. However, androgen secretions may fluctuate in these individuals which could produce normal levels on testing. Hyperandrogenaemia accounts for 85% of the causes in patients with moderately severe hirsutism and 50% in patients with mild hirsutism

(Ahmed and Jaspan, 1994) and with modern testing techniques improving, this figure is rising.

Testosterone (mainly) and its derivatives are the cause of androgen-related hirsutism. Virilising hormones are produced by the adrenal glands and the ovaries in the female. Testosterone is the most active hormone and these glands produce half of the total amount present in the body whilst the remainder is produced from peripheral conversion by adipose tissue. The causes of hirsutism are listed above with the commonest being polycystic ovary syndrome (80% plus) which has an unknown, possibly genetic aetiology. It is associated with anovulation, infertility, obesity and acne. Ovarian tumours may be virilising in nature and are believed to account for 1% of the causes of excess hair growth. Congenital adrenal hyperplasia results from an enzyme deficiency producing an "overflow" of androgen steroid production and consequently hirsutism in the afflicted individual. Acquired adrenocortical disease resulting in virilisation can occur with both adenomas and carcinomas of the adrenal gland (Cushing's syndrome). A prolactinoma results in hirsutism in 22-60% of individuals and is thought to be a direct effect of the hormone on the adrenal gland (Dawber, et al., 1992). Gonadal dysgenesis has been described in 6 individuals with 46 XY genome resulting in female genitalia and male skeletal characteristics (Moltz, et al., 1981). Androgen therapy from use (abuse) of testosterone or Danazol (which is used in the management of menorrhagia) can produce hirsutism. Iatrogenic acquired hirsutism can also occur from a surgical procedure where hair bearing skin is transplanted to a non-hair bearing site for reconstructive purposes. For example, ear reconstruction following partial or complete loss can be corrected by transplantation of a flap of hair bearing skin from the scalp to form a new helical rim. The texture, strength and contour is perfect but ultimately hair grows at the new site.

1.4.2 Treatment of Excess Hair

The primary treatment of excessive hair growth will depend upon whether a cause can be diagnosed. Endocrine imbalance can be corrected by either medical or surgical intervention. However, where an actual cause is not found, or the corrective procedure

is not successful enough, then other methods of hair eradication less systemically disturbing may be required. Current treatments available for hirsutism are listed below.

Chemical	Physical
Hormonal suppression	Shaving
Dexamethasone	Topical creams
Oral Contraceptive	Bleaching
Gonadotropin releasing hormone agonist	Plucking and waxing
Antiandrogens	Electrolysis
Spironolactone	Laser
Cyproterone acetate	
Flutamide	
Miscellaneous	
Ketoconazole	

Individuals usually request treatment for excess terminal hair growth as they generally feel that they do not conform to the values placed on them by society as a whole. As mentioned earlier, between 5 and 10% of the female caucasian population have been described as hirsute and treating only a fraction of this number would place quite a sizeable demand upon health care resources. Consequently the management of the majority of hirsute individuals is presently being performed mainly within the private sector. In addition, the lack of an effective method of producing permanent depilation has resulted in a multimillion pound business for the cosmetic industry which constantly advertises the benefits of having smooth, hairless skin.

Although depilation could be seen as being a purely cosmetic practice, the continuing evolution of reconstructive surgery has realised a potential for finding a safe, simple and effective method for removing unwanted hair from skin. The ability to transplant a flap of hair bearing skin to a non-hair bearing site and then to rid that flap of hair

would produce a much more agreeable result for the patient concerned and vastly increase the quantity of available skin for reconstructive purposes. In addition, the use of skin to replace a damaged or diseased tubular structure within the body, such as oesophagus (Kuriloff, et al., 1988) or urethra (Finkelstein and Blatstein, 1991), has been performed in the past but generally resulted in a poor outcome. In part this is due to the obstruction to flow within the tube produced by the presence and growth of hairs. This has been seen to occur particularly in the urethra where calculi have formed on the hairs ultimately preventing the flow of urine. Therefore, the development of a successful permanent depilator with the requisite abilities could have far reaching effects within medical practice as a whole.

Currently, the methods used for the treatment of excess hair can be categorised into either physical or chemical (see previous page). Chemical methods employed for the treatment of hirsutism include drugs which suppress the body's usual hormone production. Such examples would include the oral contraceptive pill, which attempts to regulate sex hormone production by placing an external, constant control on the hormone cycle so suppressing the bodies natural production. A more direct approach and one that can result in greater side effects includes the use of antiandrogens [Barth, 1991 #339] (such as flutamide and cyproterone acetate) which directly inhibit either the production or action of androgenic hormones. Other anti-androgenic drugs include spironolactone, but the side effects induced by this medication can be much greater ranging from headaches to blood pressure fluctuations. Therefore its use is only recommended under extreme circumstances.

Physical methods used for the reduction in unwanted hair growth vary in technique and success with both electrolysis and now laser being the only two stated to have a permanent effect. Shaving and bleaching per se do not reduce hair growth but merely make it less conspicuous. Shaving has been shown not to produce thicker hairs or ones that grow more rapidly (Natow, 1986). Topical creams act by dissolving the hair shaft at the disulphide bonds and is a temporary method. Side effects can include contact dermatitis, which may be aggressive on sensitive skin types. Plucking is also a temporary depilatory method and is best used in areas where the hair density is low.

The procedure can be painful and the follicle may become infected upon regrowth. Waxing requires the hairs to be of a certain length so that they can be "gripped" by the wax as it is removed. The technique is again temporary but relatively cheap and patients may not require further treatment for upto 6 weeks afterwards.

Electrolysis is a depilatory technique described as permanent removing the hair using an electrode inserted into the ostium or canal of the follicle. True electrolysis, first used over 100 years ago, involves the production of sodium hydroxide from sodium chloride and water which are present within the follicle. This occurs when an electric current is passed through the electrode. The sodium hydroxide then destroys the viable follicular tissues and hopefully prevents the hair regrowing. Thermolysis is the method most often used today and involves heat production to destroy the hair cell components via radiowaves (cf. surgical diathermy equipment). A third technique also exists which incorporates both of the previous two methods and is termed The Blend. This has been stated to be the most effective format for permanent depilation although a specific comparison of the results has not been performed (Richards and Meharg, 1995). Overall the hair regrowth rates vary between 15 and 50% and complications can include infection, hypo and hyperpigmentation and permanent scarring with keloid formation (Wagner, et al., 1985). Diphtherial endocarditis (Cookson and Harris, 1981) and the spreading of flat warts (Petrozzi, 1980) have also been reported. It is also a time consuming procedure because only one hair follicle can be treated at once.

From the text above, it becomes apparent that until recently no safe, simple or effective method was available to produce permanent depilation. Exactly who first described laser-assisted hair removal is not completely clear, but its discovery over 10 years ago has potentially revolutionised the treatment of unwanted hair. The types of laser used have varied, with a carbon dioxide laser stated to have achieved partial depilatory success on an oesophageal reconstruction using a delto-pectoral flap and a Wooky-type cervical skin flap (Kuriloff, et al., 1988) and an NdYAG laser achieving partial depilatory success upon urethras reconstructed using hair-bearing skin from the scrotum (Finkelstein and Blatstein, 1991). It is presently thought that the ruby laser

should be the most effective at depilating skin but to explain why, it becomes necessary to discuss how lasers actually work.

1.5 LASERS

1.5.1 Terminology

- The energy delivered by the laser is measured in Joules (J).
- The dose of energy delivered by the laser is measured in Joules per cm^2 and termed the fluence.
- The power delivered by the laser is measured in Joules per second or Watts.
- The pulse width or pulse duration is the time of laser exposure measured in microseconds (10^{-6}) or nanoseconds (10^{-9}).
- The chromophore of the laser is the substance within the irradiated field able to interact with the photon energy produced from the laser converting it to another more usable energy format (for example, heat).

Lasers were first theorised by Albert Einstein in 1916 but the first practical demonstration of its use did not occur until 1954. Laser is the acronym for Light Amplification by Stimulated Emission of Radiation. The laser beam is formed of packets of energy called photons. These photons are produced by a "lasing medium", which could be either a ruby crystal, CO_2, Argon or Krypton gas to name but a few, with each medium giving the various lasers their name (see Figure 1.4). An energising pump raises the atoms of the lasing medium which are contained in a chamber, or resonator, to an excited state and upon their return each emits a photon in the same phase and in the same direction as the energising photon (stimulated emission of radiation). If enough energy is given by the pump, then a population inversion can occur where the majority of the medium's atoms are in the excited state. 80% of the stimulated radiation emitted is lost as heat. The remainder is amplified by reflection between two mirrors. One is a partial reflector and allows escape of the beam from the resonator when the laser is fired. The laser beam is emitted in a collimated (in

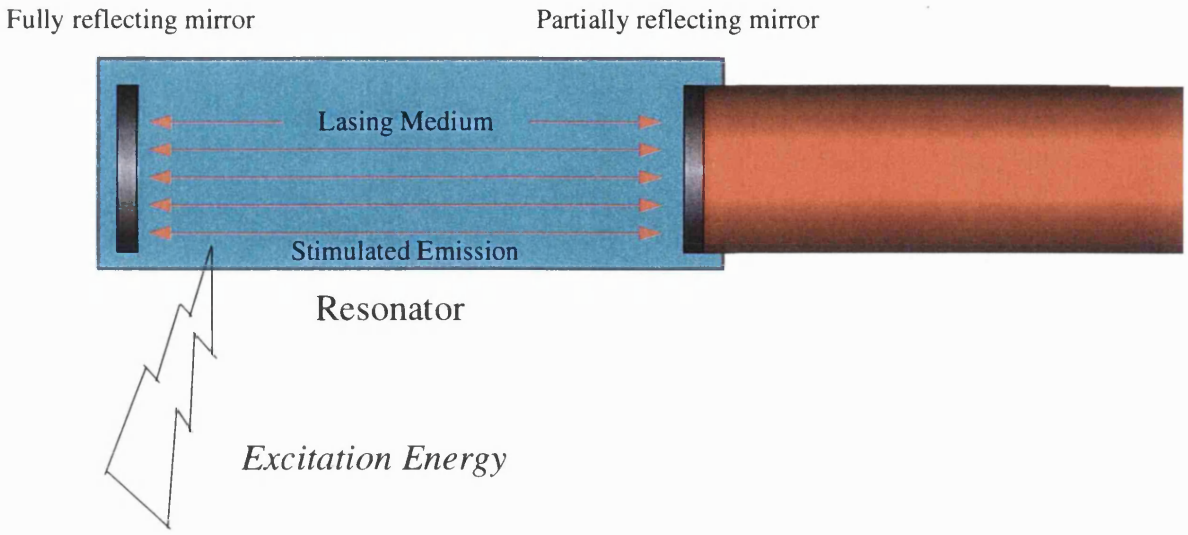

Figure 1.4: How a laser beam is produced.

parallel) and coherent (all waves are in the same phase) format. Most present day lasers are also monochromatic meaning they emit a beam of a single wavelength too. The ruby laser is at a wavelength of 694 nm which is in the visible red region of the electromagnetic spectrum (see Figure 1.5). It was the first laser to be developed and used a Xenon flash lamp to excite a ruby crystal (Maimon, 1960).

1.5.2 The Ruby Laser

The ruby laser produces a collimated, monochromatic and coherent beam of light of wavelength 694 nm by Xenon flashlamp excitation of a ruby crystal. Two different formats are currently available. These are the normal mode and the Q-switched version. Q (standing for Quality) switching is where the beam of light undergoes amplification before emission. The photon energy output, or fluence, is equivalent to a normal mode laser but delivered over nanoseconds rather than microseconds. The power is therefore a thousand times greater and this function has defined the present role of the Q-switched ruby laser as will be explained later. The beam of the normal mode ruby laser undergoes no adjustments prior to its emission.

1.5.3 Present Knowledge Regarding Laser/Skin Interaction

Being the first laser to be developed, most early experiments in the 1960's were performed using the ruby laser. The Grothus-Draper law states that for an action to occur, absorption of light must occur and it soon became apparent that the chromophore (refer to terminology above) for the ruby laser was pigmentation within the skin, be it natural such as melanin or synthetic such as carbon particles from tattooing (Goldman, et al., 1965), (Goldman, et al., 1967), (Goldman, 1983). The development of other lasers has shown that the chromophore is a function of the wavelength emitted. For example, the chromophore for the argon laser at 514 nm is haemoglobin whilst for the carbon dioxide laser at 10, 600 nm it is water. Interaction of the photon energy from any laser with its chromophore results in the conversion of that photon energy into one of three different energy formats; heat, chemical energy (free radicals particularly) and mechanical energy. It is probable that a combination of

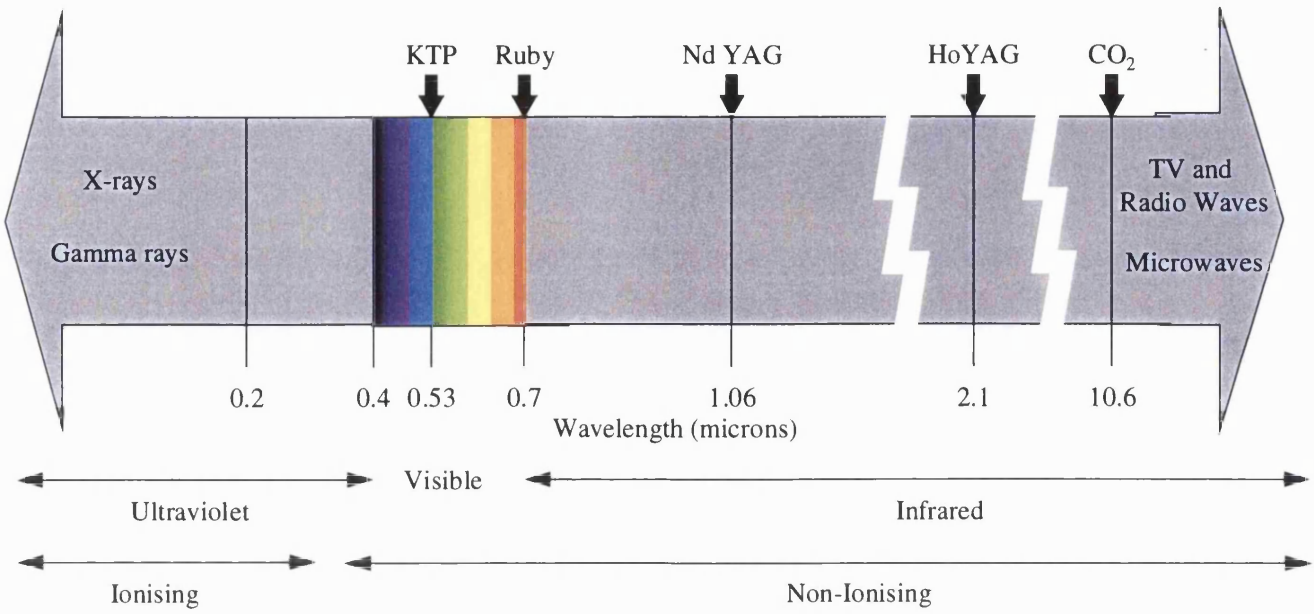

Figure 1.5: A diagrammatic representation of the electromagnetic spectrum illustrating the wavelengths at which various lasers emit light.

all three formats is produced upon laser exposure but the main expression of energy is dependent on the pulse duration of the laser. It would appear that the shorter the time of delivery of the laser beam, such as with Q-switching, then a mechanical acoustic wave, akin to an explosion, is established within the chromophore so ablating the chromophore. If the photon energy were donated over a longer time duration, as occurs with the normal mode ruby laser, then it was most likely heat that would be produced at the chromophore which could be less specific in its destruction of the chromophore alone due to local dissipation. The work by Goldman also showed that reducing the pulse duration of the laser caused considerably less damage to skin and the threshold for damage was independent of skin colour. This appeared to suggest that altering the pulse duration could selectively damage the chromophore for the ruby laser alone. Polla et al in 1987 (Polla, et al., 1987) exposed the skin of white, brown and black Guinea-pigs to a range of fluences from a Q-switched ruby laser and then examined the sites histologically. At low energy levels, damage was noted to be confined to the melanosomes within the cells of the skin alone. The greater the skin pigmentation, though, the greater the amount of damage seen within the skin, which was thought most likely to be related to the increased number of melanosomes in the target beam exerting a cumulative effect.

Work by Rox Anderson and Parrish in 1983 (Anderson and Parrish, 1983) incorporated the work of Goldman and developed it to propose the mechanism of selective photothermolysis. This stated that the photon energy from a laser required to damage or destroy its chromophore alone should be given over a time less than the time it takes for thermal diffusion to occur from that chromophore. This would effectively mean that the energy produced from photon energy conversion would be more-or-less confined to the chromophore so minimising surrounding tissue damage. In theory, for this to occur, two facts are required. First the fluence for disruption of the chromophore has to be known. This, for convenience, is taken as the heat of vapourisation of water, which is 2500 J/cm^3. Second, the "thermal relaxation time" (TRT) of the particular chromophore as mentioned above. Theoretical work by van Gemert (Gemert and Welch, 1989) has produced a formula for calculating the TRT of a chromophore, which relates it approximately, in seconds, to the square of the target

diameter measured in millimetres. Solving for this, the exposure time of an average-sized melanosome measuring 0.5 μm, to undergo selective photothermolysis is approximately 0.25 μsec. A larger target would require a longer pulse duration and a smaller target a shorter duration. Therefore the relationship can be seen to be a function of surface area to volume ratio. A smaller chromophore would release heat more rapidly therefore requiring the pulse duration to be much shorter than a larger-sized chromophore. This principle is presently used in clinical practice whereby a Q-switched ruby laser is employed for destruction of carbon particles in a tattoo and a normal mode ruby laser is used upon the larger melanosomes contained, for example, within a naevus. Although the theory is sensible, whether it can be related to heterogeneous tissue such as skin cannot be confirmed. Many melanosomes of differing sizes exist within the treatment field and each would absorb a quantity of photon energy producing, with the normal mode ruby laser, heat. It is probable that a cumulative effect would therefore occur raising the heat levels above the threshold required for tissue damage. Hence to get the desired effect may result in side effects being produced and so the relevance of the mathematical model regarding TRT in practice still remains uncertain.

Having defined, in theory, the interaction of a laser with its chromophore, the next requirement is to know how well the laser penetrates the skin to reach its chromophore. In an attempt to discern the laser pathway through the skin, skin optics were developed, which are defined as the optical properties produced by each skin layer upon exposure to a wavelength of light (Gemert, et al., 1989). Complicated mathematical models have been produced analysing the interaction of photon particles with skin in an attempt to produce a mathematical model most representative of light interaction with skin. All involve a relationship between absorption and scattering plus, in some theories such as the Diffusion theory, the mean cosine angle of scatter within the medium also being incorporated as a variable. Two such theories of radiative transfer that have been applied to wavelengths of light in the range of the ruby laser are the Kubelka-Munk theory and the Diffusion theory.

The Kubelka-Munk theory can be applied to any tissue type and wavelength of light and is relatively simple in its construction (Anderson and Parrish, 1981). The Diffusion equation, which calculates the total amount of diffuse light power that passes through a small sphere at a certain site, has been applied to occurrences resulting in strong scattering (Gemert, et al., 1989). This is usually when non-pigmented tissue is irradiated with light of wavelengths between 300 and 1000 nm. Both theories have been used upon tissues to test the models and both rely upon assumptions regarding the properties of skin. The Kubelka-Munk theory assumes homogeneity within the skin, that the incident radiation is diffuse and regular reflection occurring at the sample boundary can be disregarded. Diffusion theory assumes the same homogeneity of skin but also assumes that the influence of blood flow is negligible. Diffusion theory results overall in a rather complicated mathematical statement. Nevertheless, from these models it has been stated that the depth of laser penetration in skin depends on the wavelength-dependent optical density of the irradiated tissue with the latter term being a function of transmitted light power to incident light power (Welch, 1984). Penetration of the skin depends upon photon energy loss from the original beam pathway. This can occur firstly by reflection (remittance) at the surface (stated to be between 4 and 8% of the incident energy) and at the interface of each subsequent layer within the skin, secondly by scattering from contact with "solid objects" within the skin and finally by absorption by the chromophores. Remittance has been stated to be three times greater in caucasian than negroid skin at 694 nm (Shea and Parrish, 1991). Absorption removes the photon energy from the beam altogether, so wavelengths that produce greater scattering than absorption have an increased depth of penetration. The dermal layer is believed to have the greatest overall effect on light transmittance due to the density of the collagen fibres which markedly increase the scattering (Anderson, et al., 1979). With light of 550 nm wavelength, it has been stated that the Stratum corneum alters the beam pathway little (75% of transmitted radiation within 7.5 degrees of the normal after passing through), but that the Malpighian layer or Stratum spinosum has a much greater effect (15% of transmitted radiation recorded within 7.5 degrees of the normal after the light had traversed this layer) (Bruls and Leun, 1984). Using specimens of *ex vivo* skin also showed that the hydration of the skin affected the

pathway of 550 nm light with drier samples producing less scattering (Bruls and Leun, 1984).

The greatest penetration of skin by light has been stated to occur from approximately 600 to 1200 nm wavelength (Anderson, 1984). At these wavelengths most radiation is forward scattered to a greater extent than it is absorbed and has been stated to result in the beam penetrating distances up to several millimetres deep. A beam of light from an NdYAG laser incident upon a 2 mm thick specimen of stomach was found to have 30 to 40% of its light scattered at the surface whilst 25 to 30% was transmitted through (Halldorsson, et al., 1981). Light of 700 nm wavelength has been stated as having 37% of its incident energy at 0.75 mm depth in skin (Anderson, 1984) and a total depth of penetration between 2 and 3 mm (Rosenberg and Gregory, 1996).

The appropriateness of the Kubelka-Munk theory to be used to produce fluence-depth profiles in skin and the difficult application of the Diffusion theory has led to the use of Monte Carlo modelling (Carter and Cashwell, 1975) to attempt to produce a mathematical model adequately representing laser-skin interaction. Monte Carlo modelling can take into account the variety of physical quantities present in skin, though probably still not to an appropriate extent. However, it analyses individual photon histories and so requires many such histories to be applied before a degree of accuracy can be assured. Monte Carlo modelling has been reported by Flock et al (Flock, et al., 1989), (Flock, et al., 1989) and been compared to results obtained from a tissue phantom consisting of a phospholipid emulsion containing India ink and using light of 633 nm wavelength. The albedo, which is the ratio of the intensity of light reflected from an object compared to that it receives, could be adjusted by varying the concentrations of the constituents of the tissue phantom. Experimental data generated from this synthetic model was compared to computed data using the Monte Carlo model at varying depths. The results were reported as showing good agreement but required that the experimental data be multiplied by a constant factor, which was albedo-dependent, to match the computed data. Nevertheless, the experimental data at first stated that depth of penetration of light at 633 nm was spot size-dependent. At an albedo of 0.99099 and radius of spot 3 mm the maximum depth of penetration was

approximately 14 mm whilst at a spot size of 37 mm, depth of penetration was recorded as 20 mm. With an albedo of 0.98671 and using the same spot sizes, the depths were 11 and 15 mm respectively.

Great variance exists between the answers produced by all the mathematical models plus the synthetic experimental model described above regarding laser/skin interaction and the relevance of any or all of the studies has not been proven. Skin is such a heterogeneous tissue that it would seem only a practical demonstration of laser/skin interaction could attempt to prove the theorists correct or not.

1.5.4 Which Laser is Best Suited for Depilation?

The ruby laser has become the main depilatory laser for several reasons. First it would appear that it was the laser originally found to induce depilation when skin was exposed to its beam. The other reasons, however, depend more upon its physical properties as defined in the section above. The chromophore for the ruby laser is pigmentation, which in non-tattooed skin would mean the melanin. Work performed recently by Liew et al (Liew, et al., In press) has shown that it is the darker eumelanin that is associated with a greater depilatory success rate and that an increased quantity present increases the depilatory efficacy. Melanin, particularly in patients with dark hair colour but light skin such as a Fitzpatrick skin type 2 or 3 (Fitzpatrick, 1988) see Table 1.1 would have the melanin concentrated in and around the hair follicle. This makes the chromophore ideally placed to interact with the ruby laser. However, for permanent depilation to occur would require the heat to dissipate from the chromophore to damage and destroy the viable follicular cells at the bulge region and the hair bulb to prevent the hair from regrowing. This is why the normal mode ruby laser is believed to be the best format so the heat produced at the chromophore can diffuse away at levels great enough to cause the required damage.

The ruby wavelength of 694 nm has been stated to exist at an "optical window" (see Figure 1.6). Throughout the electromagnetic spectrum, one of the other naturally occurring pigments in skin, oxyhaemoglobin, closely mimics melanin in its absorption

of light energy. At 694 nm, however, there occurs a sudden tenfold dip in the absorption coefficient of oxyhaemoglobin compared to melanin. This "optical window" would theoretically make the ruby laser more specific by preferentially targeting melanin-containing structures and therefore producing fewer side effects.

The last reason for the use of the ruby laser for depilatory purposes relates to its penetrative qualities within skin. As mentioned in the section above, light in the wavelength range of 600 to 1200 nm has been stated as reaching the greater depths. However, whether this is still deep enough to reach the bulge region and the hair bulb cannot be assessed at present. The bulge region resides in the lower aspects of the dermis at a depth of between 1 to 2.5 mm from the skin surface (Rochat, et al., 1994). The position of the hair bulb varies with the hair cycle from being within the subcutaneous fat during anagen phase to lying adjacent to the bulge within the dermis during telogen phase. Histological assessment of damage occurring in skin specimens after ruby laser irradiation described previously would tend to infer that beam penetration was not deep enough. However, the study did not mention whether melanin pigment was noted deeper than the level at which maximal damage was seen. If this had not been the case then it could be that sufficient photon energy was actually reaching greater depths but not manifesting itself.

More recently other lasers within the wavelength range of 600 to 1200 nm have been employed to assess their depilatory capabilities. These include the Alexandrite at 755 nm and the NdYAG at 1064 nm. Both have been stated to be able to penetrate to a depth equivalent, or greater in the case of the NdYAG, to the ruby laser (Rosenberg and Gregory, 1996). The relative absorption by melanin, however, is less than the ruby laser with both laser types and this could therefore affect their efficacy requiring the addition of a chromophore to the skin in the case of the latter (Nanni and Alster, 1997). The results are compared below.

Skin colour (Unexposed skin)	Fitzpatrick skin type	Sunburn	Tan
White	1	Yes	No
	2	Yes	Minimal
	3	Yes	Yes
	4	No	Yes
Brown	5	No	Yes
Black	6	No	Yes

Table 1.1: Fitzpatrick sun-reactive skin typing. The categorising of individuals is based upon verbal response regarding first, moderate (three minimal erythema doses-MED) unprotected sun exposure for a period of 45 to 60 minutes. 1 MED is equivalent to 15 to 30 minutes of noon exposure in northern (20° to 45°) latitudes or 30 mJ/cm^2.

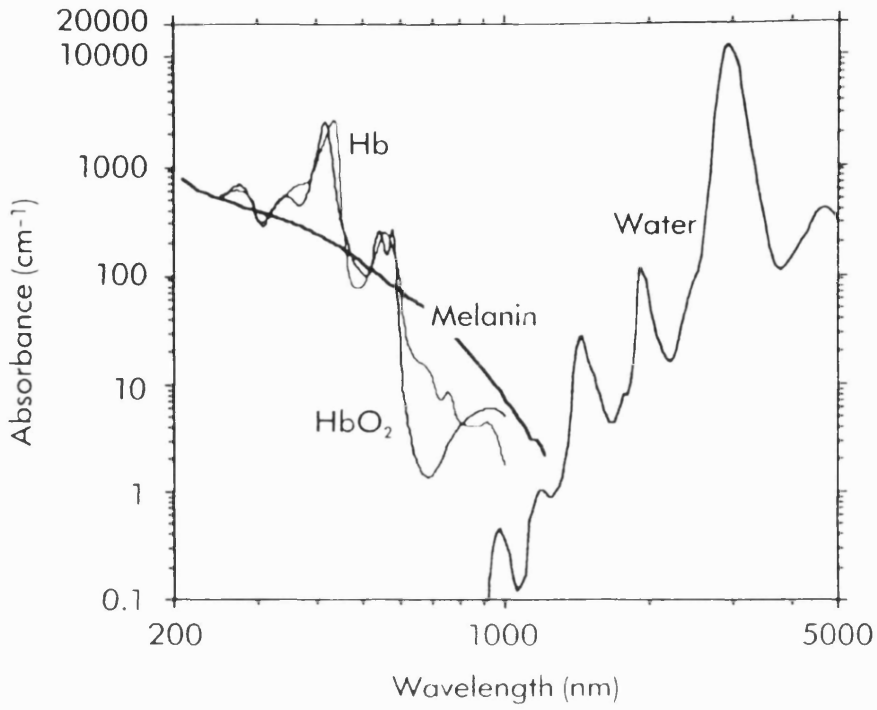

Figure 1.6: Absorption spectra of the major skin pigments according to wavelength at the concentrations they usually occur in-vivo. Note the relative difference in absorbance of melanin compared with oxyhaemoglobin at around 700 nm.

1.5.5 Present Depilatory Results

Table 1.2 summarises recent ruby laser depilatory clinical studies whilst Table 1.3 shows two studies using non-ruby lasers for comparison. The lasers used vary in type and parameter such as fluence, pulse duration and spot size. The protocols used by the authors differ and although most claim high success rates upto 12 weeks, few have published long-term results. A study by Liew et al (Liew, 1999) reporting a final follow-up of one year states that although the success of treatment is high for a small proportion of patients (9.1%), generally the success rate for permanent laser-assisted depilation is low. Further work performed by Liew et al attempted to relate anatomical variables with the extent of efficacy achieved (Liew, et al., In press). No statistically significant correlation was found with skin colour, epidermal thickness, dermal density or the length of subcutaneous hair (Liew, et al., In press). Surprisingly, total melanin content of hair revealed no statistically significant correlation either. However, the situation is complicated by the fact that melanin pigment exists in two forms, the red/yellow phaeomelanin and the brown/black eumelanin and when the relative amount of eumelanin was measured, this did positively and significantly correlate with successful hair depilation (Liew, et al., In press). In contrast, no correlation was found between permanent depilation and the growth phase of the hair, which was calculated by sampling a site adjoining the treatment area (Liew, 1999). However, recently published work performed on mice using a normal mode ruby laser with a 2 msec pulse duration showed that alopecia was induced upon hairs in the anagen (growing) phase alone (Lin, et al., 1998). These contradictory results may be explained by differences in hair-growth-phase characteristics between mice and humans. In mice, the hair follicles in telogen (resting) phase contain hair shafts, which are completely lacking in pigment throughout their subcutaneous region (Dry, 1926). In contrast, telogen hair shafts in humans remain pigmented almost to their deepest extent (brush end). Since melanin is the target chromophore, these differences may account for this apparent dichotomy. Liew et al also showed that hairs regrowing in treatment fields were significantly thinner up to 3 months after the last exposure (Liew, et al., In press), which could explain the high level of patient satisfaction reported in a number of studies. It is important to note, though, that these results were

Table 1.2: A comparison of recent depilatory studies using the ruby laser.

Author	Laser	Protocol	Patient Total	Follow-up	Results	Side-effects	Notes
Grossmann et al [Grossman, 1996 #252]	Normal mode ruby PD 0.27 msec SS 6 mm F 30-60 J/cm^2	Single exposure	13	6 months	>50 % hair reduction	Transient pigmentary changes	Cooled sapphire lens to reduce side-effects and converge the beam
Lask et al [Lask, 1997 #255]	Epitouch normal mode ruby PD 1.2 msec SS 4-5 mm F 25-40 J/cm^2	Single exposure	20	12 weeks	20 - 60 % hair reduction	Minimal temporary erythema	Prior shaving. Clear cooling gel applied at 0C prior to exposure
Gold et al [Gold, 1997 #226]	Epilight variable wavelength PD 1.5-3.5 msec SS not given F 34-55 J/cm^2	3 – 5 exposures	37	12 Weeks	60 % hair reduction	Erythema 70 % Oedema 8 % Blistering 8 % Hyperpigmentation 3 % (All temporary)	Prior shaving. Software programme varied all settings depending on patient's skin and hair type
Solomon et al [Solomon, 1998 #254]	Normal mode ruby PD 3 msec SS 7-10 mm F 5-40 J/cm^2	1 – 4 exposures	72	Average 3.5 months	Not assessed. 98.6 % patient satisfaction	Erythema Hypopigmentation 1.44 % Hyperpigmentation 2.88 % All temporary	Prior shaving. 3 weeks of pre-treatment with hydroquinone. Cooling handpiece.
Bjerring et al [Bjerring, 1998 #256]	Normal mode ruby PD 0.7-0.8 msec SS 5 mm F 10-25 J/cm^2	1 – 9 exposures (average 2.2)	133	Retrospective	Patient own evaluation. 59 % > 50 % hair reduction	Temporary hypopigmentation	Prior shaving
Dierickx et al [Dierickx, 1998 #253]	Normal mode ruby PD 0.27 msec SS 6 mm F 30-60 J/cm^2	1 exposure	13	2 years	4 (30 %) "significant " hair reduction	No scarring or permanent pigmentary changes	Cooled sapphire lens to reduce side-effects and converge the beam
Liew et al [Liew, 1999 #294]	Normal mode ruby PD 0.9 msec SS 7 mm F 8-14 J/cm^2	4 exposures at monthly intervals`	88	1 year	13.7 % hair reduction	Crusting of skin 6 % Blistering 2 % Hyperpigmentation 2 % Hypopigmentation 1 %	Prior trimming Cooling gel after treatment

Key PD - Pulse Duration, SS – Spot Size, F – Fluence

Table 1.3: A comparison of recent depilatory studies using lasers other than the ruby laser.

Author	Laser	Protocol	Patient Total	Follow -up	Results	Side-effects	Notes
Goldberg et al [Goldberg, 1997 #216]	Q-switched NdYAG (wavelength 1060 nm) PD 10 nsec SS 7 mm F 2-3 J/cm^2	Single exposure	35	12 weeks	44 – 66 % hair reduction	All had erythema Hyperpigmentation 2.8 %	Topical carbon-based solution on the skin used as a chromophore
Finkel et al [Finkel, 1997 #228]	Alexandrite (wavelength 755 nm) PD 2 msec SS 7 mm F 25-40 J/cm^2	3 – 5 exposures depending on regrowth	126	3 months	Average hair reduction 88 %	Erythema 10 % Blistering 6 % Hypopigmentation 6 % All temporary	Prior shaving. Clear gel applied at room temp. before exposure.

Key PD - Pulse Duration, SS – Spot Size, F – Fluence

all obtained with a specific type of laser and cannot be extrapolated to all laser types currently in use.

The Alexandrite laser and the NdYAG laser both appeared to achieve similar depilatory results as the ruby laser. Unfortunately, the numbers in the studies were too small and follow-up too short to produce any significant results. To improve the targeting of the NdYAG laser required the topical application of a carbon-based oil suspension to the skin so increasing the quantity of chromophore present (Nanni and Alster, 1997). How successful this was is not apparent within the paper but it is probable that the only way to improve depilatory efficacy in general would be to increase the quantity of chromophore at the target site (the hair bulge and bulb). As the presence of melanin in these areas has been described as hair cycle-dependent (Narisawa, et al., 1997) then this could account for several papers suggesting that hair cycle is associated with depilatory success. However, not only could the presence and quantity of melanin affect the efficacy but also the type as described above.

1.5.6 Present Skin Side Effects Noted

The chromophore for the ruby laser is melanin, particularly the darker eumelanin so the greater the quantity present the greater the interaction between the photon energy and the pigment. This results in more heat being produced and hence greater damage to the structures containing the pigment. Melanin and the melanocytes are concentrated at the basal layer within skin, moreso in darker-skinned individuals. Therefore, persons with a Fitzpatrick skin type (Fitzpatrick, 1988) of 3 and above are more susceptible to skin side effects which commonly take the form of superficial burning (see Figure 1.7). In addition, hypopigmentation and hyperpigmentation (see Figures 1.8a and 1.8b) can also occur after ruby laser exposure. This suggests melanin ablation with the former finding and melanocyte stimulation with the latter although the mechanisms of both are not understood.

Although laser-induced damage of skin becomes obvious over time in living organisms, the use of tissue samples required in this thesis needs a method of

Figure 1.7: Photograph showing superficial skin burning 2 days after exposure to normal mode ruby laser irradiation.

Figure 1.8a: Hypopigmentation of the skin occurring 2 weeks after exposure to normal mode ruby laser irradiation.

Figure 1.8b: Hyperpigmentation of the skin occurring 2 weeks after exposure to normal mode ruby laser irradiation.

detecting damage earlier. To this end a protein marker of cellular damage known as p53 has been used.

p53 is a protein, named for its molecular size (53 kilodaltons), which has a dual role in cellular function. It acts as a protector of the cell's genome by monitoring the integrity of the cellular DNA and accumulates upon DNA damage, switching off cell replication in the G1 phase to allow for DNA repair. If repair fails or cannot be performed then p53 can induce cellular apoptosis so preventing transmission of the faulty DNA (Lane, 1992). More than half of human cancers have been found to have either an absence of p53 protein or a mutation in the gene itself. Squamous cell carcinoma of the skin has been associated with loss of function of the p53 gene (Brash, et al., 1996). Accumulation of p53 protein within the cell has been found in transformed cells and tumours and is believed to occur because the mutant type p53 has no function resulting in the cell continuing to express it. Ultraviolet radiation (UVR) is believed to cause mutations within the p53 gene itself resulting in decreased repair elsewhere in the damaged genome, which can ultimately cause cell transformation. Thus increased expression of p53 within a cell can be associated with direct DNA damage having occurred or the cells ability to detect that it has occurred (Campbell, et al., 1993). Recent work performed on human skin exposed to Ultraviolet radiation in band A (UVA 320-400 nm), radiation in band B (UVB 280-320 nm) and radiation in band C (UVC <280 nm) showed different staining patterns for p53 throughout the epidermis. The pattern for UVB and UVC could be explained by differing penetrative abilities, so that the shorter the wavelength the less the penetration within skin. However, that for UVA, which showed basal staining predominating, could not and appeared to suggest a different mechanism of response by the basal cells to this wavelength range, though why is still a mystery (Campbell, et al., 1993).

Recent work by Nakazawa (Nakazawa, et al., 1998) using melanocytes grown either as monocells, or in co-culture with keratinocytes, has shown similarities in melanocyte responses to heat or UVB irradiation. This would appear to suggest biological similarities in melanocyte response to both these stimuli. This is supported

by the fact that heat shock proteins (mentioned below) would appear to protect cells against both high temperatures and irradiation suggesting a common pathway for cell protection (Maytin, et al., 1994). p53 protein expression was noted to be increased by multiple treatments with UVB and heat and it was thought that its expression could be taken to be a marker of general cell damage, having been induced by either of these formats (Nakazawa, et al., 1998). Therefore its expression within cells could also result from laser irradiation of exposed skin. This would therefore verify cellular damage resulting from ruby laser irradiation.

1.6 REDUCTION OF SIDE EFFECTS

Various attempts have been made to reduce the skin side effects and are included in table 1 shown above. These include the application of creams such as aloe vera before and after exposure to the beam. Cold packs have also been described after treatment but the most specific attempt to reduce side effects is from the use of a cooled converging sapphire lens. This not only cools the skin but can target the hairs individually so minimising irradiation of the surrounding skin. How well this works has not been reported and its use could be rather time-consuming as only one hair may be targeted at once. Hydroquinone application to the skin has been described, which in theory could reduce skin side effects by removing melanin from the skin altogether. Again this has not been specifically reported and it must be assumed that the hairs are bleached in addition to the skin, but to what depth is unknown. If penetration of the hydroquinone is to a depth greater than the dermis then this technique could reduce overall efficacy by removing melanin from the site where it is required.

Stress preconditioning is where living cells exposed to a sub-lethal stress can be stimulated to a heightened level of protection such that exposure to a subsequent lethal stress does not kill the cells. It was first observed in 1967, when Selye found that prior treatment of rat skin flaps by sub-lethal ischaemia reduced the amount of skin necrosis when the flaps were subsequently exposed to a 9 hour ischaemic period compared to non-pretreated controls (Selye, 1967). Murry applied the findings to a heart model using the dog and showed a reduced infarct area in the ischaemia-

pretreated group again when compared to a non-pretreated control (Murry, et al., 1986). Further work in this field has shown that the preconditioning stimulus does not have to be of the same type as the potentially lethal stimulus to adequately protect the tissue (Nolan, et al., 1978), (Vogt, et al., 1993). It is therefore possible that preconditioning skin epidermal cells could result in a reduction in skin side effects from ruby laser exposure thus enabling its use particularly in darker-skinned individuals. This protection is thought to be brought about by the induction of proteins known as Heat Shock Proteins.

1.7 HEAT SHOCK PROTEINS AND THE STRESS RESPONSE

The heat shock proteins (HSP) are a group of ubiquitous, highly conserved proteins found in cells throughout the plant and animal kingdom. Ritossa (Ritossa, 1962), who noticed the expression of a new set of proteins in Drosphila melanogaster after exposure to mild heat stress, first described their presence. They were given the name heat shock proteins on account of their induction but have subsequently been found to be expressed by a far wider range of stimuli (Welch, 1992), (Minowada and Welch, 1995) (see the Table below) and so are now more appropriately termed stress proteins (Steels, et al., 1992), (Bensaude, et al., 1996), (Morimoto, et al., 1996).

Conditions	*Agent*
Environmental stressors	Hyperthermia
	Heavy metals (Copper, Cadmium, Mercury)
	Amino Acid analogues
	Metabolic inhibitors (cyanide)
Disease states	Viral infection
	Ischaemia
	Inflammation
Physiological processes	Cell cycling
	Embryological development

The stress proteins are expressed only at low levels or not at all within cells that are not stressed. In this state they have been termed chaperones which explains their cellular role. They are believed to bind to new proteins, once their synthesis is complete, to aid folding and produce the correct tertiary structure for that protein to function normally (Craig, et al., 1993), (Hartl, 1996). These constitutive stress proteins are HSP 60, HSP 70, HSP 90 and HSP 110 (the numbering accounts for their molecular weight in kilodaltons) which, along with expression of other HSP's, undergo increased expression under conditions of stress. In this role it becomes apparent how their increased expression could result in cellular protection by the maintenance of protein structure and prevention of denaturation aiding cell survival and this is presently believed to be their mode of operation (Kaufmann, et al., 1991), (Hutter, et al., 1994), (Morris, et al., 1996).

The most inducible of the stress proteins is the HSP 70 family (Welch, 1992). The family consists of 2 proteins, the constitutive HSP 73 and the inducible HSP 72. Upon

exposure to stress, HSP 70 relocates to the nucleus to be associated with the nucleolus, described as a move consistent with a role in protecting ribonucleoproteins (Maytin, 1995). In addition, increased synthesis of the inducible form (HSP 72) occurs with a concomitant decrease in the synthesis of proteins normally synthesised at normal temperatures. The factor causing increased production is believed to be DNA damage (Muramatsu, et al., 1993), (Abe, et al., 1994). A rise in HSP production has been noted as soon as one hour after stressing (Polla and Anderson, 1987), with a greater concentration occurring in the nucleolus by approximately five hours (Muramatsu, et al., 1992). If the original stress response produces damage too great to be repaired then the cell will undergo programmed cell death. Otherwise, the increased production of the HSP's will protect the cell and this heightened state has been shown to continue for up to a few days (Marber, et al., 1993). It is this elevated state of protection which is believed to be the background to the phenomenon of preconditioning.

1.8 HYPOTHESES

The ultimate aim of the work presented in this thesis is to improve efficacy and lessen side effects resulting from normal mode ruby laser-assisted depilation via a greater understanding of its mode of action and the development of novel techniques of reducing associated epidermal damage. More specifically, the following hypotheses were addressed:

The normal mode ruby laser targets hairs within human hair-bearing skin resulting in heat production great enough to produce damage to the hair producing cells within the follicles (Chapter 3).

A photon beam from the normal mode ruby laser can penetrate human skin to a depth great enough, and have sufficient energy remaining to cause, damage to the hair producing cells of the pilosebaceous unit (Chapter 3).

The normal mode ruby laser can produce depilation and skin side effects in the black-haired mouse (Chapter 4).

A blocking chromophore is able to absorb the photon energy from a beam emitted from the normal mode ruby laser (Chapter 5).

Chromophore painted upon the skin surface can protect human skin from histological damage induced by the normal mode ruby laser (Chapter 5).

Chromophore painted upon the skin of the black-haired mouse reduces the skin side effects whilst not adversely affecting the depilatory efficacy produced by normal mode ruby laser irradiation (Chapter 5).

Human keratinocytes *in vitro* can be preconditioned by sub-lethal application of heat to protect themselves against a subsequent potentially lethal exposure to normal mode ruby laser irradiation (Chapter 6).

Human skin can be exposed to a specific temperature for a fixed time duration so as to increase Heat Shock Protein 70 expression within the cells of the epidermis without causing damage, whilst not affecting the follicular epithelium (Chapter 6).

The skin of the black-haired mouse can be preconditioned with heat so reducing or preventing skin side effects subsequently produced by exposure to normal mode ruby laser irradiation but not affecting depilatory efficacy (Chapter 7).

CHAPTER 2 - MATERIALS AND METHODS

2.1 MATERIALS

2.1.1 Animals

The animal model used for experimentation was the C57BL/10 inbred strain of black haired mouse. Males alone were used and all were purchased from Harlan UK Ltd at the age of 6 weeks.

2.1.2 Anaesthesia

The mice were weighed using a Taconic Farms Mouse Scale (Pelouze Scale Company) and the anaesthetic dosage per gram body weight calculated. Hypnorm® (Fentanyl citrate and fluanisone) was purchased from Janssen Animal Health and Hypnoval® (midazolam) was purchased from Roche Diagnostics Ltd. The anaesthetic mixture (called CRC cocktail) was made up using one part Hypnorm®, two parts "water for injection" and one part Hypnoval®.

2.1.3 Theatre Consumables

The hair shaver used was a "Sterling 2 plus" manufactured by Wahl®. The tattooing machine was supplied by Langley Ltd of Barnsley. The 6 mm diameter biopsy punch was obtained from Stiefel Laboratories. The depilatory cream used was a Tesco's Ltd. homebrand. The dermatome used for taking skin grafts from skin specimens was purchased from Zimmer Ltd.

2.1.4 Tissue Culture

All keratinocyte and fibroblast cell lines were initiated from normal skin specimens obtained from caucasian patients (mean age 32; age range 23 to 37) who underwent plastic surgical procedures at the Mount Vernon Hospital, Northwood, Middlesex.

The whole tissue skin specimens used during experimentation were obtained from patients at the Mount Vernon Hospital, apart from the specimens used in the thermal imaging experiment which were gained, in addition, from the Wellington Hospital, 8a Wellington Place, London and the King Edward VIIth Hospital for Officers, 10 Beaumont Street, London. All patients gave written consent for the use of their discarded skin for experimental purposes.

All cell culture procedures took place in a sterile, Class II laminar airflow hood (Laminair; Heraeus Instruments). Heraeus temperature controlled (37°C), humidified and gas controlled (oxygen 95%, carbon dioxide 5%) incubators were used for culturing purposes. Centrifugation was achieved using the Heraeus Labofuge. Routine monitoring of cell cultures by microscopy was performed with an Olympus CK2 inverted phase contrast microscope. Cell counting took place using a modified Neubauer haemocytometer (Weber Scientific International).

Plasticware, including culture flasks, 6 and 48 well plates, petri dishes, 20 ml centrifuge tubes, 0.22 μm filters and cell scrapers were supplied by Greiner Labortechnik. Parafilm "M"® Laboratory film was obtained from American National Can™. Dulbecco's modified Eagle's medium (DMEM), DMEM/Hams F12 medium, fetal calf serum (FCS), Dulbecco's phosphate buffered saline (PBS) and 0.05% ethylenediaminetetra-acetic acid in calcium-free PBS (versene) were supplied by Gibco Ltd. Culture media additives, including cholera toxin, epidermal growth factor, transferrin and insulin, plus the synthetic melanin were supplied by Sigma Ltd: lyothyronine was obtained from Koch-Light Ltd. Antibiotics, trypsin, di-methyl sulfoxide (DMSO) and 0.4% trypan blue were also obtained from Sigma Ltd. N-2-hydroxyethylpiperazine-N-2 ethanesulphonic acid (HEPES) was supplied by BDH Ltd.

Swiss 3T3 mouse fibroblasts cells used as feeder cells in keratinocyte culture were supplied by the Imperial Cancer Research Fund.

2.1.5 Tissue Analysis

Histology

A Histokinette 2000 automatic processor was used for the dehydration and leering stages. The blocks were embedded using a Raymond A Lamb Blockmaster III and sections cut on a Reichert-Jung Microtome. Microscopy was performed with a Zeiss Axioskop microscope. Buffered formal saline (10%), toluene, xylene, alcohol and other solvents were supplied by Genta Medical. All compounds used for staining were of the best grade and, unless otherwise mentioned, were obtained from BDH Ltd.

Sodium dodecylsulphate-polyacrylamide gel electrophoresis (SDS-PAGE) and Western Blotting

The glass sheets, spacers, rubber gaskets, upper buffer chamber gaskets, loading stands, cooling stacks and gel tanks used were supplied as the Mini Protean® II system by BIO-RAD Ltd. The sodium dodecylsulphate (SDS), the Tris (hydroxymethyl) methylamine, the hydrochloric acid and the methanol were supplied by BDH Ltd. and the acrylamide/bisacrylamide (37.5:1) solution was supplied by Boehringer-Mannheim Ltd. The ammonium persulphate, the polyoxyethylenesorbitan monolaurate (Tween 20), the N, N-dimethylformamide and the non-fat, dried milk were supplied by Sigma Ltd. The N, N, N′, N′-Tetramethylethylenediamine (TEMED) was obtained from Gibco Ltd. The Triton (t-Octylphenoxypolyethoxyethanol) X-100 was obtained from Sigma Ltd. as was the Napthol-AS-BI phosphate (sodium salt) and the Fast Red RC tablets (5-chloro-2-methoxy-benzenediazonium chloride hemi (zinc chloride) salt). The nitrocellulose paper (0.45 μm pore size) was supplied by Amersham and Whatman™ 3MM blotting paper was used in the transferring process. The protein assay kit used was the BIO-RAD *DC* (Disposable Cuvette) Protein Assay system. The protein analyser used was the Helios Unicam UV-Vis Spectrometer. The power supply was from a Flowgen Consort E714 power pack. An Eppendorff Thermostat 5320 heater was used for heating purposes. The orbital shaker used was the Luckman R100 Rotatest Shaker.

Immunohistochemistry

The p53 mouse monoclonal primary antibody (used at a 1:60 dilution on tissue sections) was supplied by DAKO Ltd. The Heat Shock Protein 70 (HSP 70) mouse monoclonal primary antibody capable of detecting, though not discerning between, the constitutive HSP 73 type and the inducible HSP 72 type of the family (diluted 1:100 for tissue staining and 1:1000 for Western Blot analysis) was supplied by Neomarkers Ltd. The secondary antibody used for all human samples was a biotinylated rabbit anti-mouse antibody supplied by DAKO Ltd and was used at a 1:350 dilution for tissue staining and a 1:1000 dilution for Western Blot analysis. The avidin-biotin complex/horseradish peroxidase kit, used for the staining of human skin sections at a working dilution of 1:100, was also supplied by DAKO Ltd. The ExtrAvidin® alkaline phosphatase used for Western Blot analysis at a dilution of 1:1000 was supplied by Sigma Ltd. The 3,3′-diaminobenzidine (DAB) peroxidase substrate kit, used on human tissue sections only, was obtained from Vector Laboratories. Immunostaining of mouse specimen sections involved the use of the mouse monoclonal HSP 70 primary antibody mentioned above, but then used a detection system specifically designed to reduce the non-specific background staining obtained when using mouse monoclonal antibodies to stain mouse tissue (Ultravision Mouse Tissue Detection System Anti-Mouse, HRP/DAB from Lab Vision Corporation).

2.1.6 Specialised Equipment

Ruby Laser

The ruby laser used in all experiments was the "Chromos 694 depilation" normal mode ruby laser and was supplied by SLS Biophile, Llanelli, Wales (Figure 2.1). The beam was of a 694 nm wavelength with a pulse duration of 900 μsec and a spot size of 7 mm. The fluence levels that could be used ranged from 0 to 17 J/cm^2 with the actual fluence emitted calibrated before each use by a built-in energy meter. The

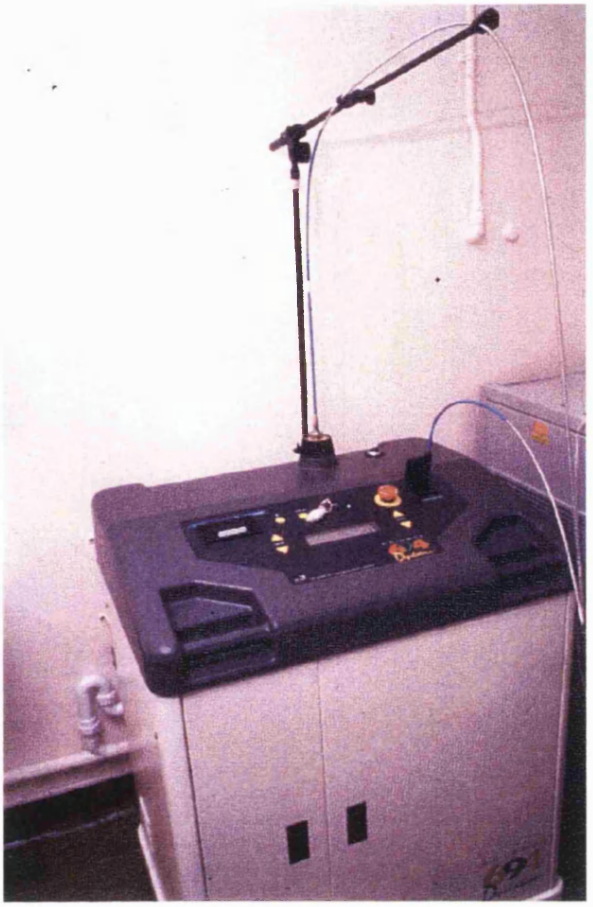

Figure 2.1: The "Chromos 694 nm Depilation" normal mode ruby laser.

Figure 2.2: The FLIR Systems "Thermovision 900" thermal imaging camera.

lowest fluence that could be recorded by this meter was 5 J/cm^2 with an accuracy of 0.5 J/cm^2. The laser fluence was adjusted by increasing or decreasing a percentage scale visible on the display ranging from 0 to 40%. A pulse of less than 5 J/cm^2 could be emitted but an accurate reading of the fluence was not obtainable using the internal meter. To remedy this, an external sensor was connected to an electron volt reader calibrated identically to the internal meter. This allowed the fluence to be calculated using the formula shown below.

The external sensor was calibrated to match the internal sensor so that 0.20 V was equivalent to 1 Joule of 694 nm light.

Therefore the energy emitted in Joules was:

$$\text{Energy (J)} = \frac{\text{Voltmeter reading (V)}}{0.20}$$

Converting this to energy density (J/cm^2) or fluence:

$$\text{Energy density (J/cm}^2\text{)} = \frac{\text{Energy (J)}}{\text{Area of the spot (cm}^2\text{)}}$$

Thermal Imaging Camera

The thermal imaging camera used was the "Thermovision 900" system loaned from FLIR Systems, Leyton Buzzard, Bedfordshire (Figure 2.2). A software package, created by the company, was used which enabled an image to be digitally recorded and incorporated onto a computer's hard-drive every 0.15 of a second. In addition, each pixel on the image (which measured 272 by 136 pixels giving a total of 36 992 pixels) recorded a temperature and so by drawing lines across the image through the desired areas, the temperature of the pixels within that line could be established and recorded into an excel worksheet™ (Microsoft Corporation, version 5.0). The lines

were copied identically onto the subsequent images taken for that run allowing the temperature changes to be assessed over time.

2.1.7 Imaging

Computer generated images of viewed histological slides were created using the Visilog© specialised software package (version 5.0) by Noesis via a JVC colour video camera, model KY F55B, mounted on the Zeiss Axioskop microscope.

A quantitative comparison of HSP 70 production between each well on a Western Blot at each of the temperatures of exposure was performed by using a Seescan image analysis computer (Seescan Ltd.). Digital images were captured, using a black and white Sony CCD video camera (Model XC-77CE) and zoom lens (18-108/2.5; Seescan), of the Western Blots illuminated upon a stabilised light box (DVV Lightboxes). Additional software programs were written by Mr Kaetan Ladhani, Research Assistant, RAFT Institute of Plastic Surgery.

2.1.8 Photography

Laser treatment sites on the mice were photographed using a Minolta X-300 35 mm camera with a telephoto lens (100 mm) and ring flash light (Starblitz 1000-Auto Macro-lite). Colour slide film (Kodak Elite Chrome ASA 100) was purchased from Jessops Photography.

2.2 TISSUE CULTURE METHODS

2.2.1 General Procedures

Media

Two types of media, fibroblast culture media (FCM) and keratinocyte culture media, (KCM) were used to culture the respective cell types. They were made up as 500 ml

aliquots, the constituents of each shown in Table 2.1, and stored at 4°C for a maximum of 1 month. Media in culture flasks was changed at least twice weekly whilst the cells were growing.

Table 2.1: Constituents of tissue culture media.

a. Fibroblast culture medium (FCM).

DMEM	90%
Fetal Calf Serum	10%
L-Glutamine	2 mM
Benzyl penicillin	100 units/ml
Streptomycin	100 µg/ml

b. Keratinocyte culture medium (KCM).

DMEM/Hams F12	90%
Fetal calf serum	10%
Cholera toxin	1×10^{-10}M
Epidermal growth factor	10 ng/ml
Hydrocortisone	0.4 µg/ml
Adenine	1.8×10^{-4}M
Transferrin	5 µg/ml
Insulin	5 µg/ml
Lyothyronine	2×10^{-11}M
L-glutamine	2 mM
HEPES	7mM
Benzyl penicillin	100 units/ml
Streptomycin	100 µg/ml

Trypsinisation/passaging

Trypsinisation is the term given to the removal of cultured cells from the base of the culture flask by the use of the protease trypsin. A slightly different technique was used for fibroblasts (human primary and murine 3T3 cell line) than for keratinocytes. The fibroblasts in the flask had the culture media removed and were washed with calcium-free PBS. This was then removed and a 0.05% trypsin in versene mix was added to the flask and the flask placed into an incubator. After approximately 3 to 5 minutes, the cells could be seen rounding and becoming detached under phase microscopy whereupon FCM was added to neutralise the action of trypsin and the cell suspension placed into a 20 ml centrifuge tube. The cells from one flask were then divided into 3 to 6 flasks according to requirements.

The technique employed for detaching keratinocytes involved washing the cells with calcium-free PBS after media removal but then adding versene alone to the flask before replacing it into the incubator. After approximately 5 to 10 minutes the feeder cells aiding the growth of the keratinocytes could be detached, leaving behind a pure population of keratinocytes. The 0.05% trypsin in versene mix was then added and the flask returned to the incubator. After approximately 10 minutes the keratinocytes could be seen to be rounding and detaching from the flask under phase microscopy whereupon KCM was added to neutralise the action of trypsin and the cell suspension placed into a 20 ml centrifuge tube. After trypsinisation, the keratinocytes from one flask were split between 3 and 7 flasks according to need.

Cell Counting

A sample of the cell suspension, whose total cell number was to be established, was pipetted onto a haemocytometer and viewed using the phase-contrast microscope. The haemocytometer grid consisted of 9 squares, with the average cell number counted in one of the squares being equal to the cell number to the power of 10^4 per ml of the cell suspension.

When estimating the number of keratinoytes it was important to include in the count only the small round cells as only these represented the viable cells from the basal layer. The larger cells seen were the suprabasal cells, which would be undergoing a form of programmed cell death (terminal differentiation) and therefore would not be able to produce a keratinocyte colony on passage. Counting the small keratinocytes therefore gave a more representative number of the cells that were alive and available for successful passage.

Trypan Blue Viability Test

The method employed for cell counting was also used to establish cell death and was performed in the same manner mentioned above. However, prior to a sample of the cell suspension being placed onto the haemocytometer, a known volume of the cell suspension was mixed with an equal volume of 0.4% trypan blue upon a sterile petri dish. Dead cells have permeable membranes and so they take up the dye appearing blue under the phase contrast microscope. A sample of the mixture was then added to the haemocytometer as described previously and the ratio of live to dead cells established. The number counted was doubled on account of the 50:50 suspension to trypan blue mix.

Feeder Cells

Keratinocytes are known to grow and replicate more successfully in culture when they are supported by a feeder population of cells. These cells were prepared from a murine fibroblast cell line known as 3T3 which were used up to passage 30 (P30) and then discarded. The 3T3 were grown in FCM in 150 cm^2 flasks and passaged (1:5 split) twice weekly. To prepare feeder cells, flasks of semi-confluent 3T3 were trypsinised as usual (see above) and counted using a haemocytometer. The cells were then pelleted by centrifugation at 1000 rpm for 5 minutes after which the cells were re-suspended in a volume of KCM calculated to produce a suspension of 2 million feeder cells per ml. The cells were then exposed to a just sub-lethal dose (6000 rads) of gamma irradiation from a cobalt 60 source. This treatment produced cells, which

although unable to proliferate, survived for approximately 4 days conditioning the medium and plastic culture surface, thus aiding keratinocyte growth. The feeder cells could be stored for up to 3 days at 4°C and used as required. The keratinocyte cultures were replenished with fresh feeders every 3 days.

2.2.2 Initiation of Keratinocyte Population

Normal keratinocyte cultures were initiated from seven caucasian patients. Each skin specimen was dissected on a 12 cm petri dish in a Class II hood to remove the fat and hypodermis. Half of the remaining skin was finely minced and then added to 10 ml 0.1% trypsin in versene in a 20 ml centrifuge tube and incubated at 37°C for approximately 2 hours. The remaining skin was used to initiate autologous fibroblast cultures (see section 2.2.4). After this period of incubation the epidermis could be seen lifting off the dermis so exposing the basal layer where the viable, replicating keratinocyte cells resided. 10 ml of KCM (Table 2.1) was then added to the mixture to neutralise the trypsin and the mix was passed through a sterile sieve to remove the collageneous matrix from the cell suspension. The cells were counted and then centrifuged at 1000 rpm for 5 minutes and the supernatant removed. The remaining pellet of passage 0 (P0) keratinocyte cells was agitated gently and re-suspended in fresh KCM. These cells were then seeded at 2 x 10^6 per T75 flask together with 1 ml of irradiated feeder cells (2 x 10^6 cells) and placed into the incubator. The first media change with fresh KCM occurred at 48 hours and thereafter twice weekly, along with replacement of feeder cells as appropriate. This regimen was continued until approximately 70-80% keratinocyte cell confluency was reached (see Figure 2.3) when the cells were passaged (section 2.2.1).

2.2.3 Initiation of a Fibroblast Population

The skin samples used to initiate keratinocyte cultures were also used to initiate fibroblast cultures. Each specimen underwent dissection as previously described (section 2.3.3) to remove the fat and hypodermis and approximately half of the specimen was cut into strips and the epidermis removed using a scalpel blade. The

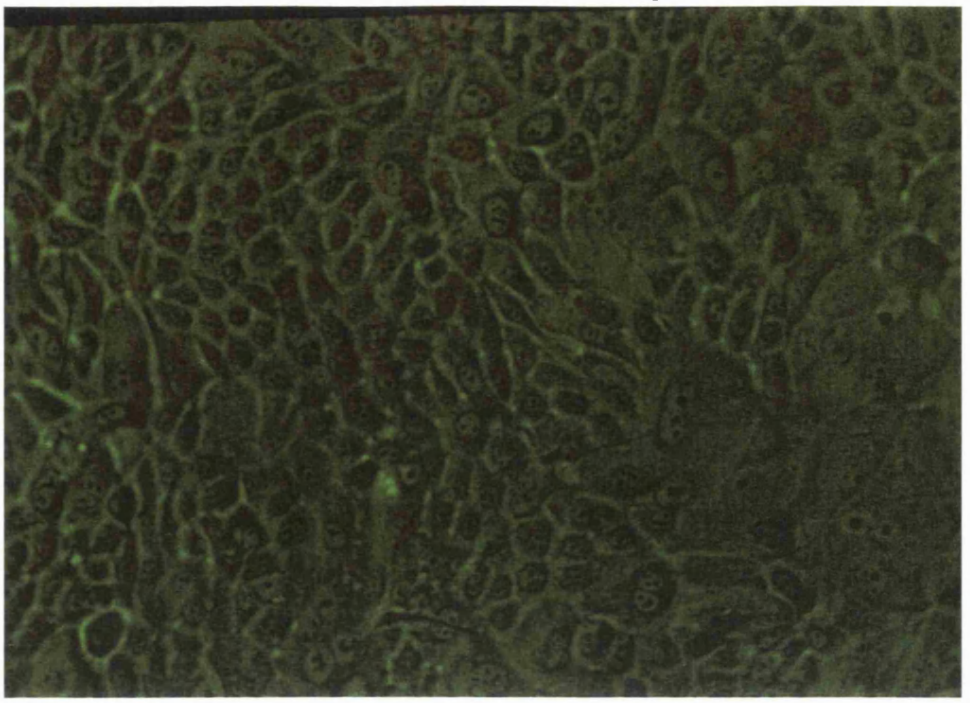

Figure 2.3: Keratinocyte cells grown in culture and viewed through an inverted phase contrast microscope. The larger cells of the colony, seen lower right, represent differentiating, suprabasal keratinocytes.

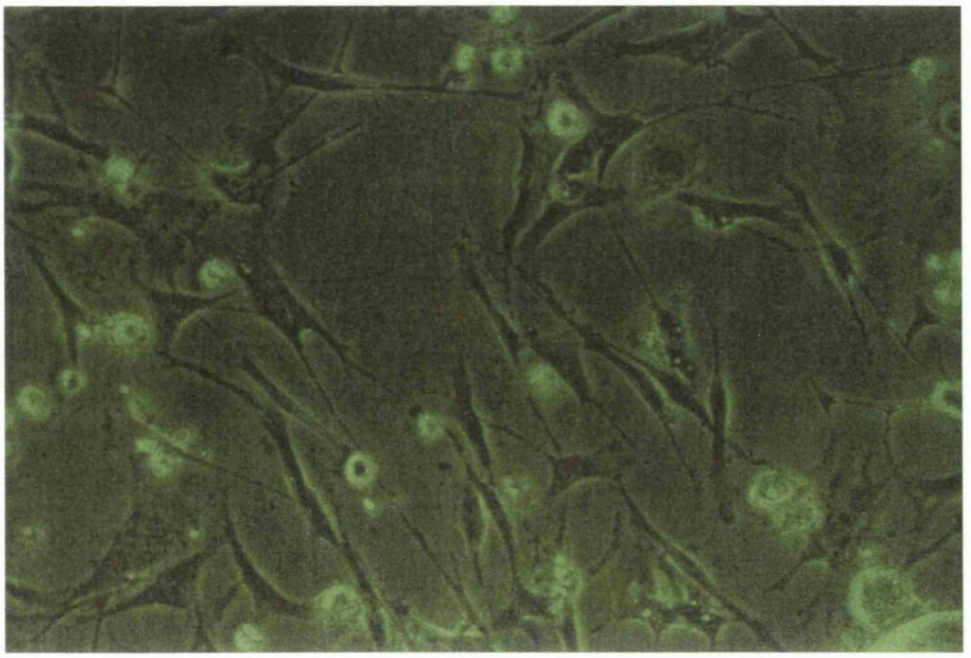

Figure 2.4: Fibroblast cells grown in culture and viewed through an inverted phase contrast microscope.

remaining dermis was then minced and placed onto the bottom of a 6 cm petri dishes with a sterile cover slip pushed onto the specimens to maximise contact between dermis and plastic base and prevent the tissue pieces from floating off the surface once media was added. FCM (Table 2.1) was added and the dishes placed into the incubator. The media was not changed for a week to prevent the forceful removal of the new growth of fibroblast cells or dermis and the loss of any growth stimulating factors produced by the cells to aid their growth and replication. Thereafter, media was changed twice weekly until the dishes were approximately 60% confluent with fibroblasts (see Figure 2.4) whereupon they were passaged using the routine trypsinisation procedure into a single T75 flask (P1 cells). Passaging thereafter was performed as detailed in section 2.2.1 when approximately 90% cell confluency was reached.

2.2.4 Cryopreservation of Cells

All keratinocyte and fibroblast cell lines were cryopreserved at P0 and P1 respectively, to establish stocks for later experimention. This took place when the T75 flasks had reached the degree of confluency stated in 2.2.3 and 2.2.4. The cells were routinely trypsinised and pelleted by centrifugation at 1000 rpm for 5 minutes. The pellet was agitated and re-suspended in 4 mls of freshly-prepared cryopreservation media (90% fetal calf serum and 10% DMSO), with 1 ml of this suspension being added to each of four cryovials. The cryovials were then wrapped in tissue paper and transferred to a minus 80°C freezer. This would allow the cells to gradually freeze at approximately minus 1°C per minute. After approximately 24 hours, the vials were transferred to liquid nitrogen for long-term storage.

Recovering the cells involved rapid thawing of the cryovial in a waterbath at 37°C, transferring the cell suspension to a 20 ml centrifuge tube and then slowly adding approximately 9 mls of KCM, or FCM as appropriate to dilute out the DMSO. The cells were then centrifuged at 1000 rpm for 5 minutes and the supernatant removed. After agitating the pellet, fresh media was added and the suspension divided between three or four T75 flasks as required. The flasks into which keratinocytes were added

had been previously seeded (24 hours before) with 2 x 10^6 feeder cells. The flasks were then placed into the incubator.

2.2.5 Organ Culture

Whole specimens of skin, which had been used for experimentation, were cultured over the short term to allow any resultant changes in protein expression to become detectable. The skin samples were placed dermis-side down upon a sterile steel mesh (made by the Bioengineering Department, Mount Vernon Hospital) within a 6 cm petri dish. FCM was then added to the dish to the level of the mesh so maintaining the specimen at the air/liquid interface. The dish was then placed into an incubator and cultured for either 5 or 18 hours depending upon the experiment (see Chapters 3, 6 and 7).

2.3 STAINING METHODS

2.3.1 Histochemistry

The majority of routine histological processing was kindly performed by Ms C Noel and Mrs E Clayton, Histologists, RAFT Institute of Plastic Surgery. All specimen sections were de-waxed using xylene, rehydrated in decreasing concentrations of alcohol and then brought to water before the staining process began.

Haematoxylin and Eosin

Sections were stained with Mayer's haematoxylin for 10 minutes. They were then washed for a further 10 minutes in running tap-water. The stain was differentiated by placing the sections into acid-alcohol for 10 seconds (1% concentrated hydrochloric acid in 70% alcohol) and then "blued" in running tap-water for 5 minutes. After that the sections were placed into 1% eosin for 5 minutes and washed in running tap-water. Sections were dehydrated by running through increasing concentrations of alcohol, cleared in xylene and mounted with a coverslip. The results are: Nuclei -

blue/black, Cytoplasm - varying shades of pink, Muscle fibres - deep pinky red, Collagen - pale pink and Fibrin - deep pink

Modified SACPIC Technique (Nixon, 1993)

The sections were stained with celestine blue for 5 minutes and then rinsed in running tap-water. Next they were placed into Gill's haematoxylin for 5 minutes and then again rinsed in running tap-water. The stain was then "blued" in Scott's tap-water for 2 to 5 minutes and afterwards rinsed in running tap-water. The sections were placed into 2% safranin for 5 minutes, rinsed in 70% ethanol which was followed by a further rinse in 95% ethanol. Differentiation occurred in absolute picric acid/ethanol for 3 minutes and the sections rinsed in 95% ethanol, then 70% ethanol and finally running tap-water. Further staining was performed in picro indigo carmine for 1 minute and then the sections rinsed in running tap-water. Dehydration through increasing alcohol concentrations then followed, the sections cleared in xylene and finally mounted with a coverslip. The results are: Nuclei - blue/black, Keratin - yellow, Collagen - blue, Inner root sheath - bright red, Outer border brush end - orange, Outer root sheath - pale green, Smooth muscle - green.

Massons Fontana

The sections were stained with a silver solution (10% silver nitrate with concentrated ammonia) and left overnight. They were then washed in distilled water and placed into 5% sodium thiosulphate for 2 minutes. After rinsing in running tap-water, the sections were stained in 1% aqueous neutral red for 3 minutes. After a final rinsing in running tap-water, the sections were dehydrated through increasing alcohol concentrations, cleared in xylene and mounted with a coverslip. The results are: Melanin - black, Argentaffin - black, Lipofuscin - black, Nuclei - red.

Massons Trichrome

Sections were stained with celestine blue for 5 minutes and then rinsed in distilled

water. They were then stained with Mayer's haematoxylin for 5 minutes and afterwards washed until blue. Differentiation with 1% acid alcohol occurred for 10 seconds before washing in running tap-water. Staining in acid fuchsin solution for 5 minutes (acid fuchsin 0.5g, glacial acetic acid 0.5cm^3 and distilled water 100 cm^3) was then followed by rinsing in distilled water. The sections were then stained in phosphomolybdic acid solution for 5 minutes (phosphomolybdic acid 1 g and distilled water 100 cm^3), drained and then stained with methyl blue solution for 2 to 5 minutes (methyl blue 2 g, glacial acetic acid 2.5 cm^3 and distilled water 100 cm^3). The sections were rinsed in distilled water and then treated with 1% acetic acid for 2 minutes before being dehydrated through increasing alcohol concentrations, cleared in xylene and mounted with a coverslip. The results are: Nuclei - blue, Muscle - red, Fibrin - red and Collagen - blue.

2.3.2 Immunohistochemistry

Detection of p53 and Heat Shock Protein 70 (HSP 70) Expression in Human Tissue

After de-waxing, the slides were placed into a plastic slide rack in a bath containing 250 ml of 10 mM citric acid at pH 6. The sections were microwaved three times for 4 minutes at 800 Watts. During this time the solution was topped-up with distilled water at the intervals. The sections were left to stand for 10 minutes in the bath before rinsing in running tap-water. The sections were washed once with Tris-buffered saline (TBS) before being ringed using a resin pen. Either the p53 mouse monoclonal or HSP 70 primary antibody was then added as required and incubated for 1 hour at room temperature. The sections were washed three times with TBS and then biotinylated rabbit anti-mouse secondary antibody added and incubated for 1 hour at room temperature. The sections were again washed three times with TBS and then avidin-biotin complex/horseradish peroxidase added and incubated for 1 hour at room temperature. The sections were washed twice with TBS and then once with Tris buffer (TB) before DAB peroxidase substrate (distilled water 5 ml, pH 7.5 buffer 2 drops, DAB 4 drops and hydrogen peroxide 2 drops) added as recommended by the

manufacturer for 10 minutes. The sections were washed once with TBS and then rinsed in running tap-water before being counterstained with haematoxylin alone. The sections were then dehydrated through increasing alcohol concentrations, cleared in xylene and mounted with a coverslip. Positive p53 protein or HSP 70 protein expression resulted in brown nuclei, negative nuclei appear blue from the haematoxylin counterstain.

Heat Shock Protein 70 (HSP 70) Detection in Mouse Tissue

The method used for detecting HSP 70 expression in the cells of sections taken from mouse biopsies required a different protocol from that outlined above and was as recommended by LabVision® in the instructions obtained with their Ultravision Mouse Tissue Detection System Anti-Mouse, HRP/DAB.

The sections were incubated, after de-waxing and rehydrating, in the hydrogen peroxide block (kit component) for 15 minutes and then washed twice in TBS. They were then microwaved in 10 mM citric acid buffered to pH 6 as above and left to stand for 10 minutes. The sections were incubated with the Ultra V block (kit component) for 5 minutes at room temperature and then rinsed once with TBS. Incubation with the Rodent block (kit component) occurred for 1 hour at room temperature before rinsing in TBS. HSP 70 primary antibody was added and the sections left for 1 hour at room temperature before rinsing with TBS. The sections were incubated with the Biotinylated goat anti-mouse (kit component) for 15 minutes at room temperature and then again rinsed in TBS. Streptavidin peroxidase (kit component) was applied and the sections incubated for 10 to 15 minutes and rinsed in TBS. DAB chromogen (1 to 2 drops - kit component) was added to 1 ml of DAB substrate (kit component), mixed and applied to the sections for incubation for 5 to 15 minutes before the sections were washed once with TBS. Counterstaining was undertaken with haematoxylin before the sections were dehydrated with alcohol, cleared in xylene and mounted with a coverslip. The positive nuclei appear brown whilst the negative nuclei are counterstained blue.

2.4 METHODS FOR SDS-PAGE AND WESTERN BLOT ANALYSIS

Western Blot analysis was performed on cultured keratinocytes alone to detect the quantity of HSP 70 produced by those cells at 5 hours and 24 hours after heat exposure to a range of temperatures for a set time of 15 minutes (see Chapter 6).

Cellular Protein Extraction

After either 5 hours or 24 hours incubation post heat exposure, the media was removed from flasks of cultured keratinocytes and the cells washed twice with 5 mls of cold calcium-free PBS (4°C). A final 5 mls of calcium-free PBS was then added to the flasks and the cells removed using a cell scraper. The resulting cell suspension was placed into a 20 ml centrifuge tube and centrifuged at 1000 rpm for 5 minutes. The supernatant was removed, the cell pellet agitated and then re-suspended in 300 µl of 1% Triton X-100 in PBS to rupture the cell membranes. This preparation was then rapidly frozen in a minus 80°C freezer.

Preparation of Gels

The glass sheets, spacers, rubber gaskets and upper buffer chamber gaskets were thoroughly cleaned and sprayed with 70% alcohol then allowed to dry in air. The gel sandwich was assembled and placed into the loading stand. A 7.5% (running) gel was made using the constituents shown in Table 2.2 and allowed to set before a 4% (stacking) gel (see Table 2.2) was added to the top of the running gel with a comb in place which produced the wells.

Protein Assay

The protein preparations were thawed and the total protein content of each sample estimated using the BIO-RAD *DC* Protein Assay Kit. This involved taking 20 µl of reagent S (a Tween 20 solution) and adding it to each ml of reagent A (an alkaline copper tartrate solution) that was required (producing reagent A'). 100 µl of each of

the samples was added to separate test tubes, 500 µl of this new reagent A′ was added to the test tubes and thoroughly mixed. 4 ml of reagent B (a dilute Folin reagent) was then added to each test tube, mixed and left to stand for 15 minutes. The light absorbencies were read using the Helios protein analyser at 750 nm and the total protein content calculated in mg/ml from a standard curve produced from a series of known protein concentrations. The samples were diluted with sample buffer (Table 2.3a) to produce a final concentration of protein of 30 µg/ml in each of the gel's wells, and then heated to 90°C for 5 minutes just prior to loading on the gel.

Electrophoresis

The gel sandwich was placed in the gel tank and running buffer (as detailed in Table 2.3b) was added to the upper and lower electrode tanks. Each of the protein preparations was loaded onto the gel (25 µl per well) along with a molecular marker control. The gel was run for approximately 1 hour at 180 volts until the dye front of the sample buffer had reached the lower end of the gel.

Western Blotting

The gel was removed from the gel sandwich and placed in transfer buffer (Table 2.3c). Whatman™ 3MM blotting paper was pre-soaked in transfer buffer and the nitrocellulose paper pre-soaked in water. A transfer sandwich was constructed consisting, in order, of a sponge pad, 3MM paper, nitrocellulose paper, the gel, 3MM paper and a sponge pad. This was placed in a frame in the following orientation; cathode, nitrocellulose paper, gel and anode, then into the tank containing transfer buffer. Transfer from gel to nitrocellulose paper took place overnight at 30 volts within a transfer chamber containing ice to maintain a cool (approximately 4°C) temperature.

The nitrocellulose paper was removed and placed in a tray containing a solution of 5% non-fat, dried milk and 0.2% Tween 20 in PBS. This was gently shaken on an orbital shaker for 2 hours. The sheet was then washed once in PBS for 5 minutes,

Table 2.2: Constituents of the 7.5% (running) gel and the 4% (stacking) gel used for the Western Blot analysis.

Reagent	7.5% gel	4% gel
Distilled Water	4.8 ml	6.1 ml
1.5 molar Tris-HCl pH 8.8	2.5 ml	
0.5 molar Tris-HCl pH 6.8		2.5 ml
SDS 10%	100 µl	100 µl
Acrylamide/Bis 30%	2.5 ml	1.33 ml
TEMED	5 µl	10 µl
Ammonium persulphate 10%	50 µl	50 µl

Table 2.3: Constituents of buffer solutions used in the Western Blot analysis.

a. Sample buffer.

Reagent	Quantity
Bi-distilled water	7.6 ml
0.5 molar Tris-HCl pH 6.8	2 ml
Glycerol	1.6 ml
SDS 10%	3.2 ml
2 β-mercaptoethanol	0.4 ml
Bromophenol Blue	0.01 g

b. Running buffer (a stock of 2 litres).

Reagent	Quantity
Bi-distilled water	2 litres
Tris base (25 mM)	6 g
SDS	2 g
Glycine (192 mM)	28.8 g

For one electrophoretic run, 300 ml of stock was diluted with 1.2 l of distilled water.

c. Transfer buffer (a stock of 1 litre).

Reagent	Quantity
Bi-distilled water	500 ml
Tris base (25 mM)	3.03 g
Glycine (192 mM)	14.4 g
Methanol	200 ml

Volume adjusted to 1 litre with bi-distilled water.

which was then removed and replaced with a 1:1000 solution of the HSP 70 primary antibody in Tris buffered saline (TBS). The nitrocellulose paper was incubated with shaking for 1 hour and then washed three times, 5 minutes each wash, in 15 mls of a 0.05% Tween 20 in PBS mix (called PBS-T). The secondary, biotinylated rabbit anti-mouse antibody diluted 1:1000 with TBS, was then added and incubated for 1 hour before washing three times, 5 minutes each wash, in 15 mls of TBS alone. The conjugated ExtrAvidin® Alkaline Phosphatase, diluted 1:1000 with TBS was then added to the paper on the shaker for one hour and removed by washing the sheet three times, 5 minutes each wash, with PBS-T again.

A substrate solution of 2 mg Napthol-AS-BI phosphate (sodium salt), with 0.2 ml N, N-dimethylformamide in 9.8 ml 0.1M Tris buffer pH 8.2 (TB) was freshly prepared and a single, 10 mg tablet of Fast Red RC added and mixed until dissolved. This solution was placed onto the sheet and shaken for approximately 20 minutes until a red precipitate had formed characterising the antigen-antibody complex. The sheet was then washed with distilled water.

The Seescan imaging equipment was used to detect the optical density of the staining in each individual lane. Comparison of lanes could be performed on the same sheet but not between lanes on differing sheets due to experimental variation. This analysis identified the temperature at which the greatest quantity of HSP 70 had been produced for that particular cell line.

2.5. METHODS - THE BLACK-HAIRED MOUSE MODEL

2.5.1. Husbandry

The mice were housed in boxes of six within the Animal House at the Northwick Park Institute for Medical Research (NPIMR) based at Northwick Park Hospital, Watford Road, Harrow, London. The mice were fed on RM1 Rodent Maintenance Diet which was supplied by Specialist Diet Services (SDS) Ltd. The mice were adult and aged approximately 6 months when used for experimentation. All surgical procedures were

performed in an adjacent surgical suite under License from the Home Office (Animals Scientific Procedures Act 1986); PIL No. 70/04480 and PPL No. 70/13714. After experimentation, the mice were housed individually to prevent further damage being inflicted upon each others wounds. Water and feed was supplied *ad libatum.* The room in which they were housed was kept at a stable temperature between 22 and 24°C and humidity between 45 and 55%. The lighting was adjusted to provide 12 hours light and darkness per day. A total of 142 mice were studied.

2.5.2. Anaesthesia

All operative procedures were performed under a general anaesthetic. Each mouse was weighed, scruffed and an intra-peritoneal injection of "CRC cocktail" (see section 2.1.2) administered (0.01 ml/g). Anaesthetic duration was short (approximately 1 hour) with the animals recovering spontaneously. 142 procedures were performed in this manner and euthanasia was by cervical dislocation.

2.5.3 Laser Procedure

The mice were either irradiated alone or irradiated secondary to an earlier procedure (for example preconditioning with heat-see Chapter 7) depending upon the experiment being performed. If the mice were being irradiated alone then they were anaesthetised by intraperitoneal injection of "CRC" cocktail but if the irradiation was a secondary event then an inhalational anaesthetic was administered. The anaesthetised mouse was laid upon a clean surgical drape and the back shaved if not already done for the first procedure. The laser fluence was checked by firing the hand-piece into the internal energy meter and then single pulses were administered as required re-checking the fluence after each exposure and adjusting if needed. Once complete, the mouse was returned to an individual box placed upon a warm mat and allowed to recover before being returned to the animal room.

2.5.4 Analysis of Results

Both clinical and histological analyses of results were performed upon the mice used.

Clinical

Clinical analysis of any skin damage occurring at the laser exposed sites was noted by the author and scored on a daily basis until fully healed. The scoring system used within Chapters 4 and 6 is shown in Table 2.4 and is the same system employed by Lin et al (Lin, et al., 1998). The author made slight adjustment to the system when it was applied to the wounds in Chapter 7 to incorporate the size of the wound produced in the laser-irradiated sites. This adjusted scoring system is shown in Table 2.5.

Hair regrowth at the laser exposed sites was assessed and scored on a weekly basis for 8 weeks employing the system used by Lin et al (see Table 2.6) (Lin, et al., 1998). Non-irradiated trimmed control sites were always scored as 3 since all the hair shafts were still present. The time scale took into account the maximum duration recorded for a complete hair cycle to occur in the black haired mouse. This timescale ensured that the hairs in the irradiated region had passed through at least one anagen phase subsequent to laser exposure (Dry, 1926).

Histological

Biopsy specimens were taken from laser exposed sites and control sites immediately after laser exposure and at 8 weeks (ie. after completing clinical observations). These were processed for routine paraffin-wax embedding and sectioned transversely throughout their depths. The sections were then stained as appropriate (see Chapters 4, 6 and 8 plus section 2.3). All sections were analysed by the author, the author's supervisor, Dr C Linge and a histopathologist, Dr P Richman, Mount Vernon Hospital, for verification when required.

Table 2.4: Classification and scoring of the laser-induced cutaneous wounds.

0	No skin damage
1	Erythema
2	Blistering / Clear exudate or crust
3	Blood-stained exudate or crust
4	Ulceration

Table 2.5: Modification of the wound scoring system shown in Table 2.4.

0	No skin damage
1	Erythema
2	Blistering / Clear exudate or crust
3	Blood-stained exudate or crust 0 to 30 % of the treatment area
4	Blood-stained exudate or crust 30 to 60 % of the treatment area
5	Blood-stained exudate or crust 60 to 100 % of the treatment area
6	Ulceration

Table 2.6: Classification and scoring of hair regrowth.

0	None (0% regrowth)
1	Sparse (0-33%)
2	Moderate (33-66%)
3	Full (66-100%)

2.6 STATISTICAL METHODS

Data throughout this thesis have been given as means +/- standard deviation. The cellular experiments were each performed in triplicate to improve statistical power. The number of patient specimens available for use within the thermal imaging experiment was limited to five pairs, which was the maximum number that could be obtained during the week that the thermal imaging camera was available for hire. This limited the statistical power of this particular experiment. For all other experiments performed using explanted tissue n=6.

Each group for the experiments performed using the black haired mouse model contained eight mice. This was a number suggested by Mr C Foy (Head Statistician, Mount Vernon Hospital, Middlesex) as being the minimum figure most likely to produce a statistical difference upon analysis of the subsequent results obtained if a difference so existed.

Ordinal data (cell survival, peak temperature recordings, heat loss rates, wound scores and depilatory scores) were subjected to the Kolmogrov-Smirnov normality test with Lillefors' correction. If the data was normally distributed, parametric comparative tests were performed and if the data failed the normality test, non-parametric comparative tests were performed. Comparison between two groups was undertaken using either a Student's t-test (parametric) or a Mann-Whitney Rank Sum test (non-parametric). For comparison of several groups a one-way ANOVA (parametric) or the Kruskal-Wallis or Dunett's (non-parametric) tests were used. All analyses were performed using SigmaStat™ statistics software, version 1.0 (Jandel Corporation).

CHAPTER 3 – THE INTERACTION BETWEEN A LASER PULSE AND HUMAN SKIN

3.1 INTRODUCTION

Although the normal mode ruby laser (NMRL) has been described, in theory, as the most appropriate and likely laser to produce successful depilation, the results published in clinical trials to date have revealed a limited long term success rate (see Table 1.1). In addition, all the studies reported regarding how the laser exerts its effects upon human skin, and therefore its apparent appropriateness, have been performed using non-biological constructs and using laws of mathematics and physics which describe a uniform, homogenous structure alone, which skin clearly is not. It has also not been proven directly whether heat is responsible for the tissue effects noted after skin has been exposed to ruby laser irradiation. Histological analysis of Guinea-pig skin after irradiation by a single pulse from the NMRL has shown damage consistent with heating (Lawrence, 1967). Heat energy has since been theorised to be the main format to which the photon energy from the NMRL is converted to when incident upon a medium containing its chromophore. If heat were therefore responsible for depilation, what is also not known is where and to what extent the heating occurs and where the heat then dissipates. Before any work could be performed to improve the efficacy and reduce the skin side effects following NMRL exposure, an attempt should be made to clarify the laser skin interaction. Preferential targeting of the hair follicle by the NMRL has not been confirmed on a practical basis although clinically the hair shaft itself can be seen to vapourise upon exposure. In addition, the ability of the chromophore melanin to convert the photon energy to heat and whether this is to an adequate extent for successful depilation still remains unknown.

Clarification of the pathway by which the NMRL beam passes through skin to exert its depilatory effect is also required. The sites to be damaged inducing permanent depilation are the bulge region and the hair bulb (see section 1.3). The chromophore

melanin is present within both these sites to a variable degree that depends on the hair cycle and the hair phenotype of the individual concerned (Narisawa, et al., 1995), (Narisawa, et al., 1997). Whether sufficient melanin is present at these sites to produce damage to these follicular stem cells upon irradiation is unknown. If it were, then the effective pathway for laser depilation could be either directly through the skin to interact with this melanin from outside of the follicle or, as the majority of melanin is present within the hair shaft, which would therefore be where the greatest quantity of heat is produced, from within the follicle. If sufficient melanin were not present at the two stem cell sites, then it would be most likely that heat would have had to diffuse from the shaft to these regions to cause cell death and the long term depilatory effect presently seen in certain individuals. Defining the depilatory pathway of the NMRL beam through the skin could have a bearing upon depilatory success and skin side effects. If protecting the skin from superficial burns and pigmentary changes requires the use of a barrier substance applied to the skin, then this could prevent the passage of the laser beam to its target and consequently depilation if the pathway was via the skin alone. If, however, the mode of action of the laser beam was to use the hair shaft as a "thermal conduit" into the skin as described, then barrier creams could theoretically be effective as the beam pathway would not be interrupted. Present thinking tends to favour the former route though this has also not been proven (Lask, et al., 1997).

In addition to establishing the beam pathway, the depth to which the NMRL can penetrate skin must also be determined. It has been stated that the laser can penetrate skin to a distance of between 2 to 3 mm. The bulge region, which resides at approximately 2/3rds the length of the hair follicle is at or greater than 2 mm deep. It could therefore be feasible that the low depilatory success rate is because the beam is unable to reach the target. Histological analysis of damage produced within skin after laser irradiation using both the Q-switched ruby laser and the NMRL has been reported in an attempt to establish skin penetration. This showed that a Q-switched laser, with a pulse duration of 40 nsec and fluence 8 J/cm^2, induced damage to a maximum depth of 0.75 mm (mean 0.381 mm) (Kopera, et al., 1997). The NMRL, which was the same model as used by the author with a pulse duration of 900 μsec

and spot size 7 mm, produced skin damage up to a depth of 1.34 mm using a fluence of 14 J/cm^2 and to 1.49 mm at 20 J/cm^2 (Liew, et al., 1999). These figures could indeed suggest that the NMRL does not penetrate skin adequately. However, the damage produced is dependent upon the correct chromophore being present. The results could also state that insufficient chromophore was present to interact with the photon energy beam to produce visible damage greater than this depth.

This chapter describes two experiments performed to assess the interaction between a beam from the NMRL and *ex vivo* human skin. The first experiment incorporates the use of a thermal imaging camera to record heat production within hair bearing skin over time along with a histological analysis to assess the site and extent of cellular damage resulting from laser exposure. The second experiment establishes the ability of a laser beam to penetrate non hair bearing skin to the regions responsible for the regrowth of hair.

3.2 AIMS

3.2.1 Thermal Imaging Experiment

- To determine the site, extent and dissipation of heat produced in *ex vivo* hair bearing skin upon NMRL irradiation.

- To determine the extent of histological damage to both the hair shaft and the follicular cells and whether they correlate.

- To discover whether a difference exists in any of the above parameters between the patient specimens.

3.2.2 Laser/Skin Penetration Experiment

- To determine the laser beam penetration profile through *ex vivo* skin at varying fluences from an NMRL.

- To determine the maximum depth of penetration of photon energy through *ex vivo* skin from an NMRL beam using varying fluences.

3.3 METHOD

3.3.1 Thermal Imaging Experiment

Hair-bearing scalp skin was obtained from five, consenting caucasian patients undergoing elective face-lift procedures. Each specimen was divided into 6 pieces of approximately 12 mm^2 and just prior to use had the dermal aspects microdissected to reveal the hair bulbs and the lower hair shafts. Sterile isotonic saline was regularly applied to the dermis during the whole procedure to prevent drying. For each specimen, two pieces were treated with the NMRL ("Chromos 694 depilation", SLS Biophile, Llanelli, Wales; pulse duration 900 μsec, spot size 7 mm), two acted as positive controls and two as negative controls (see below for further details). Those specimens undergoing laser irradiation were mounted on a cork ring on a sterile jig so that the epidermal aspect faced the laser, whereas the thermal imaging camera system ("Thermovision 900", FLIR Systems, Leighton Buzzard, England) was focused on the exposed hair bulbs of the dermal aspect. The dermal aspect was photographed to allow later comparison with the thermal images. The skin was then exposed to a single pulse of 15 J/cm^2 (typical of the clinical range) from the laser. Simultaneously, the thermal imaging system (frequency 15 Hertz) recorded the temperature changes from the dermal side over approximately 45 seconds, the time taken for all heat produced to dissipate. The 7 mm diameter target area to be exposed to the laser had been identified prior to irradiation by a helium-neon aiming beam incorporated into the laser system. Running the thermal imaging camera before ruby irradiation revealed that this "targeting" laser did not produce heat in the specimens. The target area was marked by pen outside the beam, so as not to interfere with the laser and was excised from the specimen by scalpel after the experiment.

The two skin pieces from each patient that were to be used as positive controls for cellular damage (as demonstrated by expression of p53) were exposed to ultraviolet radiation (Ultraviolet light source Nikon Ltd, model HB-10103AF, 100 Watt bulb, filtered to give wavelengths greater than/equal to 300 nm) upon their epidermal aspect for 10 minutes. These specimens were maintained throughout upon saline-damp gauze to prevent dehydration. The negative controls were exposed to air, mounted on a dry cork ring for the same time duration (1 minute and 30 seconds) as the laser irradiated specimens had been during treatment.

After the procedures, all specimens (laser irradiated and controls) were incubated at 37°C for 18 hours in culture media (Dulbecco's Modified Eagles Medium with 10% Foetal Calf Serum, 1% l-Glutamine and 1% Penicillin and Streptomycin) with the epidermis uppermost and at the air-liquid interface to mimic the skin's natural environment. The specimens were then processed for routine paraffin wax histology and sectioned tangentially (parallel to the plane of the skin surface) throughout their depths. Two consecutive 4 μm thick sections were taken for staining every fifth section. The first of the pair was stained by the modified SACPIC technique (Nixon, 1993) and the second by an immunohistochemical technique for the p53 protein. The modified SACPIC staining technique was initially promoted for its ability to differentiate the different growth phases of hair follicles, but has also been described elsewhere as being able to differentiate damaged from undamaged hair shafts in ruby laser irradiated specimens (see section 2.3.1) (Liew, 1999). The marker of cellular damage, p53, was detected as described in section 2.3.2. These sections were then counterstained with haematoxylin. Such alternate staining of two consecutive sections throughout the specimens allowed comparison of the two so establishing if a correlation existed between damaged hair shafts (demonstrated by modified SACPIC) and p53 expression within the viable cells of that same follicle. The depth to which damage to the hair shafts and p53 expression extended in each of the specimens was also estimated by knowing the thickness of each section (4μm) and the number of sections from the epidermis to the level where shaft damage or p53 expression was no longer present.

3.3.2 Laser/Skin Penetration Experiment

Large specimens of normal caucasian human skin (approximately 20 cm x 10 cm) from breast reduction procedures were taken immediately after excision from each of six patients (mean age 36; age range 28 to 44). A total of 8 skin samples of varying thicknesses were removed from each specimen using both an air-driven dermatome for thinner samples and dissecting scissors to obtain thicker samples. The skin samples were wrapped in saline damp gauze to prevent drying and removed individually only when required during the experiment.

An external energy meter (section 2.1.6) was used to accurately measure the photon energy output from the NMRL. Since the skin samples were to be placed on a coverslip to prevent contamination of the meter, various fluences from the laser were fired directly onto the meter and compared with those noted when the laser was fired through a grade 1 coverslip, which is the thinnest available.

A second pilot study was performed to clarify whether repeated firing of the laser onto the same spot of skin would not affect the subsequent light penetration measurements. A skin sample was therefore positioned on a coverslip over the energy meter as detailed above. The laser was fired three times upon the specimen at three different fluences (4.75, 9.24 and 13.41 J/cm^2) which are doses synonymous with clinical exposure, and an energy meter reading taken. This was then repeated upon a second and a third skin sample each of differing thicknesses and the results noted.

For the main experiment, the skin graft samples were removed from the saline-damp gauze in turn, trimmed to approximately 1 cm^2 and the thickness measured. If the graft samples were thin then a micrometer was used taking care not to crush the tissues. If the specimen was thicker than several millimetres and contained subcutaneous fat then Wernier calipers were used to assess depth. The skin graft samples were then placed dermis down upon a coverslip taking care not to trap any air bubbles. Excess saline was removed and the samples laser treated three times at the aforementioned fluences. The subsequent energy reading was recorded.

3.4 STATISTICS

Sample data has been presented as means (+/- standard deviation). Within the thermal imaging experiment, a comparison between temperature rise and temperature fall between all patient groups was performed by one way ANOVA method. If the normality test failed, then a Dunnett test was performed which is a one way ANOVA on ranks with a selected control. If the normality test passed, then analysis was performed using a Tukey test, which is a pairwise multiple comparison procedure. Analysis of potential correlation between depth of hair shaft damage and depth of p53 expression was performed using the Spearman's rank correlation.

In the laser/skin penetration experiment, comparisons between the energy levels recorded for each fluence of exposure were made for each single skin sample using the one way ANOVA method. However as the thicknesses of the skin samples taken from each patient specimen using the dermatome or scissors varied, a comparison between the samples from each patient specimen was not performed as it was deemed to be too inaccurate. All analyses were performed using SigmaStat™ statistics software, version 1.0 (Jandel Corporation).

3.5 RESULTS

3.5.1 Thermal Imaging Experiment

Thermal Imaging

Thermal imaging of *ex vivo*, hair-bearing skin revealed heat production at the site of the follicles alone when the specimen was exposed to a single pulse of 15 J/cm^2 from the NMRL (Figure 3.1). Figure 3.1a shows a photograph of the dermal aspect of a representative specimen of hair-bearing skin and Figure 3.1b is the thermal image taken of this specimen immediately upon irradiation (as demonstrated by the black edge visible at the top of the circular image showing that the camera was scanning at the moment of irradiation). Figure 3.1c is an image taken at approximately 0.75

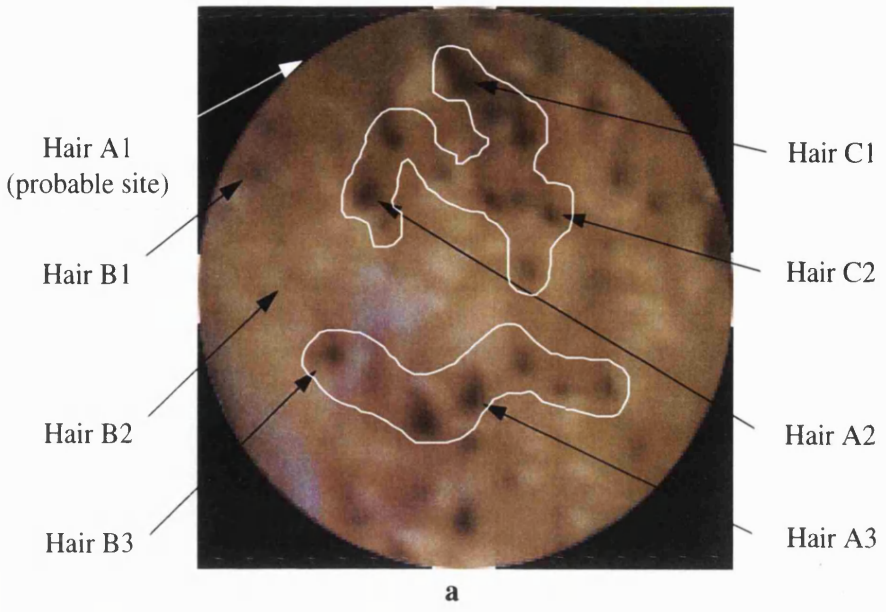

a

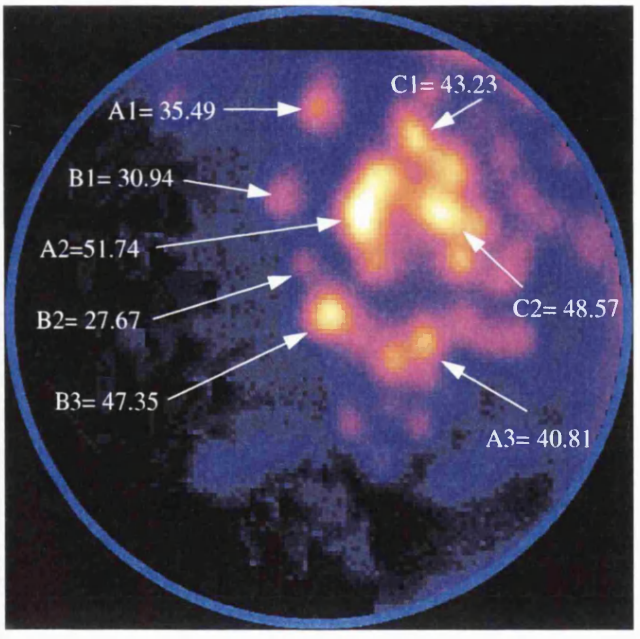

b

c

Figure 3.1:
a: Dermal aspect of a specimen from patient 3 after microdissection revealing the hair bulbs and lower hair shafts (x10). The outlined areas have identified the groups of hairs shown in the thermal image in Figure b.

b: The first thermal image of the specimen in Figure a taken during ruby laser exposure at 15 J/cm^2 and showing the peak temperatures in Centigrade obtained by the identified hairs in Figure a (x8.5).

c: A thermal image recorded at approximately 0.75 seconds after ruby laser exposure showing a reduction in temperature at the sites of the hair follicles but an increase in temperature within the intervening skin (x8.5).

seconds after laser exposure. The temperatures of the hair follicles recorded by the camera immediately upon laser irradiation (Figure 3.1b) varied between 27°C and 52°C, which is a temperature rise of between 7°C and 32°C above the background temperature of 20°C. This heterogeneous rise in temperature seen between hair follicles within the same treatment area was observed in all the samples tested. This phenomenon, from a representative skin specimen, is more clearly illustrated in Figure 3.2. Here, a line has been drawn across the thermal image which bisects a number of different hair follicles (Figure 3.2a). The temperature recorded at each pixel along the line is then plotted in Figure 3.2b over time. The range of temperature rises for all hairs (n=80) from all patient specimens was between 2°C and 32°C with the commonest being between 5°C and 10°C (Figure 3.3). When the temperature rises were grouped according to patient (Figure 3.4), four of the five patients had a mean temperature rise of 9°C, whilst the remaining patient had a mean temperature rise of 18°C. Statistical analysis using a one way ANOVA method revealed that differences in the median values of the follicular temperature rises between the patients were significantly different ($p<0.001$).

Thermal imaging revealed that the high temperatures recorded in the hair follicles reduced over time (compare Figures 3.1b and c and see Figure 3.2b) so that most hairs had virtually lost the temperature gain by two seconds after exposure. In comparison, the temperatures recorded at the intervening skin between follicles rose over time so that the greatest temperatures measured at these sites was achieved when the heat had almost completely dissipated from the follicles. When the rate of temperature change of a particular follicle and its surrounding skin was represented on the same graph (Figure 3.5), it showed that the respective temperature curves would converge and occasionally cross so that the skin could ultimately achieve a greater temperature than that individual follicle. This temperature was often then maintained for the remainder of the recording (approximately 45 seconds) and was noted to be higher than the original starting temperature by between 1°C and 5°C for all specimens examined.

The laser irradiated hair follicles showed a rate of heat dissipation that appeared to be different for each individual follicle within the same treatment site on each patient

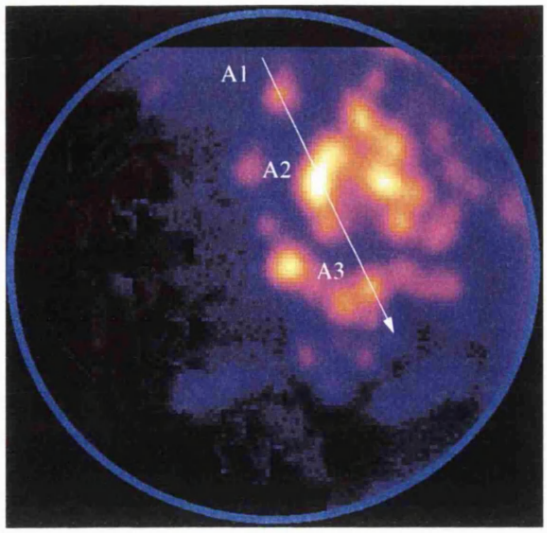

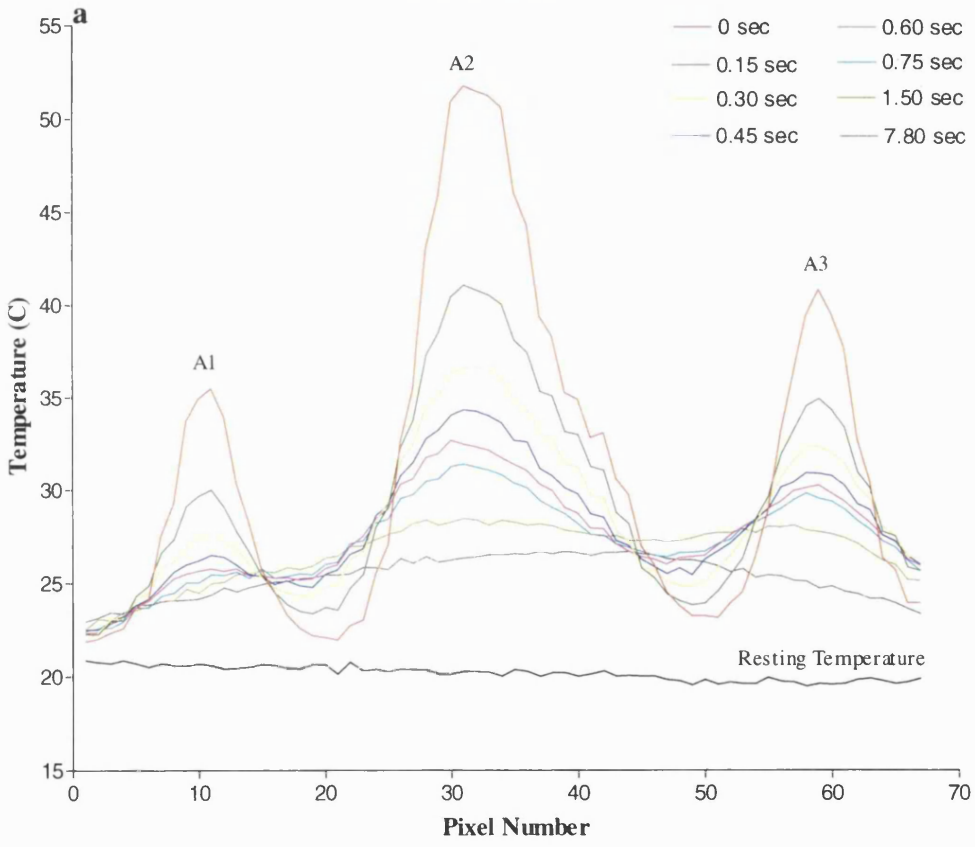

b.

Figure 3.2a: The first thermal image as shown in Figure 3.1b but with an arrow across three hairs (A1, A2 and A3) depicting the pixels along which the temperature changes were recorded over time.

3.2b: Graphical representation of the changes in temperature over time recorded by each of the pixels along the arrow shown in (a). Hairs A1, A2 and A3 have been identified and the increase in the pixel number follows the direction of the arrow.

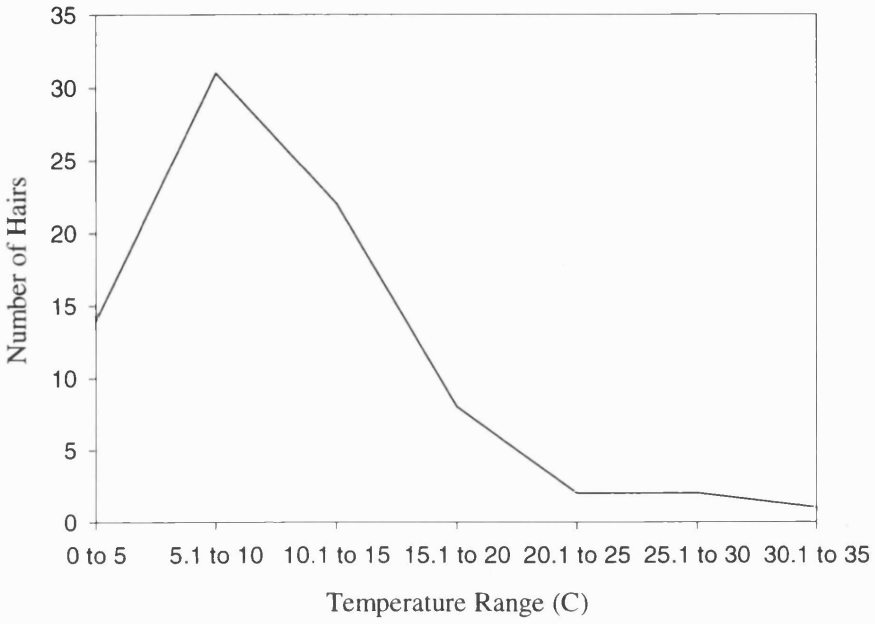

Figure 3.3: Graph showing the distribution of maximum temperature rise recorded for each hair (N=80) measured from all patients. The commonest temperature rise occurred between 5.1 and 10°C.

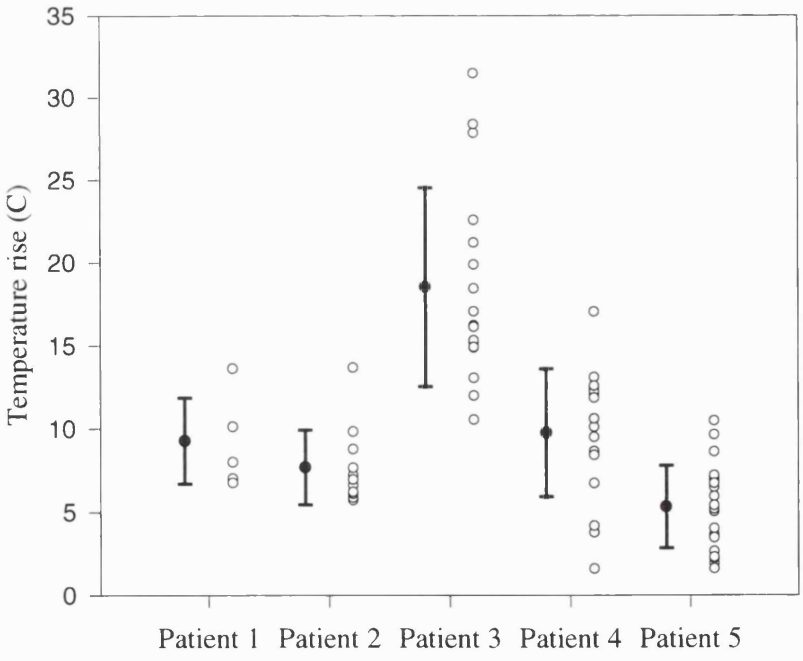

Figure 3.4: Graph showing the distribution of maximum temperature rises according to patient of all hairs measured. The range (hollow dots), the mean and standard deviation (line with a filled dot) are all shown.

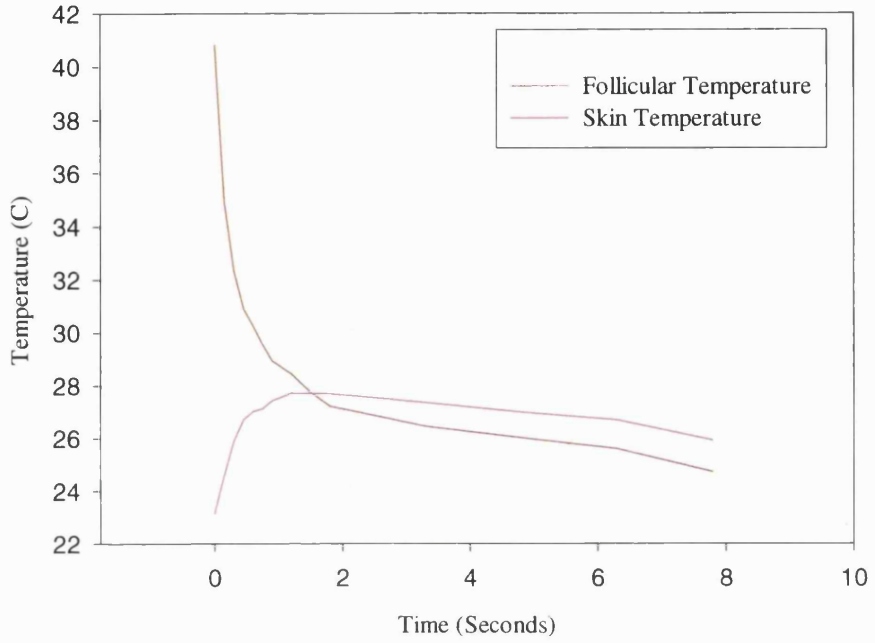

Figure 3.5: Graph showing the change in temperature over time of the hair A3 (at pixel 59) taken from Figure 3.2a and the intervening skin (at pixel 50).

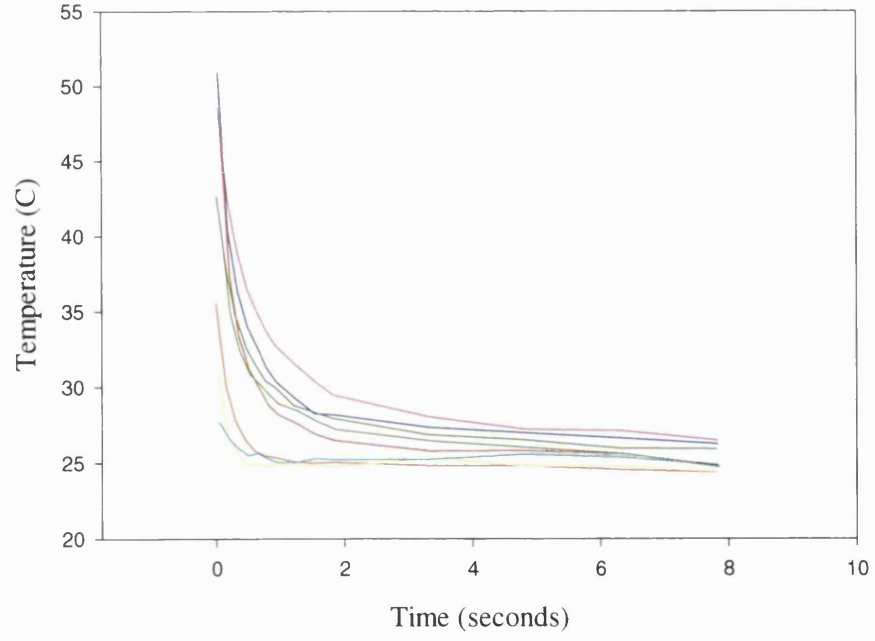

Figure 3.6: Graph showing the rate of heat loss from all hairs measured from a specimen taken from patient 3.

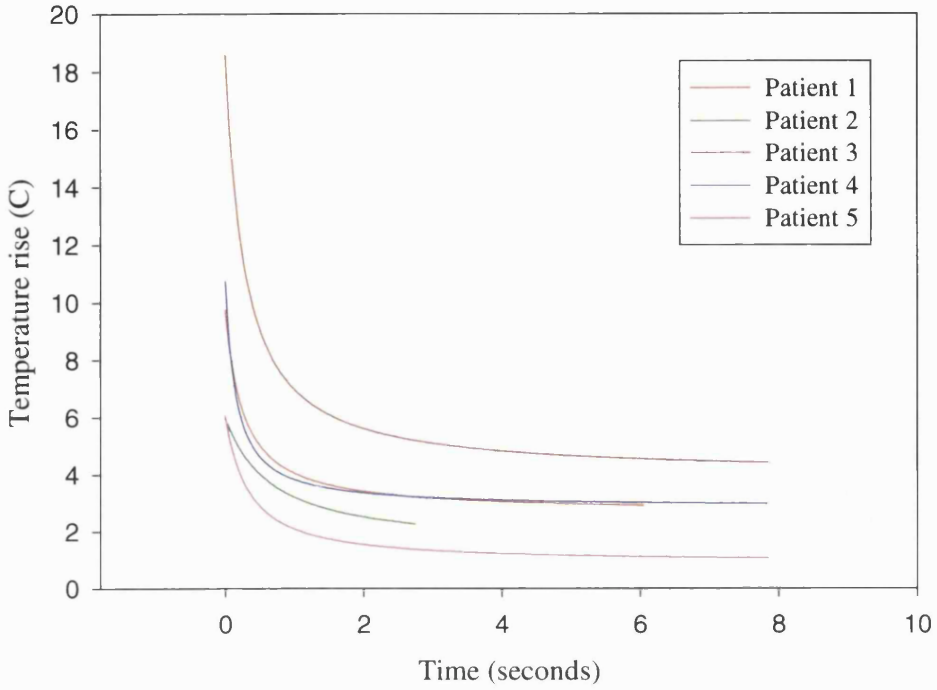

Figure 3.7: Graph showing the best fit curves for the rate of heat loss from all follicles measured according to patient.

specimen (Figure 3.6) although the significance of this could not be statistically proven. The plots of the rate of heat loss for each follicle within each specimen were adjusted to account for the time difference between the thermal imaging camera scanning each follicle in the same treatment field. The curve representing that follicle could then be moved the appropriate distance along the time axis so that its rate of heat loss could be compared in real time with others in the same image. The time taken for each follicle within each patient specimen to lose half its recorded peak temperature (the T50) was calculated from the graphs. A best fit curve representing the rate of heat dissipation of all the measured follicles from both laser specimens from each patient was then plotted (Figure 3.7). The median values of the T50 calculated for each follicle within both laser specimens from each patient were grouped according to patient and statistically compared by one way ANOVA method. This revealed no statistically significant difference in the rate of heat loss from the follicles between specimens from different patients after laser irradiation.

Histology

Modified SACPIC staining allowed identification of the anagen versus telogen growth phases of hairs (Figure 3.8) but also distinguished between damaged and undamaged hair shafts (Figure 3.9). Tangential sectioning of specimens enabled the whole of the specimen and its contained follicles to be viewed at the same time. Damage to the hair shafts was found to occur only in those specimens which had undergone laser irradiation (Figure 3.9). The percentage of hairs that were damaged was assessed for each of the patient specimens and is shown in Table 3.1. The greatest percentage of hair shafts that were damaged (78%) was seen in specimens from patient 3, whose hair follicles had undergone the greatest temperature rises (see Figure 3.4). This was, however, closely followed by specimens from patient 4, where 75% of the hair shafts exhibited damage.

Although the greatest mean and range of depth to which hair shaft damage extended was also noted in specimens from patient 3 (Table 3.1) this difference was not statistically significant from the other patients. Nevertheless, 18% of hairs in

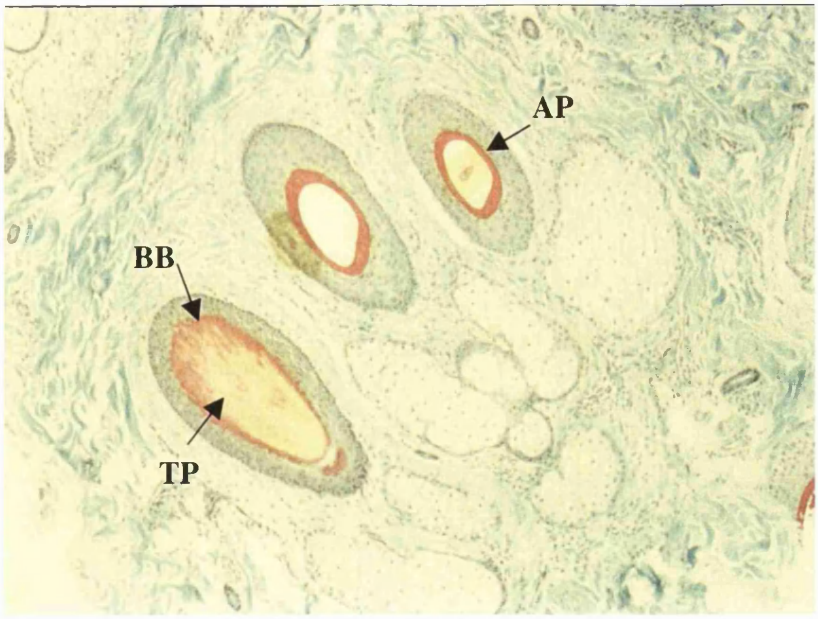

Figure 3.8: Modified SACPIC staining of a tangential section of hair-bearing skin showing a hair follicle in the anagen phase (AP) and a hair follicle in the telogen phase (TP) characterised by the brush border (BB)(x100).

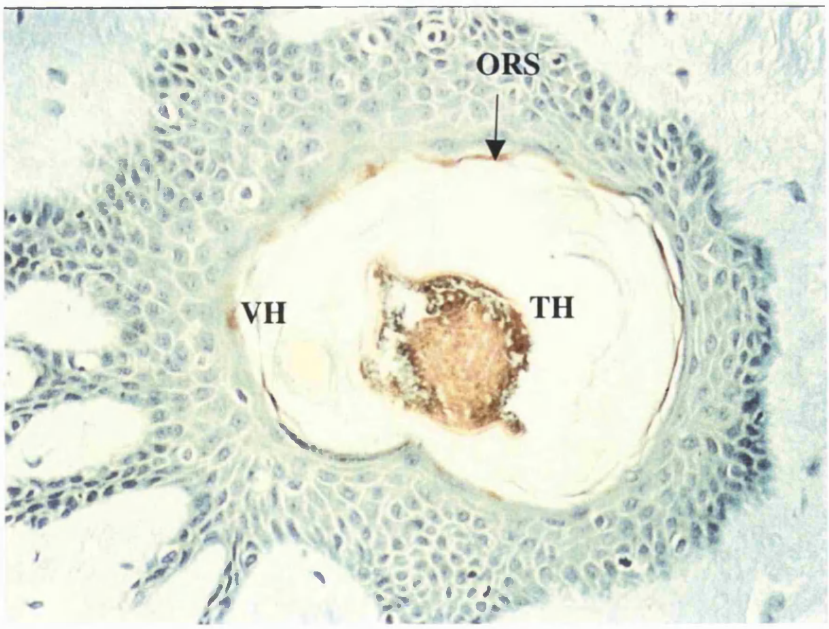

Figure 3.9: Modified SACPIC staining of a section of hair bearing skin having undergone ruby laser exposure showing a follicle containing an undamaged vellus hair (VH) and a damaged terminal hair (TH). The outer root sheath (ORS) has been disrupted (x200).

	Patient 1	*Patient 2*	*Patient 3*	*Patient 4*	*Patient 5*
% Hairs exhibiting damaged shafts (of total examined)	52 (N=86)	55 (N=56)	78 (N=90)	75 (N=122)	30 (N=135)
Mean and range of depth to which damage extended (mm)	0.37 (0-0.74)	0.33 (0-0.66)	0.39* (0-1.64)	0.29* (0-1.17)	0.27 (0-0.54)
% Hairs in telogen phase	14 (N=12)	5 (N=3)	7 (N=7)	14 (N=17)	6 (N=9)

Table 3.1: Table showing the mean percentage of hair follicles from both patient specimens exhibiting histological damage to the hair shaft, with the total number of hairs examined within both patient specimens also shown. The mean and range of depth to which damage was seen to occur to the hair shafts, according to patient, is shown (* depicts those patient specimens in which damage to the follicular hair shafts was noted to extend to the hair bulb) along with the mean percentage of hairs from both patient specimens noted to be in telogen phase.

	Patient 1	*Patient 2*	*Patient 3*	*Patient 4*	*Patient 5*
% Damaged Hairs Expressing p53	91 (N=38)	90 (N=26)	91 (N=63)	93 (N=80)	85 (N=36)
Mean and Range of Depth to which p53 Expression Reached in all Damaged Hairs (mm)	0.08 (0-0.2)	0.06 (0-0.14)	0.12 (0-0.54)	0.092 (0-0.37)	0.06 (0-0.13)

Table 3.2: Table showing the percentage of follicles containing histologically damaged hair shafts whose follicular cells expressed p53 protein. The mean and range of depth to which p53 expression was found within those damaged follicles is also tabulated.

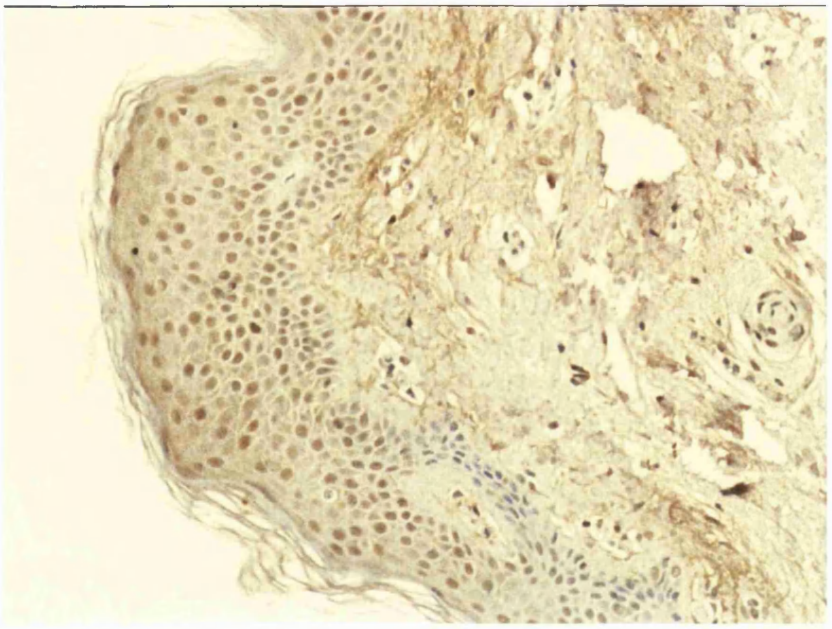

Figure 3.10: p53 immunostaining of a section of a specimen having undergone UV irradiation. Positive nuclei are stained brown and negative nuclei counterstained blue with haematoxylin. Positive nuclei are seen within cells throughout the layers of the epidermis and into the dermis (x200).

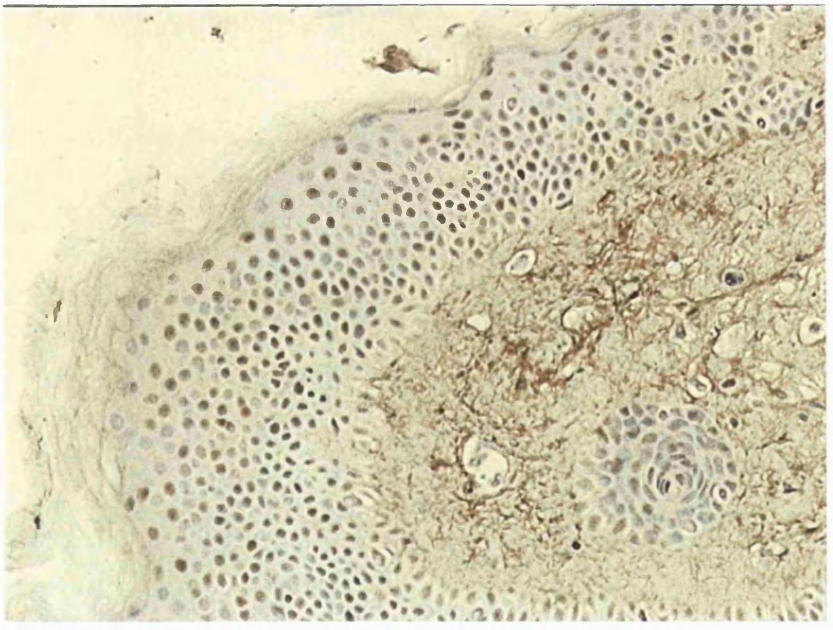

Figure 3.11: p53 immunostaining of a section of a specimen having undergone ruby laser irradiation. p53 expression can be seen to have occurred throughout the epidermal layers within the majority of cells (x200).

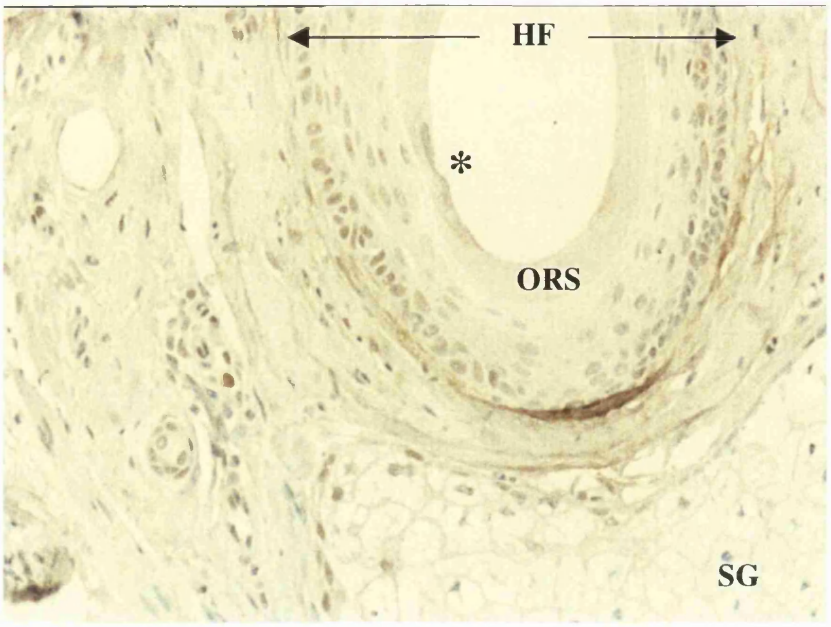

Figure 3.12: p53 immunostaining of a tangential section of a specimen from patient 3 at the level of the sebaceous gland (SG). Damage has occurred to the outer root sheath (ORS) shown by the asterisk and the cells lying adjacent to this area in both the follicle and the sebaceous gland are expressing p53 protein (x200).

specimens from patient 3 had hair shaft damage extending to the hair bulb, whereas this occurred in only 4% of hair follicles within specimens from patient 4 and in none of the specimens examined from the remaining patients.

Immunohistochemical staining for p53 expression was performed upon all specimens. All positive controls from each patient revealed p53 expression throughout the epidermis in the majority of the keratinocytes and also in dermal cells (Figure 3.10), which was not seen in sections of the negative controls. The epidermal keratinocytes of specimens exposed to a single pulse of 15 J/cm^2 from the laser also expressed p53 protein after 18 hours incubation (Figure 3.11). Unlike the positive controls, p53 staining was also seen in the viable cells lining the canals of the hair follicles whose contained hair shafts showed damage (see Figure 3.12). The cells of those follicles whose shafts did not show damage did not express p53 protein. The percentage of shaft-damaged hair follicles whose cells expressed p53 protein is shown in Table 3.2. This was consistently high throughout all patient specimens (85 to 93%). The mean and range of depth to which p53 expression occurred in the viable cells of the follicles from the laser irradiated specimens was greatest in patient 3, which achieved the greatest follicular temperature rises (Figure 3.4).

The extent to which p53 expression was seen to occur radially from the damaged follicles was usually limited to the cells of the follicles alone (specifically those of the outer root sheath) with surrounding fibroblasts, endothelial cells and glandular tissues appearing unaffected. However, the specimens from patient 3, whose follicles reached the greatest temperatures, contained follicles where positive p53 expression was often seen within the adjoining sebaceous gland too (Figure 3.12).

A statistically significant difference using one way ANOVA method was seen between the patient specimens when comparing the median values of the depths to which p53 expression was noted within the viable cells of follicles whose hair shafts were damaged ($p<0.05$). The correlation between the median depth of hair follicle damage and the median depth of p53 expression within the viable cells of those same follicles was analysed using a Spearmans Rank Correlation (SRC) test incorporating

the two specimens from each patient. This revealed a good correlation between the two median variables for each of the patient specimens. Those from patient 1 had an SRC of 0.66 ($p<0.05$), from patient 2 an SRC of 0.87 ($p<0.05$), from patient 3 an SRC of 0.66 ($p<0.05$), from patient 4 an SRC of 0.76 ($p<0.05$) and from patient 5 an SRC of 0.77 ($p<0.05$).

3.5.2 Laser/Skin Penetration Experiment

Firing the NMRL through a coverslip onto the energy meter did not change the fluence recorded by the energy meter compared to the energy recorded when the laser was fired upon the meter alone. In addition, firing the laser repetitively at the same fluence through the same skin graft sample did not result in any change in the fluence registered by the energy meter beneath. This was also noted when the fluence was varied and the sample thickness was varied too.

A plot of the energy changes versus skin thickness at the three fluences used from graft samples from a representative patient specimen has been shown in Figure 3.13. The plots at all three fluences appeared to show two very distinct rates of energy drop with depth. Linear regressions were produced for each of the three fluence plots to depict the fluence-depth profiles through *ex vivo* skin taking into account the apparent shape of the profiles according to the plots (see Figure 3.13). As mentioned, all three fluences appeared to experience a rapid drop in energy within approximately 0.6 mm depth of the skin graft samples, which amounted to approximately a 50% "energy loss" as recorded by the energy meter. It is important to clarify that by energy loss, the author means the difference in the energy recorded by the 12 mm diameter meter when the laser had been fired through the skin graft sample compared to the original incidence fluence recorded. Therefore any scattering of the beam beyond 12 mm's would not be recorded. Once the photon beam had penetrated beyond this first millimetre, the energy drop became much less marked over increasing depth resulting in the two distinct linear relationships of "energy loss" through *ex vivo* skin.

The regression lines representing the linear relationships found in the deeper regions

Table 3.3: Table showing that no change in fluence was recorded by repetitive firing of the same fluence value upon the same thickness of skin sample.

Depth (mm)	Fluence emitted (J/cm²)	Fluence recorded J/cm²)
0.54	4.75	2.60
		2.60
		2.60
	9.24	5.47
		5.47
		5.47
4.25	4.75	1.69
		1.69
		1.69
	9.24	3.66
		3.66
		3.66

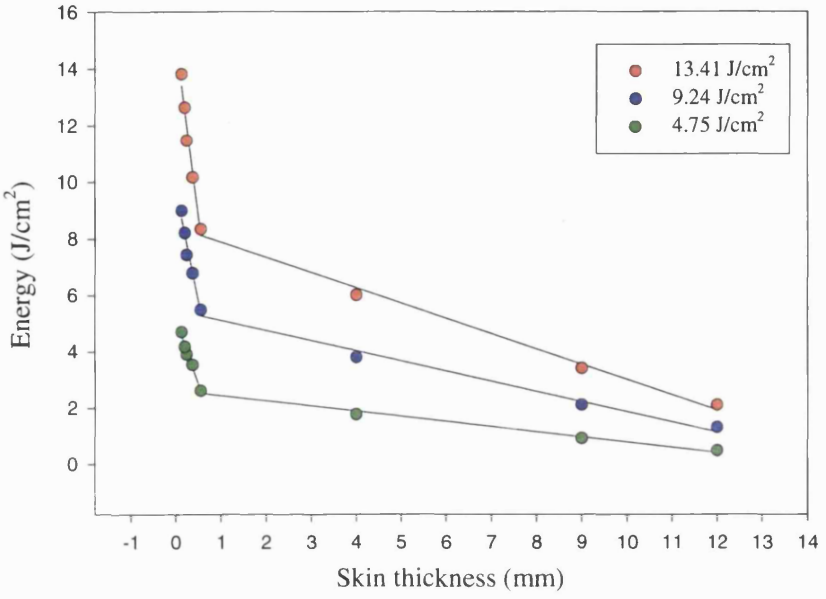

Figure 3.13: Graph representing the laser light penetration profiles at three incident fluences through *ex-vivo* skin.

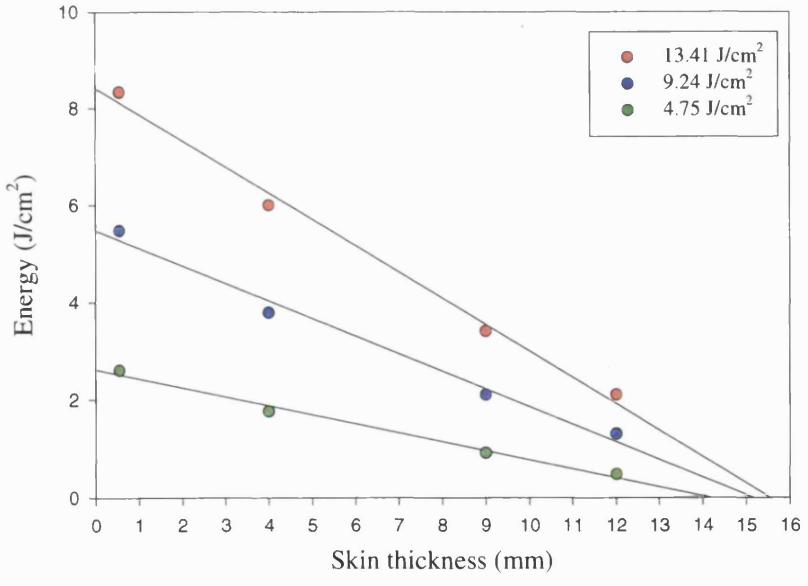

Figure 3.14: Graph showing an extrapolation of the plots in Figure 3.13 above to the x axis revealing the probable maximum depth of penetration of the ruby laser beam in *ex-vivo* skin.

Table 3.4: Table showing the maximum depth of penetration according to fluence of exposure for all 6 patient specimens.

Patient	Fluence emitted (J/cm^2)	Maximum depth of penetration (mm)
1	4.75	14.24
	9.24	15.08
	13.41	15.50
2	4.75	14.35
	9.24	14.97
	13.41	15.24
3	4.75	14.67
	9.24	15.14
	13.41	15.33
4	4.75	14.19
	9.24	14.90
	13.41	15.36
5	4.75	13.97
	9.24	14.42
	13.41	14.92
6	4.75	14.16
	9.24	14.89
	13.41	15.26

of skin were extrapolated to the x axis for each of the fluences tested and were found to converge to within several millimetres of each other (see Figure 3.14). This was performed for all 6 patient specimens tested (not shown) and gave a mean maximal depth of penetration at 4.75 J/cm^2 of 14.26 mm (SD 0.24 mm), at 9.24 J/cm^2 of 14.90 mm (SD 0.26 mm) and at 13.41 J/cm^2 of 15.27 mm (SD 0.19 mm) see Table 3.4. Comparisons by one way ANOVA method of the maximum depth of penetration according to fluence of exposure between the 6 patient specimens revealed a statistically significant difference ($p<0.001$) between the three fluences used. However, the range of this depth of penetration varied by a maximum of 1.53 mm only.

3.6 DISCUSSION

3.6.1 Thermal Imaging Experiment

This study has shown that on exposure of specimens of hair-bearing skin to a single pulse from a NMRL, heat is preferentially produced in the hair follicles presumably from the conversion of photon energy. Ruby laser does indeed therefore appear to specifically target hair follicles and this is presumably due to the greater quantity of chromophore within these specific skin appendages.

Heterogeneous temperature rises were achieved in hair follicles within the same treatment site in all patient specimens measured. This would suggest that a difference or several differences, inherent to the hair follicles, exist between them resulting in a variance in heat production. This could be due to interfollicular differences in hair pigmentation. There are two types of melanin, the red/yellow phaeomelanin and the brown/black eumelanin. Relative phenotypic expression of both by the individual is governed by genetic inheritance. Work by Liew et al has shown that the darker eumelanin is the chromophore associated with successful ruby laser-assisted depilation (Liew, et al., In press). Therefore the quantity of this particular chromophore may be important in determining the amount of heat produced and therefore the relative success of laser treatment.

A statistically significant difference in temperature rises was also noted between follicles from different patient specimens. This does not appear to correlate with the percentage of hairs in the growing phase (see Table 3.1). It would be more likely that the chromophore differed between the patients eventhough all patient specimens were taken from caucasians of a Fitzpatrick skin type 2 or 3 with similar coloured dark hair. Another possibility would be that the hairs from different patients acted differently to the heat produced with those in the specimens achieving greater temperatures having a greater combustive nature.

At present it is still unclear exactly which parts of the hair follicle need to be destroyed to prevent regrowth. It is thought that the stem cells reside at the hair bulge region (Cotsarelis, et al., 1990) which is approximately two thirds the way down a hair follicle (Rochat, et al., 1994) and also within the hair bulb during the anagen or active growth phase. During the involuting phase the hair bulb rises to the level of the bulge and it is believed that stem cells with interspersed melanocytes migrate from the bulge to the site of the old bulb. This "new" bulb then descends to the original site and a new anagen phase commences. These two sites have been described as containing melanocytes and melanin pigment to a variable extent which is cycle dependent (Narisawa, et al., 1997). Whether the chromophore is present in sufficient quantities to produce enough heat at these sites cannot be answered. It is perhaps more likely that the majority of heat is produced within the highly pigmented hair shaft and dissipation of this heat to the adjoining viable cells is the main cause of cellular damage. Heat could be seen to transfer from follicle to skin, which would lend support to this theory. Nevertheless, whether the photon energy, which eventually reaches these depths, is great enough to produce a sufficient heating effect to damage those cells is also unknown.

Heat-induced damage to the viable stem cells of the hair follicles will depend on the peak temperature achieved and the time taken for it to dissipate. The rate of heat loss appeared variable between follicles within the same treatment sites but due to the nature of the experiment statistical testing was not possible. The rate of heat loss,

when compared between patients, was found not to be significantly different. In addition, for all specimens, the heat produced had almost completely dissipated 2 seconds after irradiation. Cultured human epidermal keratinocytes have been found not to survive a one second exposure to heating over 58°C (Bowman, et al., 1997), which might imply that this factor would have a minimal influence upon successful depilation. It could also suggest that differences in thermal relaxation times may not be important in determining the extent of damage caused by laser treatment. The peak temperature however, did vary significantly between patients with one achieving markedly greater temperatures at hair follicles during irradiation. The greatest temperature rise in this experiment was 32°C suggesting that *in vivo*, the follicle would be approaching a temperature of 69°C. Cellular damage was assessed by p53 protein expression which has been stated to undergo increased cellular expression after exposure to a thermal insult (Nakazawa, et al., 1998) (Matylevitch, et al., 1998). p53 protein is able to halt cell cycling to allow the cell to repair itself or, if the damage is deemed to be too great, can instigate apoptosis. From 58°C to 72°C it has been stated that the cell undergoes a mixture of accidental cell death and apoptotic cell death with the latter alone involving p53 (Matylevitch, et al., 1998).

p53 expression was found to occur within the positive controls and the laser exposed specimens in all patient specimens. In the positive controls expression was noted within the epidermis whilst in the laser specimens, in addition to the epidermis, expression was also seen in cells lining the hair follicles, but only of those follicles whose hair shafts were seen to be damaged. p53 expression was noted to extend to a greater depth in the cells of follicles from the specimens whose follicles achieved greater temperatures. A good correlation was noted between the depth of p53 expression in follicular cells lining the hair canals and the depth of hair shaft damage by Spearmans rank correlation of median values. Damage to hair shafts was also noted to occur in laser irradiated specimens alone and this was noted to extend to the hair bulb to a greater extent in specimens from the patient whose follicular temperatures were greatest.

p53 expression within cells was found to extend in a radial fashion within the hair follicle. It is likely that some of the more severely damaged cells are incapable of expressing p53 and so the stain would probably underestimate the extent of cell death resulting from heat production. Nevertheless, the outer boundary of cells suffering from heat damage should express p53, as the temperature should decrease in a radial fashion away from the source so delineating the extent to which detectable heat-induced damage had reached. p53 expression was found to occur within the sebaceous gland of specimens from patient 3 alone whose follicles underwent the greatest temperature rises suggesting that damage could and had extended beyond the limits of the follicle itself. Figure 3.12 is a section from one of the two specimens from patient 3 and has been cut at the level of the sebaceous gland. Damage has occurred to the outer root sheath and the viable cells lying adjacent to this site both within the hair follicle and the sebaceous gland have stained positive for p53 protein. Sufficient heat could therefore have passed from the hair shaft outwards resulting in damage being inflicted upon these cells. It could also imply that damage could have occurred to the bulge region, which resides just below the sebaceous gland but in the outer root sheath, to possibly produce permanent depilation.

The thermal imaging camera showed that the skin between hair follicles in all the specimens used did not heat directly upon ruby laser irradiation but afterwards due to dissipation of heat from the hair follicles. Apart from the hair follicles, melanin within skin is confined to the epidermis. However, any heat produced at this site would not be seen by the thermal imaging camera which was focused on the dermis. This may be due to the heat production by such small concentrations of melanin being undetectable or that the thermal imaging camera cannot detect it until it has diffused through to the deep dermis. It is possible that the prolonged temperature rise seen in skin after laser exposure (up to 5°C for approximately 45 seconds) could cause the side effect of damage to the non-follicular skin structures. However, it must be remembered that these experiments were necessarily performed on skin biopsies and therefore in the absence of the effects of uninterrupted circulation. The circulation of blood undoubtedly aids the dissipation of heat from the skin considerably (Welch, et al., 1980). However, it would seem unlikely that blood flow would affect the peak

temperatures recorded at the follicles as the flow rate, when compared to the pulse duration of the laser, is much slower. It is more likely that any side effects of skin damage associated with laser depilation are mainly as a direct result of the presence of melanin within the epidermis and the consequent localised production of heat. This is in agreement with the common observation that side effects are more prevalent in patients with darker skin and ultrastructural findings of damage to the melanosomes within the keratinocytes of the epidermis (Liew, 1999).

In summary, this experiment would appear to reflect the present clinical scenario. The ruby laser does appear to interact specifically at the site of the hair follicle where heat is produced to an extent in some cases that could result in permanent damage being inflicted upon the viable hair producing cells of the hair follicles preventing hair regrowth. p53 expression was noted to occur radially beyond the extent of hair follicles in specimens from one patient which would, by implication, suggest that damage to the bulge region could have occurred as the heat traversed this region to reach the sebaceous gland.

A significant difference was noted between the median follicular temperature rises between patient specimens. This could suggest that something intrinsic to the hairs of this patient affects the maximum temperature achieved by laser treatment. A higher temperature could be reached by either increased photon energy conversion and/or combustibility of the hair shaft which accounts for the temperatures achieved by a particular follicle and the subsequent damage incurred. Further work is required to assess whether a change in the laser parameters (not possible with this laser), particularly the pulse duration, would achieve greater temperature rises or greater histological damage to the sites where it is required to do so to achieve a greater depilatory success rate.

3.6.2 Laser/Skin Penetration Experiment

The pilot studies showed that irrespective of the thickness of the skin sample used or the fluence of irradiation, repetitive firing of the laser did not affect the penetrative

properties of the skin. The two factors that would influence the penetration of any beam of light within a tissue are the absorptive capability and the scattering capability of the tissue with respect to the particular wavelength of light (Gemert, et al., 1989). Since the natural chromophore is only ostensibly present in the epidermis of hair-free skin and the high rate of energy drop continues over a much deeper range (which would include part if not all of the dermis) then the majority of the energy drop is more likely to be due to scattering rather than absorption by chromophore. Scattering of laser light occurs when the photons within the beam strike an object, which could be the collagen within the dermis (Anderson, et al., 1979) or the Malpighian layer (stratum spinosum) (Bruls and Leun, 1984), as have been suggested so becoming deviated away from the original pathway and beyond the detection of the meter. The collisions would not change the nature or structure of the object as the object would not be a chromophore for that wavelength of light therefore making this a constant feature of the specimen as was found in the experiment. The results would therefore appear to support the statement that at the wavelength used of 694 nm, scattering dominates over absorption (Anderson, 1984), (Rosenberg and Gregory, 1996), (Gemert, et al., 1989).

The energy meter recorded a loss of up to 50% of the incident fluence when the beam travelled through the first 1 mm of skin. This most likely resulted from the scattering effect mentioned and would support the hypotheses that the greatest hindrance to a photon energy beam traversing the skin was from either the Malpighian layer (Stratum spinosum) of the epidermis, the dermis or both. Beyond the depth consistent with the dermis and at the levels of the subcutaneous fat, the energy drop became much reduced over the distance travelled from the skin surface. Melanin pigment does not exist at levels deeper than the epidermis in hair-free skin and so reduced absorption could be responsible, but the most likely reason would be a change in the tissue type. The structure of fat is hugely different to that of the overlying skin epidermis and dermis and so it is quite possible that this would reduce scattering away from the original beam axis so reducing the recorded energy loss.

The linear regression lines produced for each of the three fluence values converged with increasing thickness of skin. This could suggest that a fixed proportion of the total incident fluence is lost from the original beam pathway with increasing distance travelled from the skin surface irrespective of the fluence and appeared to be consistent between skin specimens. Extrapolating the lines to the x axis where the energy would be zero, thereby predicting the maximum depth of penetration, showed that there was no statistically significant difference between the depths reached by the same fluence value between patient specimens but a significant difference did exist between the depths of penetration for the three fluence groups. It is important to state though that the difference between the maximum extrapolated penetrative depths recorded for each patient's skin specimens was only 1.5 mm and so could be accounted for by user error. If so then this would support the possibility of a fixed percentage energy drop occurring over skin depth at any fluence value resulting in a convergence of the lines and that depth of penetration of light is a function of the wavelength alone (Anderson, 1984). The findings regarding the maximum depth of penetration of the ruby laser beam at 694 nm (14.8 mm +/- 0.478) are not in agreement with the results published by several authors who have stated that this depth, at the wavelength used, was of the order of 2 to 3 mm (Anderson and Parrish, 1981), (Anderson, 1984), (Gemert, et al., 1989), (Rosenberg and Gregory, 1996). However they do match those reported by Flock et al who, using a tissue phantom, stated a maximum depth of penetration of between 10 to 20 mm depending on the albedo and radius of the laser beam (see section 1.5.2). However, notably, the figures produced by the Monte Carlo model still required adjustment to coincide with their experimental results. Nevertheless, it would appear to state that their experimental model was a reasonably accurate representation, in this respect, of *ex vivo* skin.

The average length of the adult hair follicle has been recorded at 3.85 mm and the bulge region stated as existing approximately two-thirds the way down the follicle, equating to a depth of 2.56 mm (Rochat, et al., 1994). The graph in Figure 3.14 would suggest that the energy reaching those depths through the skin was approximately 50% of the incident value. The skin used in this experiment contained no terminal hairs and their effect can only be surmised. An increase in absorption of light at 694

nm at dermal and subdermal depths would be expected with hair-bearing skin because of the chromophore present in hair follicles. In addition, light scattering may also be greater on account of the additional structures present within the target field. Both these factors could reduce the energy recorded at varying depths within the skin and so could reduce the energy reaching the areas important for permanent depilation. By how much this could occur cannot be answered and would require hair-bearing skin to be evaluated by the same technique used here.

As mentioned, only approximately 50% of the incident fluence should have reached the depth of both the bulge region and the hair bulb. Whether this energy would be sufficient to produce damage to the viable cells of these regions is unknown. Nevertheless, results of the modified SACPIC and p53 staining show that neither obvious disruption of the hair shaft nor induction of the cellular damage protein p53 reaches anywhere near the average depths of these regions. However it would suggest that a sizeable proportion of the laser energy is transmitted through the skin, the amount of which can be increased by increasing the laser fluence, but whether this is the main pathway of action cannot be stated. Work performed by Liew and colleagues showed that a greater depilatory success rate was achieved in individuals with a greater quantity of eumelanin. The results could therefore suggest that the limiting factor is the presence of the correct, or an adequate amount of chromophore in the hair follicle. Therefore, if it were possible to add chromophore to the requisite site, then the energy reaching those levels may well be great enough to produce sufficient damage.

3.7 CONCLUSIONS

- Normal mode ruby laser irradiation of hair-bearing skin produced heat localised to the hair follicles.

- Temperature rises exhibited would reach levels *in vivo* great enough to cause protein denaturation.

- Temperature rises in the intervening skin was delayed and presumably due to dissipation of heat from follicles.

- Heterogeneous temperature rises occurred at hairs within the same specimens and between patients.

- Percentage of damaged hair shafts was greatest in the specimens with the highest temperature rises.

- Hair shaft damage reached a greater depth in specimens whose follicular temperatures were higher.

- p53 staining was almost exclusive to hair follicles whose hair shafts were obviously damaged.

- p53 staining was greater in specimens whose follicles reached a higher temperature occasionally extending radially beyond the follicle itself.

- The depth to which p53 expression occurred within viable cells lining the hair follicles correlated well with the depth of hair shaft damage noted.

- The mean maximum depth of penetration of light of wavelength 694 nm in skin was 14.8 mm +/- 0.478mm and would appear not to be fluence dependent.

- Increasing the incident fluence did increase the fluence levels recorded at various depths within the *ex vivo* skin samples, though a greater percentage reduction in fluence occurred the higher the fluence with increasing depth.

- Sites of greatest "energy loss" from the original beam axis occurred in the epidermal and dermal regions of the skin graft specimens.

- Approximately half the incident fluence was available at depths consistent with the sites of the hair producing regions.

CHAPTER 4 - AN ANIMAL MODEL ASSESSING RUBY LASER-ASSISTED DEPILATION

4.1 INTRODUCTION

The published data from clinical trials performed so far report a wide variation in the efficacy of normal mode ruby laser-assisted depilation even under standardised treatment conditions. This is presumably due to large inter-patient phenotypic differences. The importance of such intrinsic differences between patients is also suggested by the results obtained in Chapter 3. Therefore an animal model where genetic variation is minimal is required to allow detailed examination of the efficacy of depilation and also to test the effects of various treatments to prevent skin side effects.

The effect of normal mode ruby laser (NMRL) irradiation upon hair bearing skin has already been studied in animal models using dogs and, more recently, mice. Grossman et al (Grossman, et al., 1996) recorded histological changes in the skin of black-haired dogs after exposure to a single pulse of either 40 J/cm^2, 70 J/cm^2 or 160 J/cm^2 fluence from an NMRL of pulse duration 270 μsec and spot size 8 mm, 6 mm and 4 mm respectively. Damage was noted histologically in the follicular epithelium and dermal collagen matrix, which increased in severity with increasing fluence of exposure, until at 160 J/cm^2, extensive damage to dermal structures, reticular dermis and adnexae was recorded. The depilatory effect of such irradiation was not examined specifically, but the histological findings reported would suggest that the NMRL targeted hair follicles in the dog and the damage induced was either fluence and/or spot size dependent. The latter has already been stated as possibly affecting laser penetrance into skin (Anderson, 1984).

Lin et al (Lin, et al., 1998) used the synchronised hair growth pattern found in the black-haired mouse to study the effects of NMRL exposure upon hair follicles in various stages of the hair cycle. Three fluences were used, 1.47 J/cm^2 (pulse duration

1.7 msec, spot size 1 cm), 2.29 J/cm^2 (1.8 msec pulse duration, spot size 1.1cm) and 3.16 J/cm^2 (2.2 msec pulse duration, spot size 1.3 cm). The results appeared to show that in the mouse, a more successful laser-assisted depilation, assessed by a subjective hair count score at 28 and 56 days post-exposure, was achieved when hairs were in the early stages of anagen. Catagen and telogen stages were associated with full hair regrowth by 28 days. It was reported that histologically dermal fibrosis had replaced degenerated hair follicles where anagen hair follicles had originally been exposed to laser irradiation. Hair follicles treated in the catagen or telogen phases were noted to be undamaged when viewed in sections.

The black-haired mouse, of which presently two strains are commercially available, C57BL/6 and C57BL/10, has been studied extensively by Dry (Dry, 1926) who recorded the hair types present, the hair growth and shedding patterns in addition to histological studies of the follicles in the various growth phases. The growth phases he divided into three parts although they are, in fact, a continuum. Firstly, the growing or anagen phase, secondly the regressing or catagen phase and finally the resting or telogen phase (see section 1.3 and Figure 1.3). These mouse strains have been described as having a non-pigmented skin and darkly pigmented follicles which undergo profound changes on transition from growing (anagen) to regressing/resting (catagen/telogen) phases. In anagen, the follicles extend to a depth of 500 μm or more from the skin surface into fat and are much larger in size (Chase, et al., 1951) with the shafts containing abundant melanin throughout their length (see Figure 4.1). This gives the mouse skin a patchy appearance with apparently pigmented regions of skin consistent with areas containing hairs in anagen phase (see Figure 4.2). In the resting phase, the hair shaft is much thinner, extends only approximately 250 μm into the skin (Chase, et al., 1951) and contains melanin pigment mainly above the level of the skin surface with little, if any, present below the skin surface (see Figure 4.3). This makes the skin containing hair in telogen phase characteristically appear pink in colour (Figure 4.2)(Chase, 1954). The anagen phase could be induced in resting hair regions by either plucking or close trimming of the hairs. This stimulated the follicles into growth in these areas after approximately 1 to 2 weeks. The bulge region, the putative site of the follicular stem cells, has been extensively studied in the mouse and is

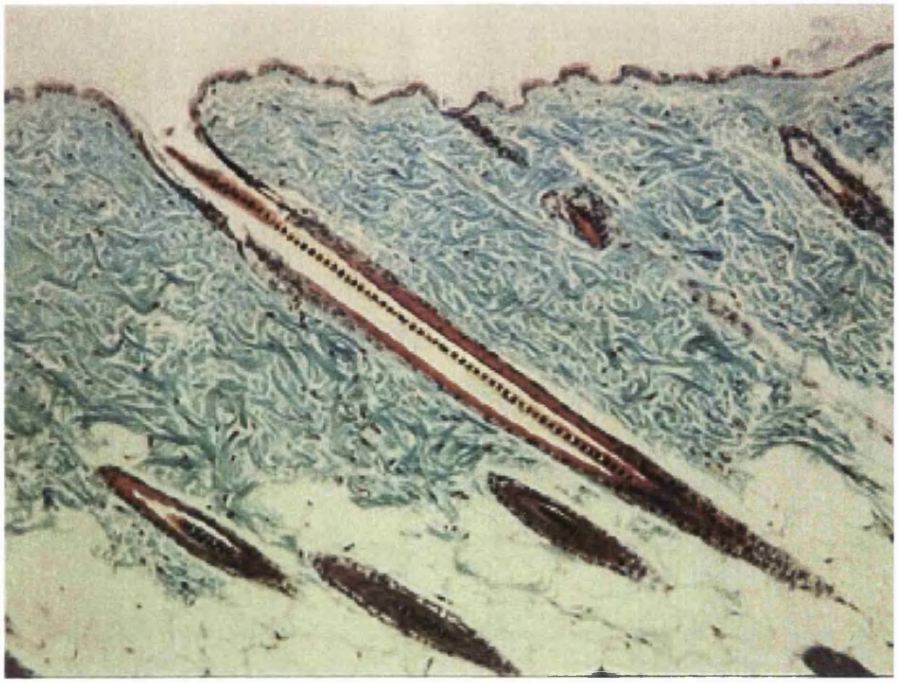

Figure 4.1: Transverse section through mouse skin showing a hair in anagen phase. Melanin can be seen throughout the length of the hair shaft (x100).

Figure 4.2: Photograph of the trimmed back of a black haired mouse illustrating the black patches synonymous with hairs in the anagen phase and pink patches synonymous with hairs in telogen phase.

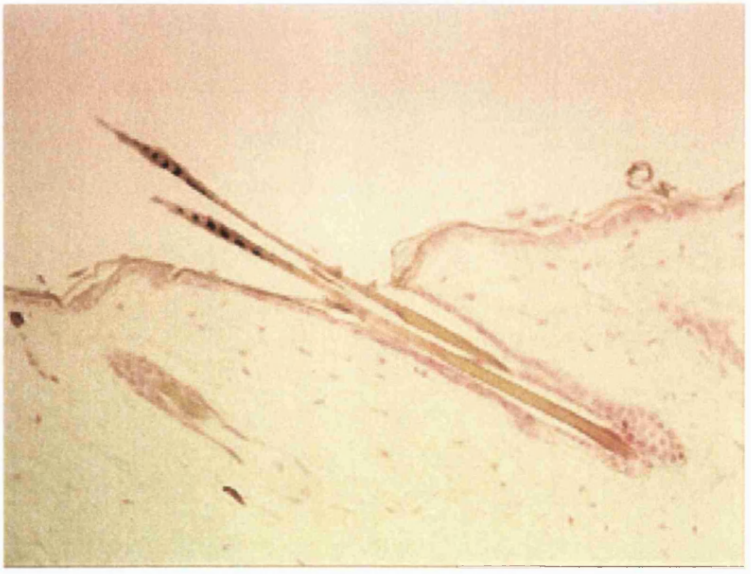

Figure 4.3: Transverse section of mouse skin stained with Massons fontana showing that for hairs in telogen phase, the melanin is restricted to that portion of the hair shaft which protrudes from the skin surface.

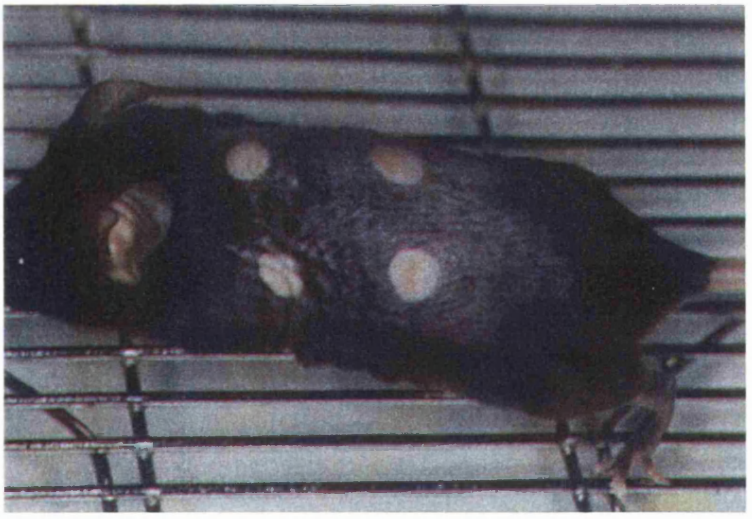

Figure 4.4: Photograph of a mouse 1 day after exposure to ruby laser irradiation with the fluences starting at top left and rotating anti-clockwise being 5, 6, 7 and 8 J/cm^2.

thought to reside just below the level of the sebaceous gland (Cotsarelis, et al., 1990). Its position does not change throughout the hair cycle.

The C57BL/10 black-haired mouse was chosen as the model for use in this thesis. The hair colour is of a uniform dark, eumelanin type throughout the diameter of the shaft, which is the ideal chromophore for the NMRL (Liew, et al., In press). The genetic inbreeding of the mouse strain also allowed a more accurate and realistic comparison of results between individual animals than would be possible in the more genetically diverse human subject. However, in contrast to humans, the epidermis of mouse skin is only 2 cells thick (Dry, 1926) which could make it more susceptible to skin side effects resulting from laser irradiation. Therefore it was important to establish the fluence range associated with depilatory success and minimal side effects.

4.2 AIMS

- To establish which fluence of laser treatment results in permanent depilation in the black-haired mouse model whilst producing minimal skin side effects.
- To confirm the findings of Lin et al (Lin, et al., 1998) on the effects of hair cycle on the efficacy of laser depilation.

4.3 METHODS

22 mice were anaesthetised and the hair trimmed from their backs. Dry, 1926 #246 described the hair growing regions as being darkly pigmented areas of skin compared to the pink regions where the hairs are either in the regressing stage (catagen) or the resting phase (telogen). Eight mice with larger pigmented areas were chosen to have those regions irradiated by the NMRL to assess its long-term effect upon growing (anagen) hairs. A further eight mice were chosen to assess the depilatory effect of the NMRL upon the resting hair sites, seen as pink in colour. The remaining six mice would be sacrificed immediately after irradiation of both growing hair and resting hair regions and 6 mm biopsies taken and processed for routine paraffin-wax histology (see section 2.3).

Each mouse was laid individually upon a clean surgical drape, 4 treatment sites were identified and each exposed to a single pulse of either 5, 6, 7 or 8 J/cm^2 from the NMRL as described in section 2.5.3 (see Figure 4.4). The appropriate mice were then sacrificed immediately after treatment and had the laser-irradiated sites biopsied along with non-irradiated, trimmed controls taken from growing and resting hair regions.

Wound evaluation was performed on a daily basis, classified and scored according to Table 2.4 until healed completely. The laser exposed sites were then permanently marked by tattooing whilst the mouse was anaesthetised to facilitate future identification. Depilatory success was scored weekly according to Table 2.6 over a time period of 56 days. All mice were then sacrificed and 6 mm biopsies taken from the previously irradiated sites along with non-irradiated trimmed controls harvested at least 2 cm away from the exposure site. These were processed for routine paraffin-wax histology (see section 2.3).

Histological evaluation was performed upon 12 randomly chosen groups of three consecutive transverse sections taken from specimens biopsied immediately after NMRL exposure. In addition, 12 randomly chosen consecutive pairs of sections taken from specimens biopsied 3 months after laser exposure were also analysed. Three staining techniques were employed upon the immediate group. Haematoxtylin and eosin (H&E) staining was used to look for the sites and the extent of cellular damage, whilst the modified SACPIC staining technique confirmed the growth phase of the hairs in addition to the extent of hair shaft damage. The third staining technique used was Massons Fontana which stains for melanin pigment (see section 2.3 for the various staining techniques).

The paired sections from biopsies taken at three months were stained with H&E to assess for cellular damage and Massons trichrome to look for any signs of scarring within the dermis synonymous with permanent skin damage (see section 2.3).

4.4 STATISTICS

Sample data are given as means +/- standard deviation. A statistical comparison of two groups was performed using the Student's t-test upon mean values but where the normality test failed then a Mann-Whitney Rank Sum test was performed upon median values. A comparison of more than two groups was accomplished using the one way ANOVA method. If the normality test failed then either a Dunnett's test, which is a pairwise multiple comparison procedure, was performed or a Kruskal-Wallis test, which is a one way ANOVA on the median values. The particular test used has been identified within the relevant results paragraph.

4.5 RESULTS

All the mice which were to be followed over the 56 day period survived the anaesthetic and made a full post-operative recovery, manifesting no systemic ill effects resulting from NMRL irradiation throughout the observational period.

4.5.1 Depilation

Resting Hair Sites

Hair regrowth was assessed on a weekly basis up to 56 days after laser exposure and scored according to Table 2.6 where full hair regrowth is scored as 3. This period of observation is over the maximum time recorded to complete a full hair cycle in the mouse so therefore any depilatory effect should be accurately established (Dry, 1926). A graph was plotted showing the mean weekly hair regrowth scores (+/- standard deviation) for the resting hair sites according to each fluence of exposure (see Figure 4.5). A statistical comparison using the Mann Whitney Rank Sum test was made between the median values of hair regrowth scores achieved weekly in laser irradiated sites treated with 5 J/cm^2 and non-irradiated trimmed controls in resting hair regions. This revealed a significant difference in hair regrowth on weeks 1 and 2 post-

irradiation ($p<0.001$) with less hair being present at the laser exposed sites, but after this time, no difference was detected.

The data from laser treatment using a fluence of 6 J/cm^2 is also plotted in Figure 4.5. A statistical comparison using the Mann Whitney Rank Sum test was made between the median values of hair regrowth scores achieved weekly at laser irradiated sites in resting hair regions and their respective non-irradiated trimmed controls. This revealed a significant difference in hair regrowth on weeks 1 and 2 post-irradiation ($p<0.001$) with less hair being present at the laser exposed sites, but after this time, no difference was also noted.

The plot representing 7 J/cm^2 is shown in Figure 4.5 too. A statistical comparison using the Mann Whitney Rank Sum test was made between the median values of hair regrowth scores achieved weekly after laser irradiation of resting hair regions compared with equivalent non-irradiated trimmed controls. This revealed a significant difference in hair regrowth on weeks 1, 2 and 3 after irradiation ($p<0.001$, $p<0.001$ and $p=0.01$ respectively) with less hair being present at the laser exposed sites, but after this time, no difference was noted.

Finally, the plot representing 8 J/cm^2 exposure is also shown in Figure 4.5. A statistical comparison using the Mann Whitney Rank Sum test was also made between the median values of hair regrowth scores achieved weekly upon laser irradiated sites in resting hair regions and respective non-irradiated trimmed controls. This revealed a significant difference in hair regrowth on weeks 1, 2 and 3 after irradiation ($p<0.001$, $p<0.001$ and $p<0.01$ respectively) with less hair being present at the laser exposed sites, but after this time, no difference was also noted.

Growing Hair Sites

Figure 4.6 shows a graph of the plots of the weekly depilatory score for the four fluences used in growing hair regions. A statistical comparison using the Mann Whitney Rank Sum test between the median values of hair regrowth scores achieved

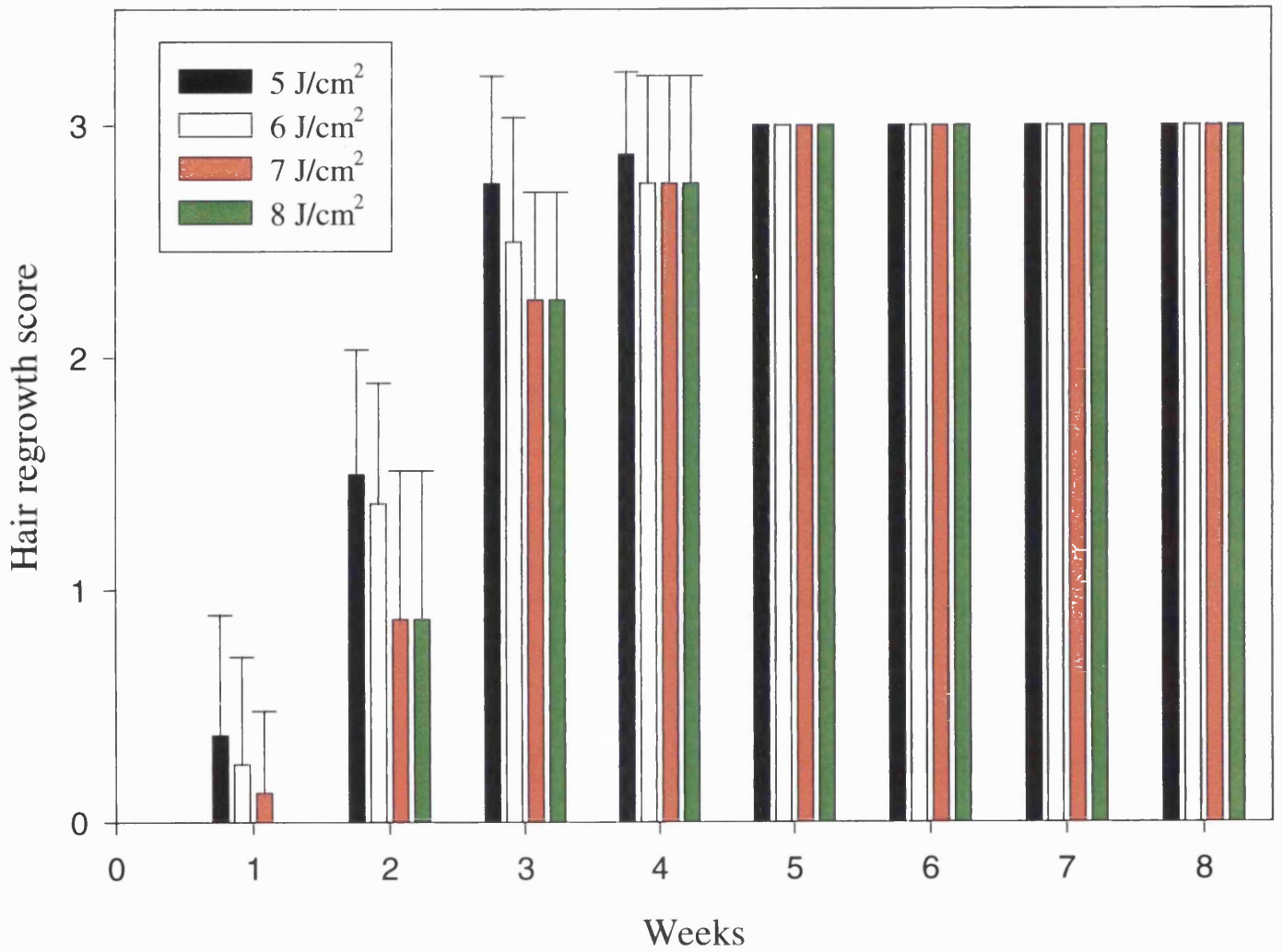

Figure 4.5: Graph representing the hair regrowth scores achieved over time in resting hair regions irradiated with different fluences.

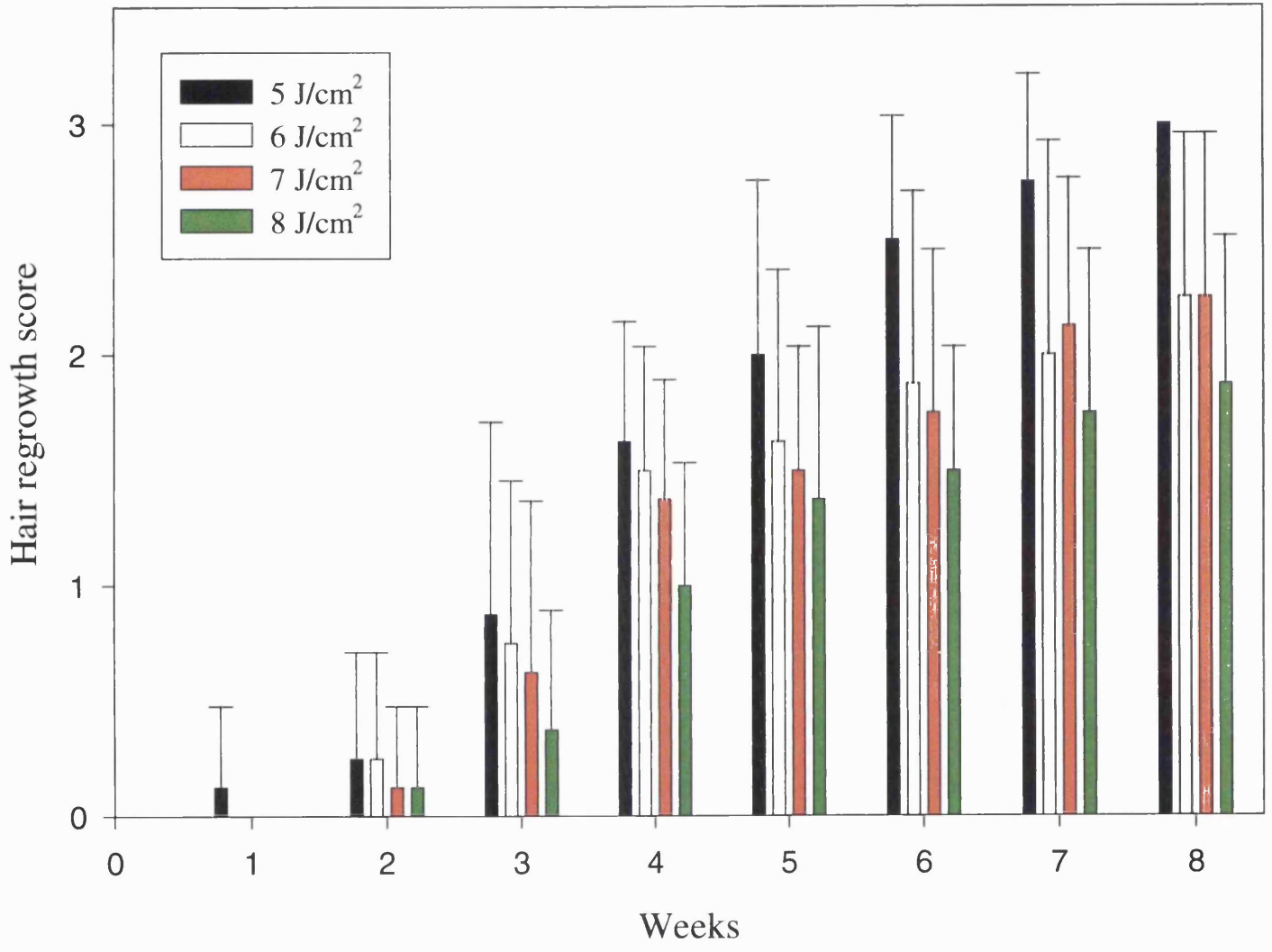

Figure 4.6: Graph representing the hair regrowth scores achieved over time in growing hair regions irradiated with different fluences.

weekly in laser irradiated sites treated with 5 J/cm^2 compared with non-irradiated trimmed controls was made for growing hair regions. This revealed a significant difference in hair regrowth up to 5 weeks after irradiation ($p<0.001$, $p<0.001$, $p<0.001$, $p<0.001$ and $p=0.01$ respectively) with the irradiated sites showing a reduced hair density. After this time the hairs had regrown to a similar extent to that seen in the non-irradiated, trimmed controls.

The plot representing 6 J/cm^2 is also shown in Figure 4.6. A statistical comparison using the Mann Whitney Rank Sum test was made between the median values of hair regrowth scores achieved weekly at laser irradiated sites in growing hair regions and their respective non-irradiated trimmed controls. This revealed a significant difference in hair regrowth up to 8 weeks after irradiation ($p<0.001$, $p<0.001$, $p<0.001$, $p<0.001$, $p=0.002$, $p=0.01$, $p=0.038$ and $p=0.038$ respectively) with the irradiated sites also showing a reduced hair density.

The plot representing 7 J/cm^2 is shown in Figure 4.6 too. A statistical comparison using the Mann Whitney Rank Sum test was made between the median values of hair regrowth scores achieved weekly after laser irradiation of growing hair regions compared with equivalent non-irradiated trimmed controls. This revealed a significant difference in hair regrowth up to 8 weeks after laser exposure ($p=0.028$, $p=0.001$, $p=0.001$, $p<0.001$, $p<0.001$, $p=0.002$, $p=0.01$ and $p=0.038$ respectively) again in favour of the irradiated sites.

Finally, the plot representing 8 J/cm^2 exposure is also shown in Figure 4.6. A statistical comparison using the Mann Whitney Rank Sum test was made between the median values of hair regrowth scores achieved weekly upon laser irradiated sites in growing hair regions and respective non-irradiated trimmed controls. This revealed a significant difference in hair regrowth also up to 8 weeks after laser exposure with the laser exposed sites showing a reduced hair count ($p<0.001$, $p<0.001$, $p<0.001$, $p<0.001$, $p<0.001$, $p<0.001$, $p=0.002$ and $p=0.002$ respectively). Figures 4.7 and 4.8 show the depilation visible 8 weeks after laser exposure at a fluence of 8 J/cm^2.

Comparison of Resting and Growing Hair Site Data

A statistical comparison between the weekly hair regrowth scores of the growing and resting hair groups was performed upon the median values using the Mann Whitney Rank Sum test. At 5 J/cm^2, this revealed a statistically significant reduction in hair present within the targeted growing hair regions compared to the resting hair regions at weeks 2, 3, 4 and 5 ($p=0.002$, $p<0.001$, $p<0.001$ and $p=0.01$ respectively) only.

Performing the same statistical comparison between the weekly hair regrowth scores achieved in the growing and resting hair groups exposed to 6 J/cm^2 revealed a statistically significant reduction in hair present within the targeted growing hair regions compared to the resting hair regions at weeks 2 to 8 ($p=0.003$, $p<0.001$, $p=0.002$, $p=0.002$, $p=0.01$, $p=0.038$ and $p=0.038$ respectively).

At 7 J/cm^2, the same statistical comparison performed between the weekly hair regrowth scores in the growing and resting hair groups revealed a statistically significant reduction in hair present within the targeted growing hair regions compared to the resting hair regions for weeks 2 to 8 after irradiation ($p=0.028$, $p=0.001$, $p=0.001$, $p<0.001$, $p=0.002$, $p=0.01$ and $p=0.038$ respectively).

A comparison between the weekly hair regrowth scores of the growing and resting hair groups exposed to 8 J/cm^2 also revealed a statistically significant reduction in hair present within the targeted growing hair regions compared to the resting hair regions for weeks 2 to 8 inclusive ($p=0.028$, $p<0.001$, $p<0.001$, $p<0.001$, $p<0.001$, $p=0.002$ and $p=0.002$ respectively).

Statistical comparison between the depilatory scores of all four fluence exposure sites for each week over the observational period was performed within both the resting hair group and the growing hair group by one way ANOVA method. For the resting hair group, this revealed no statistically significant difference in the scores between fluence groups at each of the recorded weeks. In contrast, the comparison of the

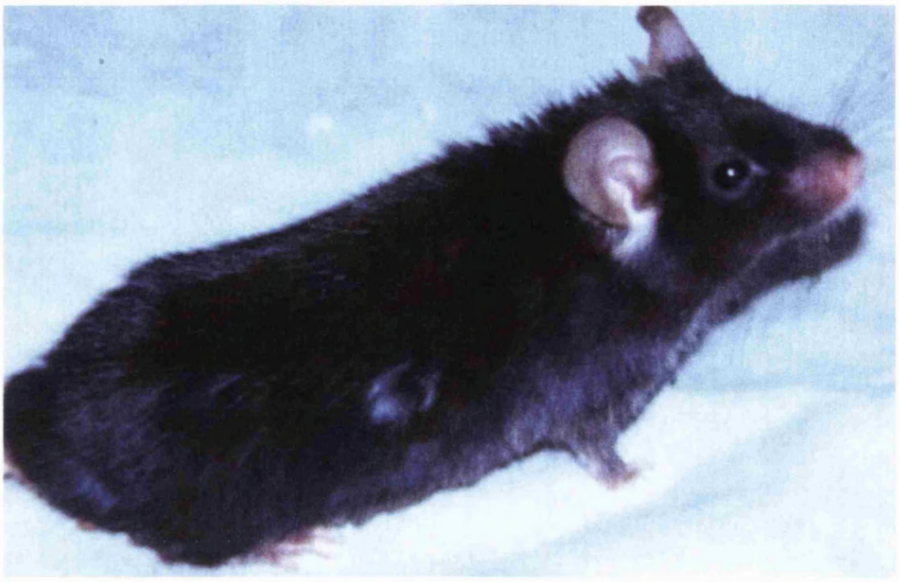

Figure 4.7: Photograph of a mouse 8 weeks after exposure to ruby laser irradiation at 8 J/cm^2 upon a growing hair region. An area of decreased hair regrowth is visible with depigmentation of the hairs regrowing in that site.

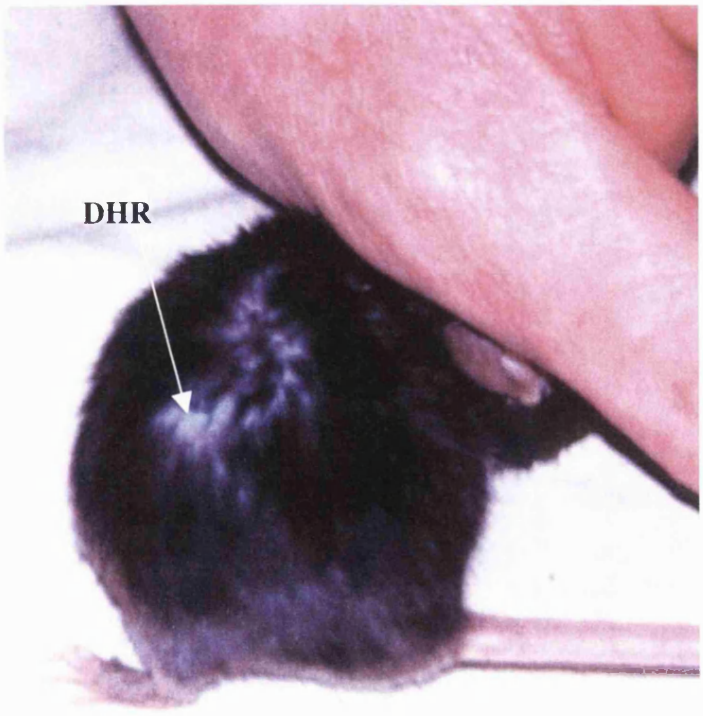

Figure 4.8: Photograph of a mouse 8 weeks after exposure to ruby laser irradiation at 8 J/cm^2 upon a growing hair region. Decreased hair regrowth (DHR) is evident in the area identified.

growing hair group revealed a statistically significant difference in the median values between the fluence groups for weeks 6, 7 and 8 ($p<0.001$).

4.5.2 Histology of Hair Damage

Modified SACPIC staining of sections taken from resting hair regions exposed to NMRL irradiation showed damage occurring to external hair shafts only, ie. to the limit of the melanin pigmentation (see Figure 4.9) and the extent of this was regardless of the fluence of exposure. Sections from growing hair regions exposed to the same range of fluences and also stained using the modified SACPIC technique showed that damage to the hair shafts extended throughout their lengths to the hair bulbs regardless of the fluence used (see Figure 4.10).

4.5.3 Epidermal Damage

All exposure sites experienced varying degrees of erythema immediately after irradiation (see Figure 4.4). Wound evaluation was performed daily until complete healing had taken place using the system described in Table 2.4.

Daily Comparison of Epidermal Damage Between Resting and Growing Hair Sites

Graphs were plotted showing the mean wound scores over time for each treatment fluence in resting hair regions (Figure 4.11) and in growing hair regions (Figure 4.12). The median values of the plots representing the 5 J/cm^2 cohort were analysed by Mann Whitney Rank Sum testing. This revealed a difference in the median values of the wound scores between the two hair groups upon days 7, 8, 9 and 10 ($p=0.001$, $p=0.015$, $p=0.003$ and $p=0.038$ respectively), with the scores in the growing hair regions being greater. The median values of the plots representing the 6 J/cm^2 cohort were also analysed by Mann Whitney Rank Sum testing. This in turn revealed a difference in the median values of the wound scores between the two hair groups also upon days 7, 8, 9 and 10 ($p=0.003$, $p=0.015$, $p=0.002$ and $p<0.001$ respectively) with

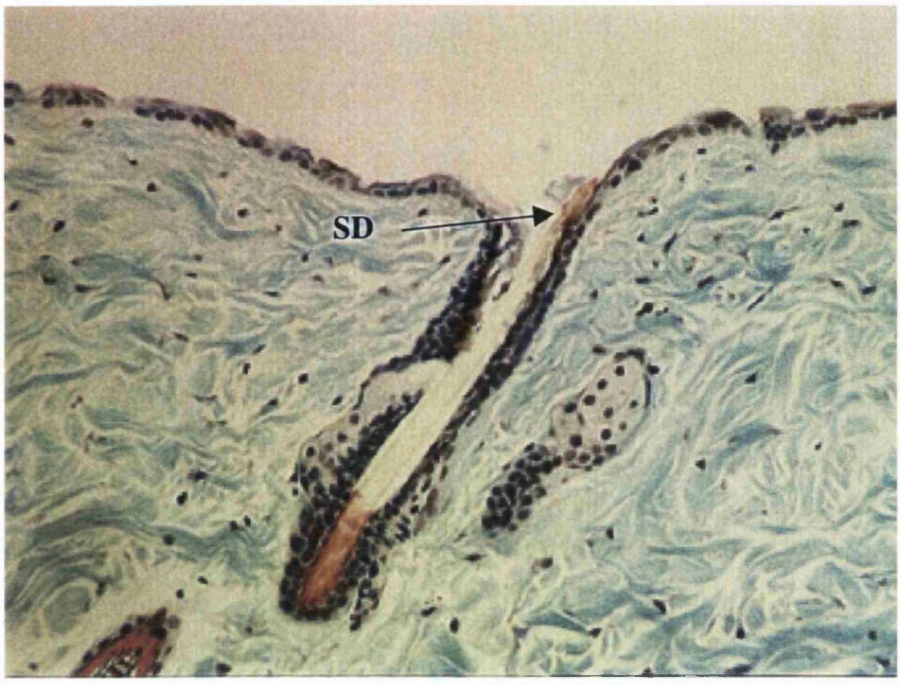

Figure 4.9: Transverse section through a resting hair region stained with the modified SACPIC technique showing a telogen hair. Ruby laser irradiation has occurred at 5 J/cm^2 and shaft damage (SD) can be seen only in the external aspect of the shaft above the level of the skin. This would coincide with the limit of the melanin pigment. The section is representative of the higher fluences too (x200).

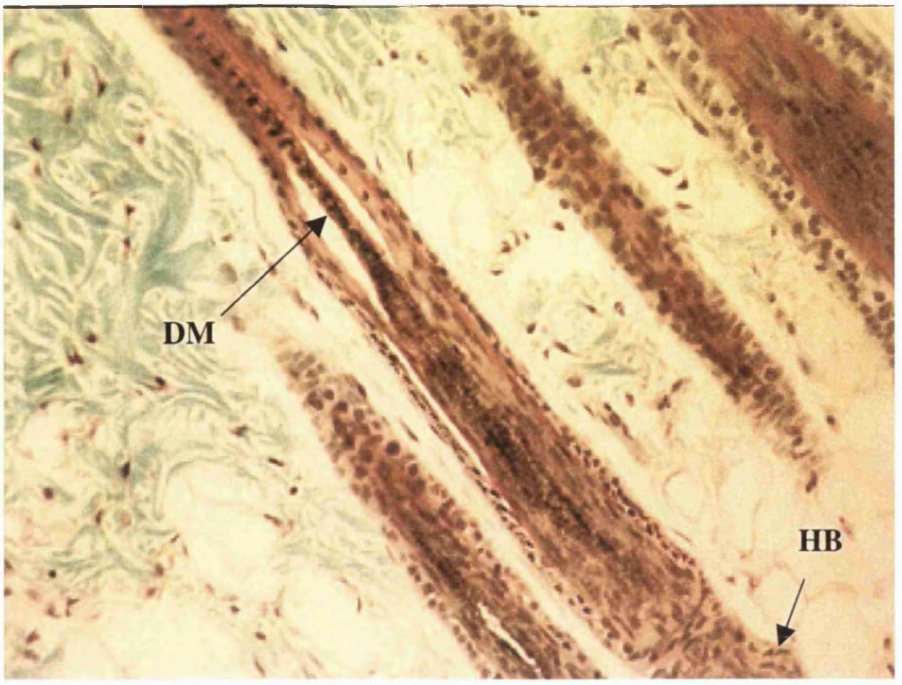

a.

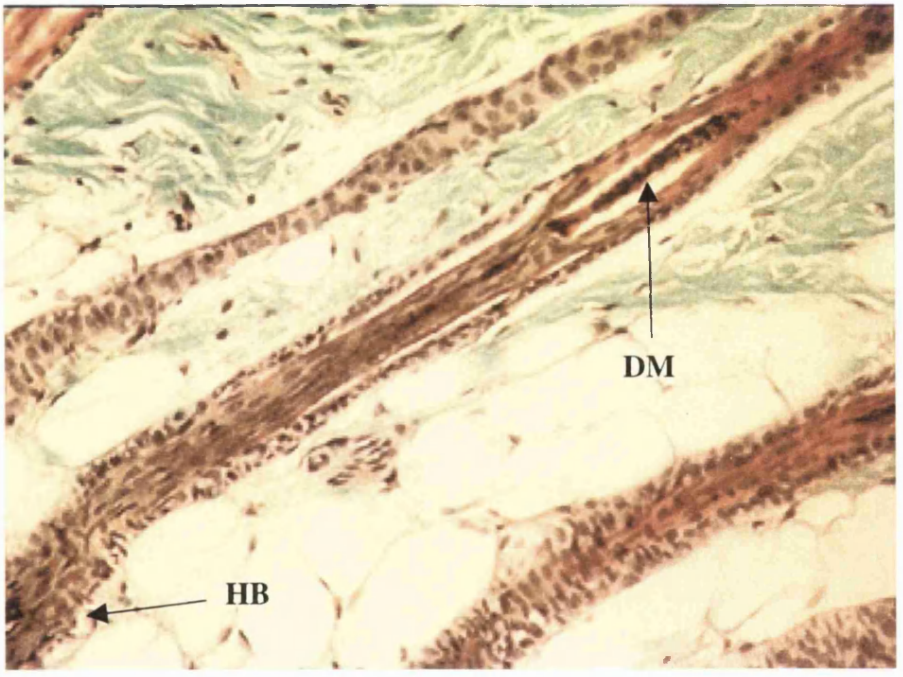

b.

Figure 4.10: Transverse sections stained with the modified SACPIC technique having been exposed to a) 5 J/cm^2 and b) 8 J/cm^2 fluence showing disruption of the melanin (DM) within the hair shafts which is greater at 8 J/cm^2 (HB = hair bulb) x200.

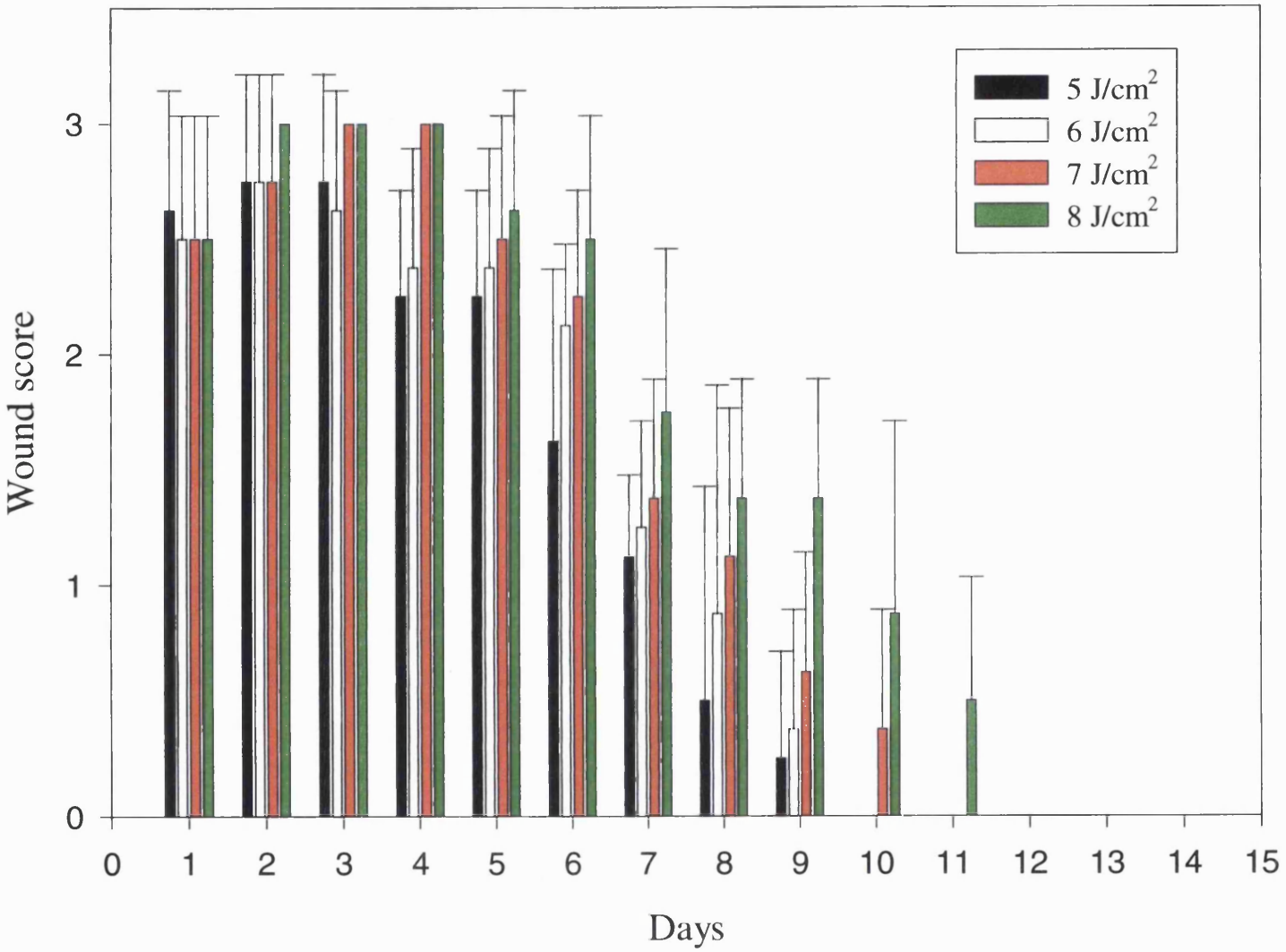

Figure 4.11: Graph representing the wound scores achieved over time in resting hair regions irradiated with different fluences.

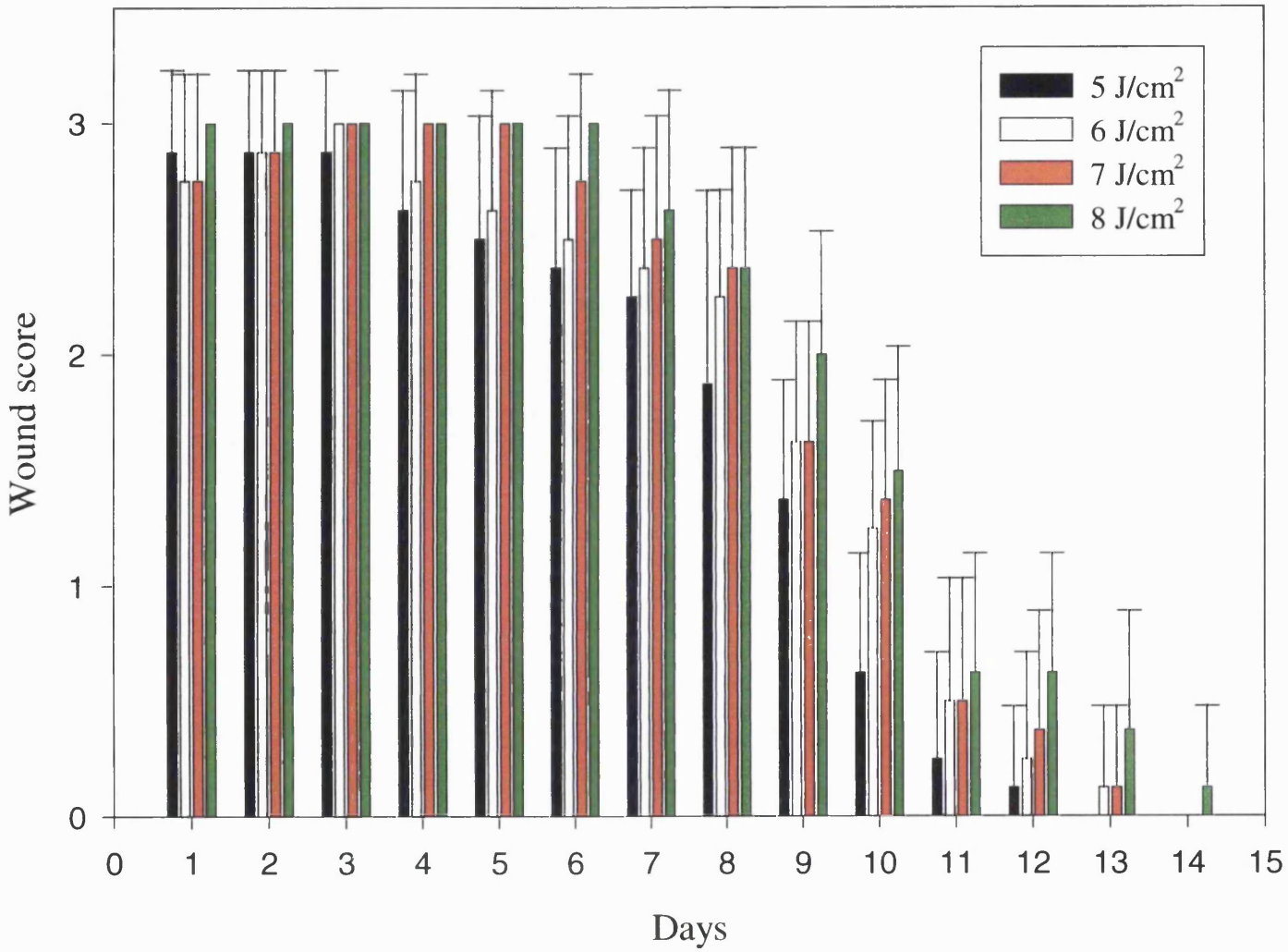

Figure 4.12: Graph representing the wound scores achieved over time in the growing hair regions irradiated with different fluences.

the scores in the growing hair regions being greater. The median values of the plots representing the 7 J/cm^2 cohort were analysed also using the Mann Whitney Rank Sum test. This revealed a difference in the median values of the daily wound scores between the resting and growing hair groups on days 6, 7, 8, 9 and 10 ($p=0.049$, $p=0.005$, $p=0.003$, $p=0.007$ and $p=0.007$ respectively) again with the greater scores achieved in the growing hair regions. Finally, the median values of the plots representing the 8 J/cm^2 cohort were analysed using the Mann Whitney Rank Sum test. This revealed a difference in the median values of the daily wound scores between the resting and growing hair groups on days 7, 8 and 11 alone ($p=0.028$, $p=0.007$ and $p=0.038$ respectively) again with the greater scores achieved in the growing hair regions.

Time Taken to Fully Heal in Resting and Growing Hair Sites

The mean time taken in days by the wounds to achieve full healing was established for all fluences within the resting hair groups and the growing hair groups and plotted according to fluence of exposure (see Figure 4.13). Within the resting hair cohort, the 5 J/cm^2 group had a mean time to heal of 8.5 days (S.D. 0.926), the 6 J/cm^2 group, 8.875 days (S.D. 0.991), the 7 J/cm^2 group, 9.875 days (S.D. 1.126) and the 8 J/cm^2 group, 11.125 days (S.D. 0.991). One way ANOVA analysis showed that a difference in the median values of the times taken to completely heal existed between the groups of the resting hair cohort which was greater than would be expected by chance and statistically significant ($p=0.001$). Within the growing hair cohort, the 5 J/cm^2 group had a mean time to heal of 11 days (S.D. 1.069), the 6 J/cm^2 group, 11.875 days (S.D. 1.126), the 7 J/cm^2 group, 12 days (S.D. 1.195) and the 8 J/cm^2 group, 12.625 days (S.D. 1.408). No statistically significant difference was revealed between these figures. A statistical comparison between the times taken to fully heal between the growing and resting hair groups at each fluence of exposure was performed. This revealed a statistically significant difference in the median values of the days taken to fully heal between the growing and resting hair sites at all four fluences ($p=0.001$, $p<0.001$, $p<0.001$ and $p=0.05$ respectively) when assessed by Mann Whitney Rank Sum testing.

Resting hair sites exposed to fluences of 8 J/cm^2 occasionally showed induction of hair growth (as evidenced by the pigmented appearance of the skin) in a distinct ring synonymous with where the laser had been incident upon the skin. This phenomenon was not seen in regions exposed to fluences lower than 8 J/cm^2 and has been described in the literature as a response of this animal to wounding (Argyris, 1967).

4.5.4 Histology of Epidermal Damage

The sections from the biopsies taken immediately were stained using H&E, the modified SACPIC technique and Massons Fontana staining (see section 2.3). The H&E sections were examined for the site and severity of cellular damage occurring post-irradiation at the four fluence values. Figure 4.14 is a transverse section from a resting hair region stained with H&E acting as a control showing the epithelial ultrastructure of mouse skin, which is approximately 2 to 3 cells thick and is supported by a collagen matrix. A resting hair is apparent within the section with its associated sebaceous gland. The bulge region has been stated to lie just below this area (Cotsarelis, et al., 1990), (Wilson, et al., 1994) and the probable location is indicated in Figure 4.14. Figure 4.15a is a transverse section stained with H&E of a specimen that underwent laser exposure at 5 J/cm^2 and Figure 4.15b is a higher magnification view of the epidermis. The epidermal cells show signs of damage with epidermal cell loss, nuclear pyknosis and cell vacuolisation. A resting follicle can also be seen, however the cells lining the follicular canal do not appear to show any signs of cellular damage. Figure 4.16a shows a transverse section through a specimen exposed to laser irradiation at 8 J/cm^2 and having been stained with H&E. The surface epithelial cells have been completely destroyed with the nuclei having all but disappeared. In contrast, though, the cells lining the hair canal do not manifest any gross histological signs of cell damage in any way, similar to the section exposed to 5 J/cm^2. Figure 4.16b is another section taken from the specimen exposed to a fluence of 8 J/cm^2, showing that not all the epidermis has been completely destroyed, with islands of epidermal cells still remaining on the surface of the dermis, though whether these cells are dying is not known.

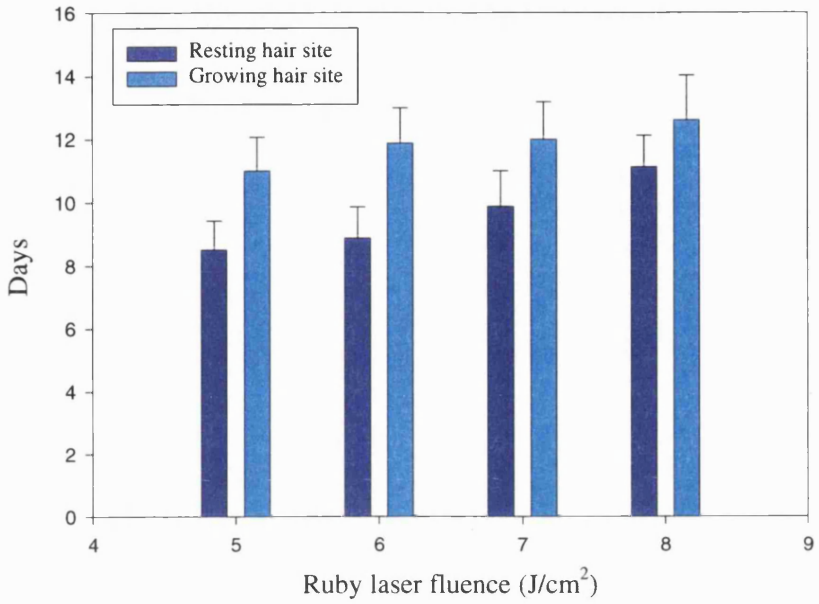

Figure 4.13: Graph representing the time taken to complete wound healing in both resting and growing hair regions as a result of ruby laser exposure at the fluences shown.

H&E sections of laser irradiated specimens from growing hair regions were also examined for both the site and extent of cellular damage. Little difference was noted in the damage occurring to the epidermal cells between those sites exposed to 5 J/cm^2 (see Figure 4.17) and those exposed to 8 J/cm^2 (see Figure 4.18). The cells lining the follicular canals within these regions also showed no obvious signs of damage.

Sections from the growing and resting (Figures 4.19a and b) hair regions that had not been exposed to NMRL irradiation were stained with Masson Fontana to show the distribution of melanin within these two skin regions. Minimal, if any, melanin was seen within the epidermal cells of mouse skin in both growing hair and resting hair regions. The cells lining the follicular canals were also noted not to contain melanin pigment. All the melanin that was noted within the sections appeared within the hair shafts alone. In the growing hair follicle, this was observed throughout the length of the hair shaft. In contrast, melanin was more-or less restricted to the external hair shaft in resting hair follicles with very little present in the hair shaft contained within the follicular canal. Sections taken from growing and resting hair regions exposed to the four laser fluences were also stained for melanin using the Massons Fontana technique. This showed that as well as melanin pigment being present within the hair shafts in the pattern previously observed, it was now also noted to be present over the surface of the epithelium. None, however, was still noted within the follicular canals (see Figure 4.20a and b).

Histological analysis of sections taken from the laser irradiated sites at 56 days post-exposure and stained with Massons trichrome were assessed for signs of scarring or fibrosis. This would characteristically occur within the dermis and foci of fibroblast cells along with disorganised collagen would reveal whether this was the case along with the site and extent. However, no evidence of scarring or fibrosis was noted within the sections examined (see Figure 4.21). In addition, examination of the sections stained with H&E taken from the same biopsy sites revealed that the epidermis had regenerated completely.

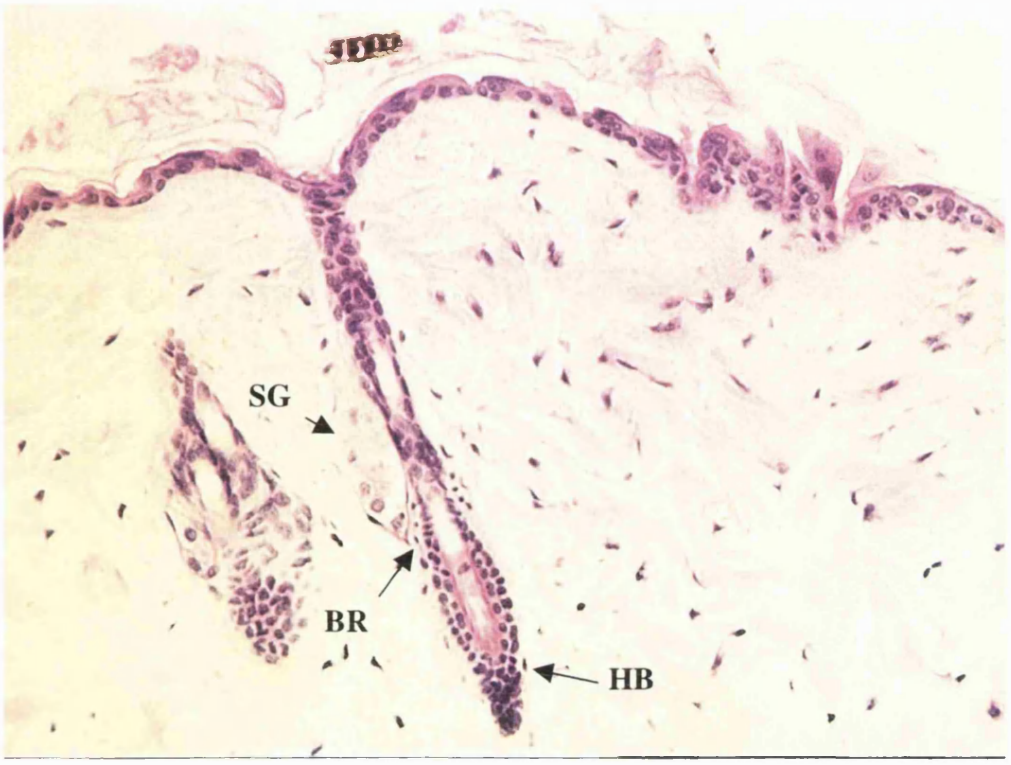

Figure 4.14: Transverse section of control mouse skin taken from a resting hair region and stained with H&E showing normal mouse epidermis. The sebaceous gland (SG), the probable bulge region (BR) and the hair bulb (HB) have been identified (x200).

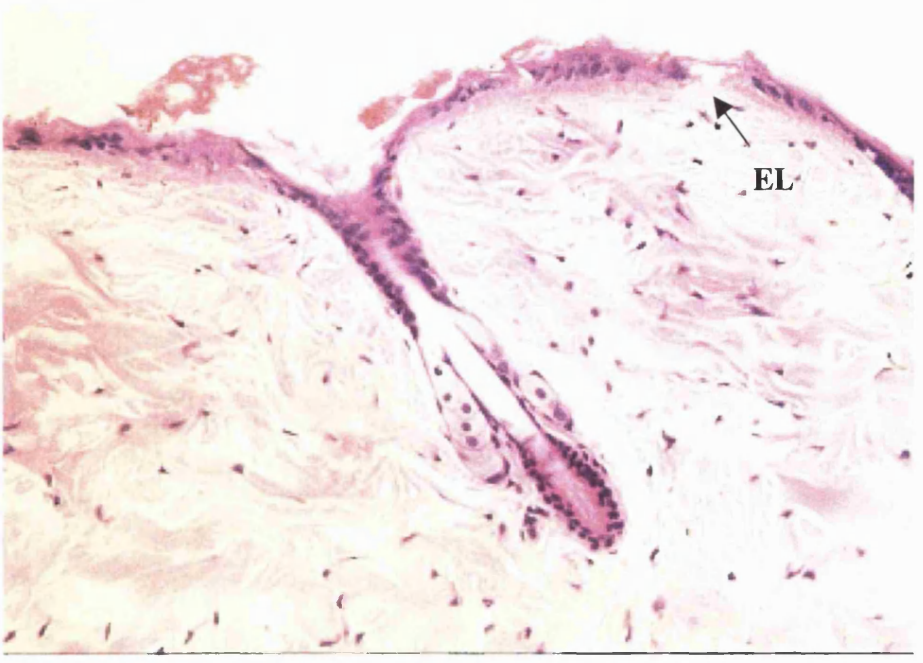

Figure 4.15a: Transverse section of a resting hair follicle within mouse skin exposed to a ruby laser fluence of 5 J/cm^2 and stained with H&E. The epidermis shows signs of damage with areas of complete loss (EL), but the cells lining the hair canal look relatively undamaged in comparison (x200).

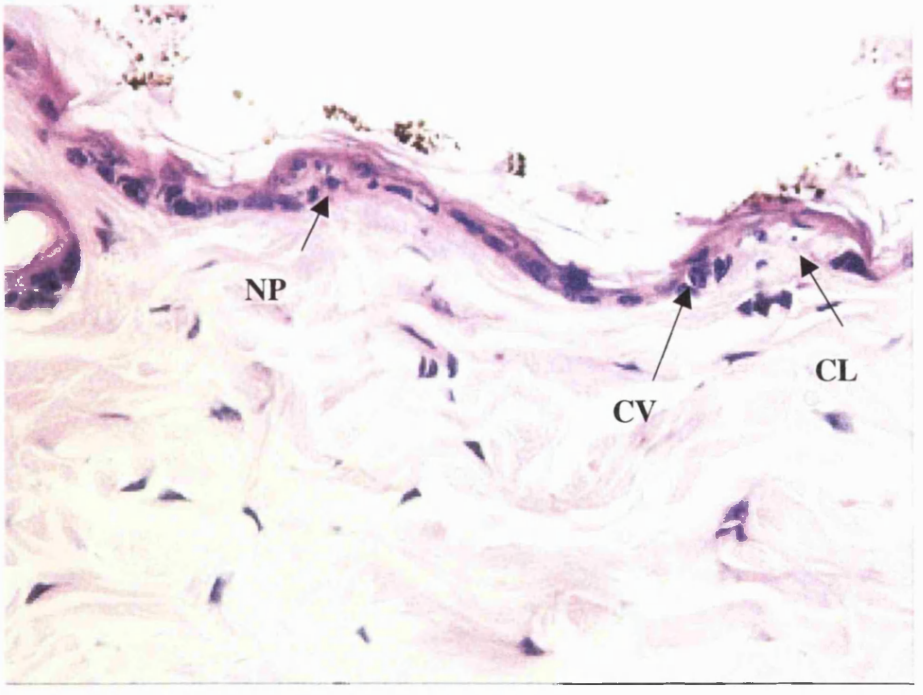

Figure 4.15b: Transverse section of mouse skin taken from a resting hair region exposed to a ruby laser fluence of 5 J/cm^2 and stained with H&E. Note that epidermal damage is present with areas of cell loss (CL), nuclear pyknosis (NP) and cell vacuolisation (CV) x400.

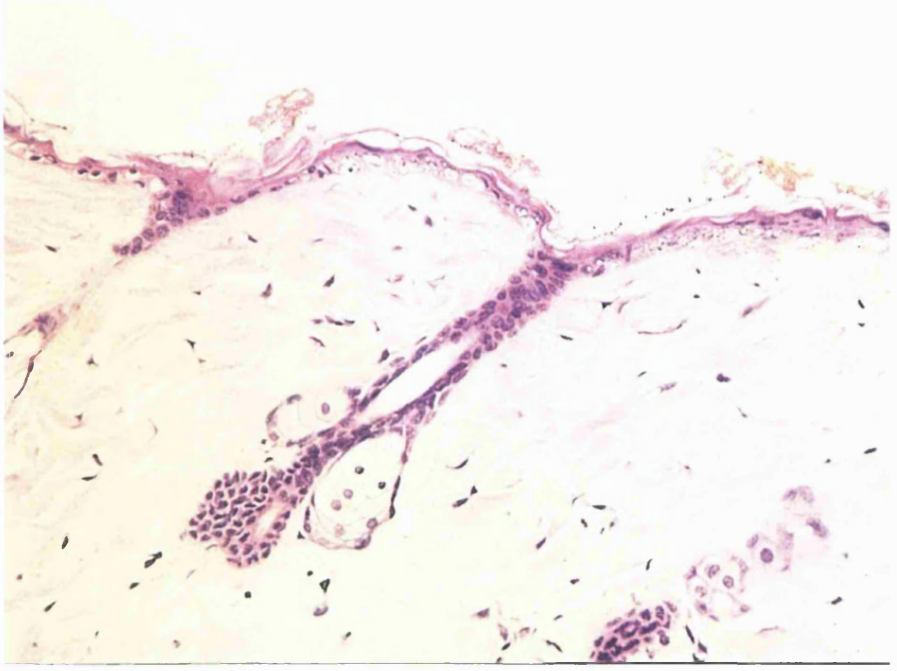

Figure 4.16a: Transverse section of mouse skin in a resting hair region after exposure to ruby laser irradiation at 8 J/cm^2. Note almost complete epidermal loss but the cells lining the hair canal appear undamaged (x200).

Figure 4.16b: Transverse section of mouse skin in a resting hair region after exposure to ruby laser irradiation at 8 J/cm^2. Note that islands of epidermal cells are still present within the treatment field although their viability cannot be ascertained (x200).

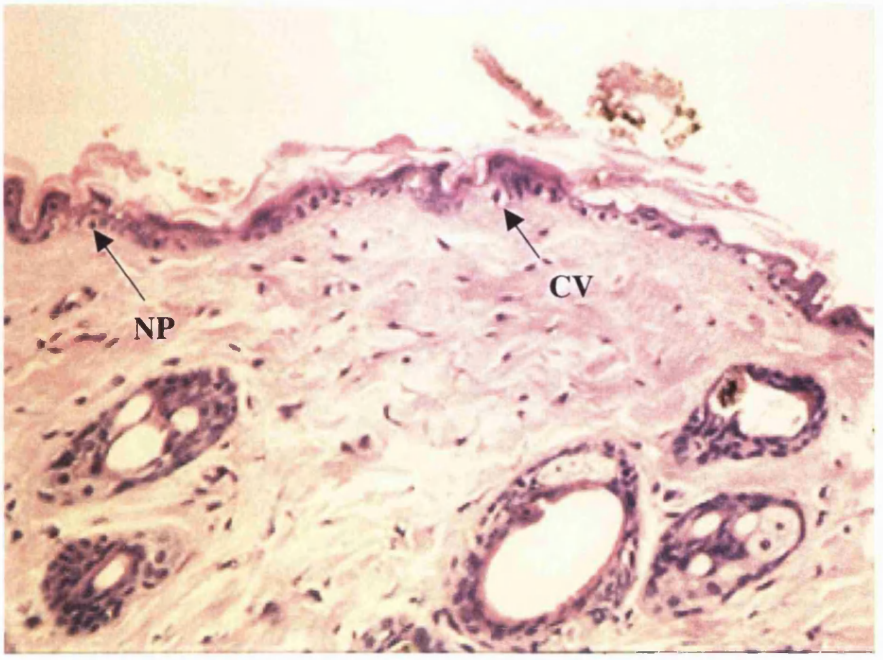

Figure 4.17: Transverse section stained with H&E of a growing hair region exposed to ruby laser irradiation at 5 J/cm^2. Note the epithelial damage, for instance cellular vacuolisation (CV) and nuclear pyknosis (NP) x200.

Figure 4.18: Transverse section stained with H&E of a growing hair region exposed to ruby laser irradiation at 8 J/cm^2. Note epithelial damage manifesting as cellular vacuolisation and nuclear pyknosis with areas of almost complete epithelial loss (EL) x200.

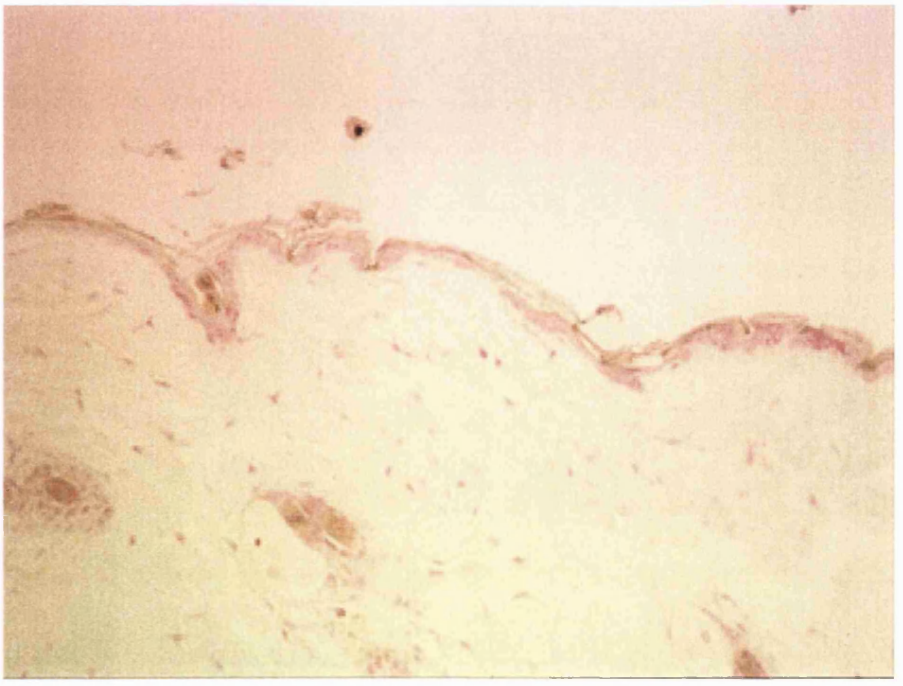

a. (x100)

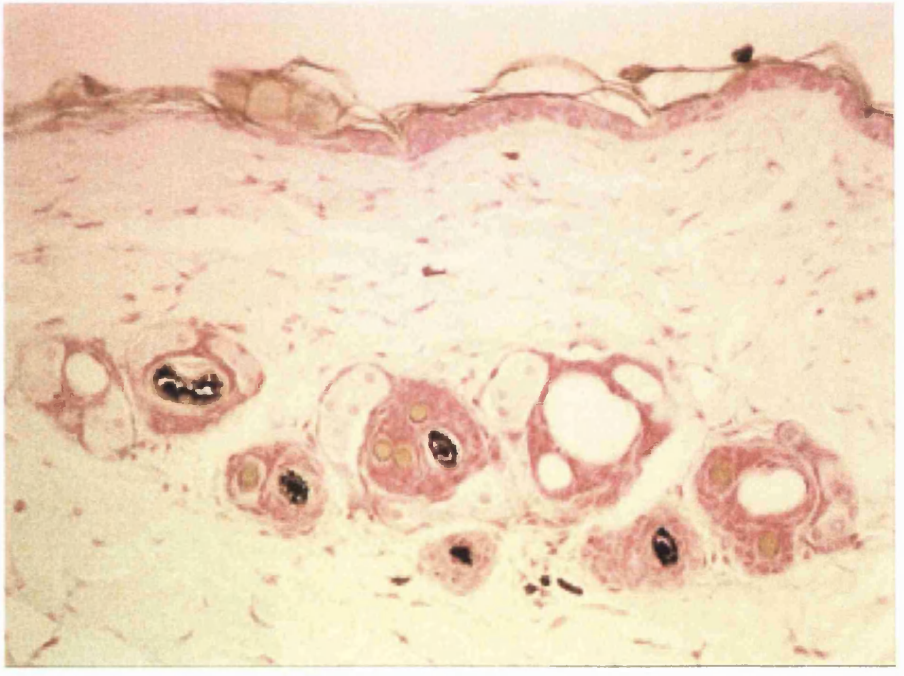

b. (x200)

Figure 4.19: Transverse section stained with Massons Fontana of a) a resting hair region and b) a growing hair region of the skin of the black-haired mouse showing no melanin within the epithelial or follicular cells.

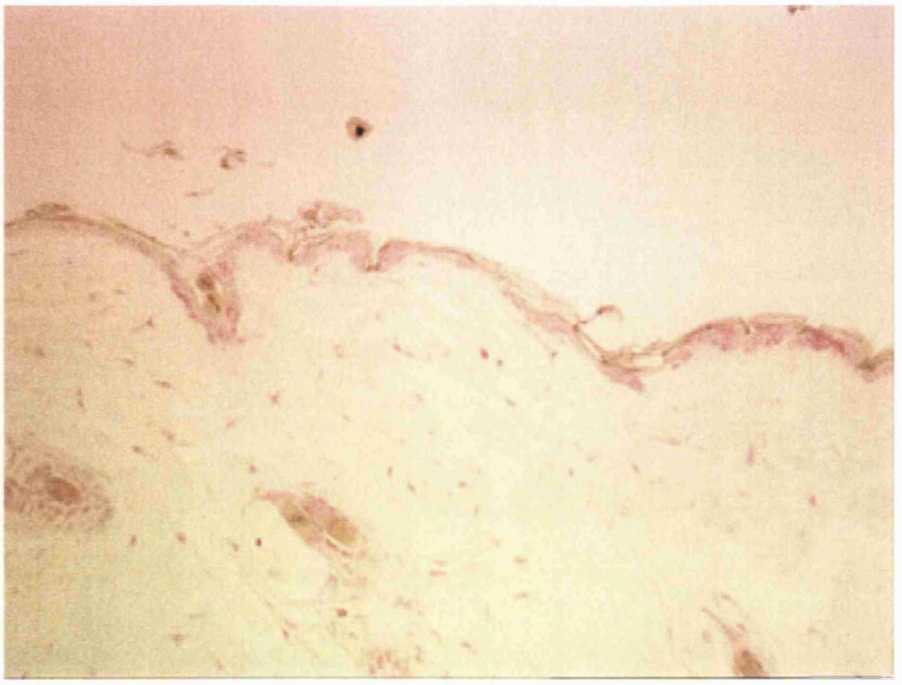

a. (x100)

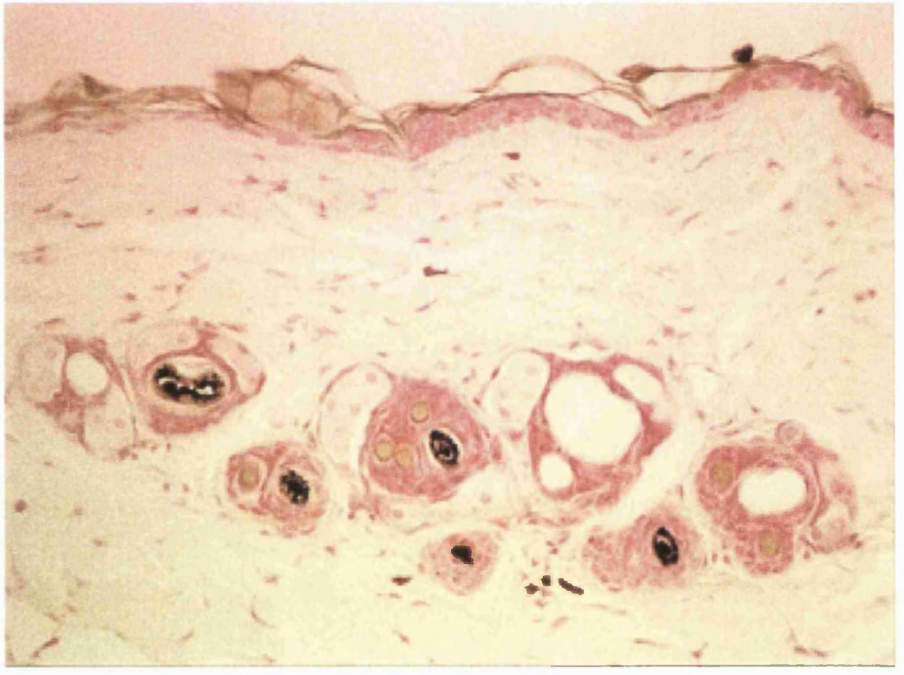

b. (x200)

Figure 4.19: Transverse section stained with Massons Fontana of a) a resting hair region and b) a growing hair region of the skin of the black-haired mouse showing no melanin within the epithelial or follicular cells.

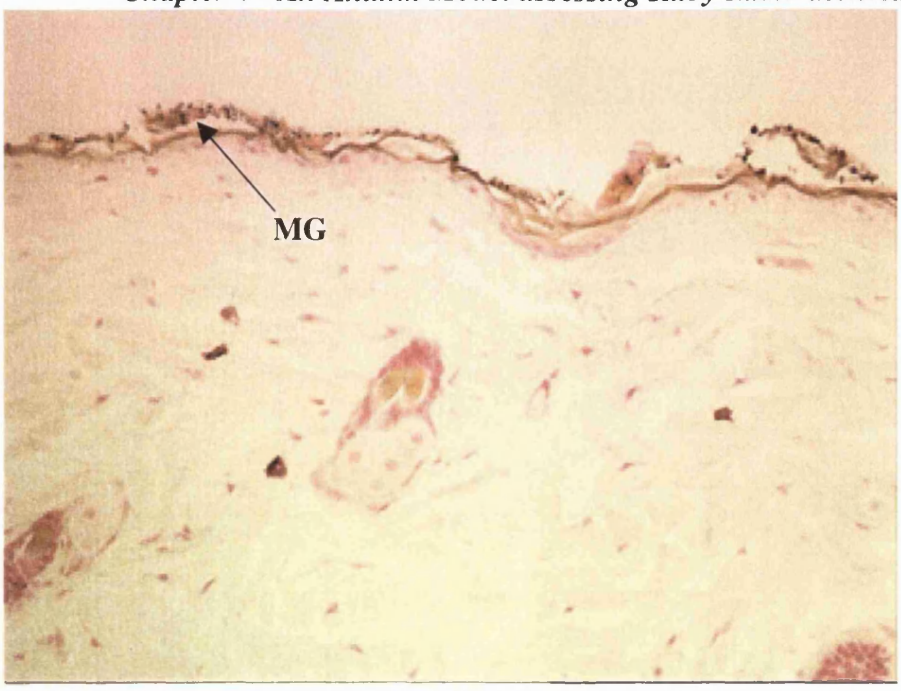

a.

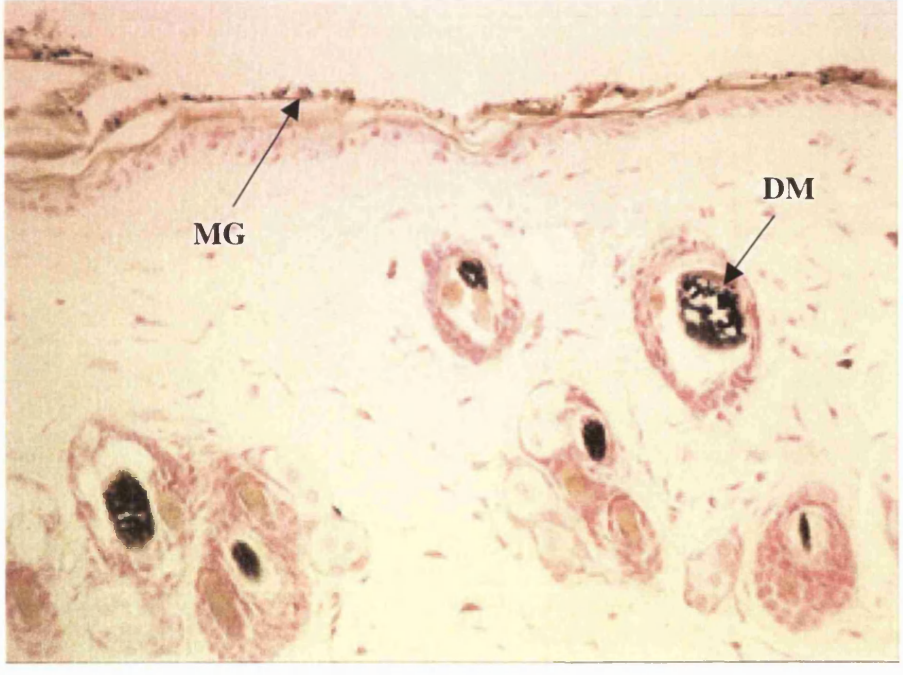

b.

Figure 4.20: Transverse sections stained with Massons Fontana of a) a resting hair region exposed to 5 J/cm^2 and b) a growing hair region exposed to 8 J/cm^2. Melanin granules can be seen scattered over the epithelial surface and disrupted (DM) within the hair follicle identified (x200).

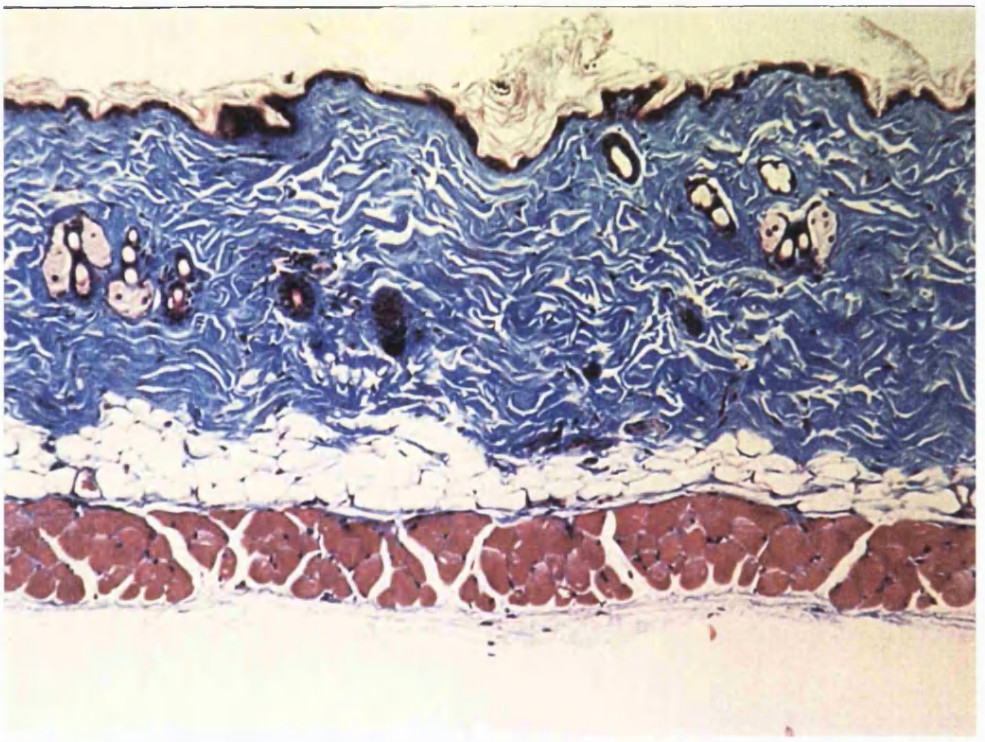

Figure 4.21: Transverse section stained with Massons trichrome of a resting hair region biopsied 8 weeks after laser exposure. No scarring or disruption is evident within the collagen of the dermis (stained blue) suggesting that the skin damage incurred as a result of laser exposure is not permanent (x100).

4.6 DISCUSSION

NMRL irradiation of both growing and resting hair sites at the fluences used within this experiment produced, clinically, immediate external hair shaft loss to the level of the skin surface. Within the resting hair group, a statistically significant reduction in the hair count was noted at 1 and 2 weeks at 5 J/cm^2 and 6 J/cm^2 and at 1, 2 and 3 weeks at 7 J/cm^2 and 8 J/cm^2 when compared to non-irradiated trimmed controls. These findings would support those declared by Lin, (Lin et al 1998) who discovered no significant difference in hair regrowth at NMRL irradiated sites within hair resting regions when compared to non-irradiated controls in the black-haired mouse at 28 and 56 days post-exposure. It was therefore reported that, within the mouse, the telogen phase was not conducive to successful ruby laser-assisted hair removal. There are two possible explanations for this. The first is that not enough photon energy was reaching the desired areas (the bulge region and the hair bulb). Second, that enough photon energy was reaching those areas but that insufficient chromophore was present to convert the photon energy to heat to produce the cellular damage required for permanent depilation. The quantity of melanin pigment, which is a known chromophore for the NMRL, is very much reduced in the mouse hair shaft during the catagen and telogen phases when compared to the shafts in the anagen phase. The NMRL should, in theory, be able to penetrate the skin to a greater distance than the depth of the bulge region and the hair bulb (Anderson, 1984) as was discovered in Chapter 3. The bulge region is situated at a fixed depth between 180 to 220 μm from the skin surface within the dermis of the mouse (Cotsarelis, et al., 1990) whilst the hair bulb has been stated to exist at about 250 μm below the skin in resting hairs and at 500 μm or greater below the skin in the early anagen phases (Chase and Montagna, 1951), (Chase, 1954). Histological examination of growing hair sections revealed damage to the hair shafts extending to the hair bulb, though whether this was direct photon energy conversion by the hair shaft or as a result of heat transfer down the shaft cannot be commented upon. Within the resting hair regions, a greater fluence could not be administered to the mouse model without selectivity being lost resulting in the production of more substantial wounding. Increasing the pulse duration could theoretically maintain the peak temperature for a longer time at the site of the

chromophore. This would then result in a controlled sustained release of sufficient heat to the surroundings rather than a sudden non-specific blast of energy, which would result from increasing the fluence alone.

Within the growing hair group, a statistically significant difference in the hair regrowth score was noted between the irradiated and non-irradiated sites between 1 and 5 weeks at 5 J/cm^2 and 1 and 8 weeks at 6 J/cm^2, 7 J/cm^2 and 8 J/cm^2. This would suggest that the fluence of 5 J/cm^2 was not sufficient upon growing hair sites to produce depilation by this laser type, but that 6 J/cm^2, 7 J/cm^2 and 8 J/cm^2 was. This could support the statement that the fluence would have appeared to have reached its maximum depilatory effect at 6 J/cm^2 and that to increase the fluence may have resulted in increasing the side effects alone. The findings in the histological sections stained by the modified SACPIC technique that hair shaft damage occurred to a similar extent at the fluences used would lend support to these clinical findings. A statistically significant difference in hair regrowth scores between growing and resting hair sites irradiated at 5 J/cm^2 was noted between weeks 2 and 5. This was increased to week 8 at 6 J/cm^2, 7 J/cm^2 and 8 J/cm^2, which could suggest that the increase in melanin content within the anagen hair follicles was enough to produce the difference seen in hair regrowth scores.

Skin damage was produced in all mice exposed to NMRL irradiation at the fluences used regardless of the growth phase of the hairs. The difference in the median values of the wound scores became statistically significant commonly at approximately one week post-irradiation at all fluences. The resting hair group healed more quickly than the growing hair group confirmed by the fact that a statistically significant difference in the time taken to fully heal was noted between the two hair phase groups at each fluence of exposure. Therefore it would seem likely that less damage had originally occurred at the resting hair sites. The greater amount of skin damage produced by laser irradiation of growing hair sites compared with resting hair sites would tend to suggest that a greater quantity of photon energy was being converted to heat in the latter regions. Whilst it is true that there is a greater amount of melanin present within the subcutaneous region of the hair shaft in growing hairs, there is little, if any,

evidence of the presence of any melanin at all within the epidermis. Therefore, how the laser exerted its effects on the epidermis can only be postulated. The possibility that the epidermis could be damaged through a build-up of heat within the hair follicles is unlikely. Although the density of hairs and the extent of their pigmentation is greater in growing regions than it is in resting regions, if the greater damage to the epidermis was caused by heat dissipation, then a gradient of damage should be evident from the follicles outwards. The cells lining the follicular canal would be most damaged along with other structures surrounding the follicle including the sebaceous glands. This was not noted when the histological sections were examined.

A second potential cause of epidermal damage could be another chromophore present within the cells of the epidermis. Work by Cheng and Packer in 1978 revealed ultrastructural damage occurring to mitochondria after exposure to visible light (400-720 nm) of intensity 300 mW/cm^2 (Cheng and Packer, 1979) It was proposed that the flavoproteins within the mitochondria were acting as a chromophore causing the damage noted. However, the cells lining the follicular canals should also be damaged and so this would appear unlikely. Viewing the sections from growing and resting hair regions that had been irradiated and stained with Massons Fontana revealed melanin pigment coating the surface of the epidermis. This could only have come from the hair shafts and so it is feasible that irradiation had caused the shafts to explode scattering the melanin pigment over the epidermis, but not into the follicular canals. If this had occurred during the pulse duration, then it could be that the remaining energy emitted interacted with the melanin now present upon the skin surface causing damage to the epidermal cells. The greater melanin content of anagen hair shafts would result in a larger quantity of melanin being scattered over the skin surface and hence greater epidermal damage. As no pigment appeared present in the hair canals, then the cells lining the canal would be left undamaged, as was observed.

Comparing the wound scores of the resting hair sites at each of the exposure fluences revealed a statistically significant difference between the scores on days 4, 6, 9 and 10. Performing the same analysis upon growing hair regions did not reveal any statistically significant difference on any of the days taken to heal. It is probable that

the wounds had reached maximal score within the growing hair regions but not in the resting hair regions resulting in the former being scored equally whilst the latter attaining different values. It must also be remembered that the experimental numbers were small.

Histological assessment performed at 56 days post laser exposure at all fluences used revealed no signs of scarring or fibrosis within the dermis. Lin et al in their experiment described sites where follicles had previously been present having been replaced by scar tissue. Whether damage to follicles must occur to this extent to prevent hair regrowth cannot be stated. However, no such dermal damage was noted in this experiment and yet depilation had still occurred at 56 days. Therefore it is possible that this may not be the case.

4.7 CONCLUSIONS

- The NMRL produced better depilatory results in the anagen (growing) hair regions than in the catagen or telogen (resting) hair regions confirming the findings of Lin et al.

- The NMRL produced a statistically significant delay in hair regrowth when compared to non-irradiated, trimmed controls up to 21 days in resting hair regions and 56 days in growing hair regions at the fluences used.

- Skin wounding appeared fluence-dependent in resting hair regions only but this may have resulted from the scoring system used.

- Skin wounding appeared to be melanin-dependent with melanin scattering onto the skin a possible vector of laser-induced damage.

- It appeared that the maximum depilatory effect of this laser was achieved in growing hair regions at 6 J/cm^2 and that any increase in the fluence would result in greater damage to the skin alone.

CHAPTER 5 - THE EFFECT ADDITIONAL CHROMOPHORE HAS UPON RUBY LASER SKIN INTERACTION

5.1 INTRODUCTION

Immediately after exposure of human skin to the normal mode ruby laser (NMRL), ultrastructural damage can be detected mainly in the basal layer of the epidermis (Liew, 1999). Damage appears limited to the site at which melanin pigment is concentrated and consequently where keratinocyte stem cells and melanocytes are situated. The ideal skin protector to prevent NMRL-associated side effects such as erythema, superficial blistering, hypo and hyperpigmentation (see section 1.5.5 and Figures 1.7, 1.8a and 1.8b) would prevent damage occurring to the progenitor cells of the basal layer whilst allowing passage of the laser beam to the bulge region and the hair bulb. One of the ways that this could be produced would be by choosing a substance which would either reflect or absorb the laser beam thereby either preventing it from entering the skin or dissipating enough of the incident energy before it reaches levels at which damage would be caused. However, if application of a substance to the skin were to prevent passage of the laser beam, then this might adversely affect depilatory efficacy. Whether this was the case or not would depend upon whether the mode of the laser required the passage of light through the skin. If the major mode of depilation, however, was by using the hair shaft as a thermal conduit into the skin, then providing the hairs remained free of the protective substance, the laser should, in theory, still work. Although work performed in Chapter 3 suggested that NMRL exposure-induced heat was specifically produced in the hair follicle rather than the adjacent skin, whether this was produced locally along the length of the shaft or simply conducted down the shaft is still unknown. Nevertheless, a high quantity of photon energy was shown to penetrate the skin reaching fluence levels at the bulge and the bulb great enough to potentially induce cell damage suggesting that the penetration of light is potentially sufficient to cause depilation.

The ability to maintain the hairs free of an opaque substance painted upon the skin would be difficult if not impossible. Therefore, this chapter concentrates on the use of a chromophore which would convert the photon energy to heat at the skin surface so potentially dissipating the energy before it reached the basal layers. Human skin contains layers of keratinising epidermal cells above the viable basal layer which is further protected by a non-viable cornified layer. Whether the distance between the skin surface and the replicating epidermal layer would be great enough to prevent heat damage reaching the basal cells is not known. In addition, the potential of this method of protecting the skin depends upon the main laser energy pathway for NMRL-assisted depilation being along the hair shaft otherwise the efficacy of depilation would be compromised.

There are no papers to the author's knowledge which have addressed the use of a pigment to protect the skin during NMRL-assisted depilation. Chromophore has been added to skin to attempt to improve depilatory success. The NdYAG laser has been advocated for depilatory purposes and appears to have achieved similar results to the NMRL over a rather short 12 week period of follow-up (see Table 1.2 (Goldberg, et al., 1997), (Nanni and Alster, 1997)). This NdYAG laser requires the application of a topical carbon-based oil suspension to the skin area undergoing depilation to act as a chromophore. Unfortunately, no long-term assessment of results has been performed and again the numbers of patients in the studies were too small for statistical significance to be achieved. Therefore it is unknown as to whether the use of NdYAG lasers with chromophore achieves better results than the NMRL laser alone. Theoretically, if it were possible to add a chromophore to the hair follicle to interact with the NMRL beam in a manner similar to eumelanin then this may improve depilatory success. With the variety of hair colours that exist in the population, not only between individuals but within the same individuals skin, it is possible that a laser of one single wavelength would not suffice to obtain complete and permanent depilation of a target area. Consequently, the only other method that could feasibly be employed to improve the targeting and effectiveness of the NMRL is that of increasing the quantity of chromophore present at the site where it is required to work. This ideally would mean the bulge region and the hair bulb, but to administer a

chromophore selectively in and around those cells would be a practical impossibility. If chromophore could be placed as close as possible to these sites, which would mean within the hair canal, then this could increase local heat production from the photon energy of the laser beam possibly improving the depilatory efficacy. However, if depilation were to occur via the "thermal conduit" route, then adding chromophore to the skin including the hair shafts may not only protect the skin but also improve depilatory efficacy.

This chapter describes four experiments in total. The first involves a study to discover the colour of chromophore best suited to either reflect or absorb the beam of photon energy emitted by the NMRL. The second looks at how well the chosen chromophore is able to protect *ex vivo* human skin from NMRL irradiation-induced cell damage histologically. The third part addresses the ability of the NMRL beam to penetrate various thicknesses of *ex vivo* skin painted with the chosen chromophore and lastly, the effectiveness of the chromophore is ascertained using an animal model.

5.2 AIMS

- To determine the colour of ink which most reflects/absorbs normal mode ruby laser light.

- To discover the histological extent of protection induced in *ex vivo* skin painted with chromophore prior to normal mode ruby laser irradiation.

- To determine the effect of adding a chromophore to the skin surface of graft samples of varying thicknesses upon the energy recorded beneath.

- To determine the protection afforded to the skin of the black-haired mouse by the addition of chromophore to the skin surface prior to normal mode ruby laser exposure.

- To determine the effect of the addition of chromophore to the skin surface of the black-haired mouse prior to normal mode ruby laser irradiation upon depilatory efficacy.

5.3 METHODS

5.3.1 The Colour Most Suited to Reflect or Absorb Ruby Laser Light

In an attempt to discover the ideal colour which would reflect or absorb the ruby laser light at 694 nm, a pilot experiment was performed. When the laser was fired upon a piece of paper coated with black ink, all the ink vapourised leaving a white patch the size of the spot behind. Therefore, different colours of ink including red, orange, yellow, green, blue, purple and black were painted onto a clear acetate sheet, which was then laid over a piece of black ink-coated paper and the exact same pulse of laser light fired upon each of the coloured squares on the acetate. The quantity of black ink removed from the paper beneath the clear acetate sheet was assessed subjectively and noted.

5.3.2 The Effect the Addition of Black Ink as a Chromophore to the Surface of *Ex vivo* Human Skin Prior to NMRL Irradiation has upon Histological Damage Noted

Specimens of normal, hair-free human skin were taken immediately after excision from each of six patients and placed onto a saline damp gauze in a 12 cm petri dish within a Class II hood. The subdermal fat was dissected away from the dermis whilst the specimen was maintained damp and the specimen then divided into four samples. One of the samples was exposed to a single pulse of 15 J/cm^2 upon the epidermis from the NMRL whilst it lay upon the gauze. The second skin sample had the epidermis painted with black ink before it too was exposed to the same fluence whilst lying upon the saline damp gauze. The third sample acted as a positive control and was exposed to ultraviolet radiation for 10 minutes upon the skin surface at a dose known to induce cellular DNA damage. The fourth was exposed to air for the same

duration as the laser specimens had been, so acting as a negative control. Both sets of controls were also maintained upon a saline damp gauze during experimentation to prevent drying.

Once each of the samples had been experimented upon, a 6 mm biopsy was taken from all treated sites and these were then placed dermis down upon a sterile steel mesh in a 6 cm petri dish. FCM was added to the level of the mesh to maintain cell viability and the dish placed in an incubator for 18 hours.

After 18 hours, the specimens were removed from the incubator and fixed immediately in 10% formal saline. Histological processing then occurred to embed the biopsies in paraffin wax which were then sectioned transversely. Immunohistochemical staining was performed to assess for expression of p53 protein within the cells of the epidermis, the site of this expression and its extent (see section 2.3.2).

5.3.3 The Addition of Black Ink to the Surface of *Ex vivo* Human Skin and its Effect Upon NMRL Light Transfer through Skin

This experiment was performed using the same methodology described in Chapter 3, section 3.2 to assess laser light penetration into *ex vivo* skin. Large specimens of skin measuring approximately 20 x 10 cm were taken from 6 consenting caucasian female patients undergoing breast reduction. 8 samples of differing thicknesses were taken from each of the specimens using an air driven dermatome and dissecting scissors. The samples were cut to 1 cm^2, their thickness measured and each placed individually on a cover slip upon the external energy meter (see section 2.1.6). A single laser pulse of 9.24 J/cm^2 was fired onto the skin surface and the meter reading recorded. Black ink was then painted onto the epidermis of the same sample before it was exposed, once again, to a single pulse of 9.24 J/cm^2 and the meter reading recorded. The laser handpiece was cleaned and the fluence emmision re-checked upon the energy meter after each sample exposure ensuring the same fluence exposure. Plots of energy drop

over distance travelled through each skin sample from the same specimen were produced with and without the application of black ink to the surface.

5.3.4 The Addition of Black Ink to the Skin of the Black-haired Mouse Prior to NMRL Irradiation and its Effect Upon Depilatory Efficacy and Skin Side Effects

22 mice were used for this procedure. All were anaesthetised by intraperitoneal injection prior to having their backs and flanks trimmed of hair. Eleven mice underwent laser treatment upon growing hair patches alone whilst the second group of eleven underwent treatment upon resting hair patches alone.

The mice were placed individually upon a clean surgical drape and the sites to undergo NMRL irradiation identified. Each mouse had four exposure sites, two where the skin had been painted just prior to laser treatment with black ink and two which remained ink-free. One of the paired target sites (which included a black ink site and an ink free site) was exposed to a fluence of 6 J/cm^2 whilst the other was exposed to 8 J/cm^2. After NMRL irradiation, each mouse was placed into an individual box upon a warm mat and allowed to recover. The laser hand-piece was cleaned after each mouse was irradiated since the black ink used created a plume after exposure which coated the end of the hand-piece potentially reducing the laser output. After cleaning, the emitted fluence was checked before the experiment continued.

Three mice were taken from each of both groups and sacrificed immediately after laser treatment. 6 mm biopsies were taken from all laser exposed sites along with biopsies from non irradiated, trimmed sites from growing and resting hair regions acting as negative controls for comparative purposes. These were fixed immediately in 10% formal saline before undergoing routine paraffin wax embedding.

The remaining mice were observed on a daily basis and the laser induced wounds scored until fully healed according to Table 2.4. The mice were then anaesthetised by intraperitoneal injection and the laser exposed sites permanently marked using a tattooing machine. This enabled the target sites to be identified later during hair

regrowth assessment.

Hair regrowth was scored weekly over a 2 month period according to Table 2.6. After this time, the mice were sacrificed and a 6 mm biopsy taken from all irradiated sites plus controls from non-irradiated hair growing and resting regions as appropriate. These were fixed immediately in 10% formal saline before undergoing routine paraffin wax embedding.

Histological analysis of paired random transverse sections was performed upon the biopsies taken from the group sacrificed immediately. One of the pairs was stained with H&E to assess the site and extent of cellular damage whilst the second was stained by the modified SACPIC technique to look for the site and extent of hair shaft damage. Sections of the biopsy specimens taken from the two groups observed over time were stained with Massons trichrome alone to assess for fibrosis or scar production within the skin.

5.4 STATISTICS

Sample data have been shown as means (+/- standard deviation). A statistical comparison of two groups was performed on the median values using the Mann-Whitney Rank Sum test. A comparison of more than two groups was performed using the one way ANOVA method. If the normality test failed then either a Dunnett's test, which is a pairwise multiple comparison procedure, was performed or a Kruskal-Wallis test, which is a one way ANOVA on the median values. The particular test used has been identified within the relevant results paragraphs.

5.5 RESULTS

5.5.1 The Colour Most Suited to Reflect or Absorb Ruby Laser Light

The pilot study showed that the colour most able to prevent the ruby laser light from removing the black ink from the paper placed beneath the clear acetate sheet was

black ink itself (not shown). The black ink coating the paper beneath the black ink square upon the acetate had been barely touched by NMRL exposure. None of the other colours tried appeared to prevent the removal of black ink which occurred to the same extent as when the laser was fired through the clear acetate alone.

5.5.2 The Effect the Addition of Black Ink as a Chromophore to the Surface of *Ex vivo* Human Skin Prior to NMRL Irradiation has upon Histological Damage Noted

Figure 5.3 shows a representative section taken from a negative control stained for p53 protein expression. It can be seen that the majority of the nuclei within the epidermal cells have taken up the haematoxylin counterstain and are coloured blue. Therefore little p53 protein expression is present. In comparison, Figure 5.4 shows a representative section taken from a positive control specimen which has been exposed to ultraviolet irradiation for 10 minutes whilst upon the saline damp gauze. This shows that the majority of the nuclei of the epidermal cells have been stained brown and are therefore positive for p53 protein expression.

Figure 5.5 is a representative section taken from a specimen having been exposed to NMRL irradiation at a fluence of 8 J/cm^2 without the addition of a chromophore to the skin surface. There is a generalised increase in cellular p53 protein expression compared to the cells within the negative control. However, expression does not appear to reach the extent of the positive control. The majority of cells within the epidermis of the laser irradiated specimen expressing p53 are in the basal layer where the viable keratinocytes reside.

Figure 5.6 is a representative section taken from a specimen having been exposed to NMRL irradiation also at a fluence of 8 J/cm^2 but with the addition of a black ink chromophore to the skin surface. The expression of p53 protein within the cells of this section is much less than that seen within the cells from the laser irradiated specimen alone. A markedly reduced number of cells, particularly in the basal layer, express p53 protein within the nuclei.

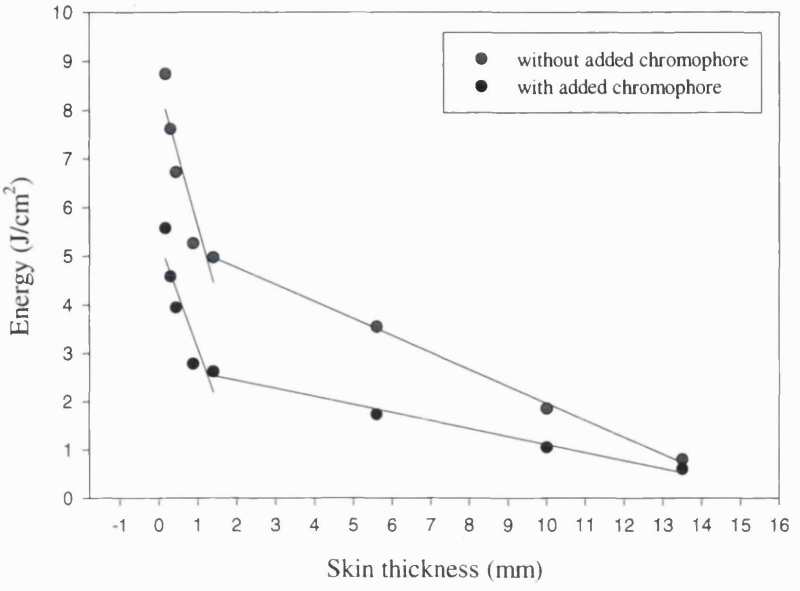

Figure 5.1: Graph representing the laser light penetration profiles through differing thicknesses of ex-vivo skin whose surfaces have either been painted or not with black ink prior to laser exposure at a fluence of 9.24 J/cm^2.

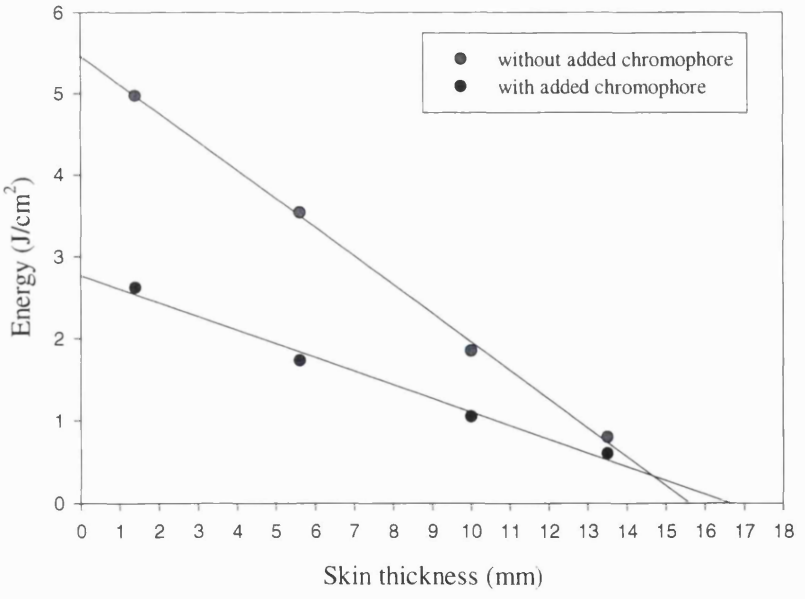

Figure 5.2: Graph showing an extrapolation of the plots in Figure 5.1 to the x axis revealing the probable maximum depth of penetration of the ruby laser beam in ex-vivo skin whose surfaces had either been painted or not with chromophore prior to laser exposure at a fluence of 9.24 J/cm^2.

5.5.3 The Addition of Black Ink to the Surface of *Ex vivo* Human Skin and its Effect Upon Laser Light Transfer through Skin

Painting black ink upon the *ex vivo* skin specimens to act as a chromophore for the NMRL reduced the energy levels recorded by the meter beneath to approximately half that noted when no ink had been painted upon the skin surface at the same fluence of exposure (see Figure 5.1). The plot of energy drop versus distance through the skin when exposed to 9.24 J/cm^2 after chromophore was added to the surface was virtually identical to the plot produced when 4.75 J/cm^2 was fired upon the same specimen without the addition of chromophore (see chapter 3, section 3.3.2 and Figure 3.13). This showed that added chromophore reduces the fluence-depth profile by approximately 50% and similar to that seen when the incident fluence was approximately half that used. When the penetration profile of the photon beam was extrapolated to the x axis (Figure 5.2), it was found to penetrate to a mean depth of 15.69 mm (SD +/- 0.39: see Table 5.1) in the specimens where chromophore had not been added prior to exposure and to 15.74 mm (SD +/- 0.49: see Table 5.1) where chromophore had been added. No statistically significant difference was detected between these two values upon Mann Whitney Rank Sum testing.

Table 5.1: Table showing the maximum depth of penetration according to fluence of exposure for all 6 patient specimens.

Patient	Maximum depth of penetration without chromophore (mm)	Maximum depth of penetration with chromophore (mm)
1	15.65	16.60
2	15.98	15.74
3	16.12	15.23
4	15.76	15.55
5	14.98	15.96
6	15.69	15.37

Figure 5.3: Transverse section of a negative control of human ex-vivo skin having undergone immunohistochemical staining for expression of p53. Virtually all the nuclei have taken up the counterstain (haematoxylin) and so appear blue (x200).

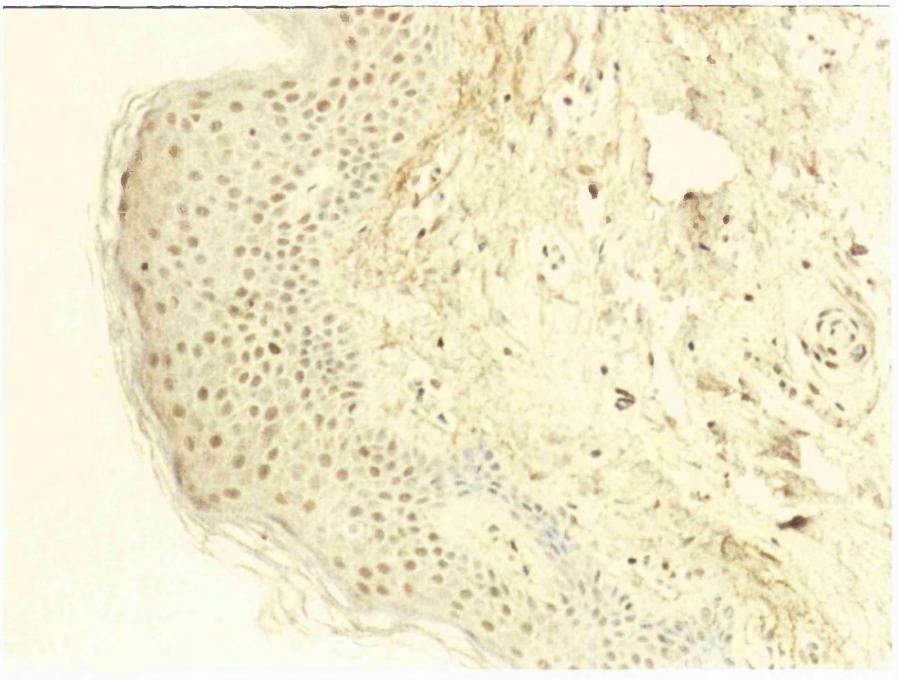

Figure 5.4: Transverse section of a positive control of human ex-vivo skin having been exposed to ultraviolet irradiation and stained for p53 protein expression. Positive nuclei (brown) are seen throughout the layers of the epidermis and into the dermis (x200).

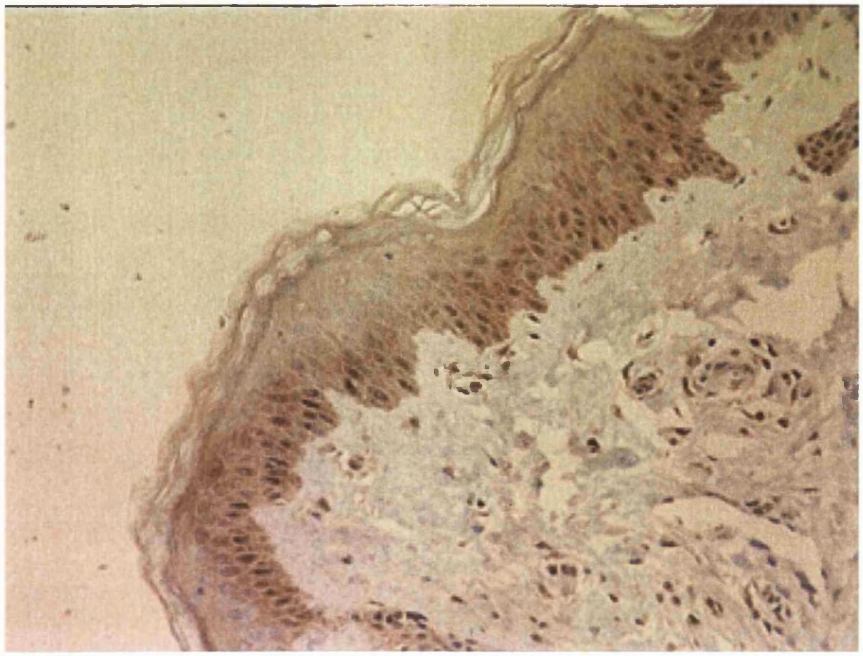

Figure 5.5: Transverse section of a specimen of ex-vivo human skin having undergone ruby laser irradiation at 15 J/cm^2 and stained for p53 protein expression. The nuclei in the basal layer and above have stained positive for the protein (brown) showing damage has occurred to the cells within this region (x200).

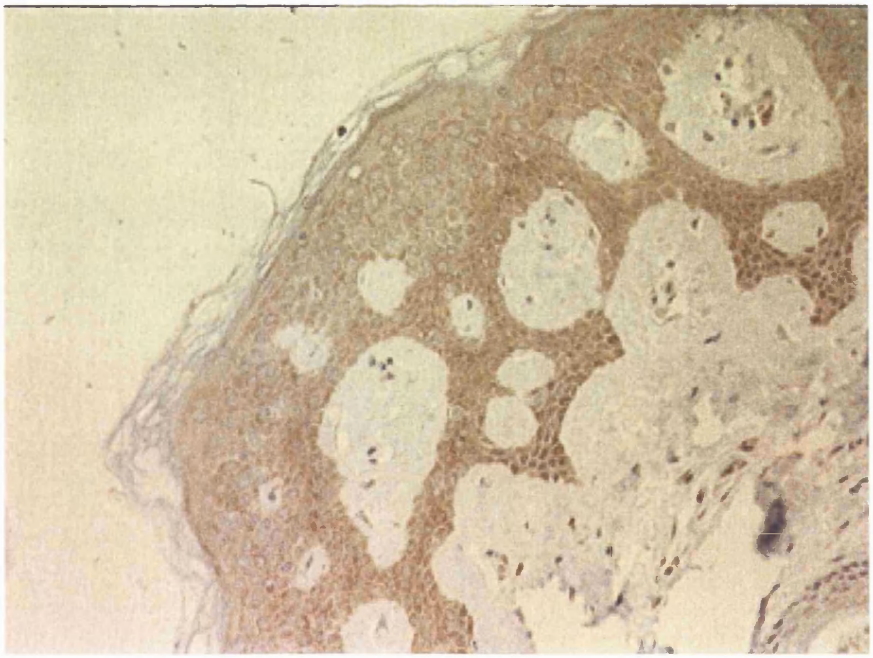

Figure 5.6: Transverse section of a specimen of ex-vivo human skin having had chromophore added to the surface prior to ruby laser exposure at 15 J/cm^2 and stained for p53 protein expression. No increase in p53 protein expression is apparent in the basal layers as compared to the section above (x200).

5.5.4 The Addition of Black Ink to the Skin of the Black-haired Mouse Prior to NMRL Irradiation and its Effect Upon Depilatory Efficacy and Skin Side Effects

Depilation

All the mice to be followed over the 8 week period survived the anaesthetic and made a full post-operative recovery, manifesting no systemic ill effects resulting from NMRL irradiation.

Growing Hair Sites

The mean weekly depilatory scores achieved upon sites where chromophore had either been added or not prior to NMRL irradiation were represented graphically according to the hair growth phase and the fluence of irradiation. Figure 5.7a represents a graph of the depilatory scores achieved upon growing hair sites irradiated at 6 J/cm^2. The median of the weekly scores of hair regrowth from both sets of irradiated mice (plus or minus chromophore) were compared with each other and with the non-irradiated, trimmed control using the Mann Whitney Rank Sum test. Both sets of 6 J/cm^2 laser irradiated sites, irrespective of the presence of chromophore, showed a significant decrease in hair regrowth from weeks 1 to 7 compared with the trimmed only control ($p<0.001$, $p<0.001$, $p<0.001$, $p=0.001$, $p=0.01$, $p=0.027$ and $p=0.038$ respectively). Statistical comparison of hair regrowth scores between mice irradiated with 6 J/cm^2 in the presence or absence of chromophore showed no significant difference between the two over the whole experimental period.

Figure 5.7b shows a plot of the hair regrowth scores in sites within a growing hair region where chromophore was either added or not prior to irradiation at 8 J/cm^2. Similarly, when the median weekly values of both sets of laser irradiated sites were statistically compared with non-irradiated trimmed controls using the Mann Whitney Rank Sum test, a significant decrease in hair regrowth was noted during the whole of the observational period irrespective of whether chromophore had been added prior to irradiation or not ($p<0.001$, $p=0.001$, $p<0.001$, $p=0.001$, $p<0.001$, $p<0.001$, $p=0.001$

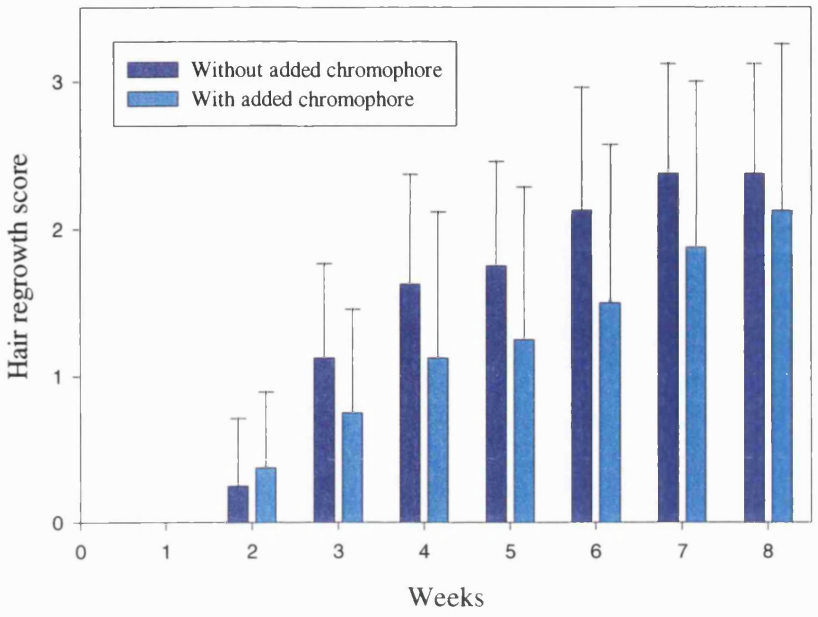

a.

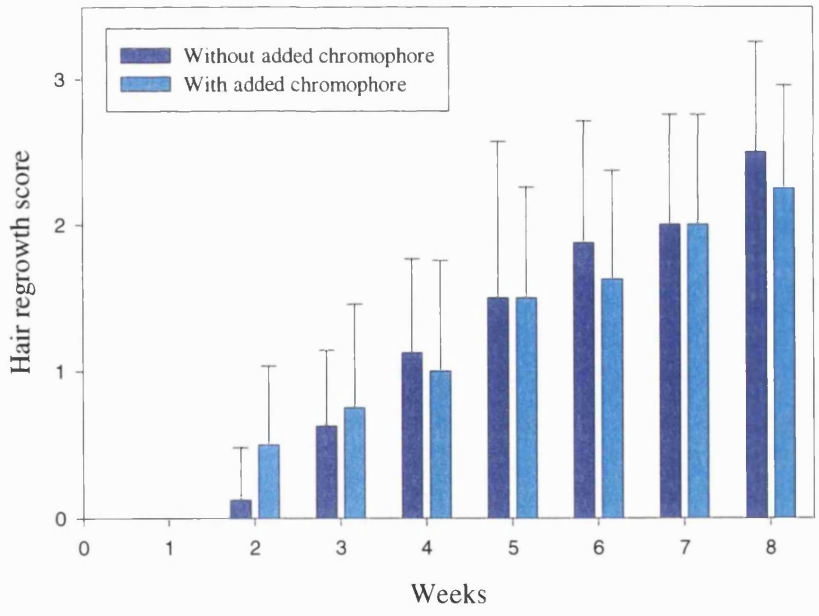

b.

Figure 5.7: Graphs representing the weekly hair regrowth scores in growing hair regions irradiated at a) 6 J/cm^2 and b) 8 J/cm^2.

and p=0.005 respectively). A statistical comparison between the median values of weekly hair regrowth scores from irradiated sites in the presence or absence of chromophore revealed no significant difference between the two. Figure 5.8 shows a site in a growing hair region 8 weeks after irradiation at 8 J/cm^2 upon which chromophore had been added prior to exposure. The reduced hair growth can be noted, but this is also typical of that seen in sites irradiated in the absence of chromophore.

Resting Hair Sites

Figure 5.9a shows a plot of the hair regrowth scores from sites in a resting hair region irradiated at 6 J/cm^2 where chromophore was either added or not prior to exposure and Figure 5.9b shows a plot of similar sites which were exposed to 8 J/cm^2. Comparing the weekly depilatory scores from chromophore added sites with non-irradiated trimmed controls revealed a statistically significant difference in the median values from weeks 1 to 4 in both the 6 J/cm^2 ($p<0.001$, $p<0.001$, $p=0.038$ and $p=0.05$ respectively) and the 8 J/cm^2 ($p<0.001$, $p<0.001$, $p=0.027$, $p=0.05$ respectively) groups, whereas the irradiated sites where chromophore was not added had a statistically significant difference in the hair regrowth scores on weeks 1 and 2 alone ($p<0.001$ and $p=0.001$) in both the laser fluence groups. A comparison between the median values of the hair regrowth scores by Mann Whitney Rank Sum test from the sites where chromophore was added and those that were irradiated alone revealed a statistically significant difference in the scores upon week 3 ($p=0.021$) in the 6 J/cm^2 group. This finding was reproduced in the 8 J/cm^2 group ($p=0.05$). No statistically significant difference in hair regrowth was noted upon comparison of the chromophore added sites exposed to 6 and 8 J/cm^2.

Skin Damage

Graphs were plotted showing the mean daily wound scores with standard deviation at both the chromophore treated and untreated sites at each of the two fluences of exposure within both growing hair regions and resting hair regions.

Figure 5.8: Photograph showing hair depilation in a growing hair region 8 weeks after ruby laser exposure at 8 J/cm^2. Chromophore had been added to this site prior to exposure.

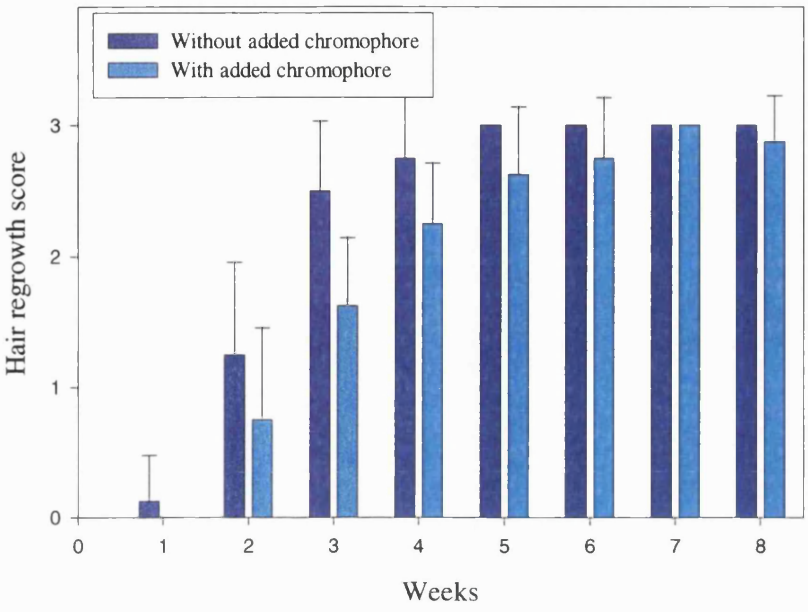

a.

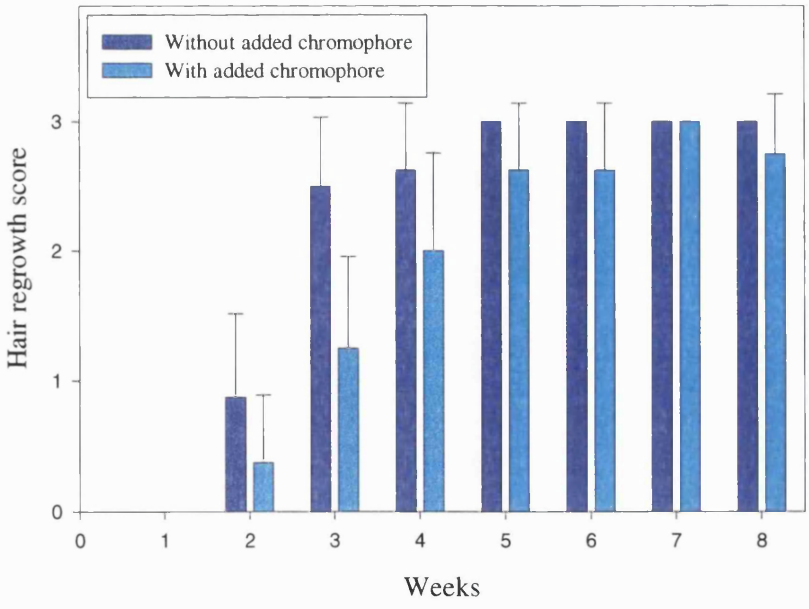

b.

Figure 5.9: Graphs representing the weekly hair regrowth scores in resting hair regions irradiated at a) 6 J/cm^2 and b) 8 J/cm^2.

Growing Hair Sites

The graph depicting the mean wound scores in growing hair regions where chromophore was either added or not prior to irradiation at a fluence of 6 J/cm^2 is shown in Figure 5.10a. The daily wound scores were always slightly greater in the group where chromophore had been added, but when the median daily values were analysed by Mann Whitney Rank Sum test, no statistically significant difference was seen on any day. The graph depicting the wound scores in growing hair regions where chromophore was either added or not prior to irradiation at a fluence of 8 J/cm^2 is shown in Figure 5.10b. The daily wound scores showed little difference between the two sites and, again, when the median values were analysed daily by the Mann Whitney Rank Sum test, it did not reveal any statistical significance between the two on any day. Figure 5.11 shows a wound in a growing hair region 7 days after NMRL exposure at 8 J/cm^2 where chromophore was not added to the site before irradiation. Figure 5.12 shows a similar site but where chromophore was added before irradiation. No difference can be seen in the extent of the wounding clinically reflecting the scores recorded.

A graph was plotted showing the mean time in days for laser exposed sites at 6 J/cm^2 and 8 J/cm^2 within the growing hair cohort to fully heal (see Figure 5.13). At 6 J/cm^2, the group where chromophore was added prior to irradiation took a mean of 13.63 days (SD +/- 1.6) whilst the group free of added chromophore took a mean of 13 days (SD +/- 1.07). Sites where chromophore was added within the same cohort prior to irradiation at 8 J/cm^2 had a mean time to heal of 13 days (SD +/- 1.85) whilst those free of added chromophore took 13.25 days to heal (SD +/- 1.39). No statistically significant difference existed in the time taken to full wound healing between sites where chromophore was added and those where it was not at both 6 and 8 J/cm^2 fluence.

Resting Hair Sites

The graph depicting the wound scores in resting hair regions where chromophore was either added or not prior to irradiation at a fluence of 6 J/cm^2 is shown in Figure 5.14a. The daily wound scores were always greater at the sites where chromophore had been added prior to irradiation and this was statistically significant when the median values were compared by Mann Whitney Rank Sum test on days 1 to 10 inclusive. The graph depicting the wound scores in resting hair regions where chromophore was either added or not prior to irradiation at a fluence of 8 J/cm^2 is shown in Figure 5.14b. The daily wound scores were also always greater at the sites where chromophore had been added prior to irradiation and this was statistically significant when the median values were compared by Mann Whitney Rank Sum test on days 1 to 12 inclusive. Figure 5.15 shows the skin damage in resting hair sites where chromophore had either been added or not prior to NMRL irradiation at 6 and 8 J/cm^2 two days after exposure. Skin damage can be seen to be much greater in the sites where chromophore was added at both 6 and 8 J/cm^2.

A graph showing the mean time to full healing within the resting hair cohort is shown in Figure 5.16. At 6 J/cm^2, the group where chromophore was added prior to irradiation took a mean of 12.62 days (SD +/- 1.77) whilst the group free of added chromophore took a mean of 9.35 days (SD +/- 1.3). Sites where chromophore was added within the same cohort prior to irradiation at 8 J/cm^2 had a mean time to heal of 13.13 days (SD +/- 1.46) whilst those free of added chromophore took 10.87 days to heal (SD +/- 0.99). A statistical comparison by Mann Whitney Rank Sum testing was made between the median values of the days taken to fully heal of the two sites within the resting hair region where chromophore had been added or not prior to irradiation at 6 J/cm^2. This showed that the site where chromophore had been added took significantly longer to heal ($p<0.001$). The analysis was repeated comparing at 8 J/cm^2. The median of the days taken to fully heal was statistically significant between the two groups when analysed by Mann Whitney Rank Sum testing ($p=0.005$) again with the chromophore added group taking longer to heal.

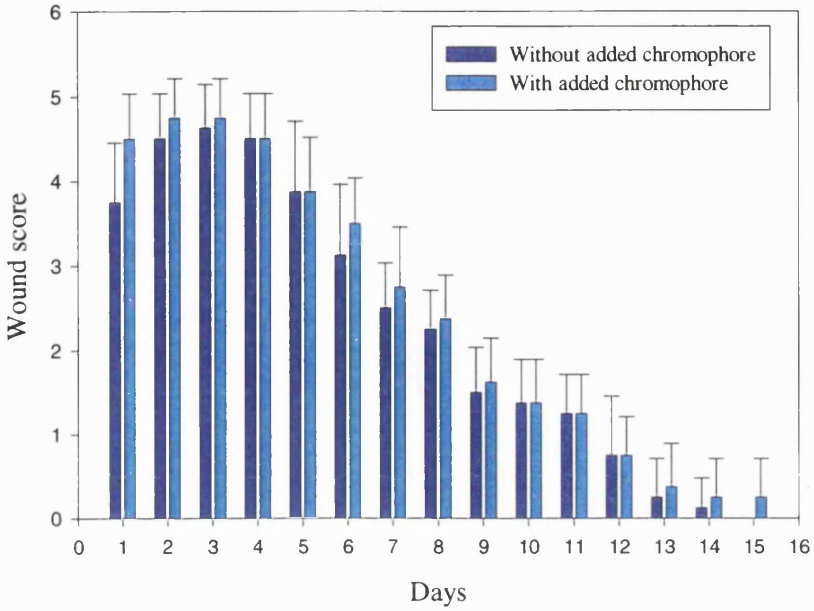

a.

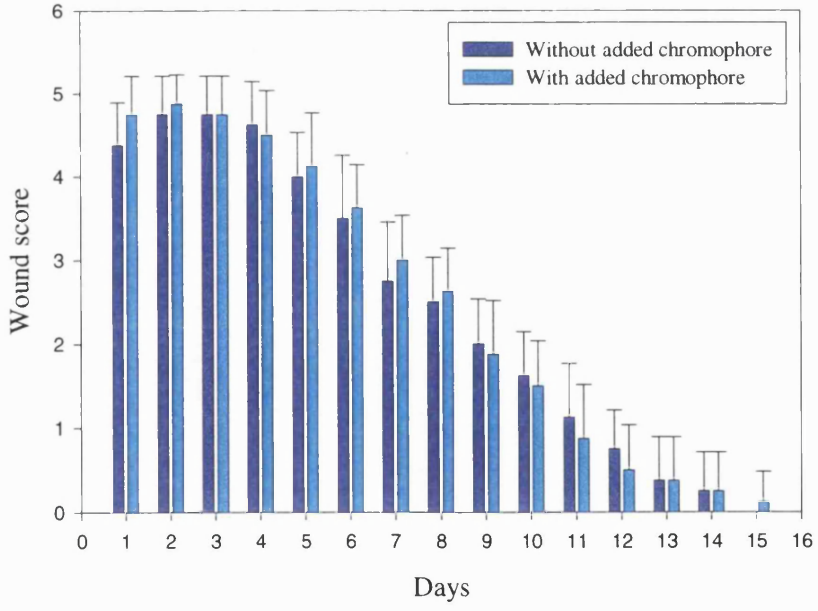

b.

Figure 5.10: Graphs representing the daily wound scores achieved upon growing hair regions where chromophore had either been added or not prior to laser exposure at a) 6 J/cm^2 and b) 8 J/cm^2 fluence.

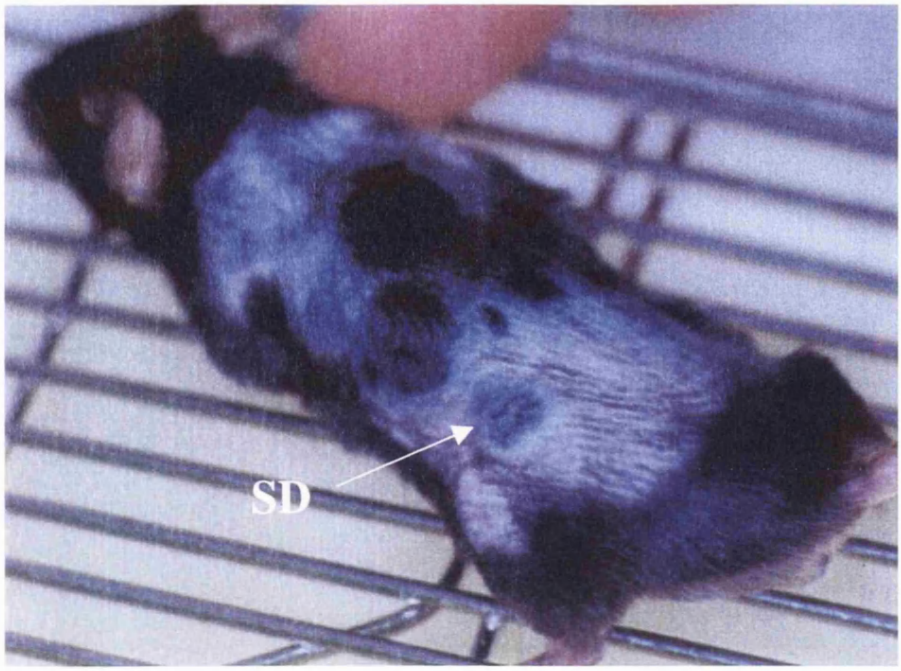

Figure 5.11: Photograph showing the skin damage (SD) in a growing hair site 7 days after ruby laser exposure at 8 J/cm^2 which did not have chromophore added prior to irradiation.

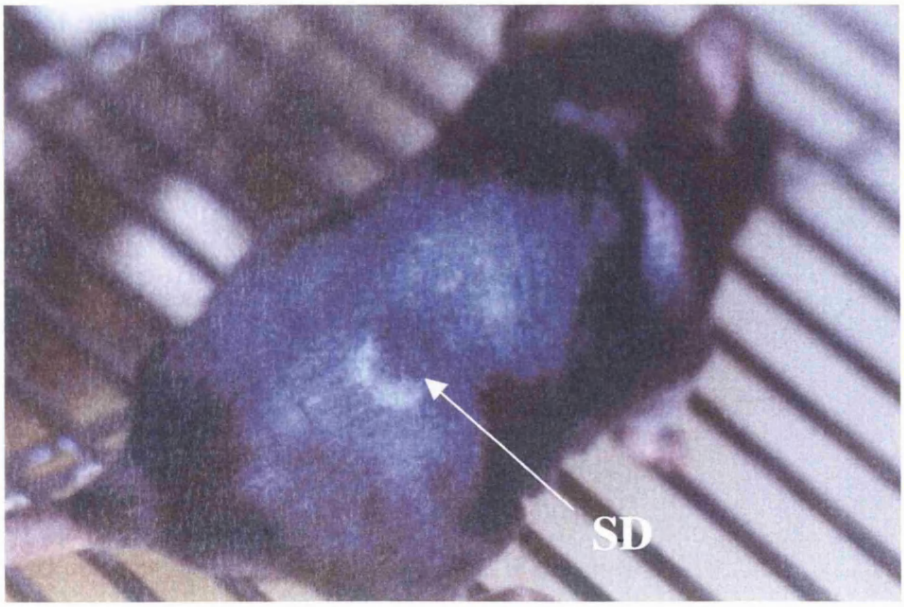

Figure 5.12: Photograph showing the skin damage (SD) in a growing hair site 7 days after ruby laser exposure at 8 J/cm^2 which had chromophore added to the site prior to irradiation.

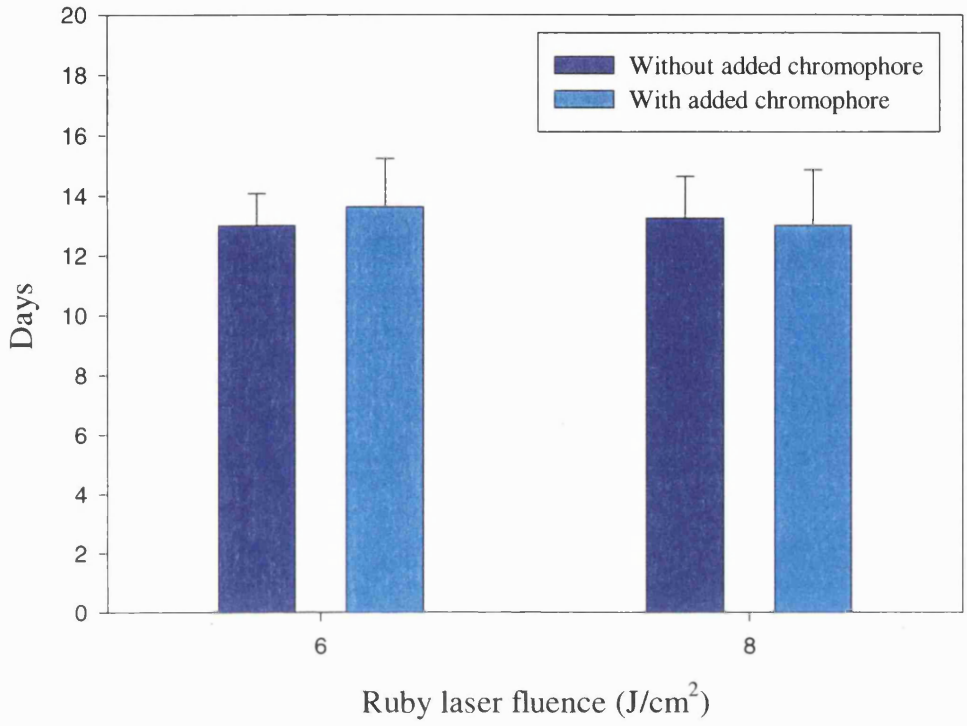

Figure 5.13: Graph showing the mean times to full healing of the skin wounds in growing hair sites which had either chromophore added or not to the skin surface prior to ruby laser exposure at 6 and 8 J/cm^2.

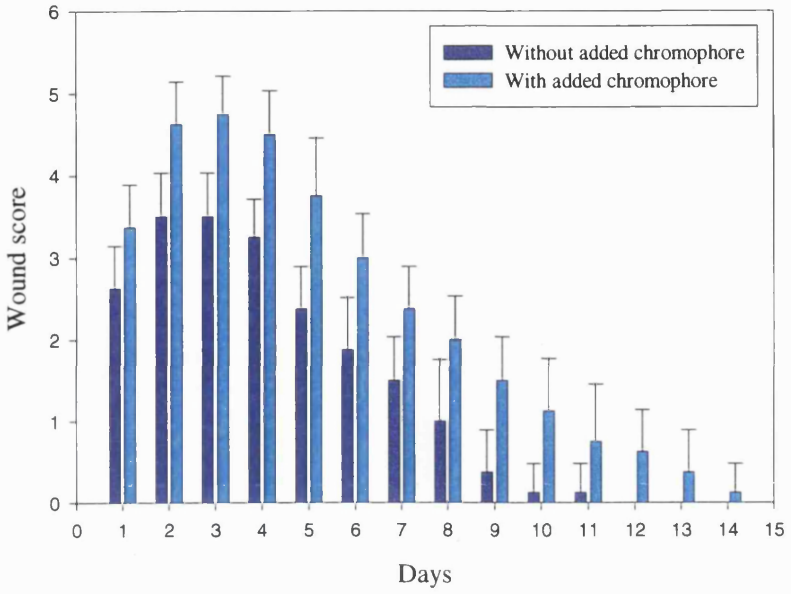

a.

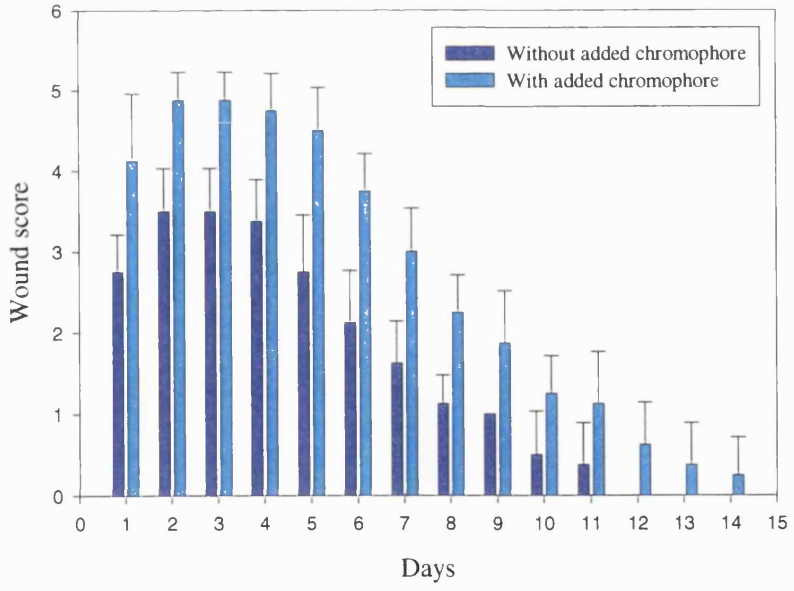

b.

Figure 5.14: Graphs representing the daily wound scores achieved upon resting hair regions where chromophore had either been added or not prior to laser exposure at a) 6 J/cm^2 and b) 8 J/cm^2 fluence.

Comparison between Growing and Resting Hair Sites

A statistical comparison was performed upon the daily median values of the wound scores of the sites in growing hair regions and resting hair regions that had had chromophore added prior to irradiation at the same fluence of either 6 or 8 J/cm^2. Using the Mann Whitney Rank Sum test, this showed no statistical difference between a growing or a resting hair region where chromophore had been added prior to NMRL exposure at the same fluence. This was noted upon all the days that it took to obtain full wound healing at those sites. A comparison between the median daily wound scores in growing and resting hair sites irradiated at the two fluences used but where chromophore was not added showed a statistically significant difference between the sites to the same extent recorded in Chapter 4, section 4.5.1.

Histology

Depilation

Modified SACPIC staining of transverse sections taken from growing hair sites where chromophore was added prior to exposure at 6 J/cm^2 and 8 J/cm^2 fluence appeared to show little difference in the extent of damage occurring to the hair shafts within the skin. In addition, damage was seen at a depth similar to that noted in Chapter 4, section 4.3.2. Figure 5.17a shows a transverse section stained using the modified SACPIC technique from a site exposed to laser irradiation at 6 J/cm^2 whilst Figure 5.17b shows a transverse section treated in the same manner but which had chromophore added prior to irradiation. The damage to the shaft can be seen to be similar. No change was noted to the extent of hair shaft damage in specimens within resting hair regions when chromophore was added to the skin before laser exposure compared to those where it had not been added (not shown).

Figure 5.15: Photograph of the back of a mouse 2 days after ruby laser exposure upon resting hair regions showing increased skin damage in the two upper sites where chromophore had been added prior to irradiation. The two cephalad sites have been exposed to a fluence of 6 J/cm^2 whilst the caudal sites have been exposed to 8 J/cm^2.

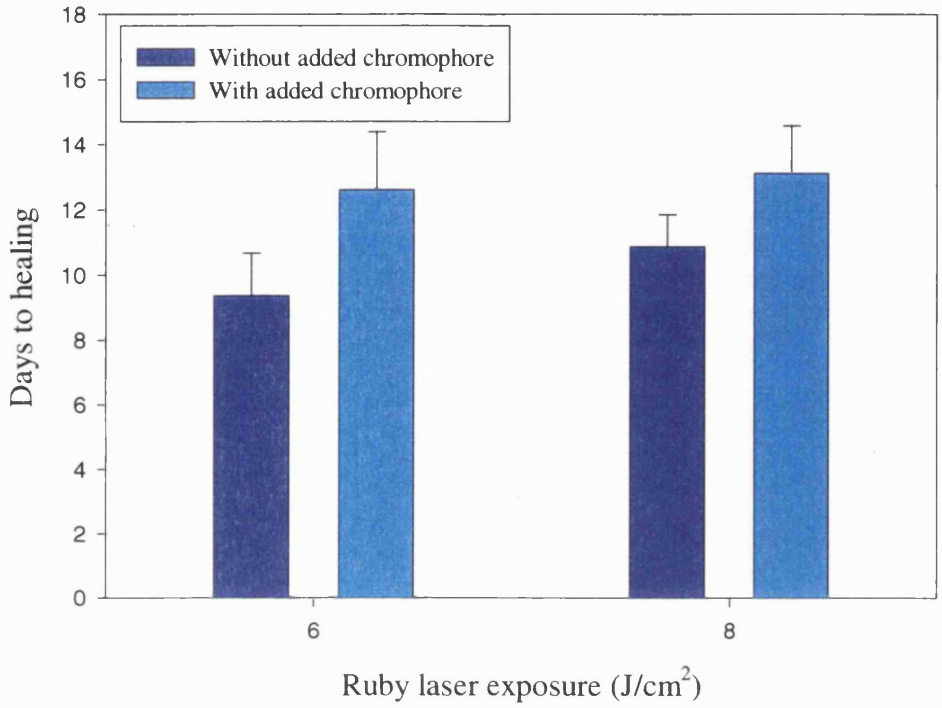

Figure 5.16: Graph showing the mean times to full healing of the skin wounds in resting hair sites which had either chromophore added or not to the skin surface prior to ruby laser exposure at 6 and 8 J/cm^2.

Skin Damage

Figure 5.18a shows a representative transverse section stained with H&E taken from a laser irradiated site alone within a resting hair region exposed to 6 J/cm^2. Figure 5.18b shows a representative transverse section stained with H&E also taken from a laser irradiated site in a hair resting region exposed to 6 J/cm^2, but that had been painted with chromophore prior to exposure. The damage to the epidermal cells is comparatively greater in the site where chromophore was added prior to irradiation. This is apparent from the increased nuclear pyknosis, cellular vacuolisation and epidermal loss which would all support the clinical findings. Figure 5.19a shows a representative transverse section stained with H&E from a resting hair region exposed to 8 J/cm^2, whilst Figure 5.19b shows a representative transverse section stained with H&E from a resting hair region exposed to 8 J/cm^2 where chromophore had been added to prior to irradiation. The damage is once again much greater in the chromophore added site compared to the site which was irradiated alone to such an extent that the epidermis has been totally removed in places. This is again consistent with the clinical findings.

Figure 5.20a shows a representative transverse section stained with H&E taken from a laser irradiated site in a growing hair region exposed to 6 J/cm^2, whilst Figure 5.20b shows a representative transverse section also taken from a laser irradiated site in a growing hair region exposed to 6 J/cm^2, but that had been treated prior to exposure with chromophore. There would appear to be little difference in damage to the epidermal cells between the two sections supporting the clinical findings. When the sections stained with H&E from the laser irradiated growing hair sites where chromophore had or had not been added prior to exposure at 8 J/cm^2 (not shown), were examined, again little difference was apparent between the two. However, the epithelial damage was present to a greater extent than the sections in Figure 5.20. This would again support the clinical findings.

Histological analysis of the sections taken from biopsy sites at three months and stained with Massons trichrome was performed to assess for signs of fibrosis and

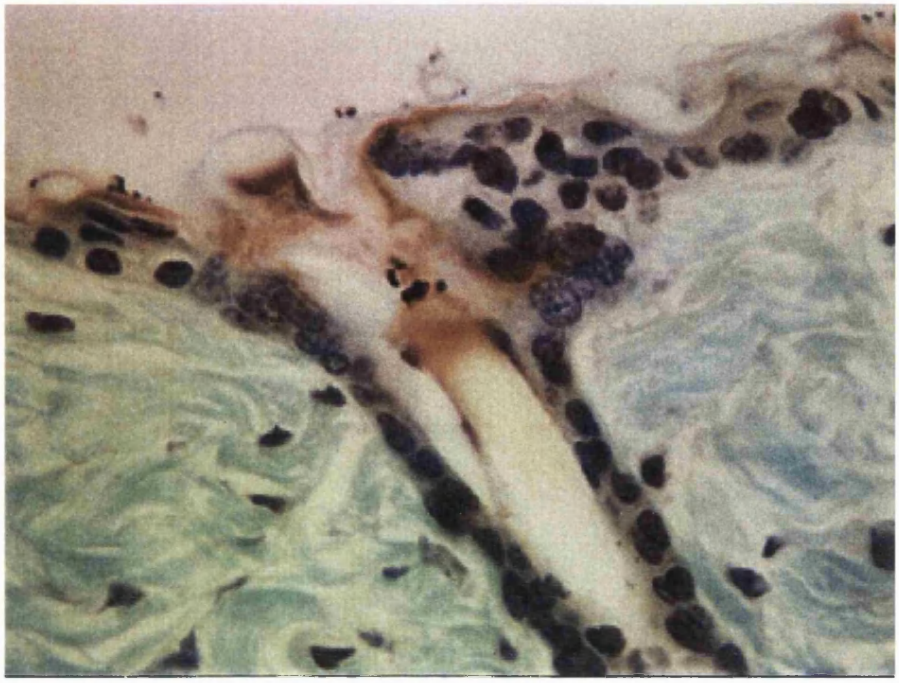

Figure 5.17a: Transverse section stained using the modified SACPIC technique showing the extent of damage occurring to the shaft of a resting hair irradiated at 6 J/cm^2 (x400).

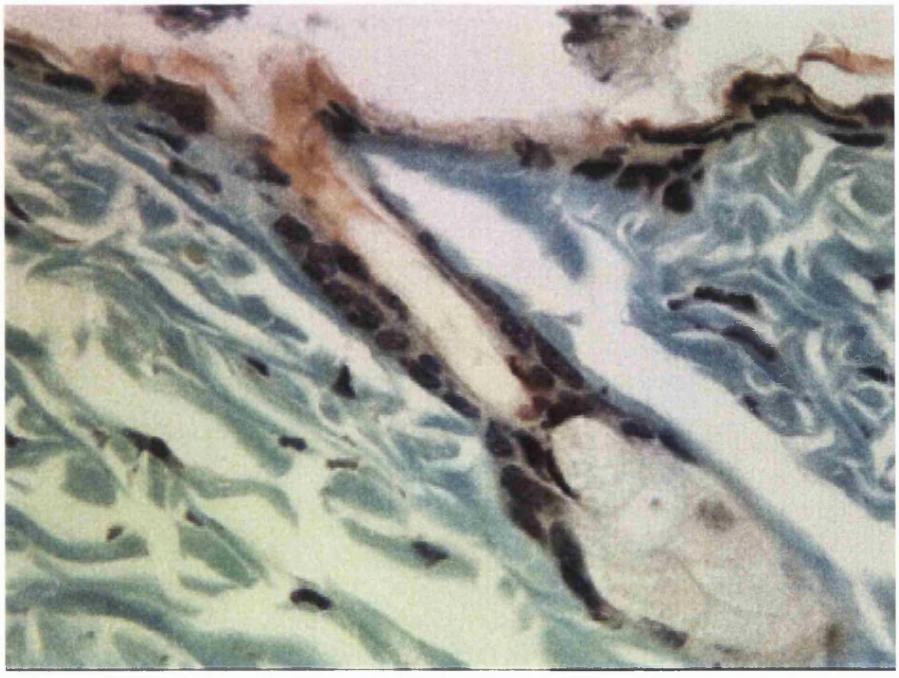

Figure 5.17b: Transverse section stained using the modified SACPIC technique showing the extent of damage occurring to the shaft of a resting hair which had chromophore applied to the surface prior to irradiation at 6 J/cm^2. Little difference is apparent in the extent of shaft damage occurring within the two sections (x400).

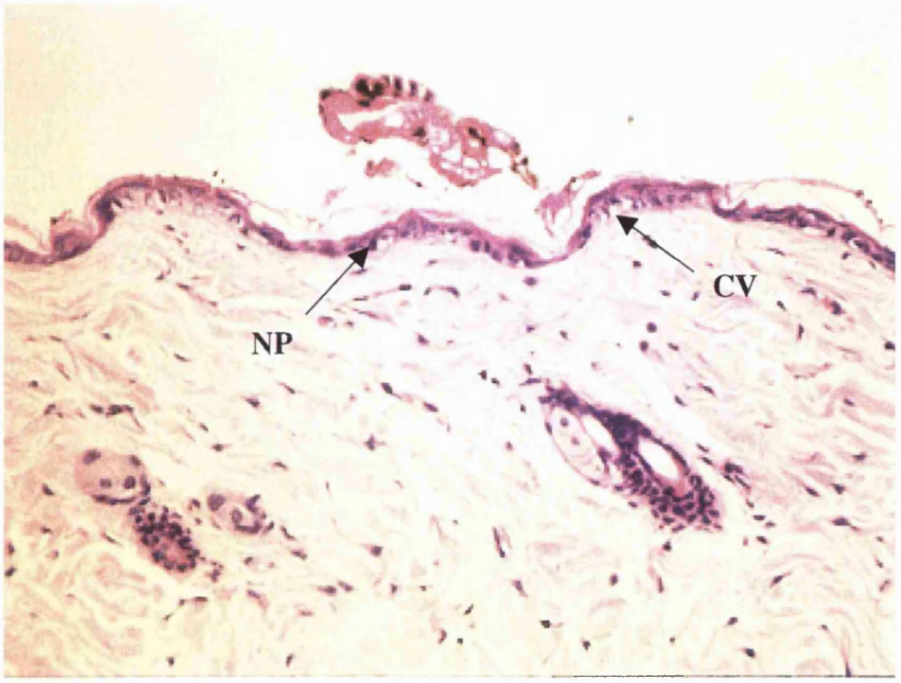

Figure 5.18a: Transverse section stained with H&E of a resting hair specimen irradiated at 6 J/cm^2 showing epithelial damage by the presence of cell vacuolisation (CV) and nuclear pyknosis (NP) x200.

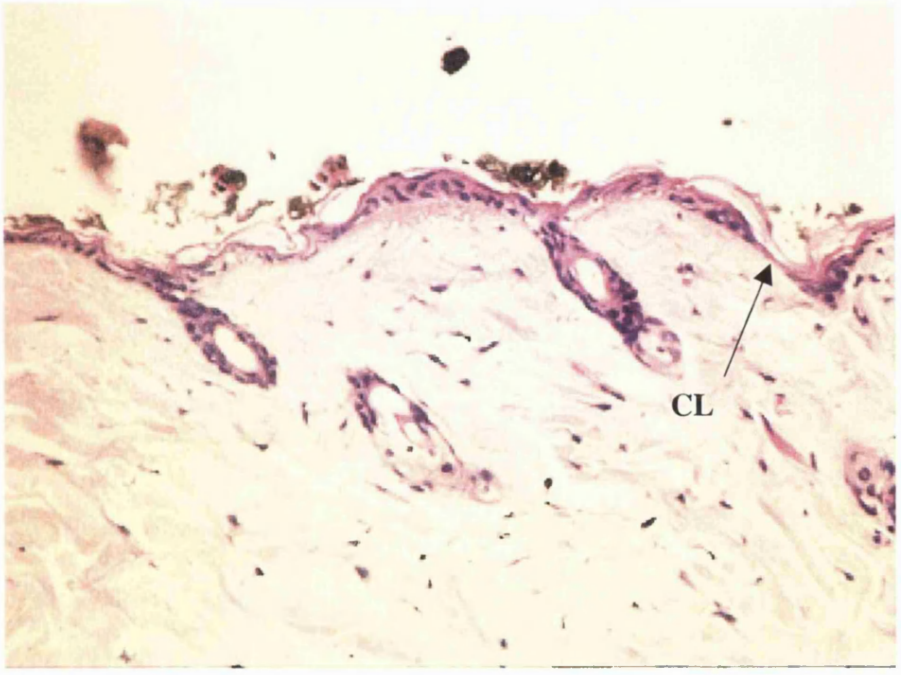

Figure 5.18b: Transverse section stained with H&E of a resting hair specimen that had chromophore added to the skin surface prior to irradiation at 6 J/cm^2. Greater damage to the skin surface has occurred than in Figure 6.6a with epithelial cell loss evident (CL) x200.

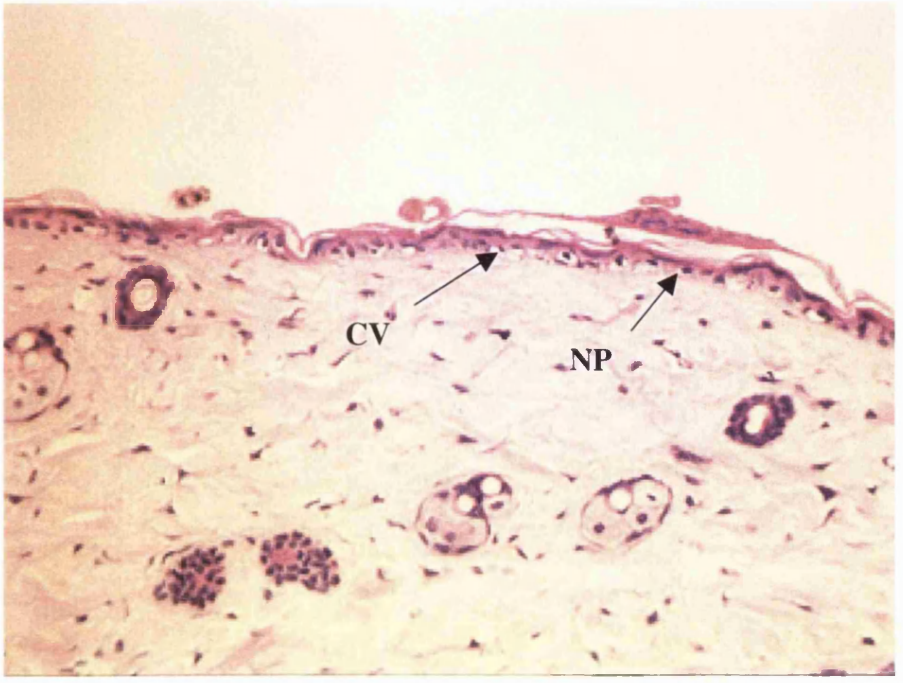

Figure 5.19a: Transverse section of a specimen of mouse skin irradiated at 8 J/cm^2 showing epithelial damage. Cell vacuolisation (CV) and nuclear pyknosis (NP) is evident (x200).

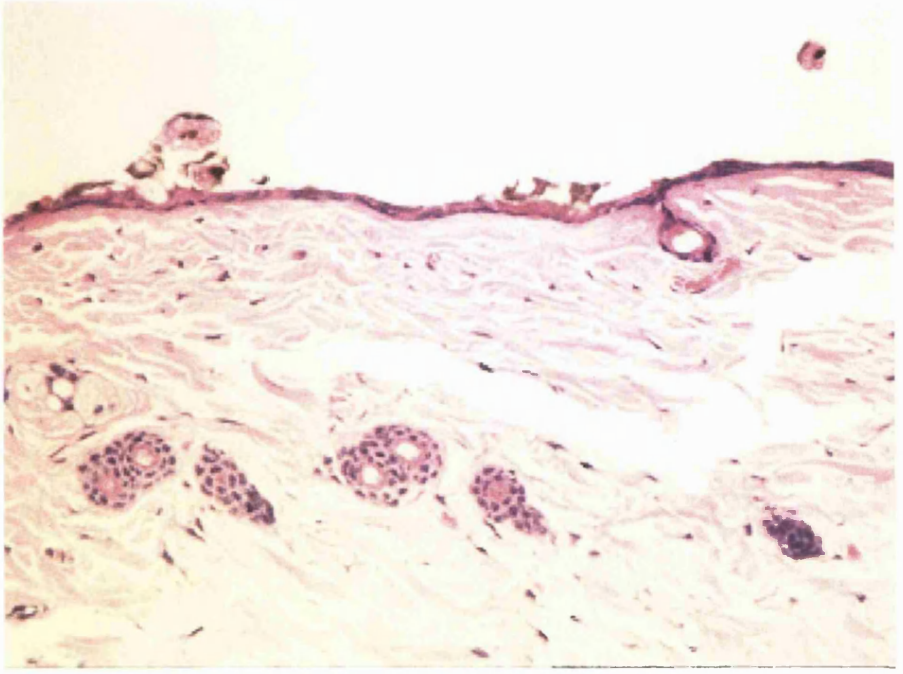

Figure 5.19b: Transverse section from a specimen of mouse skin having had chromophore added prior to irradiation at 8 J/cm^2. Virtually the whole of the epidermis has been damaged or removed as a result of laser exposure (x200).

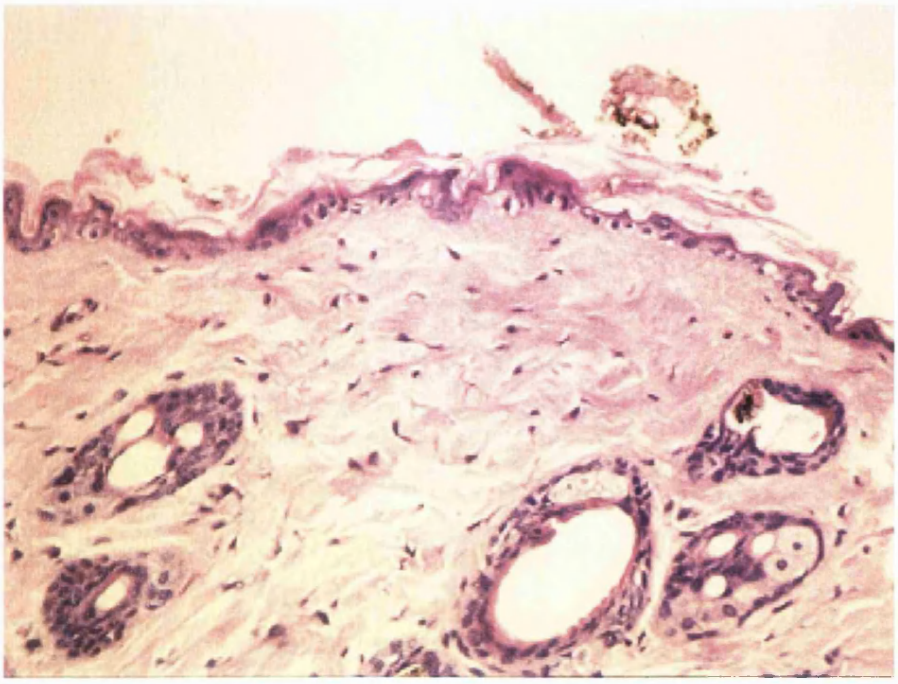

Figure 5.20a: Transverse section stained with H&E of a specimen from a growing hair region exposed to laser irradiation at 6 J/cm^2. Signs of epidermal damage are present as described before (x200).

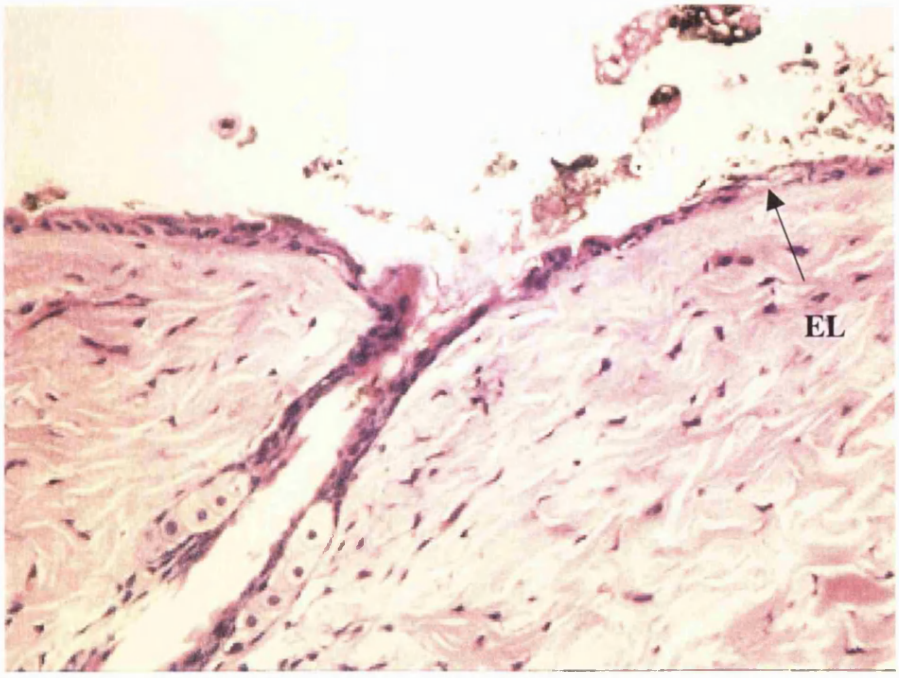

Figure 5.20b: Transverse section stained with H&E of a specimen from a growing hair region where chromophore was applied prior to laser irradiation at 6 J/cm^2. Skin damage is evident with areas of epithelial loss (EL), but the damage is similar in extent to that seen in Figure 6.9a (x 200).

scarring within the dermis. No such skin damage was identified in all the irradiated fields examined showing a very similar image to that shown in Figure 4.21.

5.6 DISCUSSION

5.6.1 The Colour Most Suited to Reflect or Absorb Ruby Laser Light

None of the coloured inks used in this experiment showed an ability to reflect the NMRL light beam. However, as mentioned, the use of such a colour would serve not only to protect the skin but most likely prevent depilation occurring at all. Black ink was able to absorb a significant amount of the NMRL beam so as to prevent any removal of ink from the paper below. This colour could therefore protect the skin but begged the question as to whether it may also reduce depilatory efficacy.

5.6.2 The Effect the Addition of Black Ink as a Chromophore to the Surface of *Ex vivo* Human Skin Prior to Ruby Laser Irradiation has upon Histological Damage Noted

The negative controls used in this experiment did not express p53 protein within the nuclei of the cells suggesting that the general processing involved within this experiment did not result in increased cellular damage. Consequently any change in p53 expression within the experimental specimens was likely to be as a direct result of the laser energy.

Histological analysis of specimens irradiated with the NMRL and stained for p53 protein showed highest expression in the cells of the basal layer. This finding of site-specific cellular damage is consistent with Liew and co-workers who reported extensive ultrastructural damage within the cells residing at this level of the epidermis after NMRL exposure. When the sections from NMRL irradiated sites, where chromophore had been added to the skin surface prior to exposure, were analysed overall p53 expression appeared to be less than in those sections taken from sites where chromophore had been absent. This was particularly noticeable in the basal

layer. This would imply that the addition of a chromophore to the surface of *ex vivo* human skin specimens prior to NMRL irradiation lessened the cellular damage, as assessed by p53 protein expression, produced in the basal layer. Whether such a decrease would be sufficient to eliminate skin side effects in clinical practice cannot be stated but it would suggest that they could at least be reduced.

The skin samples used in this experiment did not contain terminal hairs, therefore it is not possible to state what effect the presence of hair follicles would have on the protective role of the added chromophore. The majority of skin damage, which occurs in mainly dark-skinned individuals, would most likely result from direct photon energy transfer through the epidermis between the hair follicles interacting with the melanin in the skin producing a localised heating effect. The presence of these follicles would therefore be unlikely to produce findings significantly different to those recorded within the hair free specimens. Chapter 3 did show heat transfer from the follicles to skin in Caucasian specimens but the temperature rises were small.

The skin used for this procedure was breast skin and so it could be that the results are only relevant to an identical skin type to this and not to other regions of the body where skin thickness is different. However, the important aspect would be epidermal depth as this is the barrier between the heat source and the viable epidermal cells. Two types of skin epidermis have been recorded, the thin type which occurs over most of the body surface and the thick (or glabrus) type which is present on the palms of the hands and soles of the feet alone. Epidermal thickness actually varies little over the body surface making the model an accurate representation of most body sites.

5.6.3 The Addition of Black Ink to the Surface of *Ex vivo* Human Skin and its Effect Upon Laser Light Transfer through Skin

Adding a chromophore of black ink to the surface of the skin specimens through which the NMRL was fired reduced the energy recorded by the meter below. This resulted in approximately a 50% drop in energy at most depths measured when the incident fluence was 9.24 J/cm^2 compared to the readings obtained at the same

fluence when no chromophore was present. The maximum depth of penetration did not vary significantly when compared to the other fluences used (see Chapter 3, section 3.5.2) supporting the statement that penetration is wavelength-dependent (Welch, 1984). These findings show that the addition of a chromophore to the skin surface reduces the quantity of energy reaching the viable areas of the skin in the basal layers therefore potentially reducing the clinical side effects. However, whether the heat produced at the skin surface would then diffuse downwards to cause equivalent cellular damage is unknown but the experiment discussed in section 5.6.2 assessing p53 expression would suggest not. Another important finding was that the chromophore also reduced the amount of energy which would reach the regions of the hair follicle responsible for hair growth. This might subsequently reduce the potential effectiveness of the laser treatment if its mode of action was via light penetrating the skin.

5.6.4 The Addition of Black Ink to the Skin of the Black-haired Mouse Prior to Ruby Laser Irradiation and its Effect Upon Depilatory Efficacy and Skin Side Effects

Adding a chromophore to the skin within growing hair regions prior to NMRL irradiation did not significantly increase the skin wounding or healing as noted daily when compared to sites which had no chromophore added. This was the case at both fluences of exposure. In addition, the time taken to full wound healing in the chromophore added and irradiated alone sites in growing hair regions did not significantly differ at both 6 and 8 J/cm^2 fluence. These findings are further supported by the fact that histologically little difference was noted in the epidermal damage occurring between these irradiated sites. These results are at odds with the data obtained with *ex vivo* human skin in section 5.5.3 which support the hypothesis that chromophore applied to the skin surface can reduce skin damage. This apparent contradiction can be explained simply in terms of differences in epidermal thickness. Mouse epidermis is relatively thin, one to two cells thick, when compared to human skin which is usually 8 cells thick or more depending on the site. The photon energy being converted to heat in the mouse model was adjacent to the viable skin cells

whereas in human skin, the heat would have to diffuse through many more layers of the epidermis before reaching the viable cells in the basal layer. This distance could well result in adequate heat dissipation to levels below those required to induce cellular damage.

In contrast to the results in the growing hair regions, for the resting hair regions, a statistically significant difference was noted in the median daily wound scores between sites where chromophore was added and those that were irradiated alone upon days 1 to 10 at 6 J/cm^2 and 1 to 12 at 8 J/cm^2. This was supported by the finding that the time taken to fully heal in chromophore added sites at both fluences being significantly greater when compared to the equivalent fluence exposed sites where chromophore was not added in the resting hair regions and also by the histological findings. No such difference was seen in the growing hair regions. These findings would suggest that a greater quantity of chromophore was now present within the sites painted with black ink than was previously. The chromophore was therefore converting a greater quantity of photon energy to heat at the skin surface so manifesting itself by the greater degree of skin damage seen. Comparing the chromophore added sites at both fluences used in the resting and growing regions revealed no statistical difference in the daily wound scores noted. This suggested that the quantity of chromophore within the resting hair regions had been raised to amounts present in the growing hair regions and so was producing a similar degree of skin damage. Both these findings could suggest that the maximum amount of chromophore was already present within the skin of growing hair sites to produce a constant clinical picture defined by the wound scoring system used. Adding further chromophore to the target sites would therefore not increase the skin side effects that were noted clinically.

No statistically significant difference was noted between hair regrowth scores at sites where chromophore was added and those that were irradiated alone within growing hair regions. Addition of chromophore neither decreased nor increased the depilatory efficacy of the NMRL within these regions at the fluences used. An increase in efficacy may have been expected if the chromophore penetrated to the "hair-

producing" regions of the follicle. The ink used may have been too thick and the hair canal too narrow or containing sebum to allow it to enter the follicle to the limit of the inner root sheath approximately adjacent to the site of the bulge region. Interestingly, the addition of chromophore to the skin surface did not significantly decrease depilatory efficacy either. This could suggest that either enough photon energy was still able to penetrate the skin to reach its target sites or that the method of depilation is down the hair shaft which is also not affected by the addition of chromophore.

The hair regrowth scores in resting sites irradiated at the two laser fluences where chromophore had been added compared to those sites irradiated alone at the same fluences revealed a statistically significant difference between the two. This occurred upon the third week at both 6 J/cm^2 and 8 J/cm^2. This suggested that adding chromophore to resting hair regions had delayed hair regrowth. How this occurred can only be presumed but it would most likely be associated with heat production after NMRL irradiation. Either the chromophore was penetrating the hair canal producing a localised heating effect or enough heat was being produced in the external hair shaft upon the skin surface and as a direct result of heat conduction from the source, was damaging the viable follicular cells delaying hair regrowth. The fact that this delay occurred solely in resting hair regions would suggest that the addition of the chromophore had a negative, albeit temporary, effect on hair regrowth. However, it cannot be overlooked that the statistical difference between the sites was low and occurred only at one particular week. Histological assessment of sections stained with the modified SACPIC technique from resting hair regions did not show any difference in the amount or extent of hair shaft damage in sections taken from chromophore added sites and sites irradiated alone. This would not exclude heat having traversed directly through the skin to affect the hair producing regions resulting in delayed hair growth, but if it were to have been conducted through the hair shaft, then greater damage to the shaft might have been expected.

This experiment has not discounted whether the addition of chromophore within the hair canal could increase laser depilatory efficacy. It may well be that if the accuracy

of delivery of the chromophore could be improved then this method could be successful.

The findings from the *ex vivo* human skin model suggests that not only would black ink protect the skin from laser-induced damage, it does not appear to decrease the efficacy of depilation. Indeed, adding chromophore to the hair shafts of patients whose shafts contained a limited quantity of chromophore for the NMRL may well improve depilatory efficacy. One simple practical problem does remain and that is the added chromophore creates a rather noxious plume of smoke upon laser firing which coats the hand-piece requiring regular cleaning. This may simply be resolved by covering the treatment area with a translucent substance such as acetate, which will prevent such contamination.

5.7 CONCLUSIONS

- Adding chromophore to human skin appears effective in reducing skin damage resulting from ruby laser irradiation, as judged by induction of p53 expression.

- No change in depilatory efficacy was noted in growing hair regions of mice between chromophore coated and non-coated skin suggesting that the photon energy removed as a result of its conversion to heat at the skin surface was probably not required for depilatory purposes.

- Resting hair regions in mice experienced a one week delay in hair regrowth when pre-treated with chromophore compared with irradiated only sites. This may suggest that the non-pigmented hairs present are better treated by laser when coated with chromophore.

CHAPTER 6 – POTENTIAL PROTECTION FROM EPIDERMAL SIDE EFFECTS BY HEAT-PRETREATMENT - *IN VITRO* PROOF OF PRINCIPLE

6.1 INTRODUCTION

The skin side effects resulting from normal mode ruby laser (NMRL) treatment are erythema, blistering of the skin, hypo and hyperpigmentation (Gold, et al., 1997) (Grossman, et al., 1996) (Lask, et al., 1997) (Solomon, 1998) (see Figures 1.7, 1.8a and 1.8b). To date, all have been described as being temporary with histological examination of biopsies taken from the irradiated skin revealing no disruption to the collagen matrix of the dermis which would preclude the possibility of permanent scarring (Dierickx, et al., 1998). The ruby laser utilises pigmentation within the skin as a chromophore to convert the light energy to heat (Goldman, 1983). Dark-haired, light skinned individuals would in theory obtain the best depilatory results as the natural pigmentation, melanin, would be concentrated in and around the hair follicles, and little present within the intervening skin. The follicle is the site where the maximum quantity of energy needs to be converted to heat to cause maximal damage to the viable follicular components pertaining to hair growth and so potentially producing permanent depilation. The skin of darker pigmented individuals, however, contains a greater quantity of melanin within the keratinocytes of the epidermis. When ruby laser light is incident upon this skin type, a greater quantity of light energy is converted to heat at this additional skin site as well as the hair follicles. This results in the typical manifestations of mild thermal injury described in clinical practice. Hypopigmentation occurring within the skin of certain individuals with darker skin types could be explained by the melanin pigment being targeted and vapourised by the ruby laser along with selective damage to melanocytes, so preventing the rapid production of melanin and therefore repigmentation of the skin. Paradoxically, hyperpigmentation has also been described clinically, which would infer some form of melanocyte stimulation occurring, but this too has not been fully explained. It could represent a response to skin damage akin to the tanning process exhibited by the skin

upon exposure to sunlight.

To minimise the chance of skin side effects, particularly in patients of a Fitzpatrick skin type 4 or 5 (see Table 1.1), the fluence of the ruby laser is usually reduced, possibly to levels that are sub-optimal with regard to affecting permanent depilation. Preventive regimes have also been utilised, although not properly evaluated in trials, in an attempt to reduce the skin side effects and all rely on "exogenous" methods of action. For example, cooling gels, with or without aloe vera, have been applied before and/or after treatment to reduce skin temperature and subsequent heat damage. A cooled sapphire lens has been devised by a group (Grossman, et al., 1996) (Dierickx, et al., 1998) which, when placed upon the skin, also converges the laser beam upon the hair thereby achieving both skin cooling and more efficient hair targetting. The benefits, though, of these methods are at present unknown. In theory, the only really effective way to prevent skin side effects would be to remove the melanin from the epidermis altogether. One study published to date has used hydroquinone to bleach the skin, which was applied 3 weeks before treatment, but no comment was made regarding its use within the article and although patient satisfaction was described as being high, the patient follow-up was only for approximately 12 weeks (Solomon, 1998).

Whilst the previous chapter attempted to assess a rather simple barrier method of protecting the skin from laser-induced side effects, here we propose the use of an "endogenous" method of skin protection by utilising the cells own physiological response to an adverse stimulus. A cellular model has been devised and reported using cultured human dermal fibroblasts, which were preconditioned with heat and then exposed to a CO_2 laser 3 hours later. The preconditioned cells were found to undergo significantly decreased cell death when compared to the non-pretreated group 2 hours post-irradiation (Polla and Anderson, 1987). The phenomenon of pre-conditioning, first described by and attributed to Murry (Murry, et al., 1986), makes use of the inate ability of a cell to protect itself from a lethal stimulus, such as heat or ultraviolet irradiation, by prior exposure to any adverse sub-lethal stimulus not necessarily of the same type (Vogt, et al., 1993) (see section 1.8). The mediators of cellular protection

from an adverse environment are thought to be the heat shock proteins (HSP's – see section 1.7) (Hutter, et al., 1994). The types of HSP's that have been found to undergo increased expression upon cell stressing are HSP 110, HSP 90, HSP 70 and HSP 60 (Strasser, 1995). An increase in cellular sensitivity to stress has been noted after inhibition of HSP 70 expression (Johnston and Kucey, 1988). HSP 70 is the name given to represent the family of HSP's whose molecular weights are around 70 kDaltons and consists of both HSP 72 and HSP 73. The term HSP 70 has continued in the literature, perhaps rather confusingly, to represent these two proteins. HSP 73 is the constitutive form of the protein whilst HSP 72 is the inducible type and is only present under stressful conditions (Welch, 1992). HSP 72 has been stated to be the most highly induceable member of the stress protein family (Welch, 1992), is always expressed by stressed human keratinocytes (Edwards, et al., 1991) and has been stated to most likely represent the major protective stress protein within the cell (Polla, et al., 1996). The human dermal fibroblasts mentioned above were reported to express increased quantities of HSP 70 and 90, 2 hours after non-lethal heating. Exposure of cultured human skin to various adverse stimuli, for example heat, oxidative stress and UV irradiation, have all been shown to increase HSP 72 synthesis within the keratinocytes. The protein was localised to the nucleolus 5 hours after exposure to the stimulus corresponding to the site where its action would theoretically be most required to protect newly synthesised proteins (Muramatsu, et al., 1992). For these reasons the HSP 70 family was used in these experiments as the marker of cellular stress induction and also of possible cellular preconditioning.

Heat was chosen to be the mode for preconditioning because of its ease of application, with a fixed exposure time of 15 minutes. Successful pre-conditioning relies upon minimising the damage that the mild stressing agent inflicts upon the cells but also maximising the production of the potentially protective proteins (such as HSP 70) and this is the paradox that needs to be overcome before it can be correctly applied in practice. Acquired thermotolerance has been stated to last upto 24 hours in cells grown in culture (Minowada and Welch, 1995) and so HSP 70 protein was measured at 5 hours and 24 hours after exposure to stress. This chapter describes the use of two *in vitro* models to investigate the possibility of heat preconditioning protecting against

NMRL irradiation. The first set of experiments uses a simple cellular model involving the two major skin cell types, the keratinocyte and fibroblast and is detailed in sections6.2 to 6.8. The response of cells to heating has been studied and the range of temperatures at which a range of cell death would happen has been incorporated into this experiment (Uchida, et al., 1993). The temperature range also included two at 42°C and 43°C where cell death has been reported to noticeably increase (Sapareto, et al., 1978). Secondly, the relationship between the seven keratinocyte cell lines, which are the cells requiring protection from laser irradiation, temperature and HSP 70 production for the same fixed time is investigated. Lastly, the results are related to a keratinocyte model whose cells undergo preconditioning prior to NMRL exposure and the subsequent effects noted. The second set of experiments aims to repeat some of these results in the more complicated system of *ex vivo* human skin and is reported in section 6.9.

6.2 AIMS

- To titrate the temperature required to cause cell death after heat exposure for a constant 15 minutes in paired keratinocyte and fibroblast cell lines (n=7).

- To determine the temperature associated with maximal heat shock protein 70 production within the same keratinocyte cell lines after 15 minutes heat exposure.

- To determine whether preconditioning of the keratinocyte cell lines at the most effective temperature defined from the two previous procedures affords protection from damage induced by exposure to NMRL irradiation.

6.3 METHODS

6.3.1 Determining Heat-induced Cell Death of Seven Paired Fibroblast and Keratinocyte Cell Lines Exposed to a Range of Temperatures

A single cryovial from each of the fibroblast cell lines was recovered in turn and seeded into three T75 flasks (P2) (see section 2.2.3). When the flasks were approximately 80 to 90% confluent, the cells were trypsinised and seeded, at a density of 3×10^5 cells per well, into 3 wells of a six well plate, a total of eight plates being so produced (P3). The plates were incubated for 24 hours to allow cell attachment, when the media in the wells was changed and the cell confluency estimated. When the wells were approximately 80% confluent, one of the eight plates was taken from the incubator, sealed with Parafilm "M"® and floated in a waterbath at a pre-determined temperature for 15 minutes. This was repeated for the remaining seven plates with each being exposed to one particular temperature, being either 37°C, 42°C, 43°C, 45°C, 47°C, 49°C or 51°C. The eighth plate remained in the incubator to act as a negative control. After the allotted time had passed, each of the plates were removed from the waterbath and the film discarded. The FCM was exchanged in all the cultured wells for fresh FCM, that had been maintained at 37°C in a separate waterbath, before all plates were returned to the incubator.

A cell death estimation was performed in triplicate for each temperature set after 24 hours had elapsed by using the trypan blue viability test (see section 2.2.1).

The experiment to estimate heat-induced cell death within the keratinocyte population was performed in the same manner (see section 2.2.2). However, it was important to establish the correct seeding density to produce approximately 70% confluency of relatively undifferentiated cells within the well of a six well plate. Therefore, a single cryovial from one of the keratinocyte cell lines was recovered and seeded into four T75 flasks (P1) which had been incubating for the preceding 24 hours with 2×10^6 gamma irradiated feeder cells in FCM. The media was exchanged for KCM and the keratinocytes supported with twice weekly media changes and the addition of feeder

cells as appropriate. When the flasks were approximately 60% confluent, one was removed from the incubator, the 3T3 feeder cells discarded by the previously described method (see section 2.2.1) and the keratinocytes removed by trypsinisation. The keratinocytes were then seeded at a range of densities into six well plates, which were $1x10^5$, $3x10^5$, $5x10^5$, $7x10^5$, $9x10^5$ and $1x10^6$ per ml with 2 mls added to each well. The cell confluency was estimated at 24 hours and it appeared that the correct seeding density would be $7x10^5$ cells per ml producing approximately 70% confluency.

The remaining three T75 flasks were seeded into each of 3 of the wells of a six well plate at $7x10^5$ cells per ml and using eight plates in total. The plates were incubated and the media changed at 24 hours, when 70% confluency was confirmed. Seven of the plates were then removed from the incubator, in turn, sealed with Parafilm M® and floated in a waterbath for 15 minutes at the same range of temperatures mentioned above with the eighth acting as a negative control in the incubator. The plates were recovered, the film removed and the media within the wells exchanged for fresh KCM at 37°C prior to all the plates returning to the incubator.

A cell death estimation was performed in triplicate for each temperature, after 24 hours had elapsed, by using the trypan blue viability test (see section 2.2.1). The procedure was repeated identically for the remaining six keratinocyte cell lines.

6.3.2 Determining the Effect of Temperature Upon Heat Shock Protein 70 Synthesis within Seven Keratinocyte Cell Lines

Two cryovials from each of the seven keratinocyte cell lines were recovered, in turn, and grown to approximately 70 to 80% confluency in seven T75 flasks as described above. The keratinocytes were then passaged into 14 T75 flasks (P2) and again grown to approximately 70 to 80% confluency. The feeder cells were removed by incubating with versene and then fresh KCM at 37°C was added before the flasks were returned to the incubator for a minimum of 48 hours. Two flasks were then removed in turn from the incubator, the lids sealed tightly and both floated in a waterbath at one of the

seven temperatures described above. When each pair had been exposed for 15 minutes, the media was exchanged for fresh KCM at 37°C and both were returned to the incubator. This was repeated for all seven temperatures. After 5 hours incubation, one of each pair of flasks was processed for Western Blot analysis whilst the second was processed after 24 hours incubation (see section 2.4).

6.3.3 Determining the Effect of Heat Preconditioning of Keratinocytes in Culture Upon Cell Survival after Subsequent Exposure to Normal Mode Ruby Laser Irradiation

Three pilot studies were performed prior to the main experiment (see Appendix A, Appendix B and Appendix C). The first was to establish the correct seeding density of keratinocytes within a single 10 mm diameter well of a 48 well plate to produce approximately 70% confluency. This was important as too many cells would induce cell stress within the population of the well, an undesirable situation as the main experiment would hinge upon the appropriate induction of stress proteins within defined cell groups, and too few would take too long to grow to confluency without a feeder cell population being present. In addition, when passaged, only 15 to 20% of keratinocyte cells re-attach to the base of the plastic culturing container, making an estimation of the appropriate seeding cell density all the more difficult and therefore necessary to obtain. The second study was to establish the susceptibility of keratinocyte cells in culture to NMRL exposure and the range of fluences that would induce a "range" of cell deaths upto 100% within the irradiated wells. The third pilot study was a progression from the results of the second as it became obvious that a chromophore would be needed within the media bathing the keratinocyte cells to convert the incident photon energy to heat thereby producing an adequate amount of cell death for analysis. The quantity of chromophore needed and the range of laser fluences to then be used was established by this procedure.

The main experiment was designed by incorporating the results obtained from the three pilot studies and the experiments described in sections 6.3.1 and 6.3.2 above. Synthetic melanin at the two concentrations mentioned within the third pilot study

(Appendix C) was used eventhough no significant difference in cell viability had been detected upon NMRL irradiation between the two groups. It was feasible that the preconditioning could be effective up to a certain melanin concentration only, whereupon the quantity of chromophore and therefore heat produced would be too great. By using the two concentrations, a potential threshold for the chromophore could be determined. The range of fluence exposure was reduced to 1.7 J/cm^2 as no significant decrease in cell viability had occurred above this value. Preconditioning of the keratinocyte cells occurred at 45°C for 15 minutes and two groups were established with the first to undergo NMRL irradiation 5 hours after preconditioning and the second 24 hours after preconditioning (see Figure 2.5). The groups were otherwise identical in the number of control and experimental plates used. The timing of NMRL exposure would help clarify whether an optimum time existed for the protective capabilities of the induced stress proteins within keratinocyte cells.

A single cryovial of each of the seven keratinocyte cell lines was raised in turn, from frozen, into three T75 flasks by the methods described above. At approximately 80% confluency, the 3T3 feeder cells were discarded and the keratinocytes removed by trypsinisation. The India ink in agar solution mentioned in Appendices B and C was added to alternate wells as described previously and, when solidified and sufficiently cool, the keratinocytes were then seeded into the intervening wells of the 48 well plates at a density of 6×10^4 cells per well. All the plates were then returned to the incubator.

After 24 hours incubation, the media was exchanged in all cell-containing wells for either fresh KCM, KCM with 100 µg/ml or KCM with 200 µg/ml melanin in solution as appropriate. The plates were returned to the incubator.

After a further 24 hours of incubation, the plates to be pre-heated at 45°C were sealed with Parafilm "M"® Laboratory film and placed in the waterbath at 45°C for 15 minutes. This included two control plates (5 hours and 24 hours) containing wells with normal KCM, 100 µg/ml melanin in KCM and 200 µg/ml melanin in KCM, plus four of the experimental plates (two at 5 hours and two at 24 hours) each containing

wells with either 100 μg/ml or 200 μg/ml of melanin in KCM. When the heating was complete, all plates, including those not heated, had their media replaced with the same type as that present before heating and then all were returned to the incubator.

After 5 hours, a cell viability count, using the trypan blue exclusion test, was performed upon the first of the three paired rows of 3 wells within the control plates which thus represented the 5 hour group. This included the non-heated and heated controls containing normal KCM, KCM with 100 μg/ml melanin and KCM containing 200 μg/ml of melanin. Once established, the control plates were returned to the incubator and the experimental plates removed in turn and placed into the Class II hood. Exposure to NMRL irradiation occurred in exactly the same manner as mentioned in the appendices and when one plate was completed, it was returned to the incubator and the second removed. The wells of the remaining second three rows in the control plates had the media removed and were exposed to air for the same time duration as the experimental plates had been. The whole procedure was repeated identically upon the second group of plates at 24 hours after the heat preconditioning.

The cell viability for all treated and control wells was established at 24 hours after exposure by employing the trypan blue viability test (see section 2.2.1). The whole procedure was then repeated for the remaining six keratinocyte cell lines.

6.4 STATISTICS

Sample statistics are presented as means with a standard deviation. Statistical analysis of paired groups was undertaken using a Student's t-test if the normality test passed. If the normality test failed then a Mann Whitney Rank Sum test was performed. Statistical analysis between groups of more than two was undertaken using the one way ANOVA method. If the normality test passed then a Tukey test was performed, which is a pairwise multiple comparison procedure. If the normality test failed, then a Dunnett test was performed which is a one way ANOVA on ranks with a selected control. Statistical significance is expressed for each test performed. All analyses were performed using SigmaStat™ statistics software, version 1.0 (Jandel Corporation).

6.5 RESULTS

6.5.1 Determining Heat-induced Cell Death of Seven Paired Fibroblast and Keratinocyte Cell Lines Exposed to a Range of Temperatures

The viability of the fibroblasts in all three wells of each six well plate exposed to the range of temperatures is expressed as the proportion of dead cells as a percentage of the total cells counted. The temperature range employed induced upto 100% cell death in all seven fibroblast cell lines. The control plates of each of the fibroblast cell lines experienced a mean cell death of 6.6% (SD +/- 1.1%) with no significant difference between the seven cell lines and no significant difference between the seven cell lines floated in the waterbath at 37°C. Figure 6.1 shows the mean plot with standard deviation of the percentage dead cells against temperature for each of the seven fibroblast cell lines. A statistically significant variance was achieved between the mean values of the percentage of dead cells for each cell line at each temperature of exposure than would be expected by chance ($p<0.05$), apart from at 51°C. The shape of the plot for each fibroblast cell line represented an increasing sigmoidal curve with an increase in percentage dead cells occurring particularly at 45°C and then more strikingly at 47°C and above.

The viability of the keratinocytes from the three wells of the six well plates are plotted in Figure 6.2. Again upto 100% cell death was induced within these cell lines by the temperature range used, with the control plates experiencing a mean percentage dead cells of 3.9% (SD +/- 0.9). Again, no significant difference was noted between cell death in the other remaining cell lines kept in the incubator as controls and those that were floated in the waterbath at 37°C. Statistical analysis of the mean percentage of dead cells counted at each temperature for each of the seven keratinocyte cell lines showed that upto and including 45°C, no significant difference was noted between them, and this was also the case at 51°C. However, at 47°C and 49°C, a statistically significant difference was recorded, which was greater than would be expected by chance ($p<0.001$). The shape of the plot for each of the keratinocyte cell lines was

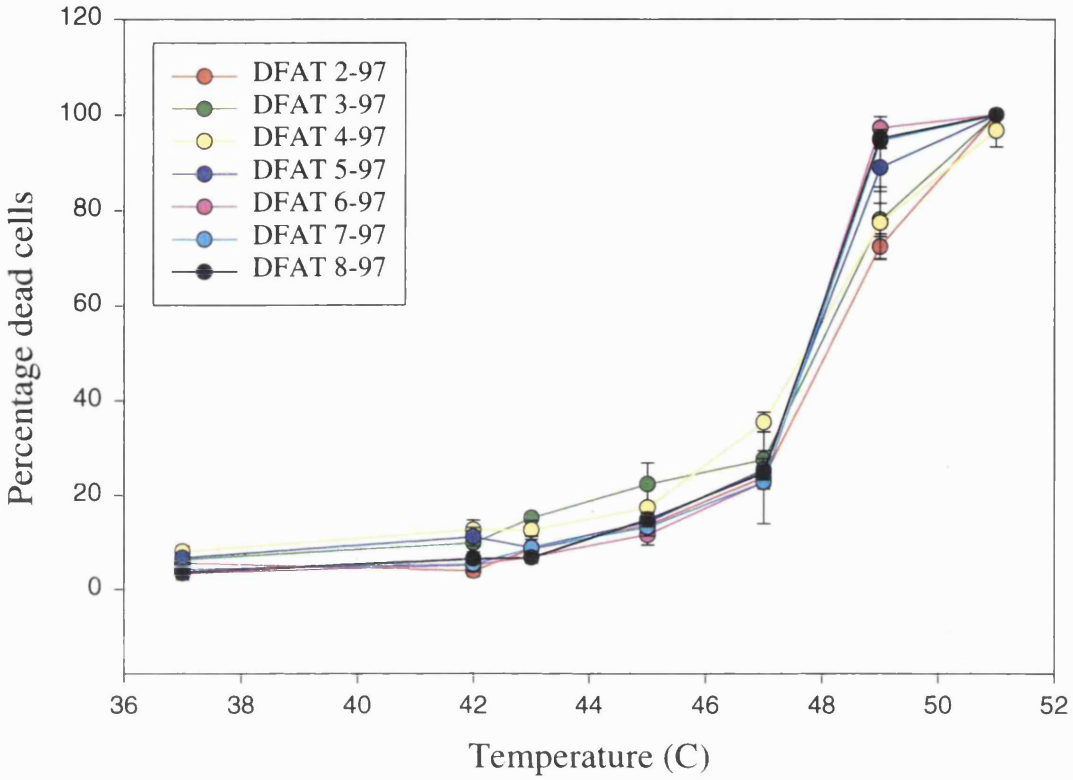

Figure 6.1: Graph showing the percentage of dead cells against temperature for each of the seven fibroblast cell lines.

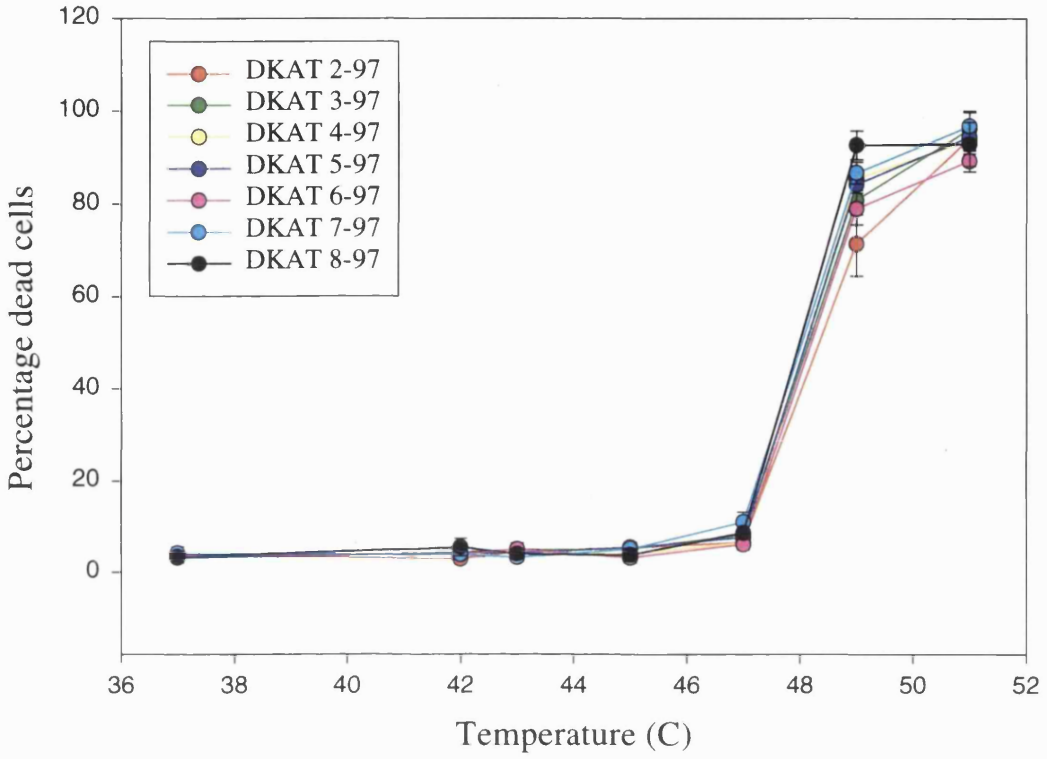

Figure 6.2: Graph showing the percentage dead cells against temperature for each of the seven keratinocyte cell lines.

again of an increasing sigmoidal type. The curves, though, were more marked with a much steeper increase in percentage dead cells generally occurring at 47°C and above.

The percentage of dead cells for all seven fibroblast cell lines at each temperature were collated and a plot of the mean values with the standard deviations performed. The same procedure was undertaken with the keratinocyte cell lines and plotted on the same graph (see Figure 6.3). This revealed that the mean values of the fibroblast death rates were always greater than the keratinocyte death rates. Statistical analysis of the percentage cell death for all fibroblast cell lines at each temperature compared to the percentage cell death for all keratinocyte cell lines at the same temperature was performed by a Mann Whitney Rank Sum test. This revealed a statistically significant difference ($p<0.001$) between the median values of both groups of paired cell types at all temperatures except 49°C.

6.5.2 Determining the Effect of Temperature Upon Heat Shock Protein 70 Synthesis within Seven Keratinocyte Cell Lines

Figure 6.4 and Figure 6.5 show two representative HSP 70-Western Blots of samples harvested 5 hours after heat shocking at the same temperature range employed for the cell death experiment described above. The first lane (blue bands) represents the molecular markers (M.M.) and the second well (37°CI) contains the sample harvested from the keratinocytes that remained within the incubator and therefore acting as a control. Subsequent wells are labelled according to the temperature to which they were exposed in the waterbath. The antibodies used show a high degree of specificity judged by the lack of background staining upon the nitrocellulose paper.

A band of the correct size within the control wells of all the Blots revealed the HSP 70 expressed constitutively within non-stressed cells for all the keratinocyte lines tested. An increasing quantity of HSP 70 protein was present the greater the temperature of exposure, up to a maximum at 45°C in the 5 hour group whereupon the quantity reduced in amount. This was a consistent finding within all the keratinocyte cell lines

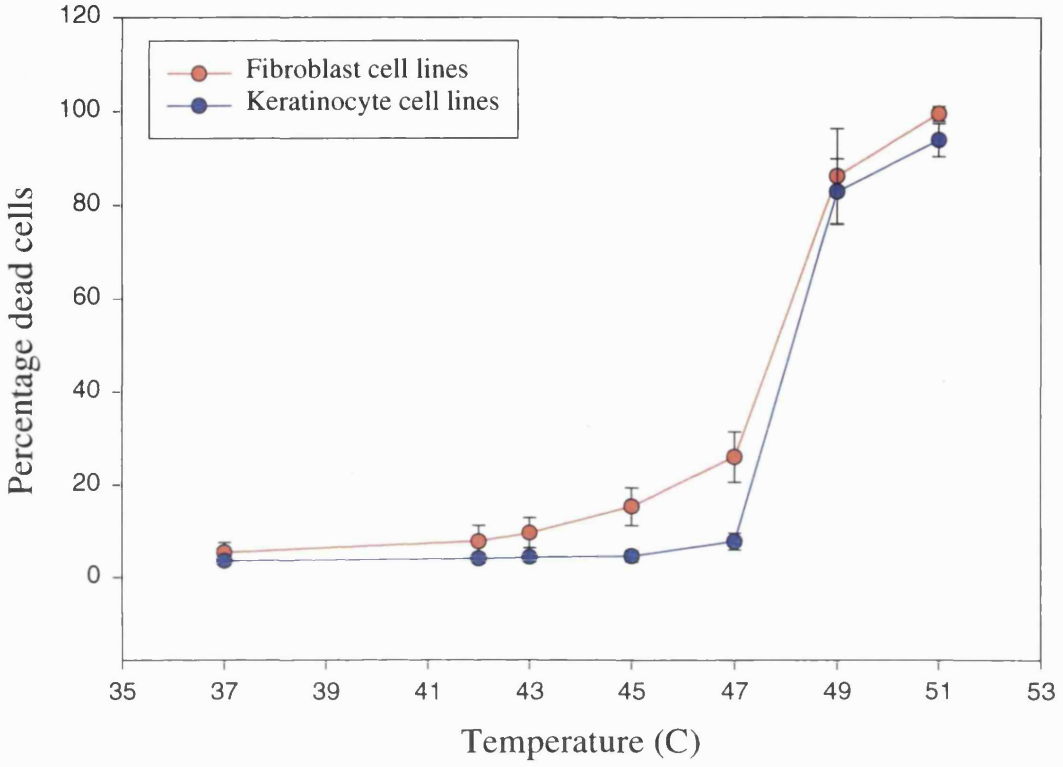

Figure 6.3: Graph showing the mean plot with standard deviation of the percentage of dead cells against temperature for all seven keratinocyte and fibroblast cell lines.

M.M.	37°C I	37°C W	42°C	43°C	45°C	47°C	49°C	51°C
Optical density x area								
	0.701	0.688	0.394	0.659	1.722	0.539	0.8	0.606

Figure 6.4: Representative Western Blot with a positive staining for HSP 70 5 hours after heat stressing at the range of temperatures shown (M.M. is molecular marker, 37°C I is 37°C in the incubator, 37°C W is 37°C in the waterbath). The product of the optical density and the area for each temperature was established by the Seescan computer and are shown beneath the relevant well.

M.M.	37°C I	37°C W	42°C	43°C	45°C	47°C	49°C	51°C
Optical density x area								
	0.642	0.675	0.410	1.801	2.833	1.283	0.312	0.924

Figure 6.5: Second representative Western Blot with a positive staining for HSP 70 5 hours after heat stressing at the range of temperatures shown (M.M. is molecular marker, 37°C I is 37°C in the incubator, 37°C W is 37°C in the waterbath). The product of the optical density and the area for each temperature was established by the Seescan computer and are shown beneath the relevant well.

and was confirmed by the Seescan analysis (see Figures 6.4 and 6.5) which shows the optical densities of the wells of the two Western Blots.

Figure 6.6 and Figure 6.7 both show two representative Western Blots from samples taken 24 hours after heat shocking at the same range of temperatures for 15 minutes. HSP 70 was once again seen to be constitutively expressed in all keratinocyte lines used and this was also noted to increase in amount with increasing temperature up to a maximum at 45°C and 47°C, whereupon it then diminished dramatically to such an extent that very little was detectable at 51°C. The Seescan computer was again employed to assess the quantity of HSP 70 produced at all temperatures and the analyses of the two Western Blots are also shown in Figures 6.6 and 6.7.

6.5.3 Determining the Effect of Heat Preconditioning of Keratinocytes in Culture Upon Cell Survival after Subsequent Exposure to Ruby Laser Irradiation

Figure 6.8 is a representative plot for all keratinocyte cell lines showing the total viable cells counted versus increasing fluence of exposure for both the preconditioned and non-preconditioned groups irradiated 5 hours after the preconditioning stimulus was applied and whose wells contained 100 μg/ml melanin. Figure 6.9 is a similar graph to Figure 6.8 except irradiation occurred 24 hours after preconditioning. Figure 6.10 is a graph showing the plot of the total viable cells counted versus increasing fluence of exposure for both the preconditioned and non-preconditioned groups irradiated 5 hours after the preconditioning stimulus was applied and whose wells contained 200 μg/ml melanin. Figure 6.11 is a similar graph to Figure 6.10 except the irradiation occurred 24 hours after the preconditioning stimulus was applied. A statistical analysis of the non-irradiated control groups before and after experimentation at both times revealed no significant difference in the cell viability for wells containing media with nil, 100 or 200 μg/ml melanin.

Increasing the NMRL fluence decreased the cell viability within all the wells when compared to the control groups ($p<0.001$). At 0.6 J/cm^2 in the 100 μg/ml group at 5 hours, the cell viability was reduced to a sixth of the control in the non-preconditioned

M.M.	37°C I	37°C W	42°C	43°C	45°C	47°C	49°C	51°C
Optical density x area								
	0.843	1.04	1.14	1.48	2.23	2.9	1.78	0.34

Figure 6.6: Representative Western Blot with a positive staining for HSP 70 24 hours after heat stressing at the range of temperatures shown (M.M. is molecular marker, 37°C I is 37°C in the incubator, 37°C W is 37°C in the waterbath). The product of the optical density and the area for each temperature was established by the Seescan computer and the results are shown beneath the relevant well.

M.M.	37°C W	42°C	43°C	45°C	47°C	49°C	51°C
Optical density x area							
	0.796	0.983	0.964	1.25	1.477	1.21	0.246

Figure 6.7: Second representative Western Blot stained positive for HSP 70 24 hours after heat stressing at the range of temperatures shown with the product of the optical density and the area shown beneath the relevant well.

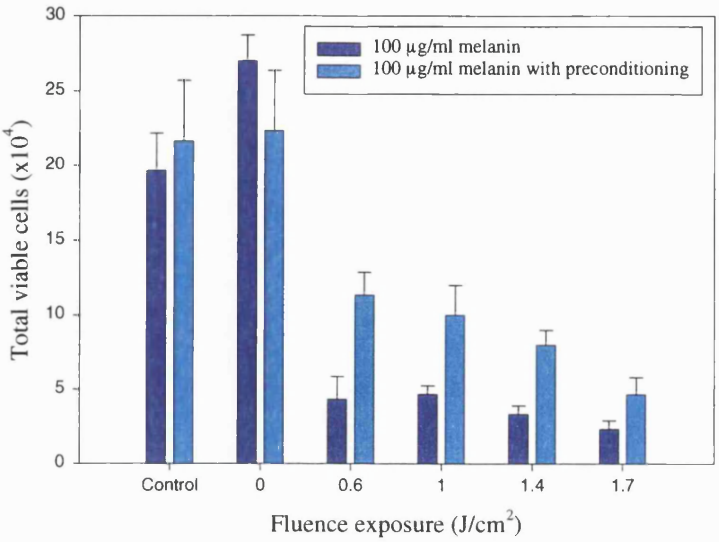

Figure 6.8: Graph showing the relationship between the total number of viable cells and increasing fluence of exposure from a normal mode ruby laser. Irradiation occurred 5 hours after heating and the wells contained 100 µg/ml melanin.

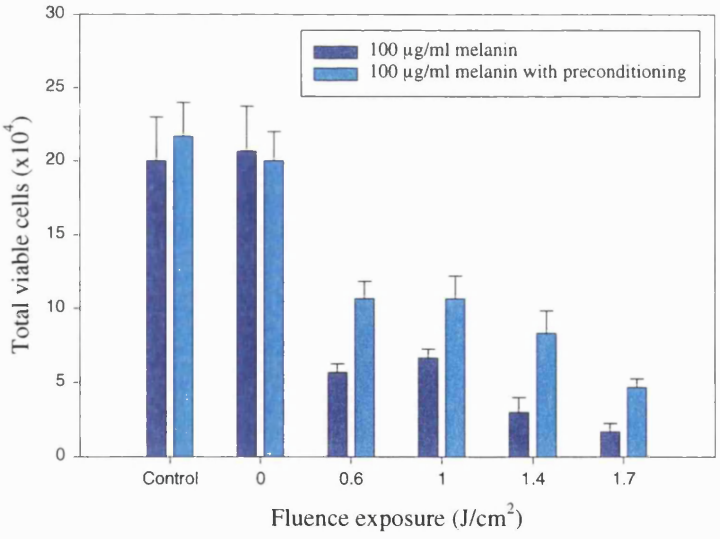

Figure 6.9: Graph showing the relationship between the total number of viable cells and increasing fluence of exposure from a normal mode ruby laser. Irradiation occurred 24 hours after heating and the wells contained 100 µg/ml melanin.

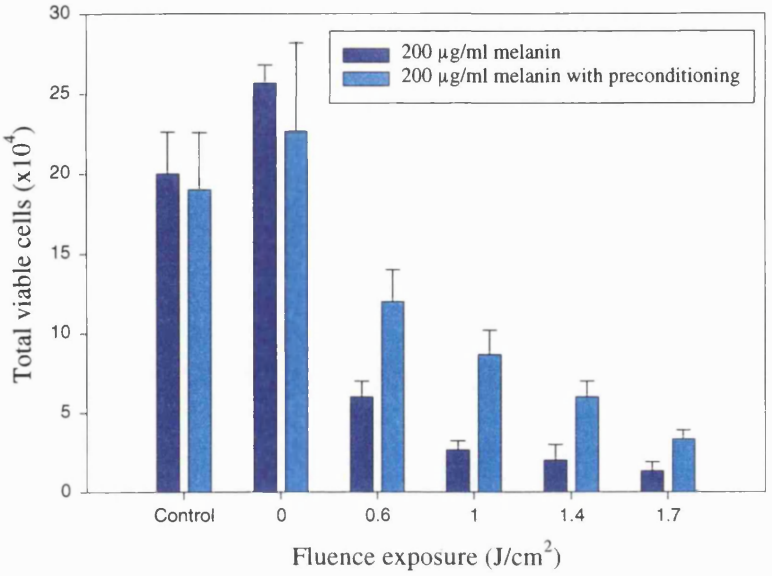

Figure 6.10: Graph showing the relationship between the total number of viable cells and increasing fluence of exposure from a normal mode ruby laser. Irradiation occurred 5 hours after heating and the wells contained 200 µg/ml melanin.

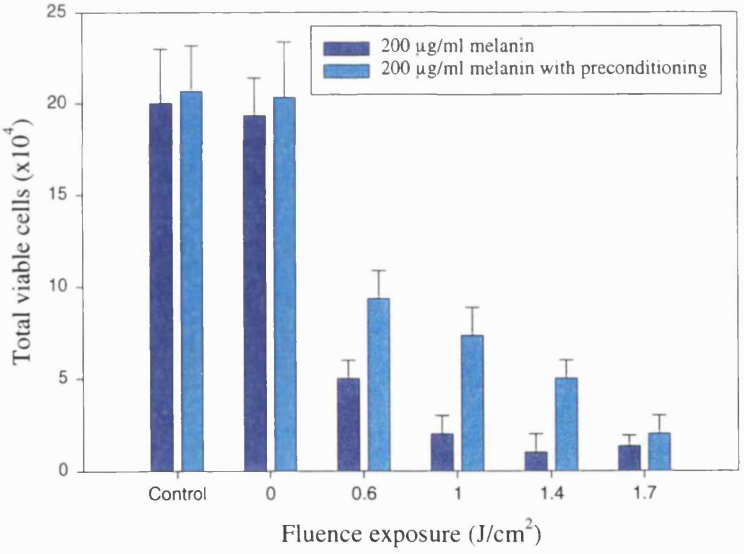

Figure 6.11: Graph showing the relationship between the total number of viable cells and increasing fluence of exposure from a normal mode ruby laser. Irradiation occurred 24 hours after heating and the wells contained 200 µg/ml.

group but only by half in the preconditioned group. When all the preconditioned and non-preconditioned groups at the same fluences were compared by a Student's t-test, then a significantly ($p<0.001$) greater number of cells survived the exposure in the preconditioned group, except at 1.7 J/cm^2, by 24 hours. A statistical comparison between the two preconditioned groupings at 5 and 24 hours revealed no statistically significant difference between the two at each fluence. When comparing the preconditioned groups with each other at the same times after pre-treatment, then a statistically significant difference in cell viability was noted between fluence exposure at 0.6 J/cm^2 and 1.7 J/cm^2.

A single analysis of the mean percentage difference in cell viability between the preconditioned wells and the non-preconditioned wells per patient culture exposed to 0.6 J/cm^2 at 5 hours revealed a greater difference in the mean values than would be expected by chance on one way ANOVA testing.

6.6 DISCUSSION

6.6.1 Determining Heat-induced Cell Death of Seven Paired Fibroblast and Keratinocyte Cell Lines Exposed to a Range of Temperatures

The control wells showed that fibroblast cultures appear to have a background proportion of dead cells of 6.6%. Heating of fibroblasts produced a slight increase in the percentage death rate upto 45°C whereupon a sudden increase was noted. This would probably be at the stage where irreversible cellular damage was occurring, particularly to cellular proteins and enzymes, resulting in the positive cells counted having either died immediately or experienced too many lethal lesions (Jung, 1986) and undergoing programmed cell death. The cell death count was performed at 24 hours, which has been stated as when the majority of cells undergoing apoptosis can be realised (Li, et al., 1996). All fibroblast cell lines followed a similar survival curve to each other supporting the likelihood of a cells inate defensive capabilities coping and then suddenly being overwhelmed ultimately producing 100% cell death at 51°C.

Although a constant background level of dead cells was noted between all the control wells of the seven fibroblasts cell lines, there was a greater difference in percentage cell deaths at all temperatures upto and including 49°C, between the seven cell lines than would be expected by chance ($p<0.05$). Culturing techniques had been identical between all seven fibroblast cell lines. In addition, the passage number of the cells was P3 which is well below the limit (generally taken to be P5) to which the phenotype of the cell would be expected to be changing and regressing to a less specialised type (Watt, 1994). Therefore, it would imply that a genetic difference, inherent to the volunteer, was present within those fibroblast cells making several of the lines more heat tolerant than others. It has been stated that an increase in protein oxidation and consequently reduced protein function within cells occurs with ageing (Stadtman, 1992). Whether the different heat sensitivities reported here are a process of ageing cannot be commented upon, but as the age range of the seven volunteers was narrow (23 to 37) then it would be thought unlikely to produce such a significant effect.

Keratinocytes had a mean background percentage of dead cells of 3.9% which was approximately half that of the fibroblasts and would perhaps correspond with a more robust cell phenotype. The percentage cell death rates of the seven keratinocyte cell lines, at each of the temperatures used, revealed no statistically significant difference except at 47°C and 49°C. This would suggest that keratinocytes from different volunteers experience a similar ability to protect themselves from heating in contrast to their fibroblasts, possibly reflecting the evolvement of this cell type to withstand the wide temperature fluctuations of the external milieu. In addition, the keratinocytes endured greater temperature insults than the fibroblast cell lines with the percentage cell death induced being less than that seen in fibroblast cultures upto 47°C ($p<0.04$ at 37°C and $p<0.001$ up to 47°C). Above 47°C the protective abilities of the keratinocyte cells appear to be lost and a sudden surge in percentage cell death occurs. An apparent contradiction is that cultured human fibroblasts have been reported to exhibit greater antioxidant enzyme activities than keratinocytes (Yohn, 1991), which would suggest that they should be more capable of defending themselves against adverse conditions.

It was stated in this paper, though, that this could be a function of the differing media in which the cells were being cultured as no universal media is presently available.

Although the response of the seven cultured keratinocyte cell lines to heat stress mimic each other closely throughout the temperature range and certainly moreso than the fibroblasts, variability again occurs at 47°C and 49°C. The passage of these cells was P2 which would make a behavioural change due to culturing unlikely. Therefore it would seem fair to suggest that once again a genetic difference in cell self-protection has been manifest.

The results from this experiment would suggest that the highest temperature at which a minimum of cell death would occur to cultured keratinocyte cells when applied for 15 minutes is 45°C. The cell death rate at this temperature for fibroblasts was significantly greater, but those cells reside deeper within the skin *in vivo* (several millimetres) and so would most likely have the heating effect reduced if not ammeliorated completely.

6.6.2 Determining the Effect of Temperature Upon Heat Shock Protein 70 Synthesis within Seven Keratinocyte Cell Lines

HSP 70 was found to be expressed within cultured human keratinocytes at all temperatures tested. It is probable that the HSP 70 band seen at 37°C at both 5 hours and 24 hours after heat exposure was the form that is expressed constitutively (HSP 73). Increasing the temperature increased the quantity of HSP 70 detected which probably reflected the production of the inducible HSP 72 form by these cells. This reached a peak within the 5 hour group at 45°C and then any further increase in temperature produced a reduction in quantity seen. The probable explanation for this was the increase in cell death seen to occur above 47°C within keratinocyte populations. A reduction in the number of viable cells would more than likely reduce the overall quantity of HSP 70 produced and hence the amount of staining detected. The reduced quantity of HSP 70 production seen at 47°C cannot be explained by an

equivalent increase in cell death, but maybe due to an accumulation of sub-lethal damage which would affect protein production.

The 24 hour group had a similar staining pattern as the 5 hour group. The keratinocytes expressed HSP 70 at all temperatures, but once again this increased in quantity with increasing temperature of exposure. The only difference noted was that the highest amount of HSP 70 was now detected at 47°C. This result supports the hypothesis that damage induced by 47°C incubation is sub-lethal and that protein production is just delayed. It has been stated that heat shock proteins have a protective role within the cell preventing it from undergoing apoptosis (Li, et al., 1996), (Strasser and Anderson, 1995) and therefore maximal expression may only be available when the cell is on the brink of apoptosis and indeed, a proportion within the culture system are undergoing that process. It could also suggest that an increased time of exposure at 45°C may further increase the quantity of HSP 70 production, but as cell death is affected by both the temperature and time of exposure (Leach, et al., 1943) then this may ultimately result in an increase in the cell death obtained.

HSP 70 would appear to be an ideal marker of cellular stress within keratinocytes, particularly when measured at 5 hours after exposure, as its rise correlated well with the presence and quantity of viable cells within the culture. As such, it could theoretically be used as a marker of successful cellular preconditioning.

6.6.3 Determining the Effect of Heat Preconditioning of Keratinocytes in Culture Upon Cell Survival after Subsequent Exposure to NMRL Irradiation

A comparison of the cell viability counts for the control wells before the experiment and at 0 J/cm^2 revealed that no statistically significant difference was seen between those wells containing synthetic melanin, those that had undergone preconditioning and those that had been exposed to air for the same time duration as the experimental wells. Consequently, any reduction in cell viability seen was most likely as a result of NMRL irradiation.

Both the preconditioned and the non-preconditioned groups whose wells contained 100 μg/ml melanin experienced a general reduction in cell viability throughout the fluence range used at 5 hours and 24 hours. This would be expected as a greater quantity of photon energy conversion would be occurring within those wells receiving a higher fluence.

A statistically significant difference was noted between the preconditioned and the non-preconditioned groups of cultured keratinocytes exposed to equivalent fluences at both 5 and 24 hours except the 1.7 J/cm^2 / 200 μg/ml melanin group at 24 hours. This represented a more-or-less common theme throughout the seven keratinocyte cell lines and would suggest that the cells can protect themselves against NMRL irradiation when preconditioned. No statistically significant difference in the cell viability of the preconditioned groups exposed to increasing fluences was revealed. This could imply that the preconditioning instills a set protective response which maintains the cell viability upto a certain level of heat stress whereupon it would once again be overwhelmed and a sudden decrease in keratinocyte viability is seen.

6.7 GENERAL DISCUSSION

The cell death experiment described emphasised the increased ability of the keratinocyte to protect itself from an adverse stimulus. The culturing techniques were identical between the fibroblasts and the keratinocytes in addition to the experimental techniques. This would appear to suggest that the keratinocyte is inherently more able to withstand extreme circumstances which defines the role it has to perform *in vivo*. The fibroblast, which resides within the dermis, is more of an "internal" cell and does not fulfil any protective role, therefore making it more susceptible to adverse conditions as shown in the experiment. What appeared interesting was that even though the keratinocytes from each of the seven cell lines exhibited a more-or-less constant response to increasing heat, this changed at 47°C and 49°C revealing that some patients cells are more susceptible to heat than others. This could imply that those cells able to withstand increased temperatures afford the patient an increased resistance to skin side effects, but it could also mean that their cells are more difficult

to destroy in the key places where this is required to work to obtain permanent hair depilation. The hair bulge at the site of the arrector pili muscle approximately a third of the way down the hair shaft (see section 1.3), is presently thought to be the source of new stem cells for regenerating hair bulbs. Those stem cells have all the characteristics of keratinocytes and would experience the adverse conditions that the keratinocytes at the skin surface would. If those cells have the same heat-resistant capabilities then it could imply that permanent laser depilation within that patient is a more difficult goal to achieve.

The fibroblasts, being more protected by skin depth, represent the cells of the internal milieu and consequently may mimic the cells of the bulb region which resides, in terminal hairs, at between 2 mm and 5 mm depth from the skin surface. Certainly those cells would not have been preconditioned in any way by extremes, but could possibly still maintain an intrinsic ability to protect themselves more capably. It would seem fair to assume that their reaction to heating would follow more closely that of the fibroblast cells. Therefore, this would suggest that the second target for ruby laser-assisted depilation, namely the hair bulb, requires less heat to destroy it than does the bulge region. This would be fortuitous as the increased depth of the hair bulb may result in less photon/heat energy from the laser reaching the cells at the bulb. It has been stated that a 50 % decay in incident ruby laser energy occurs at 1.2 mm (Anderson, 1984), although work described in Chapter 3 did not support this, but the less tolerant the cells then the better the depilatory effect will be. It is important to add, though, that the difference in cell tolerance between fibroblast and keratinocyte is a matter of a few degrees centigrade, which may well be too little.

All keratinocyte cell lines produced HSP 70 at 37°C and this increased in quantity upto and including 47°C. The fact that its presence reduced in amount when the cell viability decreased emphasised its ability to act as a marker of cellular stress. Whether in the induced HSP 72 form it is the main cellular protective protein against future adverse events cannot be answered. Other proteins have come to light, in particular interleukin-8 (Il-8), which has also been found to increase in amount within a stressed cell (Bowman, et al., 1997) and could be the main cellular protector. The experiments

therefore only used HSP 70 as a marker of maximal cell tolerance and when correlated with cell death, appeared to produce a temperature best suited for possible preconditioning with heat. The experimental model used invoked direct stimulation of the viable basal keratinocytes attached to the flask base when the flask was floated in the waterbath. These would be the cells which would require protection *in vivo*, but under those circumstances, would be separated by at least seven keratinised and cornified cells acting as a protective layer. It could be that a greater temperature than 45°C be necessary *in vivo* to produce the desired amount of stress protein production in the basal layer, which would emulate the experiment performed here. This possibility is examined in section 6.9.

A fact not addressed by this experiment was that of the process of aging upon the cell's ability to protect itself from adverse conditions. In fact to negate the effect of this, the explants for fibroblast and keratinocyte initiation were deliberately chosen from patients under the age of 40. One paper has stated that the responsiveness of heat shock factor 1, a transcription factor that mediates the response to heat shock, is reduced with age (Lee, et al., 1996). A second paper has described a decrease in the inductability of HSP 72 in normal human skin with age (Muramatsu, et al., 1996). Consequently it is possible that the benefits of preconditioning would be lost upon a more elderly patient, but to say to what extent this would be likely to occur is not possible.

Several papers, which have used ischaemia as a method of preconditioning, have stated that two windows occur in the cellular protective response. The first is within the first hour when an increased cell tolerance to a more lethal ischaemic event is noted probably related to a decrease in ATP depletion via reduced glycolysis. (Murry, et al., 1986). The second is approximately 24 hours after the episode of pretreatment, as measured by the presence of HSP 70 within the myocardial cells of the rabbit heart ((Knowlton, et al., 1990). The experiment described in this work appeared to show little difference in the quantity of HSP 70 production by keratinocytes after 5 hours and 24 hours. Although these results may appear to conflict with other published reports of HSP 70 production after bouts of ischaemia, it is important to state that a

different pathway of cell stimulation occurs when a cell is exposed to ischaemic conditions compared to heating (Yellon and Marber, 1994) because the former induces other protective enzymes such as catalase (Karmazyn, et al., 1991). Heating appears to have a more direct influence on the production of HSP 70 protein within the cell compared to ischaemia. The time of 24 hours was therefore chosen within this set of experiments to clarify the issue of HSP 70 production within preconditioned cells and also to reflect a possible clinical treatment regime that would be more tolerant to patients.

Preconditioning by heating of cultured human keratinocytes significantly increased the cell survival to NMRL irradiation. The only other similar work performed used a CO_2 laser (Polla and Anderson, 1987), which has a different wavelength (and consequently a different chromophore), a different pulse duration and used cultured human fibroblast cells instead of keratinocytes, but still achieved the same results. This would tend to support the idea of the general nature of cellular preconditioning, certainly as a response to heating and the ability of the cell to protect itself from a range of adverse circumstances. A chromophore was required within the media bathing the cells and the amount used approached physiological levels however, whether the cells responded in a physiological manner to its presence cannot be answered. As mentioned previously, it has been shown that keratinocytes do phagocytose the synthetic melanin, which would mimic the *in vivo* situation.

The experiment shows that human keratinocytes could theoretically be preconditioned by heat to protect themselves from NMRL irradiation. The model used represented as closely as possible the *in vivo* situation. However, larger quantities of energy are used in clinical practice plus it is the darker pigmented skin requiring protection. Whether the self-protecting capabilities of the keratinocytes would be overwhelmed under these circumstances cannot be addressed at present.

6.8 CONCLUSIONS

- Differential death rates exist between fibroblasts and keratinocytes when exposed to the same temperature for the same time duration, with keratinocytes able to withstand greater heat stress.

- Keratinocytes are able to withstand temperatures up to 47°C for 15 minutes with minimal cell death occurring.

- HSP 70 is expressed by heat-exposed keratinocytes to a maximum at 45°C when analysed at 5 hours post-heating and at 47°C when analysed at 24 hours post-heating.

- Preconditioning cultured human keratinocytes at 45°C for 15 minutes, 5 hours prior to exposure to NMRL irradiation significantly increased cell survival when compared to non-preconditioned irradiated keratinocytes.

6.9 THE ABILITY OF *EX VIVO* NORMAL HUMAN SKIN TO BE HEAT PRECONDITIONED BY APPLICATION OF A HEATING APPARATUS

The *in vitro* cellular work described above has shown the ability of cultured human keratinocytes to be protected from NMRL irradiation by heat preconditioning. Although the stress response invoked by heat preconditioning represents a generalised, fundamental response by all known living cells, how well the response could occur when the cells were within skin, compared to in culture, cannot be stated. The ease of response by cells in skin would need to be established to assess whether preconditioning could occur within this model. No direct measure of successful preconditioning is known. However, increased expression of the HSP 70 protein would appear a good marker judging by the successful preconditioning of keratinocytes *in vitro* described above. If it were possible to evoke a preconditioned

response within the epidermal keratinocytes of *ex vivo* skin by heating, then this would suggest that potential protection from NMRL irradiation could occur *in vivo* in clinical practice.

6.9.1 Aims

- To determine whether HSP 70 protein can be induced within the epidermal cells of *ex vivo* human skin samples by surface heating.

- To determine the association between the heating temperature and HSP 70 protein expression within the epidermal cells of *ex vivo* skin samples.

- To determine the association between the heating temperature and cellular damage within the epidermal cells of *ex vivo* skin samples.

6.9.2 Method

A single large specimen of normal human skin was taken from each of six patients who had undergone a breast reduction procedure. The specimens were each dissected within a Class II hood and the subdermal fat removed. Each of the patient specimens were then divided into six samples with the first sample acting as a negative control and the remaining five samples exposed to a particular temperature. This was either 37°C, 42°C, 46°C, 50°C or 54°C and was produced from a 15 mm diameter heating apparatus that was applied to the epidermal side of each skin sample for 15 minutes (see Figure 6.12). The experiment was performed within the Class II hood with the samples from each patient specimen laid on a sterile steel mesh in a 12 cm petri dish containing FCM upto the level of the mesh so helping to maintain cell viability. The petri dish was placed upon a thermostatically controlled heater to keep the media at approximately 37°C and was monitored by a thermometer.

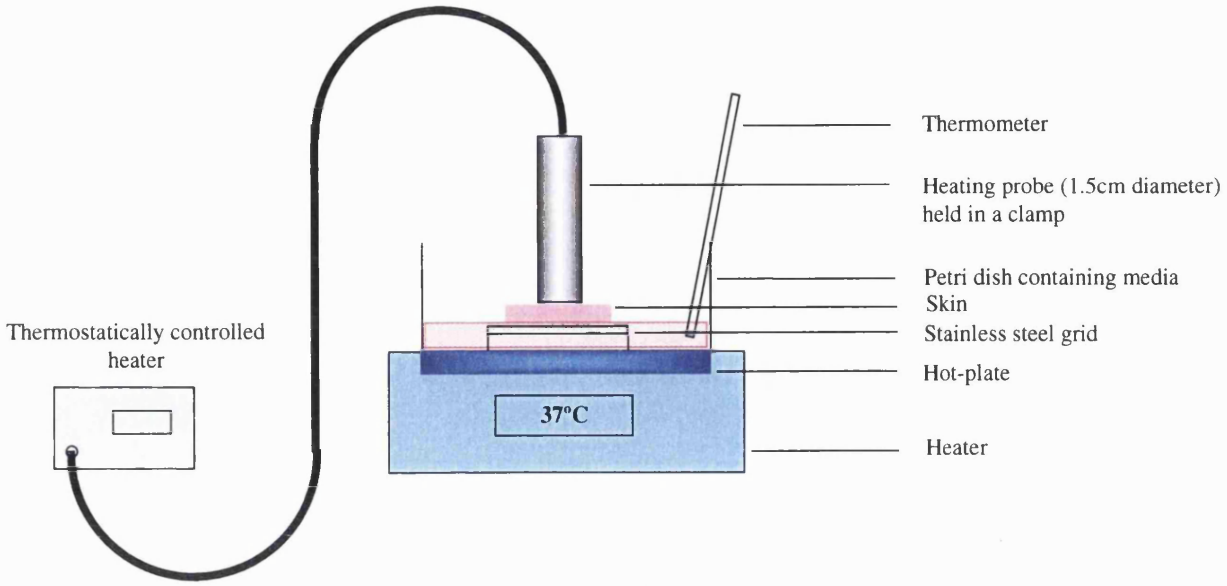

Figure 6.12: Diagrammatic representation of the experiment described in section 6.6 which was performed in a Class II hood maintaining tissue sterility.

When all the five skin samples from each patient specimen had been exposed to the pre-determined temperature via the heating apparatus, a 6 mm diameter biopsy was taken from the heated area in all five samples plus one from the negative control. The biopsy specimens were placed dermis down upon a sterile steel mesh in a 6 cm petri dish. FCM was added to the level of the mesh to again maintain cell viability and the dish placed in an incubator for 5 hours.

After 5 hours, the specimens were removed from the incubator and fixed immediately in 10% formal saline. Histological processing then occurred to embed the biopsies in paraffin wax. A random selection of 8 transverse sections was taken throughout each sample from each patient specimen and was stained for HSP 70. The counterstain haematoxylin was used and as such the same sections could also be analysed for signs of cellular damage resulting from the heating process.

6.9.3 Results

Figure 6.13 is a transverse section through a negative control sample, stained for HSP 70, which had been maintained at 37°C whilst the remaining samples were exposed to the heating probe. The nuclei have stained blue for the counterstain haematoxylin showing that no increased HSP 70 expression has occurred. In addition, no evidence of cellular damage within the epidermis is present. Figure 6.14 is a transverse section taken from the sample which had the heating probe placed on the surface at 37°C. No increased expression of HSP 70 protein is evident within the epidermal nuclei, which have taken up the counterstain haematoxylin appearing blue and once again, the cells do not appear damaged in any way. The section in Figure 6.15 is taken from a sample that was exposed to 42°C for 15 minutes. Several of the nuclei of cells within the basal layer have expressed HSP 70 but they are in the minority and no evidence of cellular damage is present. Figure 6.16 shows a transverse section through a sample exposed to 46°C and now virtually all the nuclei of the cells at the basal layer are positive for HSP 70 expression. Several of the fibroblasts within the dermis are also

expressing HSP 70 but the majority appear to be stained blue for the counterstain. No cellular disruption can be seen within the section, which would preclude heat damage.

Figures 6.17 and 6.18 show transverse sections from samples exposed to 50°C and 54°C. The cells express HSP 70 protein to the same degree as the section taken at 46°C but now increasing damage can be seen in the former section by cellular vacuolisation and in the latter by epidermal/dermal disruption.

6.9.4 Discussion

The negative control samples did not express HSP 70 within the epidermal cells suggesting that the experimental process did not place any undue stress upon the tissue samples. The section, which had been exposed to the heating probe at 37°C, also stained negative for HSP 70, which suggested that any effect of applying the heating probe itself would not induce stress within the tissue model. Increasing the temperature of exposure resulted in an increase in HSP 70 expression particularly noticeable in the cells of the basal layer which is where the protective effect is most required. This reached a maximum at 46°C and increasing the temperature further did not appear to increase the intensity of the staining for the protein. In addition, epidermal damage became evident at 50°C and was much more diffuse at 54°C.

The fibroblasts in the dermis of the section taken at 42°C show no evidence of increased HSP 70 synthesis whilst the section at 46°C shows a minimal number of fibroblasts now expressing the protein. This would suggest that the viable cells of the hair follicles residing within the bulge region in the mid to deep dermis, which would be targeted by the NMRL, would have undergone minimal heat exposure and so should not be protected by the preconditioning effect at this temperature.

The experiment has shown that human skin could be preconditioned by heat, which in turn may be able to protect against subsequent NMRL exposure. This appeared to be possible at 46°C for 15 minutes but above this temperature produced skin damage. 46°C is a temperature that may not be tolerated upon various regions of the body.

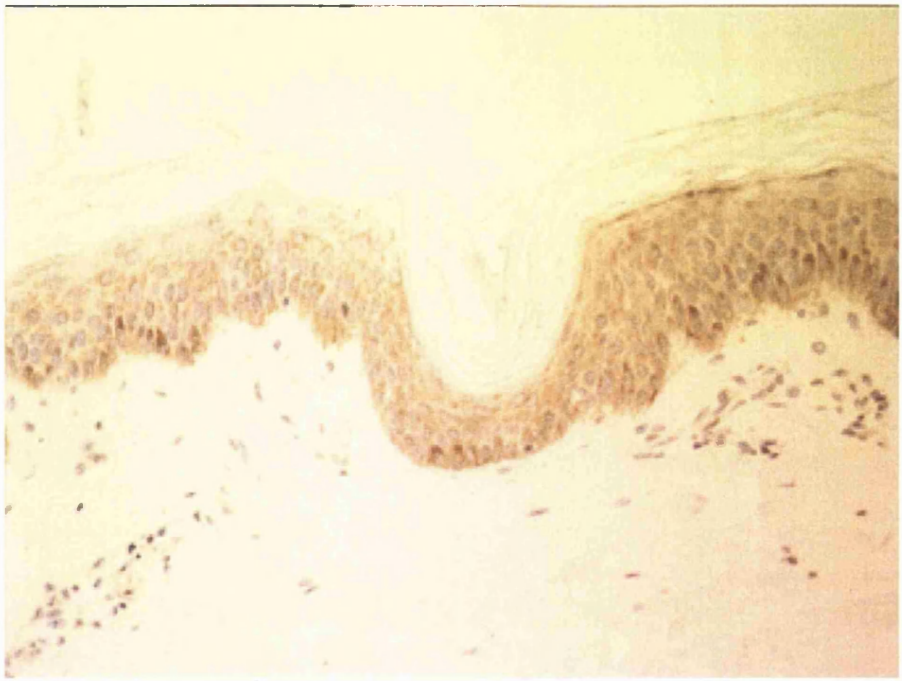

Figure 6.13: Transverse section of *ex-vivo* human skin acting as a negative control and stained for HSP 70 expression. Minimal protein expression is evident within the nuclei of all epidermal cells which appear blue from the haematoxylin counterstain (x200).

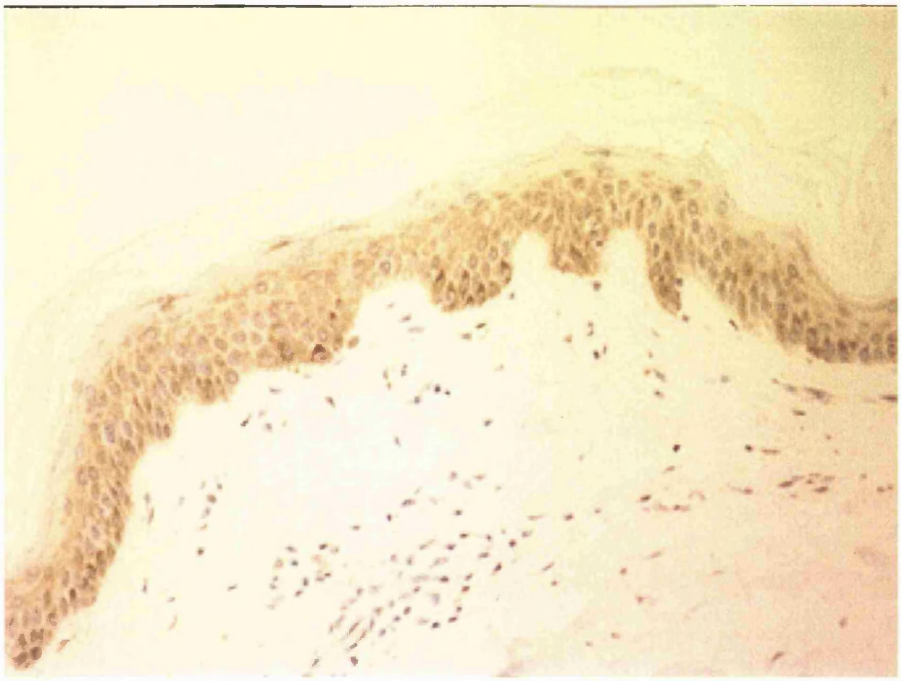

Figure 6.14: Transverse section of *ex-vivo* human skin exposed to the heating probe at 37°C and stained for HSP 70 protein. Minimal expression is evident within the nuclei of the epidermis which are blue from the haematoxylin counterstain (x200).

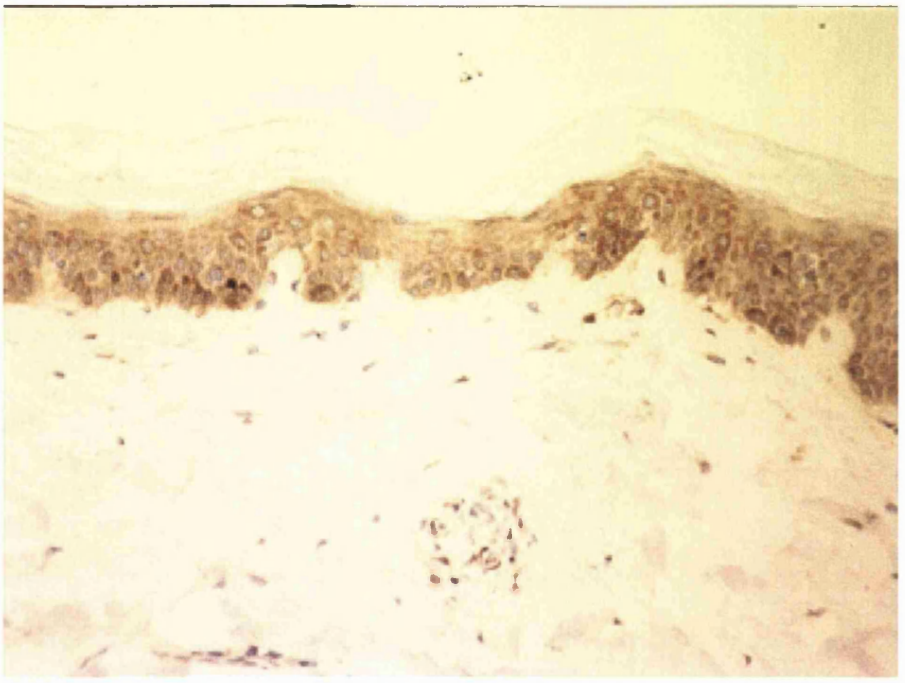

Figure 6.15: Transverse section of *ex-vivo* human skin exposed to 42°C from the heating probe and stained for HSP 70 protein. A few of the cells of the basal layer are expressing the protein with the nuclei appearing brown (x200).

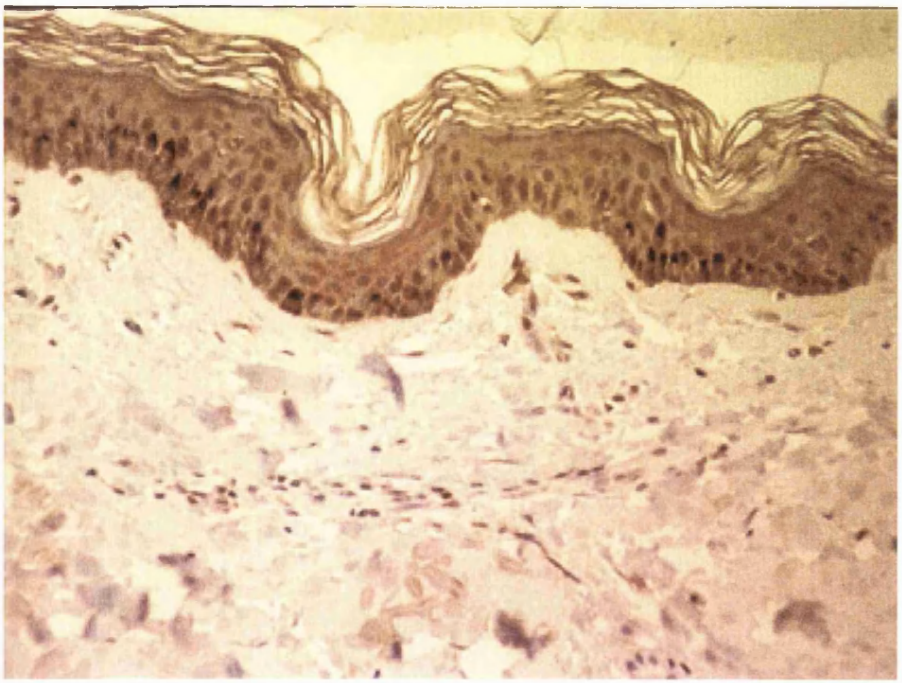

Figure 6.16: Transverse section of *ex-vivo* human skin exposed to 46°C from the heating probe and stained for HSP 70 protein. Positive expression has occurred in all nuclei denoted by the brown stain and is particularly strong at the basal layer (x200).

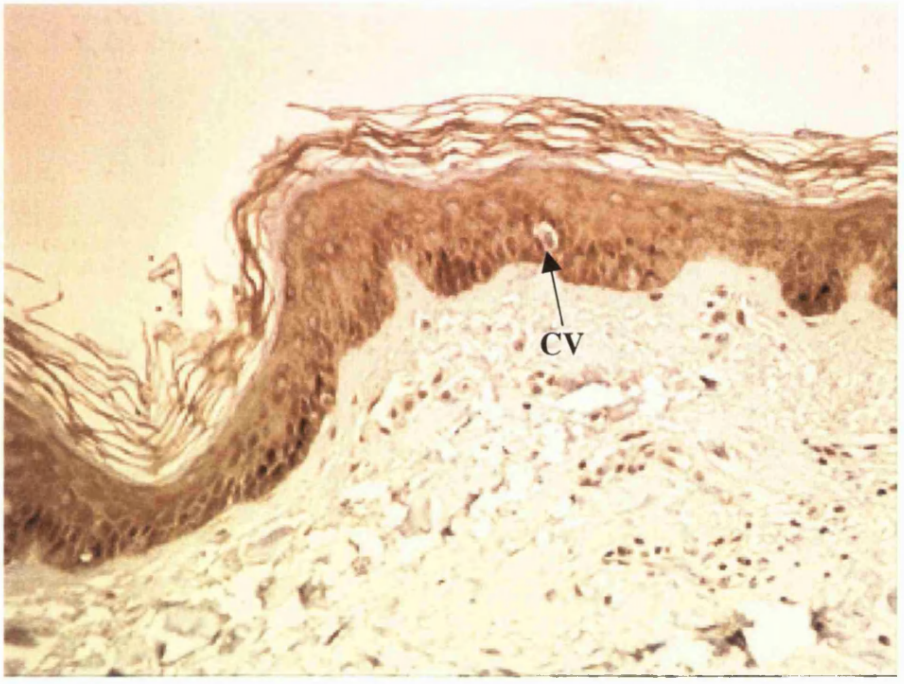

Figure 6.17: Transverse section of *ex-vivo* human skin exposed to 50°C from the heating probe and stained for HSP 70 protein. All the nuclei have stained positive for expression of the protein but cellular damage is now becoming evident in terms of vacuolisation (CV) x200.

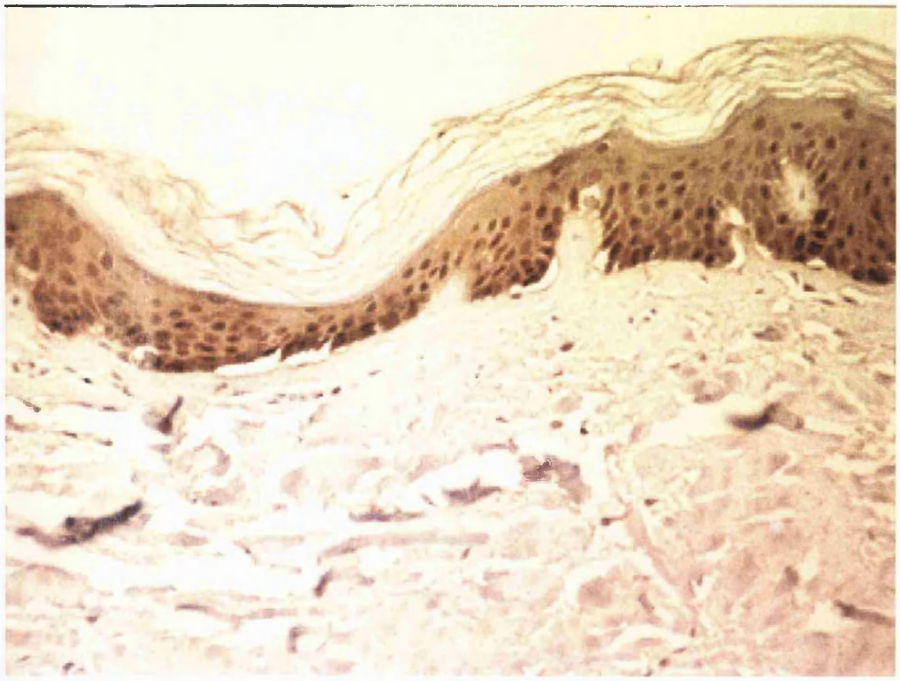

Figure 6.18: Transverse section of *ex-vivo* human skin exposed to 54°C from the heating probe and stained for HSP 70 protein. The nuclei of the cells of the epidermis are expressing the protein but increased damage is now evident in terms of the epidermis becoming removed from the dermis in places (x200).

However, to produce site specific preconditioning in the epidermis alone would theoretically require the maximum tolerated temperature for the minimal amount of time so the heating effect is limited to the skin surface alone.

6.9.5 Conclusions

- HSP 70 production can be induced by surface heating within the basal keratinocytes in *ex vivo* human skin specimens by heating of the epidermis.

- HSP 70 expression appears maximal at 46°C for 15 minutes with minimal damage evident within the epidermis of the skin specimen upon histological analysis.

- Epidermal keratinocytes within *ex vivo* human skin can be stimulated to express HSP 70 but may require a lower temperature applied for longer, since this may be better tolerated by patients.

CHAPTER 7 – POTENTIAL PROTECTION FROM EPIDERMAL SIDE EFFECTS BY HEAT PRETREATMENT - *IN VIVO* PROOF OF PRINCIPLE

7.1 INTRODUCTION

The phenomenon of preconditioning has been described in the literature relating to both cardiac and skeletal muscle protection and skin protection. Murry, 1986 #269 described increased cell survival within the heart of dogs, which had experienced prior non-lethal ischaemic conditions before a more lethal ischaemic event, when compared to non-preconditioned controls. Heat stress (Koenig, et al., 1992) (Garramone, et al., 1994) and ischaemic pre-conditioning (Gurke, et al., 1996); (Lee, et al., 1996) have both been shown to protect skin flaps and muscle flaps during the transfer process when they are subject to ischaemia/reperfusion injury. A cellular model has been devised and described using cultured human dermal fibroblasts, which were preconditioned with heat and then exposed to a CO_2 laser 3 hours later. The preconditioned cells were found to have a significantly decreased cell death when compared to the non-pretreated group 2 hours post-irradiation (Polla and Anderson, 1987).

Chapter 6 described *in vitro* experiments using a human cellular model to define the capability of cultured human keratinocytes to protect themselves from normal mode ruby laser (NMRL) irradiation after prior preconditioning with a sublethal exposure to heat. This was successfully accomplished with a statistically significant increase in the cell viability noted at a range of fluences up to 1.7 J/cm^2 when compared to non-preconditioned controls. The circumstances which preside within a culture system are, however, far removed from those which occur in the *in vivo* situation. The effects of culturing upon the activities of the cells in any cellular model are not entirely known and exactly how representative the model is remains questionable. For instance, the preconditioning heat as applied directly to the basal layer, through the flask base in chapter 6 would, *in vivo*, have to be applied through the stratum corneum, thus

implying that a higher temperature may be required than that used *in vitro* to produce the same effect. The blood flow through the pretreated field *in vivo* would also be influential by increasing the rate of heat loss from the site exposed, thereby also suggesting that a higher temperature might be required than that used *in vitro*. Pre-heating, *in vivo* would also probably induce a mild inflammatory response that may thicken the skin with oedema fluid. If the mode of effective laser depilation is via laser light passing through the skin, then this would mean that the laser beam would have to penetrate a greater distance through the skin to reach the bulge region and the hair bulb to effect depilation. It has been calculated that the divergence of the laser beam increases with increasing distance travelled through skin, which could theoretically lessen the incident fluence upon the ultimate target (Anderson, 1984). Interestingly, though, increased water content has been stated to increase thermal conductivity within the tissue, so possibly improving heat deliverence to the target cells once the photon energy has been converted (Welch, 1984).

A recent paper has suggested that Heat Shock Protein 70 (HSP 70) is expressed within the stem cells of the bulge region in mouse hair follicles, but only during the late anagen and early catagen phases of hair growth, with a significant increase towards the end of anagen (Hashizume, et al., 1997). The desired effect of preconditioning the skin must be to induce protection of the epidermal keratinocytes, particularly the stem cells within the basal layer, but not to increase the resistance of the deeper lying target cells, namely the cells of the bulge region and the hair bulb. Therefore the preconditioning effect must remain as superficial within the skin as possible, which in theory would probably mean using a higher temperature of a shorter duration in an attempt to prevent the heat from penetrating too deeply.

The C57BL/10 black haired mouse model was used for this sequence of experiments as Chapter 4 showed it to be an acceptable model for depilatory studies using the NMRL. How comparable the effects would be to the human situation cannot be stated. The cells of the skin of the mouse contain no melanin pigment and so in that respect would be comparable with a Fitzpatrick type 1/2 individual (see Table 1.1). The epidermis of the mouse skin on the back and flank is approximately 2 to 3 cells

thick and so could potentially mimic the *in vitro* cellular model more closely than human skin would, whose epidermal thickness is much greater depending upon body site. In addition it would appear that the skin damage induced in the mouse model may occur via a slightly different route than that assumed to occur in the human situation (see chapter 4). Because of this, this model may not be ideal to assess the protective efficacy of the heat preconditioning technique but may still be of use to determine whether preconditioning affects depilation.

7.2 AIMS

- To determine the ideal temperature at which to precondition mouse skin whilst producing minimal side effects, using HSP 70 protein as a marker for successful preconditioning.

- To discover whether preconditioning of mouse skin at the discerned ideal temperature protects against subsequent NMRL irradiation-induced skin side effects and to assess its overall effect upon long term depilatory efficacy.

7.3 METHODS

7.3.1 Determining the Ideal Temperature at which to Precondition the Skin of the Black-haired Mouse whilst producing Minimal Side Effects

42 mice were used in total for this procedure. All the mice were anaesthetised and the hairs trimmed from their backs. Two experimental groups and a negative control group were established prior to the experiment. The two experimental groups, n=18 for each, underwent the same protocol with the only difference being that one group was sacrificed 5 hours after heat exposure and processed for histology and HSP 70 detection whilst the other experimental group was observed macroscopically over a two month period for skin damage and hair regrowth. The negative control group consisted of 6 mice, which were trimmed only and then observed macroscopically over time. All biopsies taken were from resting hair sites 5 hours after heat exposure.

Resting hair sites were chosen because it was easier to assess whether heat preconditioning had reached the bulge region and the bulb as the hair follicles were finer. The bulge region itself is fixed within the dermis so its site does not change with hair cycling. The time of 5 hours after preconditioning was chosen for convenience as no obvious difference in the success of heat preconditioning upon subsequent skin protection had become apparent at either that time or at 24 hours (see chapter 6).

The 18 mice in both the experimental groups were divided into 6 groups of three with each group of three exposed to one particular temperature upon both sides of the back from the heating apparatus (see Figure 7.1), so therefore each temperature for each group was represented by 6 sites. The temperatures used were 37°C, 39°C, 41°C, 43°C, 45°C and 47°C and the exposure time was for 15 minutes. The mice were then returned to individual boxes placed upon warm mats and allowed to recover. When 5 hours had elapsed, the first experimental group of mice was sacrificed and 6 mm biopsies taken from the heat exposed sites. The specimens were placed into 10% formal saline for paraffin wax histology.

The second experimental group was allowed to recover in individual boxes and then returned to the mouse room. Skin wounding was assessed in the first two weeks for signs of superficial erythema or blistering from the exposure to heat and scored according to Table 2.4. Hair regrowth was assessed over a two month period using the scoring system set out in Table 2.6 to establish whether the heat pretreatment alone affected hair regrowth in the black-haired mouse.

Histological examination involved taking six paired, random, transverse sections through each of the biopsy specimens. One of the pairs was stained with H&E to assess for any histological signs of burns damage such as cell vacuolisation, nuclear pyknosis and epidermal cell loss, whilst the second section of the pair was stained for HSP 70 protein expression (section 2.3.2) within the epidermal cells, the site and the extent.

7.3.2 Determining the Consequences of Heat Preconditioning Upon the Effects of Ruby Laser Irradiation of the Skin of the Black-haired Mouse

The results gained from the experiment described above were incorporated into this procedure. The preconditioning temperature of 45°C applied for 15 minutes was used with a 5 hour time gap prior to NMRL exposure. In addition, sites of actively growing and resting hairs (discerned as previously described in chapter 4) were used to see whether the hair growing phase would affect the results.

A total of 40 mice were used in this experiment. Hair trimming was performed after intraperitoneal anaesthesia and 16 of the mice underwent preconditioning or not and then irradiation of growing hair sites; 8 at 5 J/cm^2 and 8 at 6 J/cm^2. A further 16 mice underwent preconditioning and laser irradiation upon resting hair sites in the same manner at the two fluences mentioned. The remaining 8 mice were split into two groups of four also according to hair phase and underwent the same experimental procedure, but were then sacrificed and had 6 mm biopsies taken from the irradiated sites in preconditioned and non-preconditioned areas.

The mice were exposed to the heating probe at 45°C for 15 minutes, either on one or both flanks if the mouse was large enough to accommodate the heating plate and leave room for a non-preconditioned exposure site too. Once completed, the mice were returned and housed individually in single cages placed upon a heating mat and allowed to recover.

After 5 hours, the mice were removed in turn from their cages and anaesthetised by an inhalational anaesthetic. NMRL irradiation then occurred at 5 J/cm^2 and at 6 J/cm^2 upon growing hair and resting hair regions so that at least 8 sites were represented within each of the four groups. The experimental mice were then returned to their cages and allowed to recover before being returned to the mouse room. The mice to undergo histological analysis were sacrificed and 6 mm biopsies taken from all laser exposed sites plus negative and positive (heating alone) controls. All were fixed in 10% formal saline and underwent routine paraffin wax embedding. Six paired random

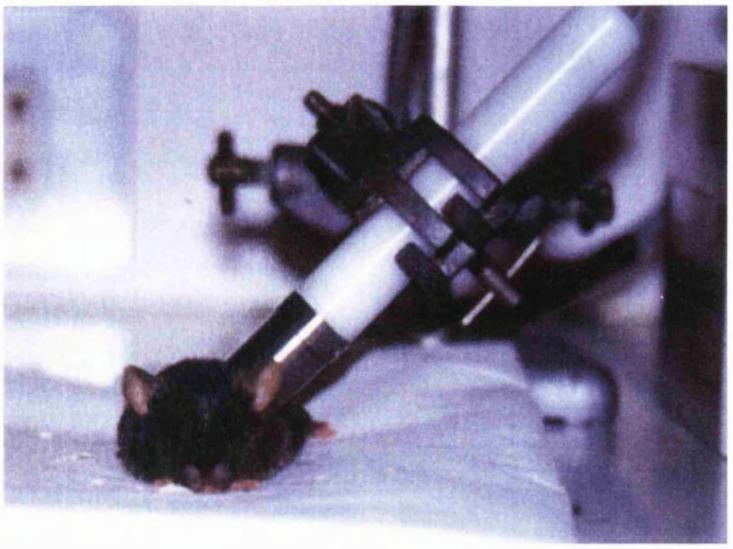

Figure 7.1: Photograph of an anaesthetised mouse being exposed to the heating apparatus.

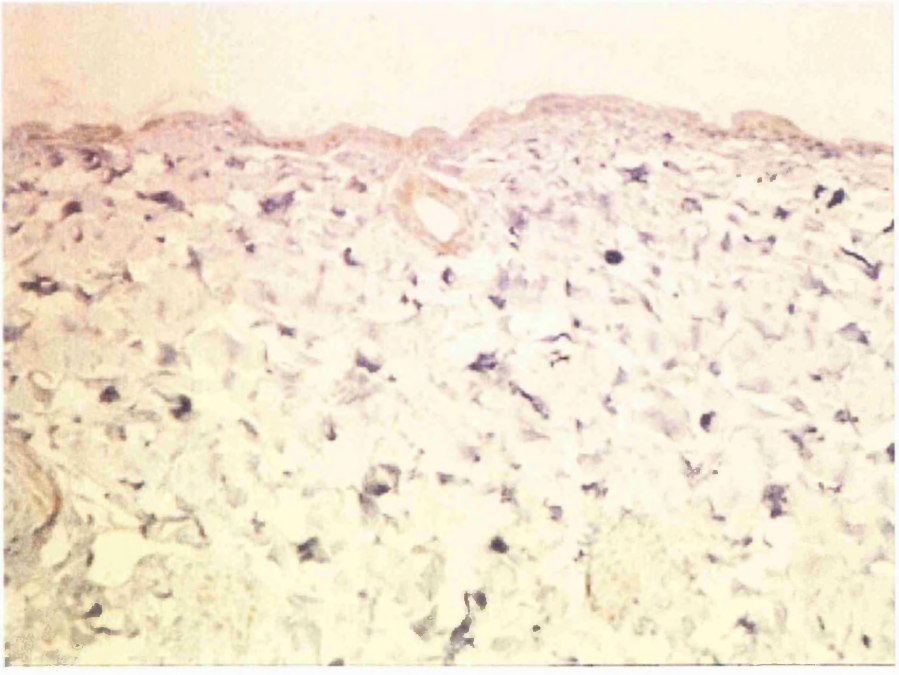

Figure 7.2: Transverse section of a specimen stained for HSP 70 having been exposed to 37°C from the heating apparatus for 15 minutes. Minimal positive expression has occurred in the nuclei of the cells within the epidermis (x200).

sections were taken in a transverse manner with one of the pairs stained using the modified SACPIC technique and the second using H&E. The modified SACPIC stained sections were compared to assess the extent of hair shaft damage occurring within preconditioned and non-preconditioned sites that had undergone NMRL exposure. The H&E sections assessed the extent of cellular damage occurring within the same specimens.

The mice were observed daily for skin damage at the sites of irradiation on preconditioned and non-preconditioned sites and scored according to Table 2.5 until complete healing had occurred. A slight modification to the scoring system was made upon the first day after the procedure when it became apparent that the previous scoring system could not take into account the difference in the size of the clinical wounding noted. Therefore, an estimate of the percentage area of wounding within the 7 mm diameter exposure site was taken to improve accuracy of the scoring system. When wound healing was complete, the mice were anaesthetised by intraperitoneal injection and the laser-exposed sites tattooed to help identify them over time. The mice were then further observed for hair regrowth over a two month period and scored weekly according to Table 2.6 to establish any change in depilatory efficacy between the preconditioned and non-preconditioned irradiated sites.

At two months, all the mice were sacrificed and representative biopsies taken from the preconditioned irradiated and irradiated alone sites with a negative and a positive (heated alone) control. Single, random transverse sections were taken after histological processing and stained using Massons trichrome to look for any signs of dermal scarring and fibrosis within the specimens.

7.4 STATISTICS

Sample statistics are shown as means (+/- standard deviation). Statistical comparison between two groups was performed upon median values using the Mann Whitney Rank Sum test.

7.5 RESULTS

7.5.1 Determining the Ideal Temperature at which to Precondition the Skin of the Black-haired Mouse whilst producing Minimal Side Effects

Macroscopic Analysis

Application of the heating apparatus to the trimmed flanks of the mice up to a temperature of 47°C for 15 minutes did not induce any gross clinical signs of a burn wound in any of the mice. No systemic ill effects were manifest in any of the mice post-operatively.

The eight week follow-up of the experimental and negative control groups revealed no difference in the hair regrowth rates between them and no apparent difference in the final hair density upon the flanks of the heat exposed and non-heat exposed mice.

Histological Analysis

Figure 7.2 is a representative transverse histological section of mouse skin taken from a biopsy specimen five hours after being exposed to the heating apparatus at 37°C for 15 minutes and immunostained for HSP 70 protein. The majority of the surface epithelial cells do not appear to be expressing HSP 70 protein with the nuclei, having been counterstained with haematoxylin, appearing blue. The proportion of epidermal cells expressing HSP 70 increased with increasing temperature used, reaching a maximum at 47°C.

Figure 7.3 is a representative transverse histological section of a biopsy specimen taken from a resting hair region five hours after being exposed to the heating apparatus at 45°C for 15 minutes. Immunostaining for HSP 70 protein shows that the surface epithelial cells all appear to be expressing the protein and to a greater extent than any of the cells shown in Figure 7.2. HSP 70 has also undergone comparatively increased expression in the viable cells of the follicular canal to the level of the

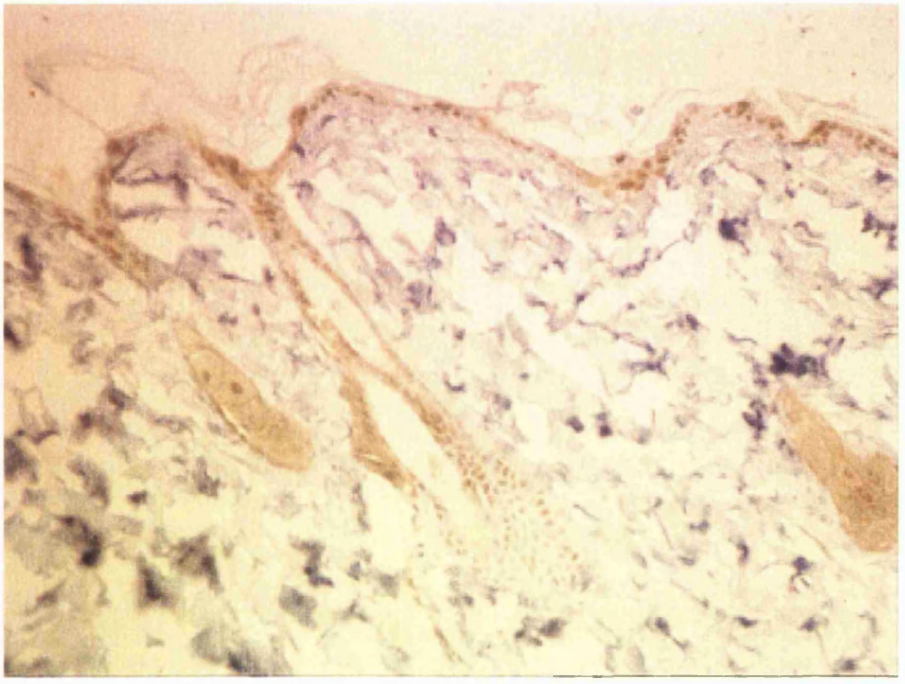

Figure 7.3: Transverse section of a specimen stained for HSP 70 having been exposed to 45°C from the heating apparatus for 15 minutes. Increased expression has occurred within the nuclei of the cells of the epidermis and also the cells lining the hair follicles to the extent of the sebaceous gland (x200).

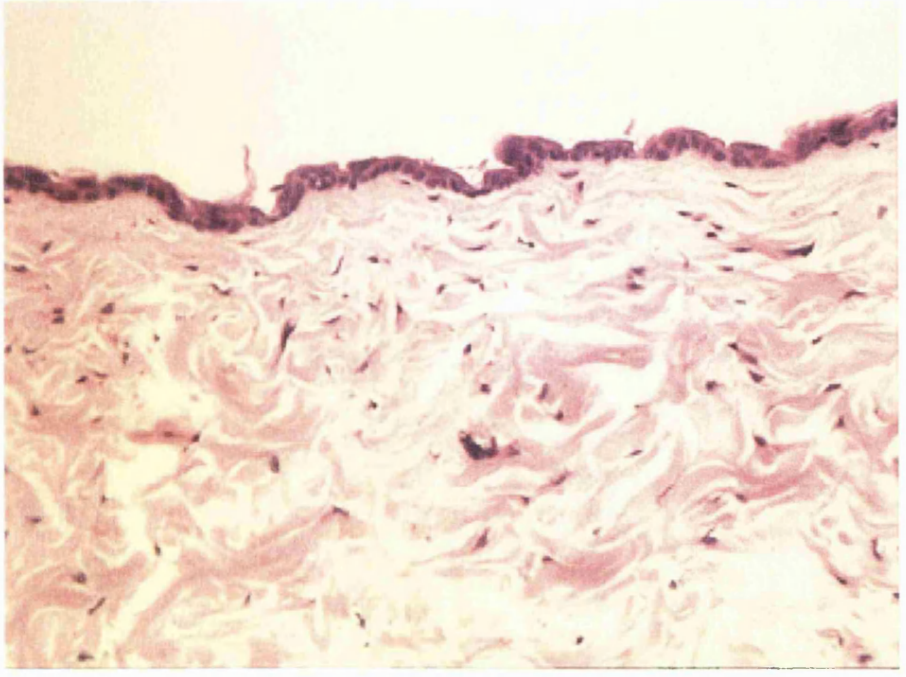

Figure 7.4: Transverse section of a specimen stained with H&E having been exposed to 45°C from the heating apparatus for 15 minutes. No evidence of cellular damage is apparent within the epidermis (x200).

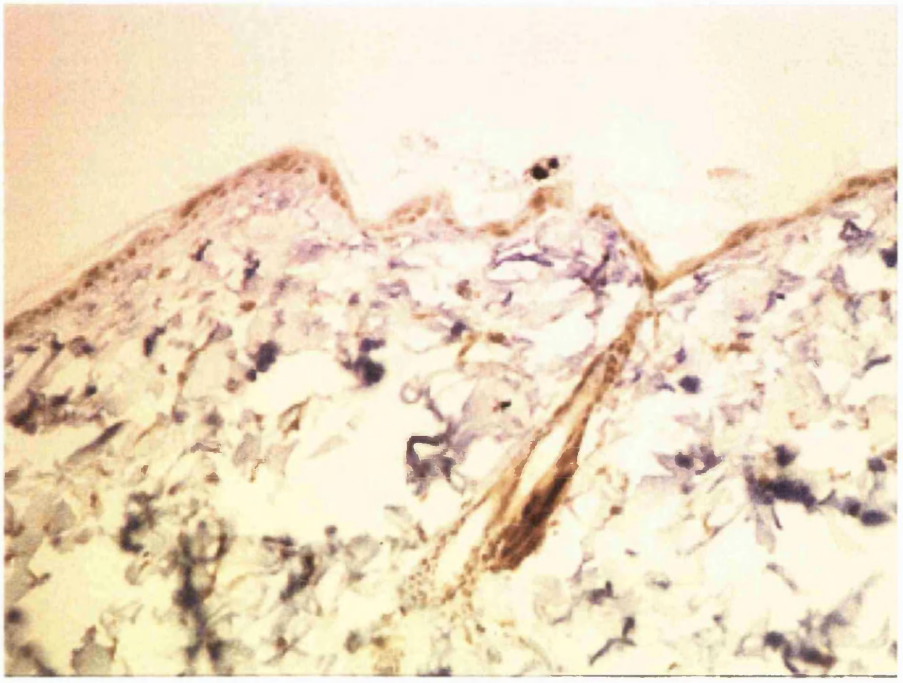

Figure 7.5: Transverse section of a specimen stained for HSP 70 having been exposed to 47°C from the heating apparatus for 15 minutes. Increased expression is present within the nuclei of the epidermis and throughout the cells of the follicle to the hair bulb (x200).

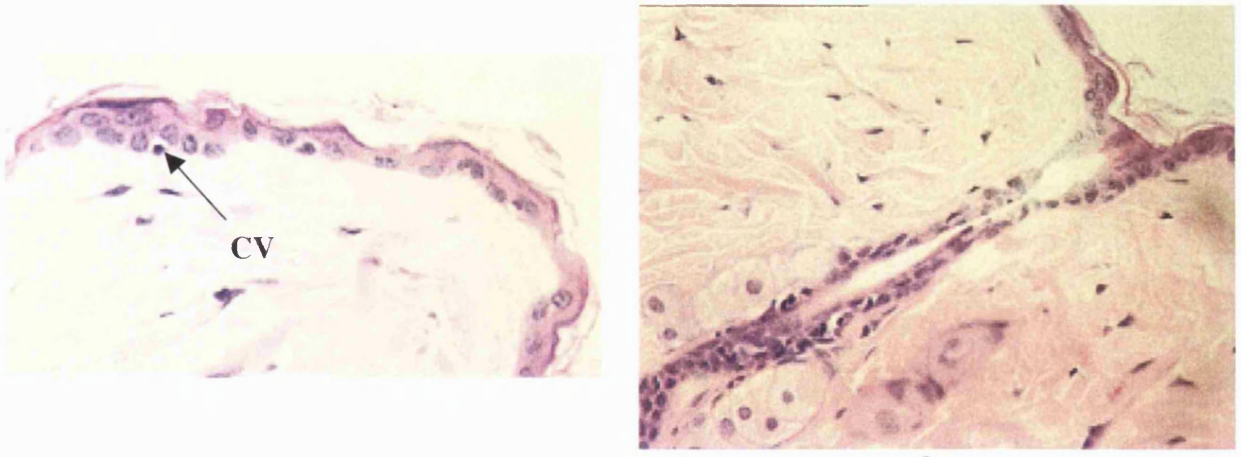

a. **b.**

Figure 7.6a: Transverse section through mouse epidermis exposed to 47C for 15 minutes showing damage to the epidermal cells (CV=cell vacuolisation) x400.

b: Transverse section through mouse skin in a hair resting region exposed to the same temperature as a) showing damage to the cells lining the follicular canal (x200).

sebaceous gland. The follicular cells at a deeper level within the skin than the sebaceous gland express the protein to a lesser extent until at the hair bulb itself, only a few have been stained for expression of HSP 70. The section shown in Figure 7.4 is a transverse section stained with H&E looking for signs of cellular damage within the cells of the epidermis. This is not apparent in the representative section shown or in any other sections examined at this temperature.

Figure 7.5 is a representative transverse histological section of a biopsy specimen from a resting hair region five hours after being exposed to the heating apparatus at 47°C for 15 minutes. This section has been stained for HSP 70 and it would appear that this protein is heavily expressed within the surface epithelial cells. In addition, the viable cells of the follicular canal within this section also appear to express an increased quantity of HSP 70 extending to and including the hair bulb itself. A greater number of cells of the hair bulb have stained positive for HSP 70 when compared to the cells of the hair bulb from the specimen exposed to 45°C.

Figure 7.6a is a representative section taken from the specimen exposed to 47°C for 15 minutes and biopsied after 5 hours having been stained with H&E. The nuclei within several of the skin surface keratinocytes can be seen to have degenerated by the apparent increase in staining density. In addition, vacuolisation is evident around several of the nuclei and this would appear to confirm increased damage to the cells upon exposure to 47°C for 15 minutes. Figure 7.6b is an area from the same specimen but showing a follicle of a resting hair. Nuclear damage is apparent within several of the viable follicular cells lining the hair canal at the level of the sebaceous gland, which would again suggest irreversible cellular damage occurring within the hair follicle as a result of the heating process at that particular temperature.

7.5.2 Determining the Consequences of Heat Preconditioning Upon the Effects of Ruby Laser Irradiation of the Skin of the Black-haired Mouse

Macroscopic Analysis

Skin Damage

All the mice followed over the 8 week period survived both anaesthetics with no apparent systemic ill effects noted. Figure 7.7a shows the mean daily plots (+/- standard deviation) of the wound scores achieved on the eight mice within the 5 J/cm^2 fluence group which underwent either preconditioning or not upon sites containing resting hairs. The scores can be seen to always be higher in the non-preconditioned group throughout the time taken to heal. Statistical analysis of the median values by Mann Whitney Rank Sum test revealed a significant difference in these values on the second day alone ($p=0.028$).

Figure 7.7b shows a graph of the mean daily wound scores (+/- standard deviation) seen on the eight mice within the 6 J/cm^2 group, which underwent either preconditioning or not upon sites containing resting hairs. This revealed that the mean scores were again always lower in the preconditioned group throughout the period of wounding. Statistical analysis by Mann Whitney Rank Sum test upon the median wound scores revealed that no significant difference was encountered in the scores upon day 1 post-operatively, but from days 2 to 4 inclusive, a statistically significant difference was noted ($p=0.021$, $p=0.028$ and $p=0.038$ respectively) and this was repeated on day 8 ($p=0.05$). No difference was noted on days 5 to 7 and 9 to 10 inclusive. Figures 7.8 and 7.9 shows the preconditioned and non-preconditioned sites upon a mouse two days after being exposed to a laser fluence of 6 J/cm^2. The wound area in the non-preconditioned site can be seen to be greater than the preconditioned site.

The two graphs representing the growing hair cohort each exposed to 5 and 6 J/cm^2 from the NMRL are shown in Figures 7.10a and 7.10b respectively. At 5 J/cm^2, the

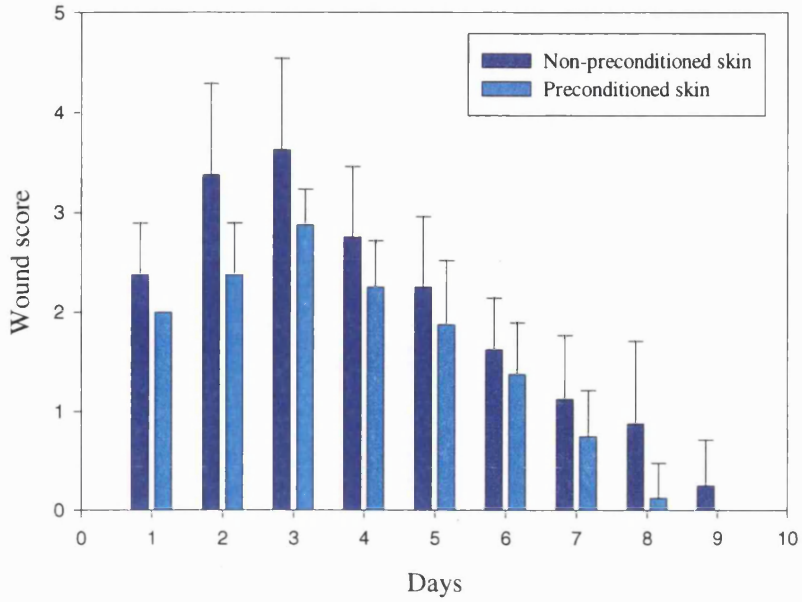

a.

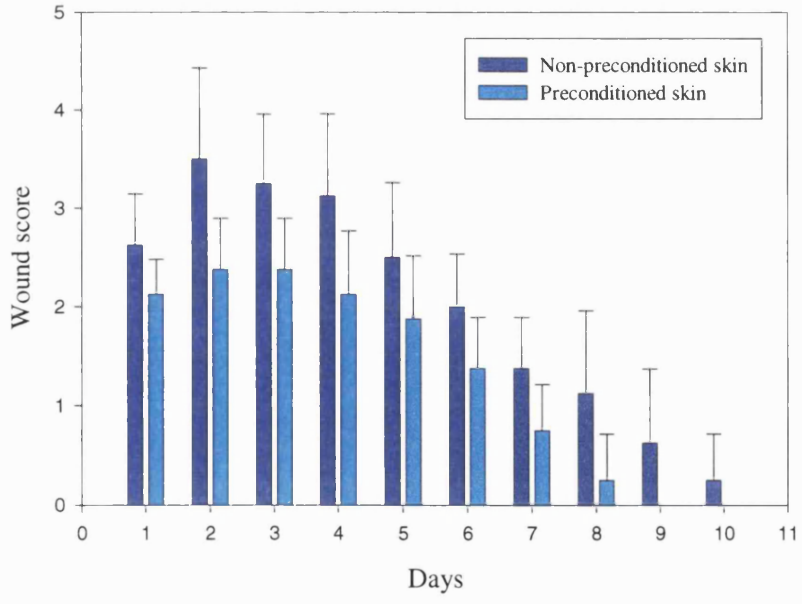

b.

Figure 7.7: Graphs showing the wound scores achieved in preconditioned and non-preconditioned sites in resting hair regions at a) 5 J/cm^2 and b) 6 J/cm^2.

mean wound scores are always less in the preconditioned than the non-preconditioned group but to a lesser extent than the difference observed in resting hair regions (Figure 7.7). However, no statistically significant difference was found in the scores upon each of the days it took for complete healing to occur when a Mann Whitney Rank Sum test upon the median values was performed. These results were repeated when the 6 J/cm^2 group was analysed. This showed that again the mean scores in the preconditioned group were always lower than the non-preconditioned group but statistical analysis revealed no difference between the two groups throughout the time it took to completely heal.

The graph shown in Figure 7.11a shows the mean time in days (+/- standard deviation) that it took for the NMRL-induced skin wounds upon resting hair sites exposed to 5 and 6 J/cm^2 fluence to completely heal. The non-preconditioned sites at 5 J/cm^2 took an average of 8.75 days to heal (S.D. +/- 1.0) whilst the preconditioned sites took an average of 7.87 days (S.D. +/- 0.64). Statistical analysis of these figures showed no significant difference in the times taken to heal between these two groups. The mean time to heal of the non-preconditioned wounds exposed to 6 J/cm^2 was 9.5 days (S.D. +/- 1.2) whilst the preconditioned group was 8 days (S.D. +/- 0.75). Statistical analysis by the Mann Whitney Rank Sum test revealed a significant difference in the median values of the times taken for the wounds to completely heal ($p<0.001$).

The graph shown in Figure 7.11b shows the mean time in days (+/- standard deviation) that it took for the laser-induced skin wounds upon growing hair sites exposed to 5 and 6 J/cm^2 fluence to completely heal. The mean values are less in the preconditioned groups than the non-preconditioned groups at both laser fluences, although to a lesser extent than those values shown in the resting hair cohort. A statistical comparison of the median values by Mann Whitney Rank Sum test revealed no significant difference in the time taken to complete wound healing within the hair growing sites exposed to a laser fluence of either 5 or 6 J/cm^2.

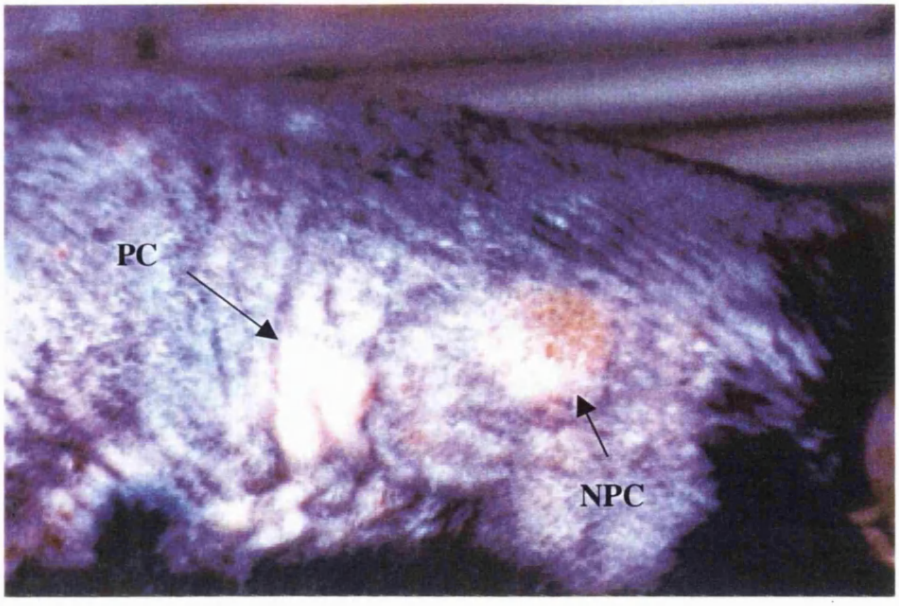

Figure 7.8: Photograph showing a non-preconditioned (NPC) and preconditioned (PC) laser exposed site in a resting hair region 2 days after irradiation at 6 J/cm^2.

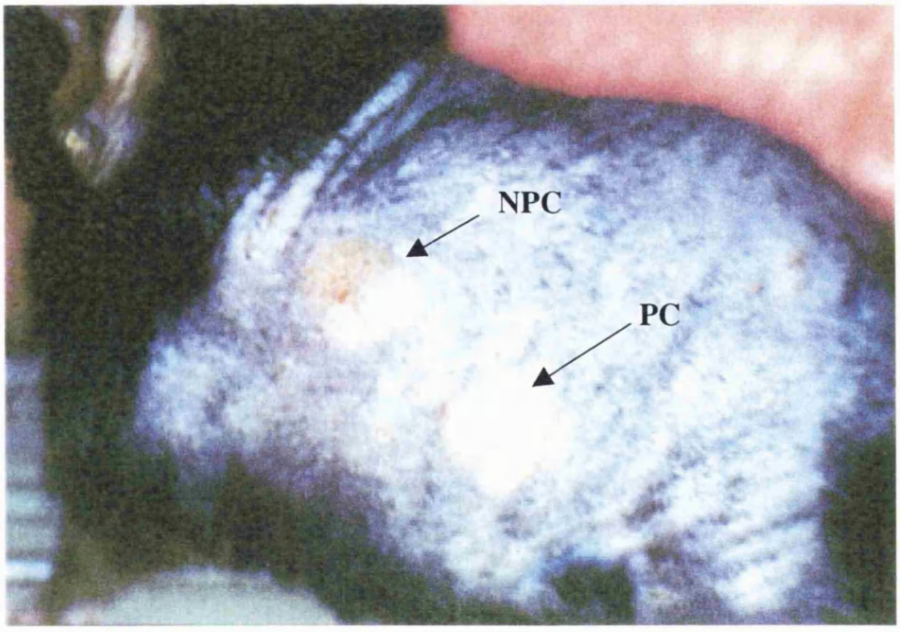

Figure 7.9: A photograph also showing a non-preconditioned (NPC) and preconditioned (PC) laser exposed site in a resting hair region 2 days after irradiation at 6 J/cm^2.

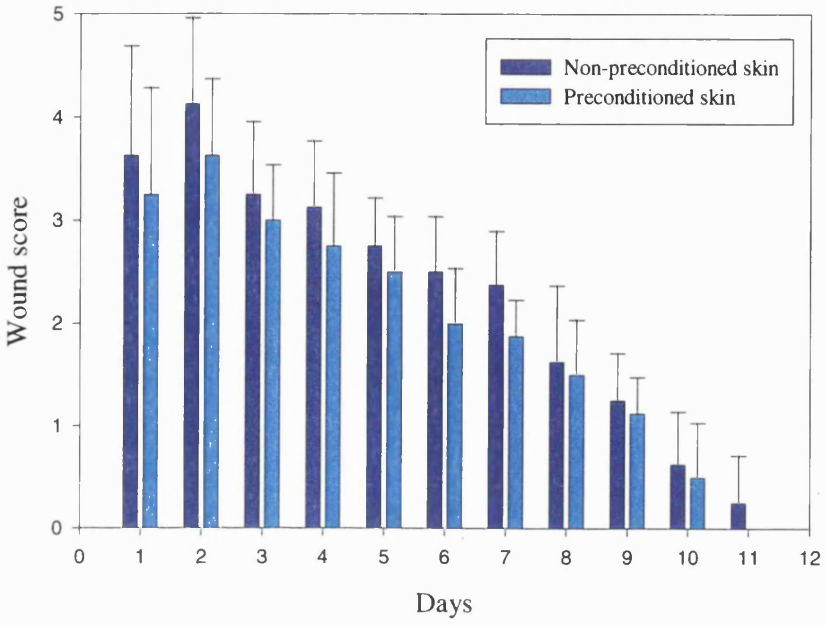

a.

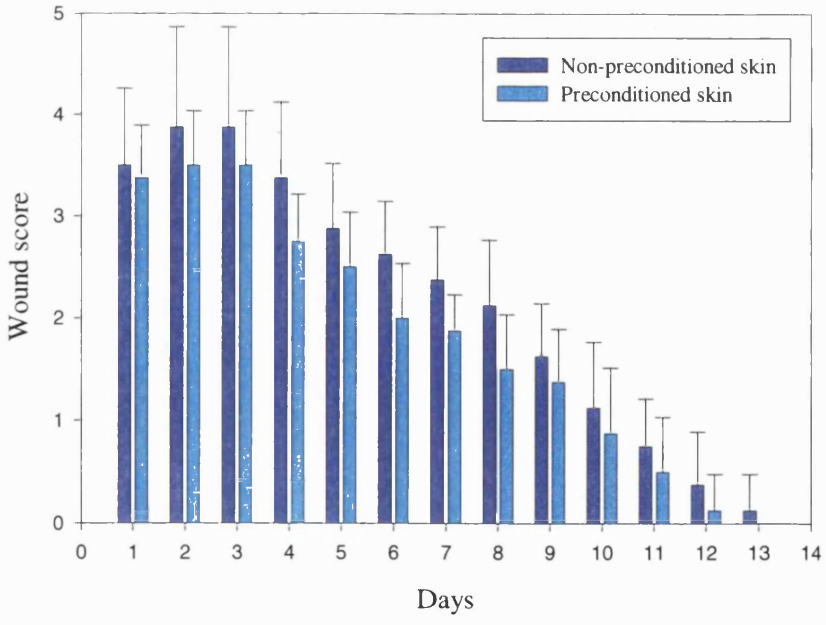

b.

Figure 7.10: Graphs showing the wound scores achieved in preconditioned and non-preconditioned sites in resting hair regions at a) 5 J/cm^2 and b) 6 J/cm^2.

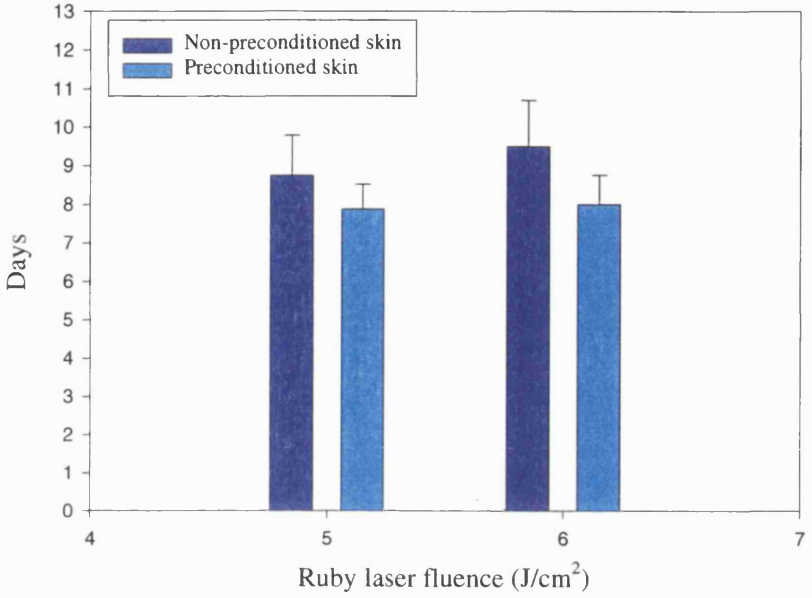

a.

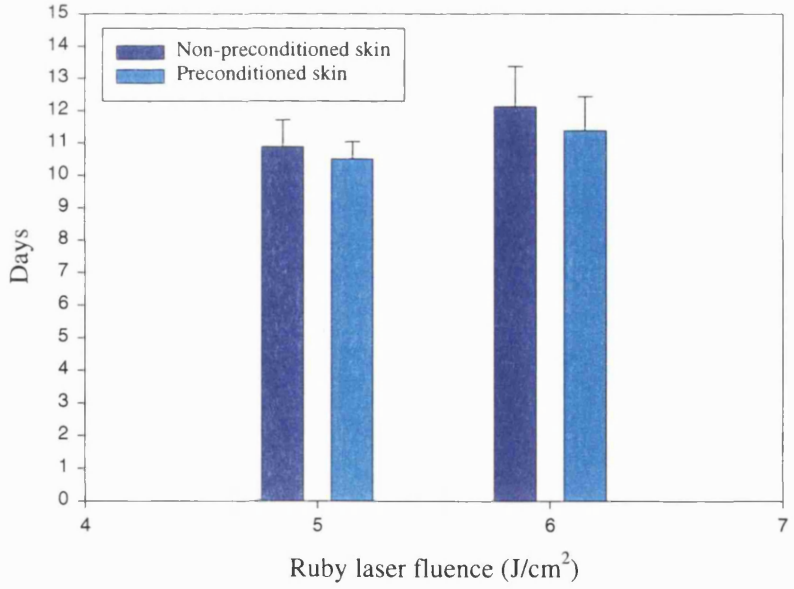

b

Figure 7.11: Mean time in days for the laser induced wounds to heal in preconditioned and non-preconditioned sites a) in resting hair regions and b) in growing hair regions.

Depilation

Figure 7.12a shows a graph of hair regrowth score versus the time in weeks after NMRL exposure in the preconditioned and non-preconditioned sites exposed to a laser fluence of 5 J/cm^2 upon resting hair sites. Immediate hair loss was noted after irradiation upon both preconditioned and non-preconditioned sites comparable to that seen and described previously (see Chapter 4, results section 4.3.1). The hair regrowth that occurred over the ensuing weeks was comparable between the preconditioned and non-preconditioned groups with no statistically significant difference noted in the scores.

Figure 7.12b shows a graph of hair regrowth score in resting hair sites versus the time in weeks after NMRL exposure from the preconditioned and non-preconditioned sites exposed to a laser fluence of 6 J/cm^2. Immediate hair loss occurred after irradiation upon both preconditioned and non-preconditioned sites. The hair then gradually regrew until both groups had achieved full hair regrowth by 5 weeks post-irradiation. No statistically significant difference was noted in the hair regrowth scores from the two groups during the intervening weeks and once again, this was comparable with the scores achieved within the experiment recorded earlier (see Chapter 4).

Figure 7.13a shows a graph of the mean hair regrowth scores achieved in the preconditioned and non-preconditioned groups over the eight week period from growing hair sites irradiated at 5 J/cm^2. Full depilation was achieved immediately after laser exposure in both preconditioned and non-preconditioned groups. No statistically significant difference was noted in the median values of the hair regrowth scores obtained from both preconditioned and non-preconditioned sites by Mann Whitney Rank Sum testing over the eight week period. When the median values from the preconditioned group were compared with those from non-irradiated trimmed controls by the Mann Whitney Rank Sum test, then a statistical difference was noted from weeks 1 to 6 inclusive (cf. Chapter 4).

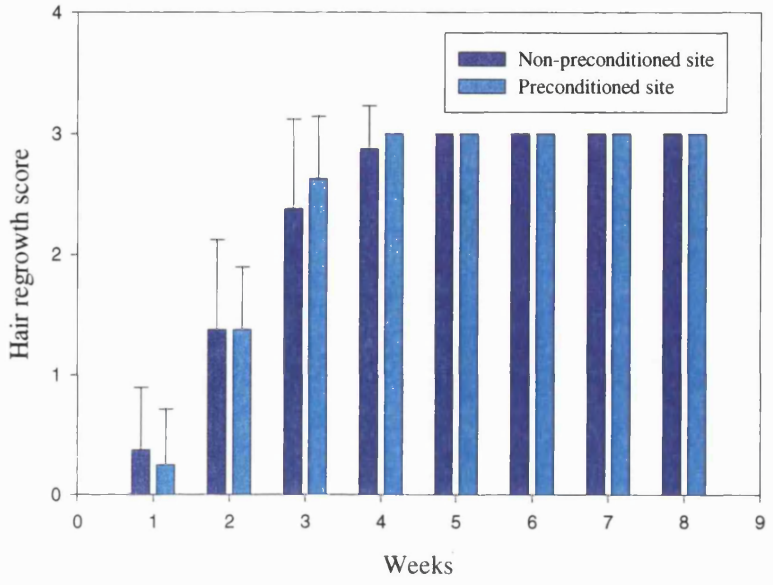

a.

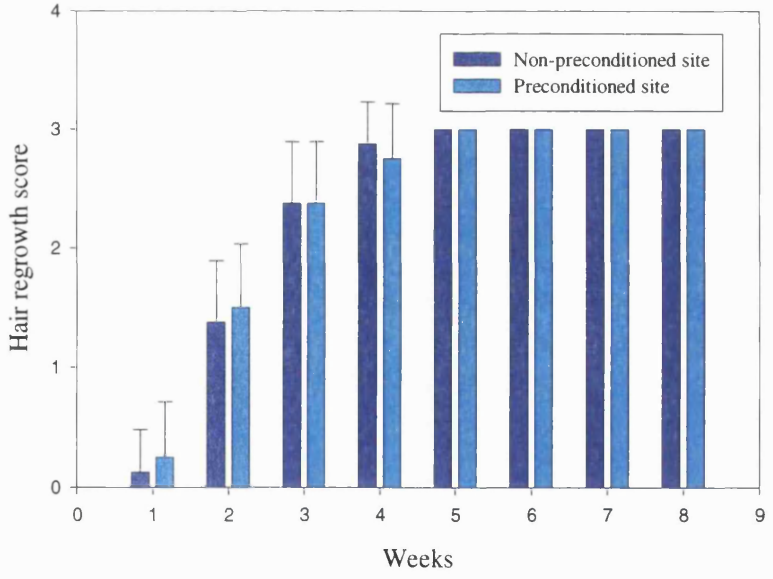

b.

Figure 7.12: Graphs representing the hair regrowth over time in resting hair regions that were either preconditioned or not prior to laser exposure at a) 5 J/cm^2 and b) 6 J/cm^2.

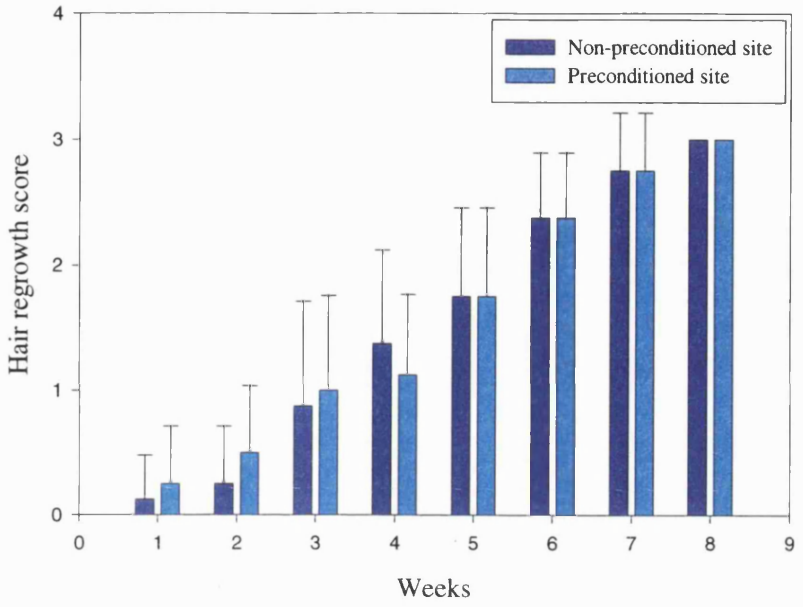

a.

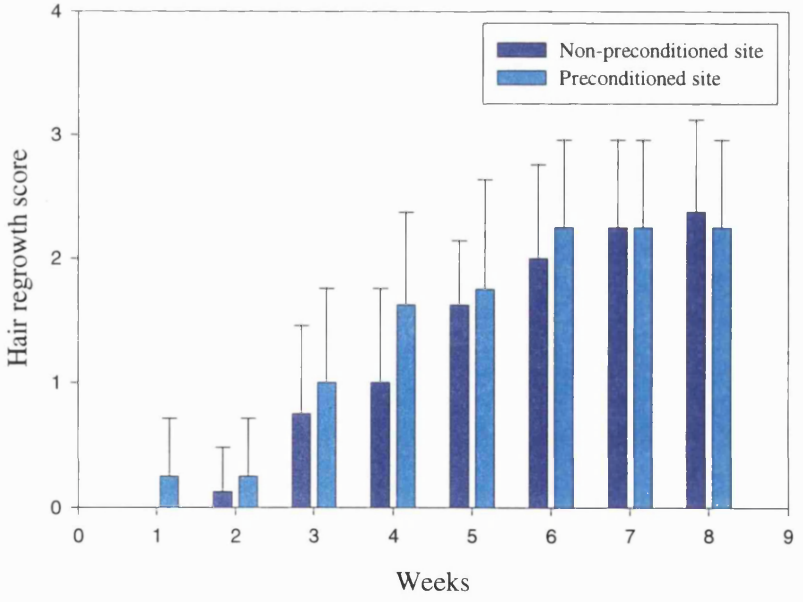

b.

Figure 7.13: Graphs representing the hair regrowth over time in growing hair regions that were either preconditioned or not prior to laser exposure at a) 5 J/cm^2 and b) 6 J/cm^2.

Figure 7.13b shows a graph of the mean hair regrowth scores achieved in the preconditioned and non-preconditioned groups over the eight week period from growing hair sites irradiated at 6 J/cm^2. Full depilation was achieved immediately after laser exposure in both preconditioned and non-preconditioned groups. No statistically significant difference in the median values of the hair regrowth scores was noted between the two groups on Mann Whitney Rank Sum testing during the whole 8 week period. However, a statistically significant difference was noted in hair regrowth when the preconditioned group was compared with non-irradiated shaved controls during the whole of the eight week period, which was again similar to results reported earlier (cf. Chapter 4).

Histological Analysis

Histological assessment was performed upon sections obtained immediately from biopsy sites which had been exposed to NMRL irradiation at either 5 or 6 J/cm^2 fluence on either growing or resting hair sites that had been either preconditioned or not prior to exposure. Those sections that were stained for H&E were assessed for the site and the extent of cellular damage. Figure 7.14a shows a representative section taken from a site exposed to 5 J/cm^2 fluence in a resting hair region whilst 7.14b shows a representative section also taken from a resting hair site exposed to the same laser fluence but preconditioned with heat 5 hours previously. A greater amount of cellular damage was noted within the epidermis of the non-preconditioned section compared to the preconditioned section which would support the clinical findings. Figure 7.15a shows a representative section taken from a growing hair site exposed to 5 J/cm^2 whilst 7.15b shows a similar section preconditioned beforehand. The difference in the amount of histological cellular damage was not as noticeable between these two specimens compared with that seen for resting hair regions. Figure 7.16a shows a representative section taken from a resting hair site exposed to 6 J/cm^2 fluence whilst 7.16b shows a similar representative section that had been preconditioned beforehand. The difference in epidermal cellular damage between the two sections is quite marked with the preconditioned site showing less signs of cellular disruption. Once again, this would support the clinical findings. Little

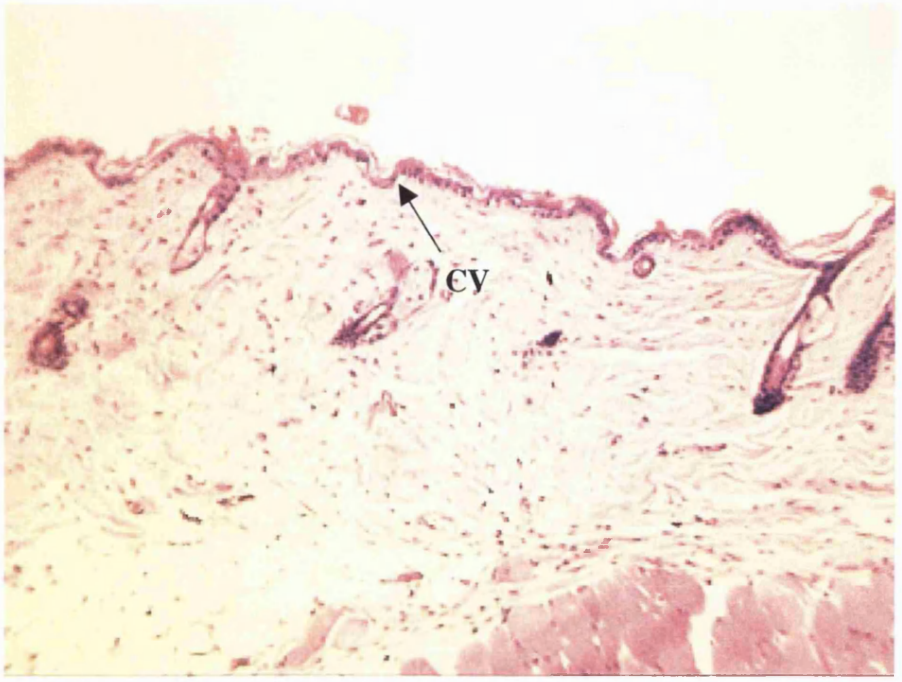

Figure 7.14a: Transverse section through a resting hair region stained with H&E having been exposed to ruby laser irradiation at 5 J/cm^2. Note the extent of the epidermal damage in terms of cell vacuolisation (CV) x100.

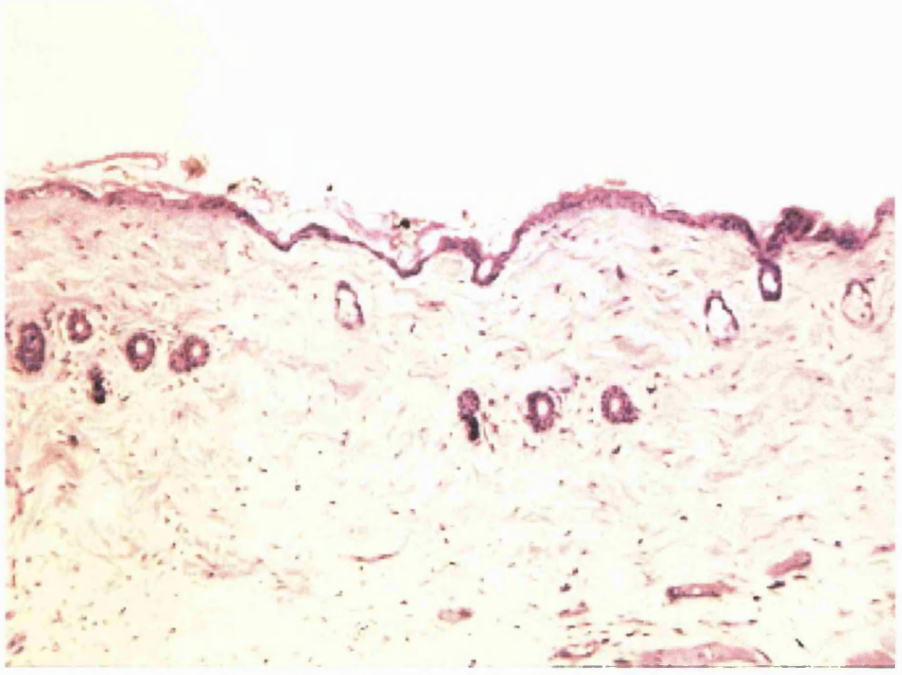

Figure 7.14b: Transverse section through a resting hair region stained with H&E having been preconditioned 5 hours before exposure to ruby laser irradiation at 5 J/cm2. Note decreased epidermal cell damage compared to Figure 8.11a above (x100).

Figure 7.15a: Transverse section through a growing hair region stained with H&E having been exposed to ruby laser irradiation at 5 J/cm^2. Note the increased extent of epidermal damage in terms of cell vacuolisation (CV) compared to the irradiated resting hair region (Figure 8.11a) x100.

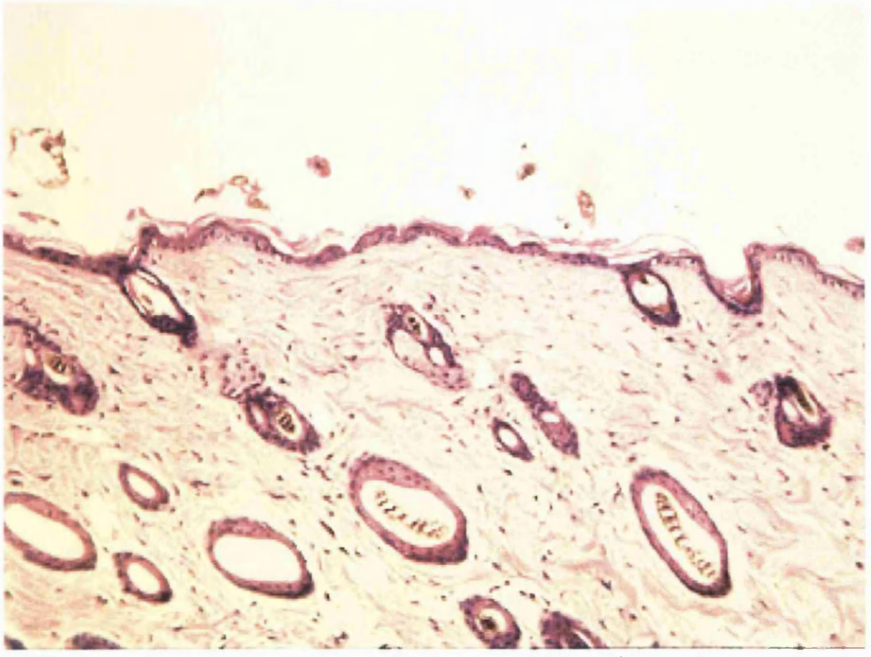

Figure 7.15b: Transverse section through a growing hair region stained with H&E having been preconditioned prior to ruby laser irradiation at 5 J/cm^2. Note the decreased extent of epidermal damage in terms of cell vacuolisation (CV) compared to the irradiated growing hair region above (Figure 8.12a) x100.

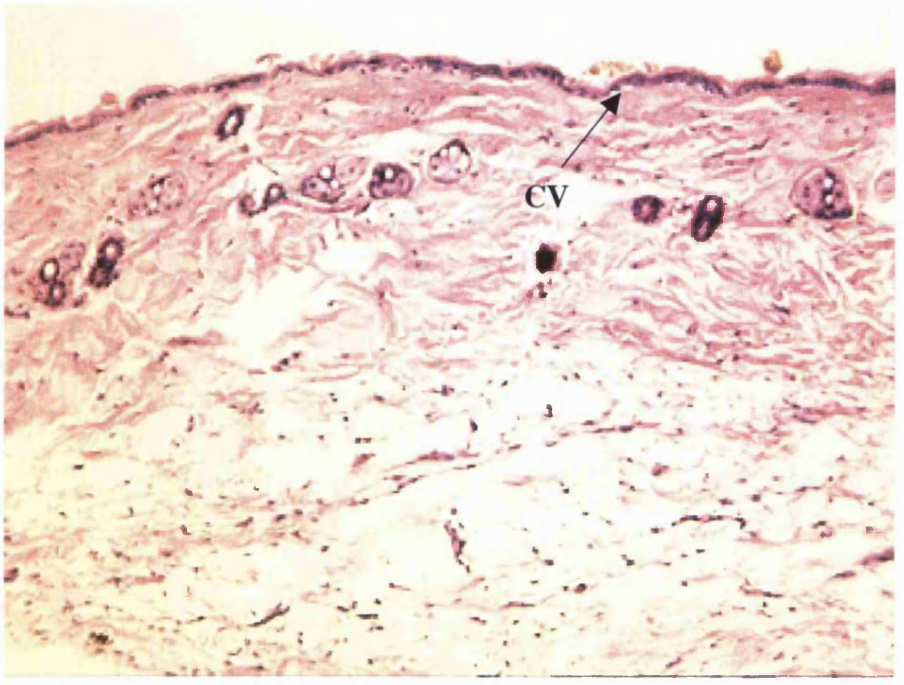

Figure 7.16a: Transverse section through a resting hair region stained with H&E having been exposed to ruby laser irradiation at 6 J/cm^2. Note the extent of the epidermal damage in terms of cell vacuolisation (CV) x100.

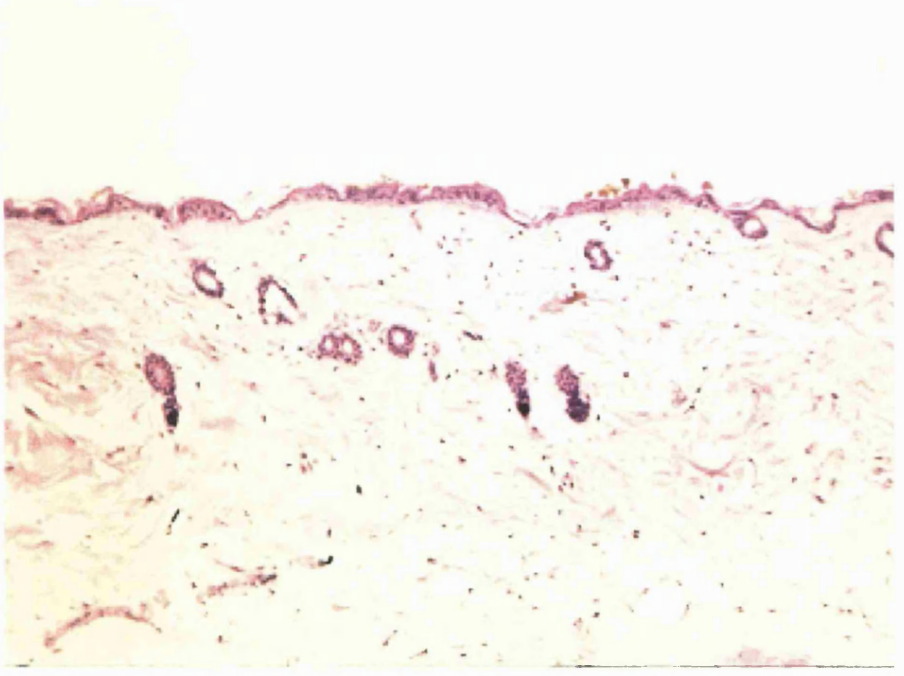

Figure 7.16b: Transverse section through a resting hair region stained with H&E having been preconditioned prior to exposure to ruby laser irradiation at 6 J/cm^2. Note minimal epithelial damage has occurred (x100).

difference was noted histologically in terms of cellular damage and disruption between representative sections taken from growing hair sites exposed to 6 J/cm^2 fluence which were preconditioned and those which were not (not shown) also reflecting the recorded findings.

Histological examination of sections taken from growing and resting hair regions eight weeks after laser exposure were stained with Massons trichrome for any sign of scarring or fibrosis. No evidence was noted of this within the dermis of the mouse skin (not shown), which was consistent with histological findings described in Chapter 4.

7.6 DISCUSSION

7.6.1 Determining the Ideal Temperature at which to Precondition the Skin of the Black-haired Mouse whilst producing Minimal Side Effects

Macroscopic observation of heat preconditioned mouse skin or the trimmed only negative controls showed that the heating process, up to a temperature of 47°C for 15 minutes was not great enough to induce any signs of burn injury. In contrast, however, sections of specimens taken from each of the exposed sites at 5 hours after heating and stained with H&E did show that microscopic cellular damage had occurred at the highest temperature tested. This damage manifested as nuclear degeneration and cellular vacuolisation within the surface epithelial cells ie the epidermal cells. Although the damage was only randomly observed across the exposed site, and was obviously insufficient to cause any obvious clinical signs of damage it would appear that this temperature was too great for preconditioning as it in itself caused damage to the epidermis. The sections taken from the sites exposed to 45°C for 15 minutes revealed little if any cellular damage to the surface.

Immunostaining of the sections for HSP 70 protein revealed minimal constitutive expression within the skin surface epithelial keratinocytes of the negative control specimen at 5 hours. The representative section taken from the site exposed to 45°C

showed an increase in HSP 70 expression to the level of the sebaceous gland but little increase deeper than that. This is important as the bulge region in the mouse resides just below the sebaceous gland which is the site where laser-induced damage might be most required in order to effect permanent depilation. The image shown is that of a resting follicle, but it is important to stress that the bulge region does not change in position throughout the hair cycle whereas the hair bulb does, rising to lie adjacent to the bulge during the catagen and telogen phases. The hair bulb in this image would appear to show minimal signs of preconditioning again confirming the limited depth to which the stimulus from the heating process has extended.

The HSP 70 immunostained sections from specimens exposed to 47°C show a further increase in the quantity of HSP 70 expression within the keratinocytes of the skin surface epithelium. The positive staining is evident within cells extending down into the canal of the hair follicle and deeper than the level of the sebaceous gland. This would imply that preconditioning is also occurring to the cells of the bulge region which would not be desirable as this may reduce the efficacy of the laser where depilation is concerned. The image also shows increased staining within the cells of the hair bulb, which would again confirm the deeper extent to which the heating stimulus has reached.

Observation of the heat preconditioned sites compared with the negative controls examining any difference in hair regrowth patterns or rates revealed no obvious difference between the two groups. This was to be expected as only a deep partial thickness or full thickness burn would induce death within the follicular cells producing a reduced hair density at the heat exposed site. Any less of an injury could well have caused increased hair density resulting from the stimulatory effect of the skin damage which has been well documented (Chase and Montagna, 1951), (Argyris, 1967). The fact that this was not seen would support the histological findings of only minimal skin surface epithelial damage.

The results from this experiment show that the ideal temperature for preconditioning of mouse skin prior to NMRL irradiation is 45°C for 15 minutes. It is this temperature

that is associated with minimal histological cell damage, whilst preconditioning the surface epithelial cells without producing potential protection within the target areas, particularly the bulge region. In addition, no effect was noted on hair growth patterns.

7.6.2 Determining the Consequences of Heat Preconditioning Upon the Effects of Ruby Laser Irradiation of the Skin of the Black-haired Mouse

Skin Damage

The possible mechanisms of laser-induced epidermal damage in the mouse have been discussed in chapter 4, however it is clear that they may not be the same as those in human skin. Summarised briefly, the damage inflicted upon the mouse skin appeared to be from the scattered melanin pigment from the hair shafts acting as a chromophore upon the skin surface since no melanin was detected within the epidermis. In contrast, melanin is present within the basal and suprabasal layers of the epidermis in human skin and is thought to be the source of heat damage associated with laser treatment. It is important to bear this in mind when attempting to assess the wound healing results of this chapter.

Surprisingly, despite an apparent protective effect of heat preconditioning on cultured cells and indeed *ex vivo* skin samples (see chapter 6), in growing hair regions of the mouse model no significant difference in wound scores was detected between the preconditioned and non-preconditioned sites. This suggests that the protective mechanisms of heat shock protein expression, known to be induced in this model by preconditioning (see above section), were overwhelmed by the amount of heat reaching or produced in the epidermis. Whether this would be the case in the human situation cannot be assessed since the anatomical differences between the skin of the two species are large. Compared with humans, excessive heat may reach the viable layers of mouse epidermis due to a number of different factors. Firstly the density of hairs is far greater in mouse skin compared to human skin and also mouse hair contains a much higher concentration of melanin compared even with the most highly pigmented human hair. Finally mouse epidermis is much thinner than that seen in

humans, which may allow an increased proportion of the heat produced at the skin surface to reach the viable layers of the epidermis.

The possibility that the effects of preconditioning would not be overwhelmed when laser-treating human skin may be insinuated from the results found in resting hair regions, where a significant difference was indeed found between preconditioned and non-preconditioned regions when irradiated at 6 J/cm^2, preconditioning being mildly protective. Resting hair regions in mouse skin are more comparable than growing hair regions to the situation found in human skin in some respects: the degree of skin damage is significantly lower in resting hair regions compared to growing hair regions, there is a greatly reduced density of hairs (although the number of follicles per unit area is the same) but it is still higher than that found in human skin and a reduction in hair pigmentation (at least below the skin surface). Notwithstanding these results appear inconclusive due to the unknown mechanisms of epidermal damage within this model.

Depilation

The question of whether preconditioning of skin protects from laser-induced skin side effects is immaterial if the technique reduces the depilatory efficacy. It affect on hair regrowth was therefore assessed. Over an 8 week observational period, no difference in the rates of hair regrowth was noted upon all irradiated sites either preconditioned or not and either within resting hair regions or not. This implied that heat preconditioning did not affect the rate of hair regrowth and confirmed that the protective effect did not reach the progenitor regions of the follicles. This would support the histological findings of minimal HSP 70 production at the sites of the bulge region and the hair bulb.

The results obtained were from sites exposed to a normal ruby laser with set parameters of pulse duration and spot size. It is unknown whether the use of a different laser or even the same laser type but different parameters would have a similar effect. Nevertheless, since the response of cells to increased environmental

stress is generalised and has the ability of protecting that cell against many different types of stresses, then the only way of exceeding the cells protective capabilities would be by increasing the energy delivered to the site. So it should be that an element of protection should be conferred upon the cells regardless of the laser type or parameters used.

As stated earlier, the effect of preconditioning would appear to be overwhelmed, certainly in sites where the melanin and hence the chromophore content was greater. This would imply that preconditioning can only work to a certain extent and that to improve this further may require the addition of other protective modalities presently in clinical use such as application of creams or hydroquinone, cooling devices and the use of the converging sapphire lens. None of these regimes have been assessed in a clinical trial and so their worth at present is unknown but a synergistic effect could be possible between them.

7.7 CONCLUSIONS

- Heat shock protein 70 can be induced in the epidermal cells of mice.

- This can occur at a temperature (45°C) and a time duration (15 minutes) so as to confer protection upon the epidermal cells but not to the cells of the hair follicles where maximum damage is required subsequently (bulge region and bulb).

- Preconditioning of mouse skin using the formula described can protect the epidermal cells from subsequent ruby laser irradiation and does not adversely affect depilatory efficacy.

- Used either alone or in association with other cooling techniques, the role of preconditioning in the human prior to ruby laser irradiation could be beneficial in reducing the skin side effects presently noted.

CHAPTER 8 - DISCUSSION

Clinical trials performed to date have shown that the normal mode ruby laser (NMRL) can successfully remove unwanted hair but the overall efficacy and permanence of the technique remains unclear. The trials themselves have been inconclusive largely due to the differences in both patients and treatment protocols used (see Table 1.1 and 1.2). The time of follow-up was also often short-term and varied between the studies, making comparisons difficult. Nevertheless, it is clear that the technique, as presently used, is not optimally effective for the majority of patients. A contributory factor to this inefficiency is that most patients are sub-optimally treated, where the fluence used is concerned, due to the technique's tendency to cause epidermal damage.

The work in this thesis aims to improve the efficacy of this technique in two ways: firstly by attempting to obtain a better understanding of its mode of action and secondly by determining methods of reducing the severity of epidermal damage produced which would allow the use of higher fluences in clinical practice.

In order to achieve this objective, laser/skin interaction was first assessed using a thermal imaging camera which determined the site, extent and distribution of any heating within *ex vivo* human hair-bearing skin during and after irradiation. Interaction was investigated further by the use of an external energy meter and differing thicknesses of skin, which consequently established penetrative capabilities of NMRL light through human skin. An animal model of laser depilation and epidermal damage was characterised. Two potential skin protective regimes were then assessed; the first used the external application of a chromophore to the skin surface acting as a physical block and the second manipulated the skin's own protective mechanisms.

8.1 RELATING THE SCIENTIFIC EXAMINATION OF LASER-SKIN INTERACTIONS TO THE RESULTS ACHIEVED CLINICALLY

The two experiments reported in Chapter 3 attempted to define the interaction

between the laser and human skin as far as was possible given the resources available. Using the thermal imaging camera, a beam of light from the NMRL was shown to specifically target hair follicles contained within *ex vivo* human hair-bearing skin, manifesting itself by temperature increases within the follicle which then dissipated to the surrounding stroma. In addition, in some hairs the extent of the temperature increase was seen to be great enough to cause protein denaturation and by inference, sufficient to cause lethal damage to cells. Indeed, the laser exposure was clearly seen to cause damage to the hair shafts and to the surrounding follicular cells, as shown by modified SACPIC staining and p53 expression respectively. The depth at which damage was detected by the two stains was found to correlate well and appeared to be directly associated with the peak temperatures achieved by the follicles within the patient specimens reaching the bulge region in most and the hair bulb in some follicles. When peak temperatures were compared between patient specimens, a significant difference was noted between them suggesting that this was a property individual to each patient. Heterogeneous temperature rises also occurred between follicles within the same treatment site suggesting that the characteristics of each hair follicle which determined the heat production varied between follicles within the same patient. By contrast, the mean rate of follicular heat loss for each of the patient specimens was comparatively similar, confirmed by analysing the time taken for the follicles to lose half the peak temperature (T50). This implied that peak follicular temperature was the important factor associated with increased follicular cell damage and potentially permanent depilation, rather than the rate of heat loss. These results suggest that the heat produced and therefore potentially the susceptibility to destruction by laser depilation varies between the hair follicles within the same piece of skin and also between patients. This would explain the partial efficacy of this technique seen for most patients and the differences in the degree of efficacy seen between patients.

The use of an external energy meter revealed that a beam of photon energy from a ruby laser penetrated *ex vivo* skin to a mean depth of 14.8 mm (+/- 0.478 mm) which was considerably greater than had previously been theorised excepting one study which used a phantom skin model. These findings appeared to confirm that maximum

depth of skin penetration was not fluence dependent. However, increasing fluence levels did increase the proportion of energy present throughout the penetration depth, particularly at the depths where damage was required to cause permanent depilation, namely the bulge region and the bulb. In addition, the energy at these sites was approximately half that of the original incident fluence, because greatest energy loss occurred within the first millimetre of skin. Whether the energy reaching these sites is sufficient to cause permanent cellular damage is unknown.

Neither of the experiments described above answered whether heat is produced locally within the subcutaneous hair shaft and follicle or whether it is confined to the external hair shaft alone and is then conducted down the hair shaft into the follicle. Clarification of this question is important for the future improvement of treatment strategies and lasers themselves.

Further work using a laser with variable fluence and pulse duration would be interesting to see whether either of these factors could affect heat production and cellular damage obtained. In addition, calorimetric analysis of the hairs taken from patients whose specimens would be irradiated could also help clarify whether the combustive qualities of the hair shafts influenced peak temperature achieved, or whether, as has been suggested before, this is simply related to the amount and type of melanin present.

8.2 CHOICE OF MODELS TO INVESTIGATE RUBY LASER-ASSISTED DEPILATION

Chapter 4 detailed experiments discerning how well the black-haired mouse responded to ruby laser irradiation in terms of both depilation and the skin side effects produced. In order to establish ways of protecting skin, it is first important to discover the treatment levels that best mimic the clinical situation in terms of producing both successful depilation and clinical side effects. These fluence values were ascertained within this chapter, but it became apparent that the ruby laser was only able to effectively depilate hairs that were actively growing and not those in the resting phase

within this model. This finding confirmed that reported by Lin et al who suggested that growth phase played an integral part in depilatory success, however, this may not be the case in humans. In the mouse, melanin is concentrated throughout the hair shaft of follicles which are in anagen, but only in the shaft external to the follicular canal in telogen hair. This situation does not occur in humans, where pigmentation of the hair shaft remains constant irrespective of which phase the hair is in. Therefore, examination of depilation within the mouse model should be restricted to growing hair regions.

The acceptibility of the mouse as a model of NMRL-induced epidermal damage, however, is questionable. It is proposed that the skin damage induced in the black-haired mouse following NMRL exposure occurred in a manner different than that seen in humans. It appeared that melanin had been scattered over the skin surface during laser irradiation and it was these melanin fragments which may have acted as chromophore to produce the damage to the comparatively delicate epidermis.

8.3 CHROMOPHORE BLOCKS AND THEIR ROLE IN SKIN PROTECTION

In a search to find the colour which might best protect skin by reflecting the beam of the ruby laser, black ink was chosen as it was discovered that this chromophore most reduced the energy penetration from the NMRL in a simple, non-biological model. This chromophore was further found to induce a protective effect when painted upon *ex vivo* human skin that was subsequently irradiated and stained for cellular damage using the p53 antibody detection kit. There was reduced cell damage at the basal layers after laser exposure when compared to non-painted, irradiated controls. It therefore seemed that although a large quantity of heat was probably produced at the skin surface, enough had been safely dissipated before it reached the viable stem cells within the basal layer thus reducing the amount of damage to these cells. This could in theory mean that human skin would be protected from ruby laser-induced side effects by prior painting with black ink. This experiment was performed using non-hair bearing skin, so the effect of increased melanin within the skin from hair shafts could not be ascertained. In addition, the effect upon depilation could not be established in

this system. It is possible that by preventing passage of the laser beam through the skin, then this could adversely affect the efficacy. Consequently, it was decided to examine the effect of painting the skin with chromophore on the laser/skin penetration profile of differing thicknesses of skin. This revealed a reduction in the light penetration profile amounting to approximately half that for the same incident fluence without added chromophore. This suggested that if the depilatory pathway was directly through skin, then efficacy would more than likely be reduced.

In an attempt to establish both the protective and the depilatory effects of chromophore added to the skin prior to ruby laser exposure, the black-haired mouse animal model was incorporated into the study. Two fluences that were both shown in chapter 4 to induce successful depilation and skin side effects were used and animals were irradiated upon growing and resting hair regions. The results of the resting hair regions were initially surprising showing greater epidermal damage and slightly increased depilatory efficacy in the regions which had been painted with black ink compared to those not painted. In growing hair regions, no significant difference was noted in the depilation and skin side effects produced in painted and non-painted areas. The explanation for the increased damage seen within painted resting hair regions could be accounted for by the fact that the greater quantity of heat produced by the added chromophore was not safely dissipated, as in human skin, before it reached the viable layers of mouse skin due to it being comparatively delicate and thin. Why the growing hair regions did not show a similar statistically significant difference in skin damage as the resting hair region cannot be answered, but it could either reflect potential inaccuracies of the scoring system, or numbers used in the study were too small. Nevertheless, the damage seen in growing areas with or without prior painting was similar in extent to that seen in painted resting regions. This observation may suggest that the amount of damage seen is already maximal in the growing regions due to the greater density of pigmented hairs present, which are thought to cause epidermal damage by fragmenting during the laser pulse and covering the skin surface. The amount of damage seen in the resting regions is presumably less due to the reduced size and hence melanin content of the hairs present.

Importantly, depilation appeared not to be affected by the addition of chromophore to the skin surface. Again, whether this can be related to the human situation, where the skin is much thicker by comparison, is questionable but it does suggest that adding chromophore to the skin surface may not reduce depilatory efficacy.

Further studies of interest would be to perform a clinical trial using black ink painted upon the skin surface to establish whether an improvement in the skin side effects occurs after ruby laser exposure and whether this affects depilatory success. One potential practical problem to the use of the chromophore upon skin is the fact that a large plume of smoke is produced after irradiation which dirties the handpiece and makes regular cleaning important to maintain the correct fluence delivery.

8.4 HEAT PRETREATMENT AND ITS ROLE IN SKIN PROTECTION

It was mentioned in Chapter 1 that various authors have established pretreatment of living tissues with a non-lethal noxious stimulus as a way of potentially reducing cell damage and death within that tissue from a subsequent lethal stimulus. Heat was chosen as the simplest method of preconditioning to assess. First of all the required temperature associated with maximal preconditioning and minimal cell death was established for two of the major cell types in skin, keratinocytes and fibroblasts. The experimental work did show that a differential rate of cell death was present between the two cell types such that keratinocytes could withstand greater temperatures than fibroblasts. This most likely reflected the evolutionary role for which keratinocytes have developed namely to withstand wide variations in the temperature of the external milieu. Further to this, successful preconditioning was detected by an increase in cellular Heat Shock Protein 70 expression. This was established by Western Blotting which showed that the temperature best suited for preconditioning keratinocytes, assessed by the greater quantity of HSP 70 expression, was 45°C for 15 minutes and that the time gap between pretreatment and exposure could be either 5 or 24 hours, as a similar amount of HSP 70 expression occurred at both times.

The damaging effects of NMRL irradiation was assessed simply upon cultured keratinocytes and found not to cause any discernable damage or cell death. An *in vitro* model was therefore established which would help assess whether heat pretreatment of cultured human keratinocytes could increase the survival rate after laser exposure when compared to non-pretreated keratinocytes. Since keratinocyte culture contains little if any natural melanin, initial experiments found that addition of chromophore to the culture media required in order to see keratinocyte damage and killing by NMRL irradiation (see Appendices).

This model was used to discover whether heat preconditioning could protect cultured keratinocytes against ruby laser irradiation *in vitro*. The results showed that a significant decrease in cell death occurred when the heat preconditioned group was compared to non-preconditioned controls. This implied that heat preconditioning could be effective under clinical circumstances and should be further investigated within the animal model. The experiment also showed that staining for increased HSP 70 expression within keratinocyte cells could be used as a marker for successful preconditioning.

To establish whether HSP 70 could be induced within cells of the whole tissue, samples were taken of normal human skin which were then exposed to heat at varying temperatures before being cultured in media for 5 hours and fixing in formal saline. Increased expression of HSP 70 was noted within the keratinocytes of the specimens which suggested that the epidermis of human skin could also be successfully preconditioned.

Having established an *in vitro* proof of principle regarding the positive protective effect of cellular preconditioning, it was important to discover whether the same circumstance existed in an *in vivo* model. However, as with the cellular model, it was necessary to determine the correct temperature associated with successful preconditioning whilst inducing minimal, if any, skin side effects. In addition, in the animal model it was also important to ensure that preconditioning occurred only to those cells which required protection, namely the epidermal keratinocytes, whilst not

protecting those cells which require damaging, namely the stem cells of the bulge region and the hair bulb. To do this, mice were exposed to heat at varying temperatures, the treatment sites biopsied after 5 hours and stained for HSP 70 expression. The site and extent of HSP 70 expression was analysed and the temperature associated with maximal expression in epidermal cells alone was noted. Other sections taken were stained with haematoxylin and eosin for signs of cellular damage. This established a temperature of 45°C for 15 minutes as being most likely to induce a successful preconditioning response without causing obvious damage to the skin surface.

Heat preconditioning the skin in resting hair regions of the black-haired mouse significantly decreased skin damage as evidenced by a decrease in mean time of the laser exposed sites to fully heal and supported histologically by a decrease in cellular damage noted. This occurred only at a fluence of 6 J/cm^2, not at 5 J/cm^2 and was not noted in the growing hair regions. Why this difference was present cannot be answered. One possible reason could be that a greater quantity of chromophore is present in the growing hair regions producing an amount of heat too great for the preconditioning response to protect against. Conversely, the fluence of 5 J/cm^2 was too low to produce a noticeable difference in skin damage. It could also be that the numbers used were too small in these groups to establish a statistically significant difference. Just as important was the finding that preconditioning did not affect the success of depilation. This appeared to show that given the correct temperature and duration of pretreatment, skin protection could occur without losing depilatory efficacy.

Future work in this area could apply these results to a clinical trial with the aim of assessing the role of preconditioning upon skin protection from subsequent laser exposure. It would be necessary to establish a temperature tolerated by the patient but which would be adequate to induce cellular protection first before laser treatment. The practicality of the procedure should be simple in the sense that it would need a heating plate to be placed over the site to be treated at least 5 hours and even possibly up to 24 hours before irradiation. Both skin damage and depilation would then be assessed

over time in a manner similar to that described in Chapter 7. In addition, it could be anticipated that all laser types could be protected against using the method described here as their mode of actions are similar.

8.5 THE FUTURE OF LASER-ASSISTED DEPILATION

Laser-assisted depilation has now entered the list of treatments for hirsutism and can produce permanent hair loss. It is more convenient than the only other method of permanent depilation, namely electrolysis, by having the ability to treat large areas of skin with immediate results. However, at present it is probably too fixed a modality, in terms of wavelength and pulse duration available to be able to successfully treat the large variety of hair types that exist upon human, particularly caucasian, skin. Nevertheless, the treatment does result in patient satisfaction which is a key factor in successful treatment. It may be that adding chromophore to the skin surface or heat preconditioning can benefit those individuals who suffer side effects as a result of laser exposure and hence may allow the use of higher fluences and thus increase the efficacy of treatment. It may also be that by changing the laser parameters according to hair and skin type can change the interaction of the laser with skin increasing the efficacy and reducing the side effects. Newer models of laser have now been developed able to emit variable wavelengths and pulse durations of laser light and the results are eagerly anticipated. Laser-assisted depilation is now an integral part of the management of hirsutism and it is felt will continue to develop to benefit the patient.

APPENDICES

The following appendices present pilot studies aimed at establishing a simple *in vitro* model of the laser-depilation-associated side effect of epidermal damage. This model could then be used to perform preliminary assessments of potentially protective pre-treatments (see Chapter 6).

Appendix A

Establishing the Correct Seeding Density of Keratinocytes Required for the *In vitro* Model of Epidermal Damage

The experiments detailed in appendices B, C and Chapter 6 require a simple model of the epidermis *in vitro*, such as cultured keratinocytes. The most widely used method of culturing keratinocytes (Rheinwald and Green, 1975) involves seeding the cells at relatively low densities and allowing them to proliferate over time to give sufficient cell numbers for experimentation. However, the behaviour of keratinocytes in this culture system creates potential problems, with the cells not only proliferating but also differentiating with time to form multilayered, stratified sheets of epithelium which closely mimic the epidermis *in vivo*. This structure complicates both the experimental design and the interpretation of results where the experiments planned in this thesis are concerned. The reasons for this are two-fold; first of all any viability study would be complicated by the presence of differentiated cells (as these are undergoing a form of programmed cell death) and secondly, since the viable progenitor cells in this system are sandwiched between the plastic and multiple layers of differentiating cells, they may not be affected by any additions to the media (the importance of which will become clear in Appendix C).

A potential way to remove the complications of differentiation would be to culture the cells in low calcium media which results in the growth of a relatively undifferentiated monolayer of cells. This possibility was, however, rejected since the relatively ubiquitous role of calcium in many cellular functions may adversely affect the results.

An alternative method of producing an undifferentiated monolayer of keratinocytes is to seed them at very high densities (enough to produce near confluency upon their adhesion and spreading on the culture dish surface) and to use them within 48 hours before significant differentiation could occur. This appendix therefore relates the establishment of the correct seeding density required to achieve an approximately 70% confluent monolayer in 24 to 48 hours.

Methods

A single cryovial of keratinocytes (P0) was recovered from frozen stocks and seeded into three T75 flasks. When 70 to 80% confluent, the flasks were triturated to remove the 3T3 feeder cells (see section 2.2.1), the keratinocytes were trypsinised, counted and seeded into the wells of a 48 well plate at a range of densities, in triplicate. These densities were 5×10^3, 1×10^4, 2×10^4, 3×10^4, 4×10^4 and 5×10^4 cells per well, with 0.5 ml of medium in each well. This procedure was repeated using three different strains of P0 keratinocytes.

Results and Discussion

The wells were examined using phase contrast microscopy at 24 and 48 hours after seeding. A seeding density of 3×10^4 keratinocyte cells per well of a 48 well plate gave rise to a monolayer of keratinocytes which were approximately 70% confluent, with little evidence of stratification at both the 24 and 48 hour time points. This seeding density was consequently used for further experimentation.

Appendix B

Does Laser Treatment of the *In vitro* Model Cause Similar Levels of Cell Damage and Death to That Seen *In vivo*?

In order to examine the potential protective effects of any pre-treatment in an *in vivo* model, it first had to be established whether laser treatment of the *in vitro* model mimicked the skin damage seen clinically. A pilot study was therefore performed to discover if ruby laser could induce cell death in a cultured keratinocyte population within the wells of a 48 well plate. An important point to take into account is that these cultured cells contain little if any melanin (the laser's chromophore) which they obtain *in vivo* from melanosomes donated by surrounding melanocytes. Nevertheless, it is possible that the pigmented flavoproteins within the mitochondria of the cells can act as a chromophore when exposed to ruby laser irradiation and thus lead to cell damage (Cheng and Packer, 1979). If cell damage and death did not occur in this model then the addition of the natural chromophore (melanin) to the wells might be necessary to induce cell death and thus mirror the clinical situation.

Methods

Alternate wells of two 48 well plates were filled with a 10% solution of agar containing India ink and 0.02% sodium azide (Figure B.1). This black gel would serve as a "barrier chromophore" preventing the reflection of laser light from one well to its neighbours upon exposure. Keratinocytes were seeded into the gel-free wells of the 48 well plates at the appropriate density (3×10^4 cells/0.5 ml/well - see appendix A). One additional plate acted as a control and this had two rows of three wells seeded with cells. The remaining two plates were experimental and had three alternate wells in each of four rows seeded with cells. Each row represented a triplicate set of wells to be used for a single fluence level, in a range of 0.6 to 3.2 J/cm^2 (see Figure B.1). The plates were placed in the incubator for 24 hours after seeding and then had the media changed for fresh KCM to remove any non-adherent cells before being replaced in the incubator for a further 24 hours prior to experimentation.

The experiment began by performing a cell viability count using the trypan blue viability test (see section 2.2.1) upon the first row of three wells in the control plate. These counts are designated Time 0 counts. The experimental plates were then removed in turn from the incubator and placed, one at a time, into the Class II hood. The media was removed from the first set of three wells and those wells then exposed to a single pulse of 0.6 J/cm^2 from the ruby laser*. The media was then replaced and this procedure was repeated for each successive set of three wells using exposures of progressively higher fluences as detailed in Figure B.1. The control plates were removed from the incubator and the remaining set of 3 wells were exposed to air for the same duration as the wells in the experimental plates had been during laser irradiation. These wells were designated 0 J/cm^2. The media was then replaced and these plates returned to the incubator.

A cell viability count was performed after 24 hours had elapsed for all the control and experimental wells using the trypan blue viability test (see section 2.2.1).

Results

The mean total viable cells (+/- standard deviation) was calculated for each of the set of three wells in the control and experimental plates and plotted as a bar graph (see Figure B.2). A Student's t-test revealed no statistically significant difference in the median values between the control wells at Time 0 and those at 0 J/cm^2. When the experimental groups were analysed statistically using a one way ANOVA method, the results showed that no statistically significant difference existed in the mean number of viable cells within the wells exposed to different fluences and either of the control well sets.

A 48 well plate is approximately 10 mm in diameter but the spot size of the ruby laser used was only 7 mm. To ensure that the whole well base was exposed to the laser meant increasing the distance of the hand piece from the well base, which in turn would increase the spot size to 10 mm. This distance was maintained throughout this experiment and all subsequent experiments where the ruby laser was used on cultured cells in a 48 well plate. Although a lower fluence (J/cm^2) was produced in the target area because of the increased spot size, it could be calculated using the formula shown in section 2.1.6. Ruby laser exposure of the wells took place on a piece of black paper to minimise the reflection of the beam from the metal surface of the hood.

Figure B.1: Diagrammatic representation of the second pilot study (see Appendix B) to determine the ruby laser fluence required to induce keratinocyte cell death.

Control plate

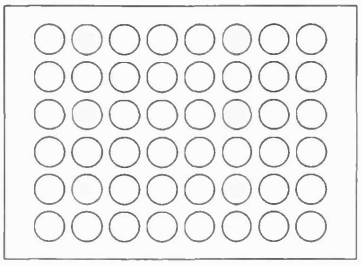

Key

○ Wells containing keratinocytes

● Wells containing ink in agar

Note the numbers represent the fluence values in J/cm^2

Experimental plates

0.6 1.0 1.4 1.7

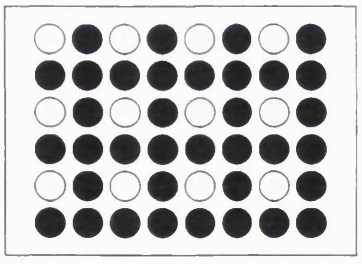

2.1 2.4 2.9 3.2

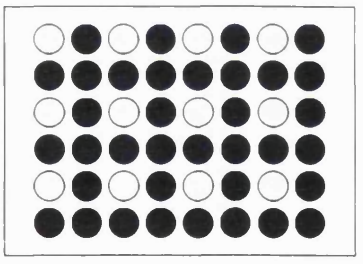

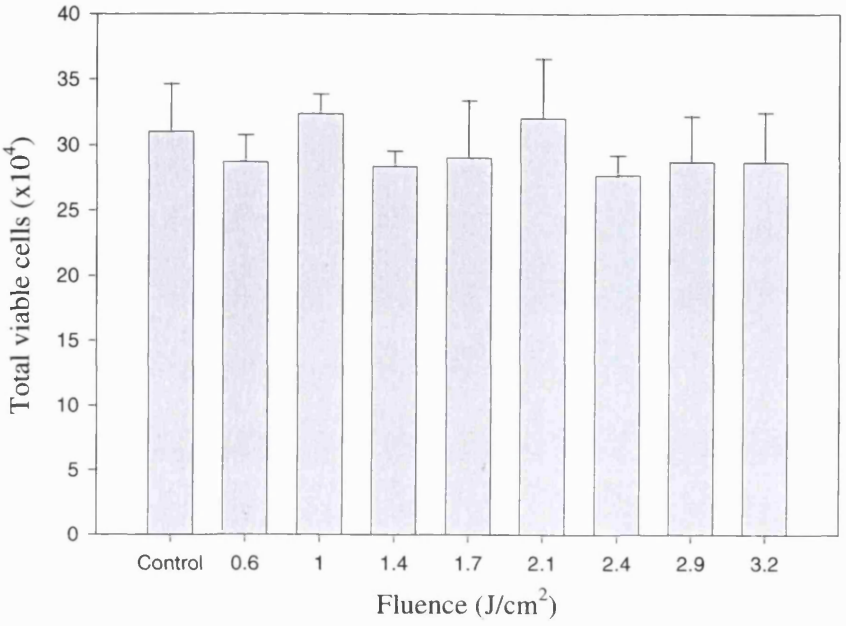

Figure B.2: Graph representing the cell death of cultured human keratinocytes after exposure to ruby laser irradiation at a range of fluences (see Appendix B).

Discussion

No statistically significant difference in cell viability was seen between the two sets of controls used within this experiment. This would appear to imply that exposure to air for the same duration as the experimental wells did not decrease the cell viability within those wells. Consequently it would appear likely that any decrease in cell viability within the experimental wells would be as a result of ruby laser exposure.

No statistically significant difference in cell viability was noticed between all the experimental wells and the control wells. This would suggest that the cultured human keratinocytes were not sufficiently damaged by ruby laser irradiation under the experimental conditions used to induce cell death.

The results would appear to confirm a requirement for a chromophore within or adjacent to the keratinocytes if ruby laser induced cell death is to occur to cultured human keratinocyte cells. The chromophore should preferably be inert, non-toxic and as close to the normal physiological chromophore as possible so as to mimic the *in vivo* situation as closely as possible.

Appendix C

The Effects of the Addition of Synthetic Melanin to the *In vitro* Model

The pigment chosen to act as a chromophore within keratinocyte cultures was synthetic melanin (supplied by Sigma Ltd.). Working concentrations of 100 μg/ml and 200 μg/ml were used which was approximately compatible with physiological levels (Menon, et al., 1985). Work by Dr C Linge (personal communication) has shown that keratinocytes readily phagocytose melanin placed in the culture medium within 24 hours, thus mimicking the *in vivo* situation.

Methods

A sterile synthetic melanin concentrate was therefore produced by adding 40 mg of melanin to 20 ml PBS and autoclaving at 120°C, 2 atmospheres pressure for 30. This was then diluted with KCM as appropriate.

Keratinocytes were seeded into five, 48 well plates at 3 x 10^4 cells/0.5 ml/well with one of the plates as the control, shown in Figure C.1. The plates were then incubated for 24 hours to allow the keratinocytes to attach and spread. The media within the wells was then removed and replaced with either KCM alone or KCM containing a 100 μg/ml or a 200 μg/ml solution of melanin as depicted in Figure C.1. The experimental plates were set out in the same format as the experiments described in Appendix B. All plates were returned to the incubator for 24 hours.

A cell viability test was then performed upon the first set of each of the three paired sets in the control plate using trypan blue (see section 2.2.1), which are designated as Time 0 counts. Each set of triplicate wells in the experimental plates was then exposed to the fluence levels depicted (see Figure C.1). The media was removed prior to irradiation, but the cells were not washed in order to keep the chromophore in-situ. The control wells were then exposed to air for the same time duration as the experimental wells had been. All plates were returned to the incubator and a cell viability test was performed upon all wells after a further 24 hours.

Figure C.1: Diagrammatic representation of the third pilot study (see Appendix C) to discover the effect of varying concentrations of melanin and ruby laser irradiation upon cultured human keratinocytes.

Control plate

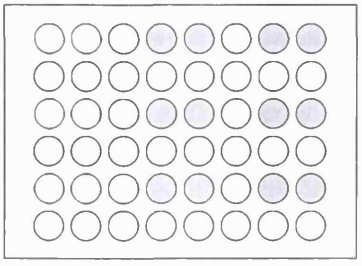

Key

- Wells containing ink in agar
- Wells containing KCM alone
- Wells containing 100 μg/ml melanin
- Wells containing 200 μg/ml melanin

Experimental plates

100 μg/ml melanin

0.6 1.0 1.4 1.7

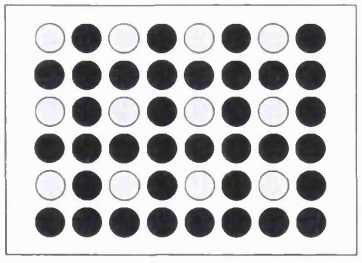

2.1 2.4 2.9 3.2

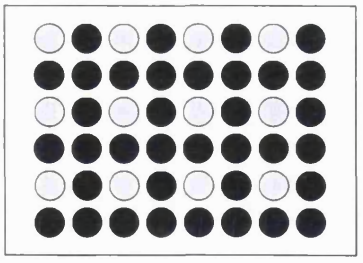

200 μg/ml melanin

0.6 1.0 1.4 1.7

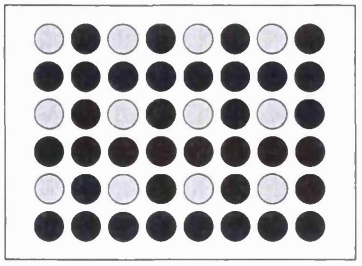

2.1 2.4 2.9 3.2

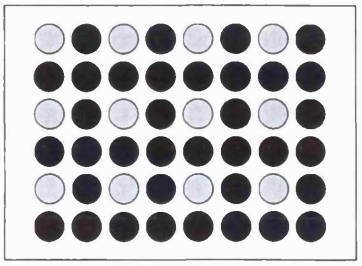

Note the numbers used represent the fluence value in J/cm^2.

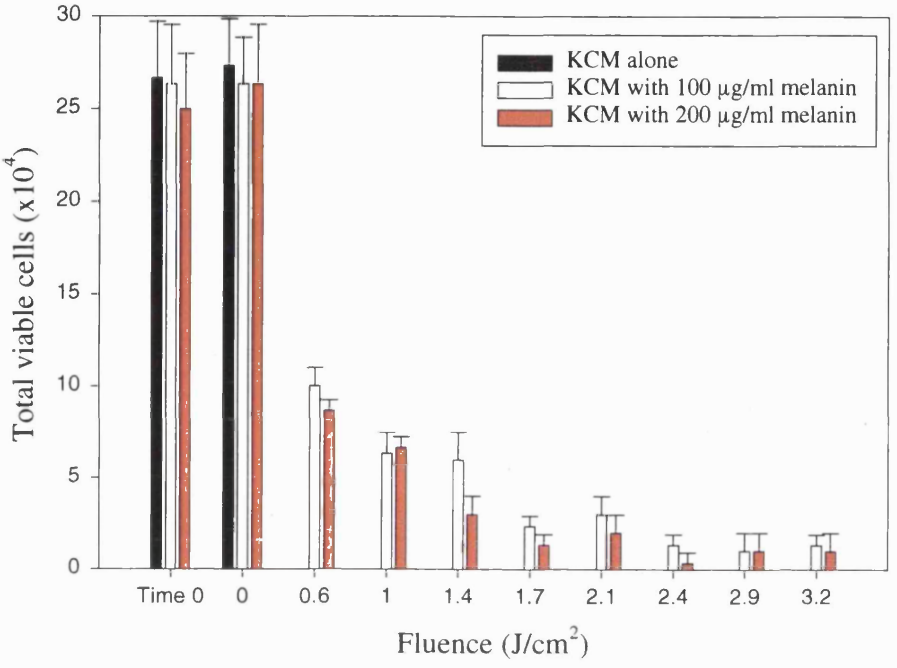

Figure C.2: Graph representing the cell death of cultured human keratinocytes with the addition of two concentrations of synthetic melanin after exposure to ruby laser irradiation at a range of fluences.

Results

The mean total number of viable cells (+/- standard deviation) of the controls and of the two melanin concentration groups exposed to different laser fluences were plotted (see Figure C.2). Statistical analysis of the results from the control wells at Time 0 by one way ANOVA showed no significant difference in cell viability between the wells containing KCM alone and those containing synthetic melanin at either concentration (100 μg/ml and 200 μg/ml). A comparison of the mean cell viability of the control wells at Time 0 and 0 J/cm^2 by one way ANOVA again revealed no statistically significant difference.

For both the 100 and 200 μg/ml melanin concentration groups, a large, significant drop in keratinocyte cell viability was noticed between the groups exposed to the lowest (0.6 J/cm^2) fluence of ruby laser and the respective control wells at 0 J/cm^2 (Student's t-test, $p<0.001$). Further statistical analysis by one way ANOVA of each of the fluence groups within the 100 μg/ml concentration category revealed that there was a greater difference in the mean viability values upto 1.7 J/cm^2 than would be expected by chance ($p<0.05$). The same result was obtained when the 200 μg/ml melanin concentration category was analysed in the same way. Above 1.7 J/cm^2, no significant difference in cell viability was found between the fluence groups for either category.

A comparison of the keratinocyte cell viability between the two melanin concentrations at each fluence exposure by a Student's t-test revealed no statistically significant difference.

Discussion

Adding either concentration of synthetic melanin (100 μg/ml and 200 μg/ml) to the media bathing keratinocytes in culture did not significantly affect cell viability when compared to the viability of the wells containing KCM alone at Time 0, nor in the non-laser treated controls (0 J/cm^2). This would suggest that synthetic melanin did not

exert a significantly toxic effect upon the cultured human keratinocytes over the whole time course of the experiment. Statistical analysis by one way ANOVA comparing the control wells of Time 0 and 0 J/cm^2 also revealed no difference in cell viability. This would appear to suggest that once again, as recorded in the experiments in Appendix B, exposure to air for the same duration as the experimental wells did not significantly decrease cell viability. Also given that under similar conditions (see Appendix B) but in the absence of a chromophore that laser treatment of keratinocytes did not cause damage, it would therefore seem fair to suggest that any change in cell viability recorded would be most likely as a result of ruby laser's action upon the added melanin.

The normal mode ruby laser appeared to induce a statistically significant decrease in cell viability within the keratinocyte population whose media now contained synthetic melanin as a chromophore. Statistical analysis using a Student's t-test between the non-exposed (0 J/cm^2) triplicate group and the group exposed to 0.6 J/cm^2 revealed a significant difference between the two mean values ($p<0.001$) at both melanin concentrations used. The extent of cell viability decreased with increasing fluence to a minimum at 1.7 J/cm^2 whereupon greater fluence values did not decrease cell viability any further (see Figure C.2).

Further statistical analysis by Student's t-test between the two melanin concentrations at the same fluence levels revealed no significant difference in cell viability throughout the range of fluences to which they were exposed. It might be expected that double the quantity of chromophore available within the 200 μg/ml wells might increase the cell death seen after laser exposure. Feasible explanations include the possibility that the two melanin concentrations used may be above the optimum level required to fully convert the laser photon energy to heat. Another explanation could be that only the melanin that has been internalised by the keratinocytes causes laser-induced cell death. Keratinocyte phagocytosis of melanin may have reached a maximum at the 100 μg/ml concentration, thus rendering any increase in added melanin unnecessary.

Finally, these results show that a monolayer of cultured keratinocytes, when incubated with synthetic melanin provides a good approximation of the epidermal cell damage/death events seen upon laser irradiation of skin. This model provides a simplified system in which to perform initial testing of any potentially protective pre-treatments and as such is used extensively in Chapter 6.

REFERENCES

Abe T, Konishi T, Hirano T, (1994), Possible correlation between RNA damage induced by hydrogen peroxide and translocation of heat shock protein 70 into the nucleus. *Biochem Biophys Res Commun,* 206:548-555

Ahmed B, Jaspan J, (1994), Hirsutism: a brief review. *Am J Med Sci,* 308(5): 289-294

Anderson R, (1984), Laser tissue interactions. In: Goldman MP, Fitzpatrick RE eds, Cutaneous laser surgery-the art and science of selective photothermolysis. *St Louis Mosby Year Book, Inc,* 1-18

Anderson R, Hu J, Parrish J, (1979), Optical radiation transfer in the human skin and application in *in vivo* remittance spectroscopy. *Proceedings of the symposium on bioengineering and the skin; MTP Press Ltd, London*

Anderson R, Parrish J, (1981), The optics of human skin. *J Inv Dermatol,* 77:13-19

Anderson R, Parrish J, (1983), Selective photothermolysis: precise microsurgery by selective absorption of pulsed radiation. *Science,* 220:524-527

Argyris T, (1967), Hair growth induced by damage, In: Advances in biology of the skin. 12:339-356

Bensaude O, Bellier S, Dubois M, Giannoni F, Nguyen V, (1996), Heat shock induced protein modifications and modulation of enzyme activities; in Stress-inducible cellular responses. U Feige, RI Morimoto, I Yahara and BS Poila. Basel: Birkhauser Verlag. 199-219

Billingham R, (1958), A Reconsideration of the Phenomenon of Hair Neogenesis

with Particular Reference to the Healing of Cutaneous Wounds in Adult Mammals. In: Montagna W, Ellis RA eds. The Biology of Hair Growth. New York: Academic Press. 451-468

Bowman P, Schuschereba S, Lawlor D, Gilligan G, Mata J, DeBaere D, (1997), Survival of human epidermal keratinocytes after short-duration high temperature: synthesis of HSP 70 and IL-8. *Am J Physiol,* 272:C1988-C1994

Brash D, Ziegler A, Jonason A, Simon J, Kunala S, Leffell D, (1996), Sunlight and sunburn in human skin cancer: p53, apoptosis and tumor promotion. *J Inv Dermatol,* 1:136-142

Bruls W, Leun JVD, (1984), Forward scattering properties of human epidermal layers. *Photochem Photobiol,* 40(2): 231-242

Campbell C, Quinn A, Angus B, Farr P, Rees J, (1993), Wavelength specific patterns of p53 induction in human skin following exposure to UV radiation. *Cancer Res,* 53:2697-2699

Carter L, Cashwell E, (1975), Particle transport simulation with the Monte Carlo method. *Tech Inform Centre, Office of Public Affairs, US Energy Res Develop Admin*

Casey J, Burger H, Kent J, Kellie A, Moxham A, Nabarro J, (1966), Treatment of Hirsutism by Adrenal and Ovarian Suppression. *J Clin Endocrinol Metab,* 26:1370-1374

Chase H, (1954), Growth of the hair. *Acta Derma Venereol,* 34:113-126

Chase H, Montagna W, (1951), Relation of hair proliferation to damage induced in the mouse skin. *Proc Soc Exper Biol Med,* 76:35-37

Chase H, Rauch H, Smith V, (1951), Critical stages of hair development and pigmentation in the mouse. *Physiol Zool,* 24:1-7

Cheng L, Packer L, (1979), Photodamage to hepatocytes by visible light. *Febs Letters,* 97(1): 124-128

Choudry R, Hodgins M, Kwast TVd, Brinkmann A, Boersma W, (1992), Localisation of Androgen Receptors in Human Skin by Imunohistochemistry: Implications for the Hormonal Regulation of Hair Growth, Sebaceous Glands and Sweat Glands. *J Endocrinol,* 133:467-475

Cotsarelis G, Sun T, Lavker R, (1990), Label-retaining cells reside in the bulge area of pilosebaceous unit: Implications for follicular stem cells, hair cycle and skin carcinogenesis. *Cell,* 61:1329-1337

Cookson WO, Harris AR, (1981), Diphtheroid endocarditis after electrolysis. *Br Med J (Clin Res Ed)* 282: 1513-1514

Courtois M, Loussouarn G, Hourseau C, Grollier J, (1995), Ageing and hair cycles. *B. J. Derm,* 132:86-93

Craig E, Gambill B, Nelson R, (1993), Heat shock proteins: molecular chaperones of protein biogenesis. *Microbiol Rev,* 57:402-414

Danforth C, (1925), Hair. In: Am. Med. Assoc. Press, Chicago.

Dawber R, Ebling F, Wojnarowska F, (1992), Disorders of Hair, In: Champion RH, Burton JL, Ebling FJG, eds. Textbook of Dermatology. Oxford: Blackwell Scientific Publications. 4:2533-2571

Dierickx C, Grossman M, Farinelli W, Anderson R, (1998), Permanent hair removal by normal-mode ruby laser. *Arch Dermatol,* 134:837842

Dry F, (1926), The coat of the mouse (Mus Musculus). *J Genet,* 16:287-340

Durward A, Randall K, (1949), Studies on Hair Growth in the Rat. *J Anat,* 83:325-335

Ebling F, Hale P, Randall V, (1991), Hormones and Hair growth. In: Goldsmith LA, ed. Biochemistry and Physiology of the Skin 2nd edn. Oxford University Press.

Ebling F, Johnson E, (1964), The action of hormones on spontaneous hair growth cycles in the rat. *J Endocrinol,* 29:193-201

Edwards M, Marks R, Dykes P, Merrett V, Morgan H, O'Donovan M, (1991), Heat shock proteins in cultured human keratinocytes and fibroblasts. *J Inv Dermatol,* 96(3): 392-396

Ferguson K, Wallace A, Lindner H, (1965), In: Biology of Hair Growth ed. Lyle AS, Short BF. Angus Robertson, Sydney. 655-677

Ferriman D, Galway J, (1961), Clinical assessment of body hair growth in women. *J Clin Endocrinol & Metabol,* 21:1440-1447

Finkelstein L, Blatstein L, (1991), Epilation of hair-bearing urethral grafts using the neodymium:YAG surgical laser. *J Urol,* 146:840-842

Fitzpatrick T, (1988), The validity and practicality of sun-reactive skin types I through VI - editorial. *Arch Dermatol,* 124:869-871

Flesch P, (1954), Hair Growth. In: Physiology and Biochemistry of the Skin. Univ. of Chicago Press. 601-661

Flock S, Patterson M, Wilson B, Wyman D, (1989), Monte Carlo modeling of light propagation in highly scattering tissues - 1: Model predictions and comparison with diffusion theory. ***IEEE Trans Biomed Engin,*** **36(12): 1162-1168**

Flock S, Wilson B, Patterson M, (1989), Monte Carlo modeling of light propagation in highly scattering tissues - 2: Comparison with measurments in phantoms. ***IEEE Trans Biomed Engin,*** **36(12): 1169-1173**

Friedenthal H, (1908), Das Dauerhaarkleid des Menschen. jena G. Fisher.

Garramone R, Winters R, Das D, Deckers P, (1994), Reduction of skeletal muscle injury through stress conditioning using the heat shock response. ***Plast Reconstr Surg,*** **93:1242-1247**

Gemert MV, Jacques S, Sterenborg H, Star W, (1989), Skin Optics. ***IEEE Trans Biomed Eng,*** **36(12): 1146-1154**

Gemert MV, Welch A, (1989), Time constants in thermal laser medicine. ***Las Surg Med,*** **9:405-421**

Giacommetti L, (1965), The Anatomy of the Human Scalp. In: Advances in Biology of the Skin. Vol VI Ageing. Ed: Montagna W. Pergamon Press, Oxford. 97-120

Gold M, Bell M, Foster T, Street S, (1997), Long-term epilation using the epilight broad band, intense pulsed light hair removal system. ***Dermatol Surg,*** **23:909-913**

Goldberg D, Littler C, Wheeland R, (1997), Topical suspension-assisted Q-switched Nd:YAG laser hair removal. ***Dermatol Surg,*** **23:741-745**

Goldman L, (1983), Optical radiation hazards to the skin. In; Sliney D, Wolbarsht (eds): Safety With Lasers and Other Optical Sources: A Comprehensive Handbook. New York, Plenum Press. 167-169

Goldman L, Rockwell J, Meyer R, Otten R, Wilson R, Kitzmiller K, (1967), Laser treatment of tattoos: a preliminary survey of three years' clinical experience. *JAMA,* 201:841-844

Goldman L, Wilson R, Hornby P, Meyer R, (1965), Radiation from a Q-switched ruby laser: effect of repeated impacts of power output of 10 megawatts on a tattoo of man. *J Inv Dermatol,* 44:69-71

Grossman M, Dierickx C, Farinelli W, Flotte T, Anderson R, (1996), Damage to hair follicles by normal-mode ruby laser pulses. *J Am Acad Dermatol,* 35:889-894

Grossman MC, Dierickx C, Farinelli W, Flotte T, Anderson RR, (1996), Damage to hair follicles by normal-mode ruby laser pulses. *J Am Acad Dermatol,* 35(6): 889-94

Gurke L, Marx A, Sutter P, Frentzel A, Salm T, Harder F, et al., (1996), Ischemic preconditioning improves post-ischemic skeletal muscle function. *Am Surg,* 62:391-394

Halldorsson T, Rother W, Langerholc J, Frank F, (1981), Theoretical and experimental investigations prove Nd:YAG laser treatment to be safe. *Las Surg Med,* 1:253-262

Hartl F, (1996), Molecular chaperones in cellular protein folding. *Nature,* 381:571-579

Hashizume H, Tokura Y, Takigawa M, Paus R, (1997), Hair cycle-dependent expression of heat shock proteins in hair follicle epithelium. *Int J Dermatol,* 36:587-592

Hutter M, Sievers R, Barbosa V, Wolfe C, (1994), Heat shock protein induction

in rat hearts. A direct correlation between the amount of heat shock protein induced and the degree of myocardial protection. *Circulation,* 89:355-360

Ito M, Tazawa T, Shimaza N, (1986), Cell Differentiation in Human Anagen Hair Follicles Studied With Anti-hair Keratin Monoclonal Antibodies. *J Inv Dermatol,* 86:563-569

Johnston R, Kucey B, (1988), Competitive inhibition of hsp 70 gene expression causes thermosensitivity. *Science,* 242:1551-1554

Jung, (1986), A generalised concept for cell killing by heat. *Rad Res,* 106:56-72

Karmazyn M, Mailer K, Currie R, (1991), Acquisition and decay of heat shock enhanced post-ischaemic ventricular recovery. *Am J Physiol,* 259:H424-H431

Kaufmann S, Schoel B, Embden Jv, Koga T, Wurttenberger AW, Munk M, et al., (1991), Heat shock protein 60: implications for pathogenesis of and protection against bacterial infections. *Immunol Rev,* 121:67-90

Kligman A, (1961), Pathologic dynamics of human hair loss. *Arch Dermatol,* 83:175-198

Knowlton A, Brecher P, Apstein C, (1990), Rapid expression of heat shock protein in the rabbit after brief cardiac ischaemia. *J Clin Invest,* 87:139-147

Koenig W, Lohner R, Perdrizet G, Lohner M, Schweitzer R, Lewis V, (1992), Improving acute skin flap survival through stress conditioning using heat shock and recovery. *Plast Reconstr Surg,* 90:659-664

Kopera D, Hohenleutner U, Stolz W, Landthaler M, (1997), *Ex vivo* quality-switched ruby laser irradiation of cutaneous melanocytic lesions: persistence of S-100-, HMB-45- and masson-positive cells. *Dermatol,* 194:344-350

Kuriloff D, Finn D, Kimmelman C, (1988), Pharyngoesophageal hair growth: the role of laser epilation. ***Otol Head Neck Surg,*** **98(4): 342-345**

Lane D, (1992), p53, guardian of the genome. ***Nature,*** **358:15-16**

Lask G, Elman M, Slatkine M, Waldman A, Rozenberg Z, (1997), Laser-assisted hair removal by selective photothermolysis. Preliminary results. ***Dermatol Surg,*** **23(9): 737-9**

Lawrence JC, (1967), ***In vitro*** **studies of skin after irradiation by a ruby laser.** ***Br J Plast Surg,*** **20(3): 257-62**

Leach E, Peters R, Rossiter R, (1943), Experimental thermal burns, especially the moderate temperature burn. ***Quart J Exp Physiol,*** **32:67-89**

Lee H, Schroeder C, Shah P, Babu S, Thompson C, Belloni F, (1996), Preconditioning with ischemia or adenosine protects skeletal muscle from ischemic tissue reperfusion injury. ***J Surg Res,*** **63:29-34**

Lee Y, Manalo D, Liu A, (1996), Heat shock response, heat shock transcription factor and cell ageing. ***Biol Signals,*** **5:180-191**

Li W, Chen C, Ling C, Li G, (1996), Apoptosis in heat-induced cell killing: the protective role of HSP 70 and the sensitization effect of the c-myc gene. ***Rad Res,*** **145:324-330**

Liew S, (1999), Ruby laser-assisted hair removal: clinical efficacy and evaluation of cutaneous changes. ***Thesis submitted for the degree of Doctor of Medicine***

Liew S, Grobbelaar A, Gault D, Sanders R, Green C, Linge C, Ruby laser light irradiation on ***ex vivo*** **scalp skin: clinical implication (depth of penetration).** ***Ann***

Plast Surg

Liew S, Ladhani K, Grobbelaar A, Gault D, Green C, Linge C, (In press), Ruby laser-assisted hair removal results in reduction in the coarseness of regrowing hairs: fallacy or fact. ***Br J Plast Surg***

Liew S, Ladhani K, Grobbelaar A, Gault D, Sanders R, Green C, et al., (In press), Ruby laser-assisted hair removal: success in relation to anatomical factors and melanin content of hair follicles. ***Plast Reconstr Surg***

Lin TY, Manuskiatti W, Dierickx CC, Farinelli WA, Fisher ME, Flotte T, et al., (1998), Hair growth cycle affects hair follicle destruction by ruby laser pulses. ***J Inv Dermatol,*** **111(1): 107-13**

Lynfield Y, (1960), Effect of pregnancy on the human hair cycle. ***J Inv Dermatol,*** **35:323-327**

Maimon T, (1960), Stimulated optical radiation in ruby. ***Nature,*** **187:493-494**

Marber M, Latchman D, Walker J, Yellon D, (1993), Cardiac stress protein elevation 24 hours after brief ischemia or heat stress is associated with resistance to myocardial infarction. ***Circulation,*** **88:1264-1272**

Matylevitch N, Schuschereba S, Mata J, Gilligan G, Lawlor D, Goodwin C, et al., (1998), Apoptosis and accidental cell death in cultured human keratinocytes after thermal injury. ***Am J Pathol,*** **153(2): 567-577**

Maytin E, (1995), Heat shock proteins and molecular chaperones: Implications for adaptive responses in the skin. ***J Inv Dermatol,*** **104(4): 448-455**

Maytin E, Wimberley J, Kane K, (1994), Heat shock modulates UVB-induced cell death in human epidermal keratinocytes: evidence for a hyperthermia-

inducible protective response. *J Inv Dermatol,* 103:547-553

McKnight E, (1964), The prevalence of hirsutism in young women. *Lancet,* 1:410-413

Menon I, Persad S, Ranadive N, Haberman H, (1985), Role of superoxide and hydrogen peroxide in cell lysis during irradiation *in vitro* of Ehrlich ascitic carcinoma cells in the presence of melanin. *Can J Biochem Cell Biol,* 63:278-283

Minowada G, Welch W, (1995), Clinical implications of the stress response. *J Clin Invest,* 95:3-12

Moltz L, Schwartz U, Pickartz H, (1981), XY gonadal dysgenesis aberrant testicular differentiation in the presence of H-Y antigen. *Obstet Gynecol,* 58:17-23

Morimoto R, Kroeger P, Craig E, (1996), The transcriptional regulation of heat shock genes: a plethora of heat shock factors and regulatory conditions. In: Stress-inducible cellular responses. U Feige, RI Morimoto, I Yahara and B Poila Basel, Switzerland: Birkhauser Verlag. 139-163

Morris S, Cumming D, Latchman D, Yellon D, (1996), Specific induction of the 70-kD heat stress proteins by the tyrosine kinase inhibitor herbimycin-A protects rat neonatal cardiomyocytes. A new pharmacological route to stress protein expression? *J Clin Invest,* 97:705-712

Muramatsu T, Hatoko M, Tada H, Shirai T, Ohnishi T, (1996), Age-related decrease in the inductability of heat shock protein 72 in normal human skin. *B J Dermatol,* 134:1035-1038

Muramatsu T, Tada H, Kobayashi N, Yamji M, Shirai T, Ohnishi T, (1992), Induction of the 72kD heat shock protein in organ-cultured normal human skin. *J Inv Dermatol,* 98(5): 786-790

Muramatsu T, Yamashina Y, Tada H, (1993), 8-Methoxypsoralen plus UVA induces the 72-kD heat shock protein in organ-cultured normal human skin. *Photochem Photobiol,* 58:809-812

Murry C, Jennings R, Reimer K, (1986), Preconditioning with ischemia: a delay of lethal cell injury in ischemic myocardium. *Circulation,* 74:1124-1136

Nakazawa K, Sahuc F, Damour O, Collombel C, Nakazawa H, (1998), Regulatory effects of heat on normal human melanocyte growth and melanogenesis: comparative study with UVB. *J Inv Dermatol,* 110:972-977

Nanni C, Alster T, (1997), Optimizing treatment parameters for hair removal using a topical carbon-based solution and 1064-nm Q-switched Neodymium:YAG laser energy. *Arch Dermatol,* 133:1546-1549

Narisawa Y, Hashimoto K, Kohda H, (1995), Scanning electron microscopic observations of extracted terminal hair follicles of the adult human scalp and eyebrow with special reference to the bulge area. *Arch Dermatol Res,* 287:599-607

Narisawa Y, Kohda H, Tanaka T, (1997), Three-dimensional demonstration of melanocyte distribution of human hair follicles: special reference to the bulge area. *Acta Derm Venereol (Stockh),* 77:97-101

Natow A, (1986), Chemical removal of hair. *Cutis,* 91-92

Nixon A, (1993), A method of determining the activity state of hair follicles. *Biotech Histochem,* 68(6): 316-325

Nolan J, Venuto R, Goldmann S, (1978), Role of endotoxin in glycerol-induced renal failure in the rat. *Clin Sci Mol Med,* 54:615-620

Oliver R, (1966), Whisker growth after removal of the dermal papilla and lengths of follicle in the hooded rat. *J. Embryol Exp Morph,* 15(3): 331-347

Petrozzi JW, (1980), Verrucae planae spread by electrolysis. *Cutis*, 26(1): 85

Pinkus H, (1958), Embryology of hair, In: Montagna W, Ellis RA eds, Biology of hair growth. New York Academic Press. 1-32

Polla B, Anderson R, (1987), Thermal injury by laser pulses: Protection by heat shock despite failure to induce heat shock response. *Las Surg Med,* 7:398-404

Polla B, Kantengwa S, Francois D, Salvioli S, Franceschi C, Marsac C, et al., (1996), Mitochondria are selective targets for the protective effects of heat shock against oxidative injury. *Proc Natl Acad Sci USA,* 93:6458-6463

Polla LL, Margolis RJ, Dover JS, Whitaker D, Murphy GF, Jacques SL, et al., (1987), Melanosomes are a primary target of Q-switched ruby laser irradiation in guinea pig skin. *J Invest Dermatol,* 89(3): 281-6

Price V, (1975), Testosterone metabolism in the skin. *Arch Dermatol,* 111:1496

Rabinowitz S, Cohen R, (1983), Anxiety and hirsutism. *Psychol Report,* 53:827-830

Randall V, Ebling F, (1991), Seasonal changes in human hair growth. *B J Dermatol,* 124:146-151

Randall V, Thornton M, Messenger A, (1992), Cultured Dermal Papilla Cells from Androgen Dependent Human Hair Follicles (e.g. Beard) Contain More Androgen Receptors Than Those From Non-Balding Areas of the Scalp. *J Endocrinol,* 133:141-147

Rheinwald JG, Green H, (1975), Serial cultivation of strains of human epidermal keratinocytes: the formation of keratinizing colonies from single cells. *Cell*, 6(3): 331-343

Richards R, Meharg G, (1995), Electrolysis: observations from 13 years and 140 000 hours of experience. *J Am Acad Dermatol,* 33(4): 662-666

Ritossa F, (1962), A new puffing pattern induced by temperature shock and DNP in Drosophila. *Experientia,* 15(12): 571-573

Rochat A, Kobayashi K, Barrandon Y, (1994), Location of stem cells of human hair follicles by clonal analysis. *Cell,* 76(6): 1063-1073

Rook A, (1965), Endocrine Influences on hair growth. *B Med J,* 609-614

Rosenberg G, Gregory R, (1996), Lasers in aesthetic surgery. In: What's new in plastic surgery. *Clinics in plastic surgery,* 23(1): 29-48

Rushmer R, Buettner K, Short J, Odland G, (1966), The skin. *Science,* 154:343-348

Saitoh M, Uzuka M, Sakamoto M, (1970), Human hair cycle. *J Inv Dermatol,* 54(1): 65-81

Sapareto S, Hopwood L, Dewey W, Raju M, Gray J, (1978), Effects of hyperthermia on survival and progresion of chinese hamster ovary cells. *Cancer Res,* 38:393-400

Selye H, (1967), Ischemic necrosis: prevention by stress. *Science,* 156:1262-1263

Setty L, (1966), A Comparative Study of the Distribution of Hair of the Hand and Foot of White and Negro Males. *Am J Phys Anthropol,* 25:131-138

Setty L, (1968), The Distribution of Hair of the Lower Limb in White and Negro Males. *Am J Phys Anthropol,* 29:51-55

Shea C, Parrish J, (1991), Nonionising radiation and the skin. In: Physiology, biochemistry and molecular biology of the skin, Goldsmith LA. Eds. Oxford University Press. 910-927

Solomon MP, (1998), Hair removal using the long-pulsed ruby laser. *Ann Plast Surg,* 41(1): 1-6

Stadtman, (1992), Protein oxidation and aging. *Science,* 257:1220-1225

Steels E, Watson K, Parsons P, (1992), Relationships between thermotolerance, oxidative stress responses and induction of stress proteins in human tumour lines. *Biochem Pharmacol,* 44:2123-2129

Strasser A, (1995), Bcl-2 and thermotolerance cooperate in cell survival. *Cell Growth Differ.,* 6(7): 799-805

Strasser A, Anderson R, (1995), Bcl-2 and thermotolerance cooperate in cell survival. *Cell Growth Differ,* 6:799-805

Szabo G, (1958), The regional frequency and distribution of hair follicles in human skin. *In: Montagna W, Ellis RA eds, Biology of hair growth. New York; Academic Press,* 33-38

Trotter N, (1924), The life cycles of hair in selected regions of the body. *Am J Phys Anthropol,* 7:427-437

Uchida N, Kato H, Ishida T, (1993), A model for cell killing by continuous heating. *Med Hypo,* 41:548-553

Vogt B, Croatt A, Alam J, Nath K, (1993), Prior treatment with endotoxin confers resistance to the glycerol model of acute renal failure: the role of heme oxygenase and ferritin. *J Am Soc Nephrol,* 4:761A

Wagner R, Tomich J, Grande D, (1985), Electrolysis and thermolysis for permanent hair removal. *J Am Acad Dermatol,* 12(3): 441-449

Watt F, (1994), Cultivation of human epidermal keratinocytes with a 3T3 feeder layer, In: Cell Biology: A Laboratory Handbook. New York: Academic. 83-89

Welch A, (1984), The thermal response of laser irradiated tissue. *IEEE J Quant Electr,* QE20(12): 1471-1481

Welch A, Wissler E, Priebe L, (1980), Significance of blood flow in calculations of temperature in laser irradiated tissue. *IEEE Trans Biomed Eng,* BME-27:164-166

Welch W, (1992), Mammalian stress response: Cell physiology, structure/ function of stress proteins and implications for medicine and disease. *Physiolog Rev,* 72(4): 1063-1081

Wilson C, Cotsarelis G, Wei Z, Fryer E, Margolis-Fryer J, Ostead M, et al., (1994), Cells within the bulge region of mouse hair follicle transiently proliferate during early anagen: heterogeneity and functional differences of various hair cycles. *Differentiation,* 55:127-136

Yellon D, Marber M, (1994), HSP 70 in myocardial ischaemia. *Experentia,* 50:1075-1084

Yohn N, Yrastorza, Buno, Leff, Hake, Repine, (1991), Disparate antioxidant enzyme activities in cultured human cutaneous fibroblasts, keratinocytes and

melanocytes. *J. Inv. Derm,* 97(3): 405-409